Lock n Load

A Digital Solution for Emergency Timber Shelters

Empowering Designers and Seekers

AMIR GHADIRI LANGARI

Amir Ghadiri Langari

Master Thesis Research

5824737

MSc in Architecture, Urbanism, and Building Sciences
Building Technology Track

Mentors
Dr. serdar asut
Prof.dr. Mauro Overend

Delft University of Technology
Faculty of Architecture and the Built Environment

29 October 2024

Acknowledgement

This thesis would not have been possible without the guidance and expertise of my mentors, Dr. Serdar Asut and Prof. Dr. Mauro Overend. Their insights, feedback, and unwavering support have been instrumental throughout this research journey.

I also extend my sincere gratitude to Dr. Simona Bianchi and Gilbert Koskamp. While not my official mentors, their willingness to lend their expertise and encouragement at critical junctures has been invaluable. Their belief in my work and their reassurance that I was on the right track provided much-needed motivation.

To my awesome friends, thanks for keeping me sane and for all the help with the technical stuff. You know who you are – you're the best!

To my Parents, thank you for supporting me coming all the way to another continent for my studies. I love you both and appreciate your understanding for all those missed family calls.

And finally to my partner Patricia, thanks for putting up with me during those stressful nights and for being the best cheerleader ever. You were basically writing this thesis with me! I especially needed to hear those "you're doing a great job" pep talks, so thank you for that.

Abstract

This thesis delves into the potential of timber as a sustainable and efficient material for constructing emergency shelters, particularly in post-disaster scenarios where rapid and accessible housing solutions are critical. The research focuses on the development of "Lock n Load," a digital tool designed to streamline and optimize the design, construction, and delivery of timber frame shelters.

A primary challenge addressed in this thesis is the limited availability of skilled labor in post-disaster situations. "Lock n Load" tackles this challenge by automating complex design tasks, enabling individuals with minimal construction experience to participate in building their own shelters. The tool incorporates a user-friendly interface that simplifies the design process, making it accessible to a wider range of individuals.

Another key aspect of this research is the emphasis on utilizing readily available resources. By optimizing the use of timber and incorporating local sourcing, "Lock n Load" promotes sustainability and reduces reliance on external materials. This approach not only minimizes environmental impact but also allows for faster and more cost-effective shelter construction.

The research methodology includes a case study that investigates various design and optimization methods for timber structures. This case study provides insights into the structural performance and material efficiency of different timber frame designs, informing the development and refinement of "Lock n Load".

Lock n Load offers an innovative solution to address the urgent need for effective emergency shelters by bridging traditional timber construction with modern digital tools. "Lock n Load" empowers individuals to take an active role in their own shelter construction, promoting self-reliance and community participation in post-disaster recovery efforts. The tool's focus on sustainability, efficiency, and accessibility makes it a valuable resource in addressing the challenges of providing rapid and resilient housing solutions in times of crisis.

Contents

List of Mathematical Symbols

$\sigma_{c,o,d}$: Compressive stress

$f_{c,o,d}$: Design compressive strength

N_{ED} : Design axial compressive force

k_{mod} : Modification factor for the impact of load duration and moisture content

$f_{c,og}$: Characteristic compressive strength

y_{M} : Partial factor accounting for the material properties

$\sigma_{m,y,d}$: The bending stress about the y-axis

$f_{m,y,d}$: Bending strength

$M_{y,ED}$: Bending moment around the y-axis

w_{y} : Section modulus about the y-axis

$f_{m,g,k}$: Characteristic bending strength

τ_{d} : The design shear stress

$f_{v,d}$: The design shear strength

v_{ED} : The design shear force

$f_{v,g,k}$: The characteristic shear strength of timber

k_{cr} : The factor for the potential cracking of the timber

$\sigma_{c,o,d}$: The design compressive stress acting on the timber

$f_{c,o,d}$: The design compressive strength of the timber parallel to the grain.

k_c : The modification factor for load duration and moisture content.

N_{ED} : The design axial force (compression)

$f_{c,o,g,k}$: The characteristic bending strength of the timber

y_M : The partial safety factor for material properties

$w_{creep,g}$: The creep deformation due to dead load

$w_{inst,g}$: The immediate deflection under dead load

k_{def} : The factor accounting for creep's influence under sustained load

$w_{creep,lead}$: The Creep due to Live Load fo rLeading Variable Action

$w_{creep,q}$: The creep deformation from leading variable action

$w_{inst,q}$: The immediate deflection under leading variable action

ψ_{acmp} : The factor adjusting for the loading duration for accompanying load Variable Action

$w_{creep,acmp}$: The Creep due to Accompanying Variable Action

List of abbreviations

CNC: Computer Numerical Control

ESBM: Equivalent Steel Bolt Method

FEM: Finite Element Model

FEA: Finite Element Analysis

MOE: Modulus of Elasticity

MT: Mortise and tenon

PMT: Pegged Mortise and tenon

Introduction

Shelter, more than just a physical structure, is fundamental to human well-being and a critical determinant of health outcomes (Shaw, 2004). It serves as a habitable sanctuary, offering security, privacy, and a sense of dignity to its occupants (Shelter Center, 2010). In the face of natural disasters – earthquakes, hurricanes, landslides, tornadoes, tsunamis, and typhoons – the vulnerability of developing countries is starkly exposed. Inadequate building practices and lax planning codes often render homes in these regions tragically susceptible to damage or complete destruction (Schilderman, 2004). The absence of timely and adequate emergency or temporary shelter can lead to the proliferation of overcrowded, and hoc dwellings. These makeshift settlements, while a testament to human resilience, frequently become breeding grounds for a host of health concerns (VanRooyen and Leaning, 2005). The escalating frequency of natural disasters, compounded by the effects of climate change and humanitarian crises, underscores the urgent and growing need for effective emergency shelter solutions worldwide, particularly for vulnerable populations (Allen, 2006; Ashton, 2000; Wilson, 2011).

Timber, with its unique blend of characteristics, emerges as a compelling option that addresses both the immediate and long-term needs of those affected. Historically, particularly in areas abundant in timber, farmers readily built their own shelter. This skill, passed down through generations, fostered a deep connection between them and their homes. The process was so commonplace that even traveling merchants in Russia carried tools to construct their own makeshift offices. Whether in the Carpathian Mountains, the Alps, or in Japan, self-built farm houses remained a tradition well into the 20th century, showcasing how easily accessible this practice was when timber was plentiful (Zwerger 2015).

Beyond the timber structure itself, the artistry of **joinery**, as ancient as history itself, especially in regions abundant in timber, played a crucial role in these self-built structures. For instance, the Potala Palace and Jokhang Temple in Tibet, built with methods dating back over 4500 years, still stand today. Likewise, the Dou-gong bracket system (figure 1.1) originating around 770 BC, continues to be used in traditional timber buildings throughout China, Korea, and Japan. Even in ancient Egypt, archaeological finds and artistic depictions reveal the use of woodworking tools like saws, chisels, and mallets, highlighting the long history of carpentry and joinery (Arlet 2021). In timber structures, connections play a crucial role in ensuring the overall strength, durability, and effective load transfer of the entire system. Metal fasteners (figure 1.2) are currently the predominant method for joining timber components together. However, while joinery became obsolete because of its labor-intensive nature and the need for high-level skills, the advent of digital fabrication technologies has renewed interest in joinery (Siem 2017).

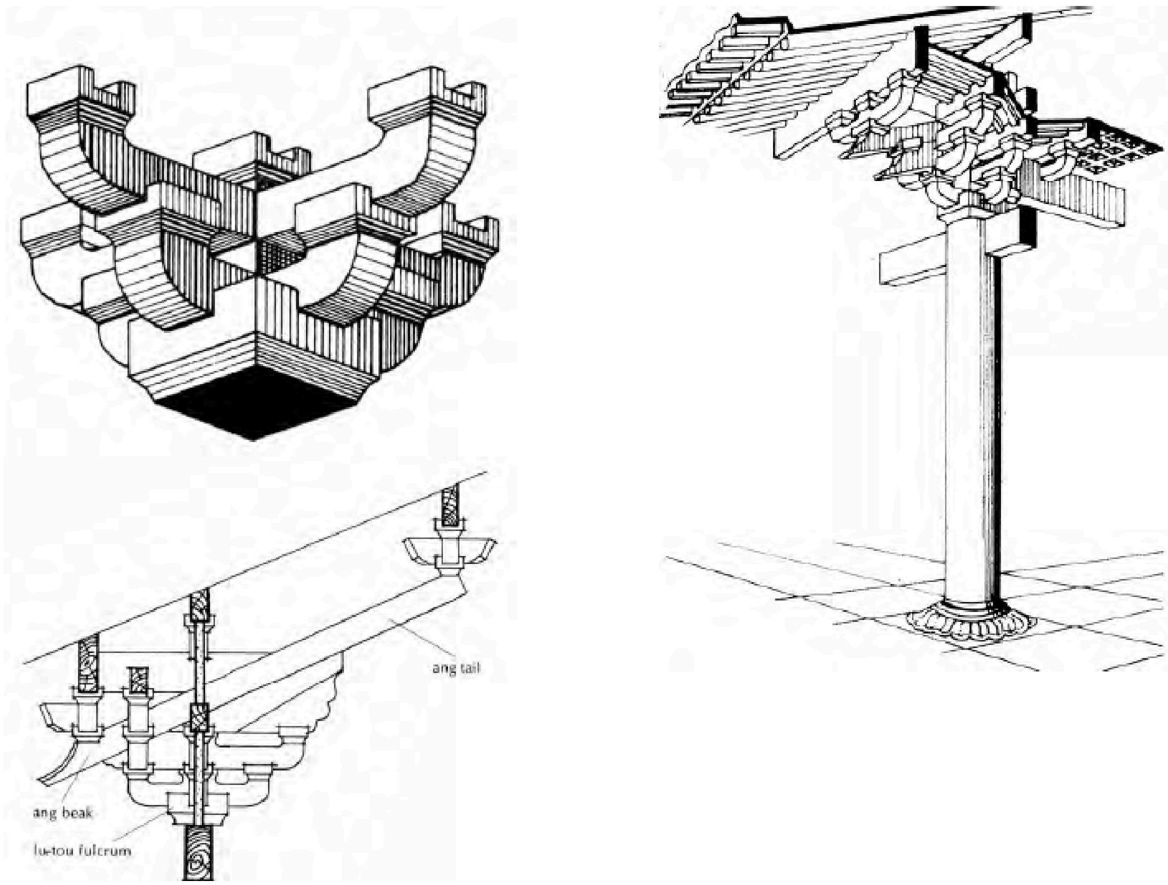

Figure 1.1: Dou-gong bracket system | Chinese architecture

Instances of recent connections can be seen in projects like the Yusuhara Wooden Bridge Museum in Japan (2010) by Kengo Kuma and Associates (figure 1.3), the Tamedia Office Building in Switzerland (2013) by Shigeru Ban Architects, and the Writers Theatre in the USA (2016) by Studio Gang Architects (Fang, Moradei et al. 2019). While the demand for carpenters skilled in manual joint carving is decreasing, there is a growing need for experts who can bridge the gap between traditional timber knowledge and modern construction practices (Hudert 2019).

Figure 1.2: examples of timber structures with steel connections a: (Gensler 2015), Matthew Millman Photography and b: Photo by Vermont Timber Works Inc.

Figure 1.3: Yusuhara Wooden Bridge Museum in Japan (2010) by Kengo Kuma and Associates

Rationale for Timber Shelters: Advantages and Opportunities

After a disaster, time is of the essence. Timber's **lightweight** nature and **prefabrication** potential allow for **rapid assembly** of shelters, ensuring that people are provided with a safe haven as quickly as possible. This swift response can be life-saving, particularly in harsh weather conditions or when access to affected areas is challenging (Falk 2019; Casagrande 2021; Barreca 2022). There are numerous examples of modern structures being rapidly constructed using wood (figure 1.4, figure 1.5).

Figure 1.4: The Rigot Collective Dwelling Centre in Geneva was built to quickly house 370 refugees. Constructed from prefabricated wooden modules, this two-building complex is designed to be taken down within ten years.

Another significant advantage inherent to timber structures, particularly those employing joinery, lies in their capacity for **non-destructive** assembly and their inherent compatibility with **Design for Deconstruction** principles. This potential for joinery to facilitate Design for Deconstruction stems directly from its characteristic of enabling non-destructive assembly, a feature not typically encountered within the construction industry (Fang 2020). This inherent capacity for non-destructive assembly and Design for Deconstruction proves particularly advantageous in the context of temporary shelters. Such structures often require rapid deployment and eventual dismantling, making the ability to assemble and disassemble without damage or waste a critical factor.

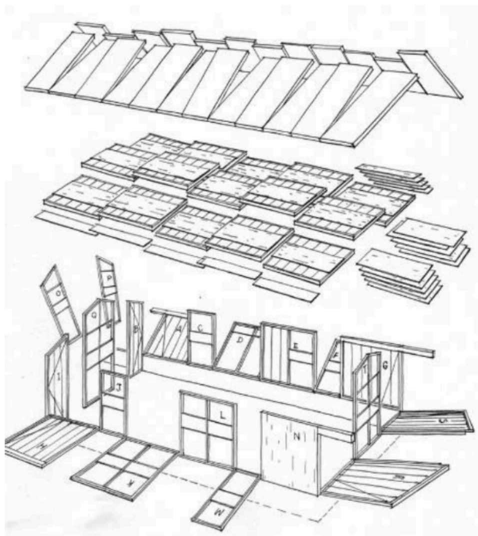

Figure 1.5: Techbuilt: Modern, Modular, Quick assembly and Made for the Masses

Another factor contributing to timber's suitability for emergency shelters is its **natural abundance, particularly in forested areas**. This readily available resource eliminates the need for extensive material transportation, allowing individuals to focus their efforts on shelter construction rather than resource acquisition.

Furthermore, timber's relatively soft nature allows for easy manipulation with **basic tools** (figure 1.6) commonly found in survival situations, enabling individuals to construct shelters rapidly and efficiently. This accessibility and ease of use make timber an invaluable resource in survival scenarios, where the need for shelter is often urgent and critical.

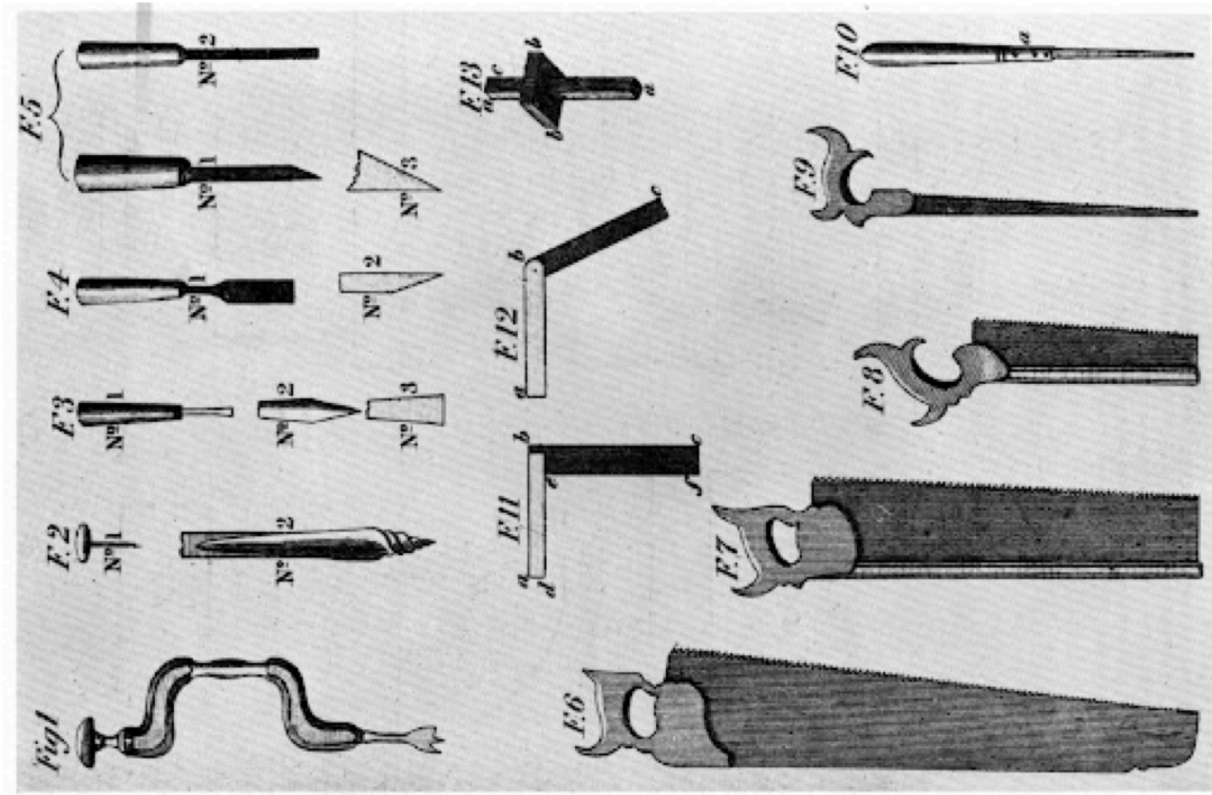

Figure 1.6: Simple tools used in timber framing

In addition, while timber's **environmental friendliness** may not be the primary reason for its use in emergency shelters, it's certainly a noteworthy benefit. As research like (Gustavsson 2006; Skog 2015; Stern 2018) shows, timber often boasts lower embodied carbon than traditional building materials, further enhancing its appeal. Also study by (Fang 2020) establishes the sustainability benefits of timber dry joints compared to conventional materials such as steel and concrete. The study demonstrates that employing interlocking joints as a building method holds significant potential for reducing the embodied carbon in structures. A key environmental distinction of timber lies in its adaptability, making it particularly valuable for emergency shelter construction. Unlike many short and mid-term shelter options that lack flexibility, timber structures can be disassembled, reused, and even upgraded to meet evolving needs, extending their lifespan and reducing waste. To fully utilize wood's benefits, we must extend its lifespan in buildings through adaptable designs or component reuse. However, current practices hinder this, necessitating a shift in building and product design to promote wood recycling (Hudert 2019).

Given timber's **availability**, **adaptability**, **environmental benefits**, potential for **reuse**, **upgrade**, **rapid** and **low-dependency assembly**, it seems that timber-based structures present a promising solution to the escalating need for effective emergency and mid-term shelters in crisis situations.

Problem Statement

Though timber joinery and interlocking systems show great promise for improving emergency shelters, there are challenges to overcome before they become widely used.

However, various **obstacles** currently hinder the full realization of this vision:
While timber's abundance makes it an appealing construction material, its effective utilization demands more than mere availability. Designing **safe** and **resilient** timber structures necessitates a **profound understanding of structural engineering principles**. This entails not only a comprehensive grasp of **wood's diverse properties** and behaviors under stress but also proficiency in structural calculations and adherence to **building codes**.

The **intricate nature of timber** design further amplifies the **complexity**. Each structure, unique in its size, purpose, and environmental context, requires meticulous consideration. A well-conceived design, encompassing factors like foundation type and local climate, ensures the structure's longevity and functionality.

In the past, the knowledge of working with timber and constructing shelters was a **generational** inheritance. This knowledge encompassed an intuitive understanding of timber's properties, sizing rules-of-thumb, and climate-responsive design principles, refined through centuries of hands-on experience. Each generation contributed to an ongoing optimization process. (Zwerger 2015) . However, the advent of industrialization and modernism, accompanied by the rise of new materials, disrupted this lineage. The once-commonplace skills of timber construction were gradually eclipsed, creating a disconnect between people and their built environment. This loss of traditional knowledge represents a break in the **chain of experience**.
Even in contemporary practice, timber joinery remains reliant on experiential knowledge. However, a disconnect exists between the design of timber joinery and that of other construction methods. No country has used structural reliability concepts for timber joint design equations, as **the safety levels** are hard to assess except for simple cases (Smith 2002). This is

different from wood member design, where reliability concepts are already used in several countries. While the sizing of timber members adheres to established structural analysis methods and material specifications, the detailing of joinery connections falls outside these codified boundaries. This necessitates reliance on engineering judgment and the builder's experiential knowledge, a practice that can introduce variability and uncertainty into the design process (Schmidt 2019). This **absence of standardized guidelines** and analytical methods for joinery connections hinders advancements in joinery design. The lack of a systematic framework limits the ability to rigorously assess the strength and stiffness of these connections, impeding innovation and optimization in timber construction (Shanks 2009).

The growing scale and complexity of modern wood construction demand a renewed focus on joinery design to facilitate **circularity**. Despite the potential for disassembly, reuse, and recycling offered by traditional principles, current practices often hinder achieving these goals. This necessitates a shift in design philosophy to **prioritize connections** that enable circular construction throughout the building lifecycle, from factory to site (Zwerger 2015).

In addition, the **need for optimisation** of the structural performance of temporary timber shelters was specifically underscored by the aftermath of the 2011 Great East Japan Earthquake. As survivors were compelled to live in temporary housing for durations far exceeding the initial two-year design period, these wooden units experienced significant deterioration, necessitating extensive repairs (Iwata 2023). The range of repair categories, from cracks in walls to damage to wooden foundations, highlights the necessity for a comprehensive database that not only records these issues but also facilitates the identification of future optimizations in timber shelters and structures. Beyond optimization for higher capacity, refining the construction process and accelerating the assembly of timber shelters, enhancing their overall livability emerges as another crucial objective.

In addition, the design of emergency shelters is inherently constrained by **contextual factors** that significantly impact their effectiveness and feasibility. Limited availability of materials, logistical complexities in transportation and deployment, and the need to adapt to diverse climatic conditions pose significant challenges to creating shelters that are both functional and resilient. These limitations necessitate innovative approaches that balance immediate needs with long-term sustainability, ensuring that emergency shelters are adaptable to the specific

context in which they are deployed.
Moreover, designing effective emergency shelters presents a significant challenge: balancing the diverse **personal preferences** of displaced individuals with the **constraints of limited resources** and **urgent needs**. What may be a suitable design for one person may not meet the needs of another, highlighting the complexities of delivering suitable shelters in times of crisis.

These obstacles underscore the challenges associated with the rapid deployment of timber shelter systems for structurally sound temporary shelters in post-disaster situations. To fully utilize the potential of timber shelter in disaster relief, it is crucial to address these challenges. This necessitates research into **more efficient, integrated design methods** and **faster verification** and **optimizing processes**, ultimately enabling the provision of **timely**, **effective**, and **sustainable** shelter solutions.

Research Objectives

The vision is to empower individuals to become active participants in assembling their own shelters, reducing reliance on specialized skills and labor. This approach would allow people to inhabit temporary, transitional, or even permanent structures that are **tailored to their needs** and preferences, to the greatest extent possible within the constraints of their circumstances.

The primary aim of this thesis is to develop a **digital tool** that **streamlines** and **enhances** the process of **delivering**, **designing**, **optimizing**, **provision** and **fabricating** post-disaster timber shelters for emergency use, benefiting disaster **victims**, shelter **designers**, **manufacturers** and other **stakeholders** involved in the **supply chain**.

Research Questions

Can a **digital tool** be created to **simplify**, **improve**, and **integrate** the process of **delivering**, **designing**, **optimizing**, and assembling post-disaster timber shelters for emergency use, providing benefits to **disaster victims**, **shelter designers**, and other key **stakeholders** in the **supply chain**? **How**?

Methodology

The research methodology consists of three distinct phases, **literature** and **background review**, **Case study**, and the **development** of the **tool** (Lock n Load).

literature review

The literature review begins with an exploration of **existing timber shelters** and structures, showcasing how others have navigated the challenges outlined in the problem statement. These examples highlight the key objectives for optimization. Subsequently, the investigation delves into the **properties** and **structural applications** of **timber**, providing a foundation for the design and parameters of the ensuing case study. Finally, the review explores the field of **timber structure optimization**, branching into **whole-structure optimization** and the **optimization of joints** and connections. These insights inform the methodological choices, design processes, and optimization strategies implemented in the case study.

Case study

The case study begins with the **preliminary design** of a timber frame, considering architectural and practical factors relevant to an emergency shelter. Next, Eurocode 5 guidelines are used to define the parameters and limitations for **optimizing** the **timber frame**. Once the most efficient cross-sections for the timber frame members are determined, the case study focuses on designing and optimizing the chosen connection: the pegged mortise and tenon joint. Two approaches are used to optimize this joint. First, an **analytical** method is developed, using a steel bolt equivalent model and iterative calculations to find the best joint dimensions. Then, a **numerical simulation** (**FEM**) is created to test and optimize the joint with a wider range of factors. The combination of these two optimization approaches led to the final design.

Development of Lock n Load (the Tool)

The tool's designer section was built upon the foundation of a single, optimized timber frame block from the case study. All necessary components for this block were developed in Python, showcasing how timber frame design and optimization can be largely **automated** and incorporated into a **design library** for further refinement. Additionally, a panel for **shelter-seekers** was created to allow for **customization** based on available resources and individual preferences. The **supply chain** component was also developed, integrating **manufacturers** and **timber providers** with the other two elements of the tool.

Research outline

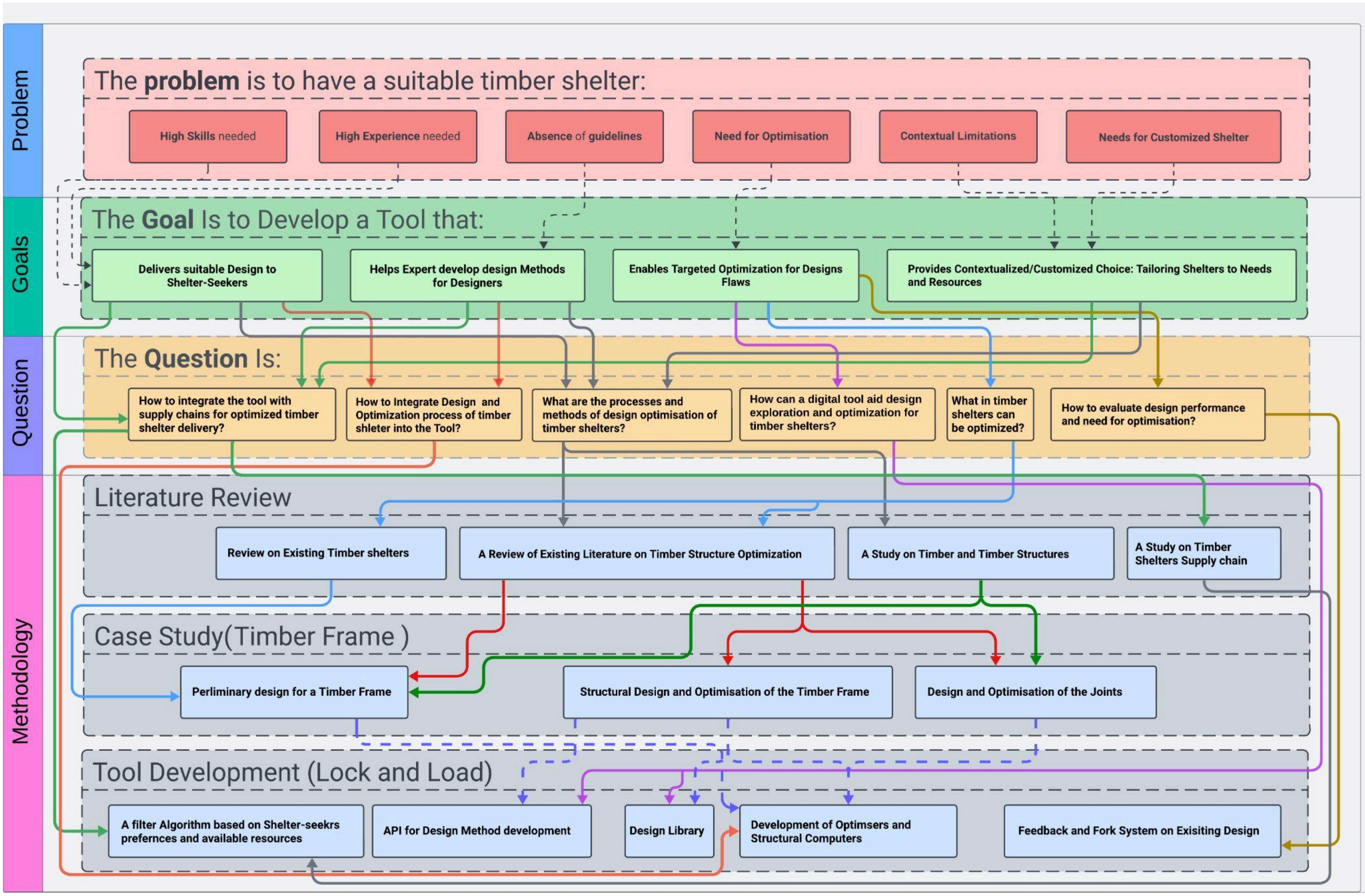

Figure 1.7: Research outline

"In the construction of houses, choice of woods is made. Straight un-knotted timber of good appearance is used for the revealed pillars, straight timber with small defects is used for the inner pillars. Timbers of the finest appearance, even if a little weak, are used for the thresholds, lintels, doors, and sliding doors, and so on. Good strong timber, though it be gnarled and knotted, can always be used discreetly in construction."

The Book of Five Rings: Miyamoto Musashi, 17th Century

Literature review

This section presents a review of existing timber shelters relevant to the thesis's research questions. Subsequently, a comprehensive examination of the literature concerning the analysis, simulation, and optimization of timber structures and their constituent components is provided.

Review of Existing Timber Shelters

This section explores existing timber shelters and structures, examining the **objectives** that designers prioritized during the optimization and design processes. By analyzing these choices, the key factors that contribute to the creation of a suitable and optimized timber shelter were determined.

Liina Transitional Shelter

The Liina Transitional Shelter (figure 2.1) was designed to address the immediate need for shelter in the aftermath of disasters. Its key features are its **flat-pack shipping** and **rapid assembly**, even in areas with limited infrastructure and resources. The design specifically **avoids** the need for **complex tools**, **heavy machinery**, or **electricity**, **enabling deployment in challenging conditions** (ArchDaily 2011).

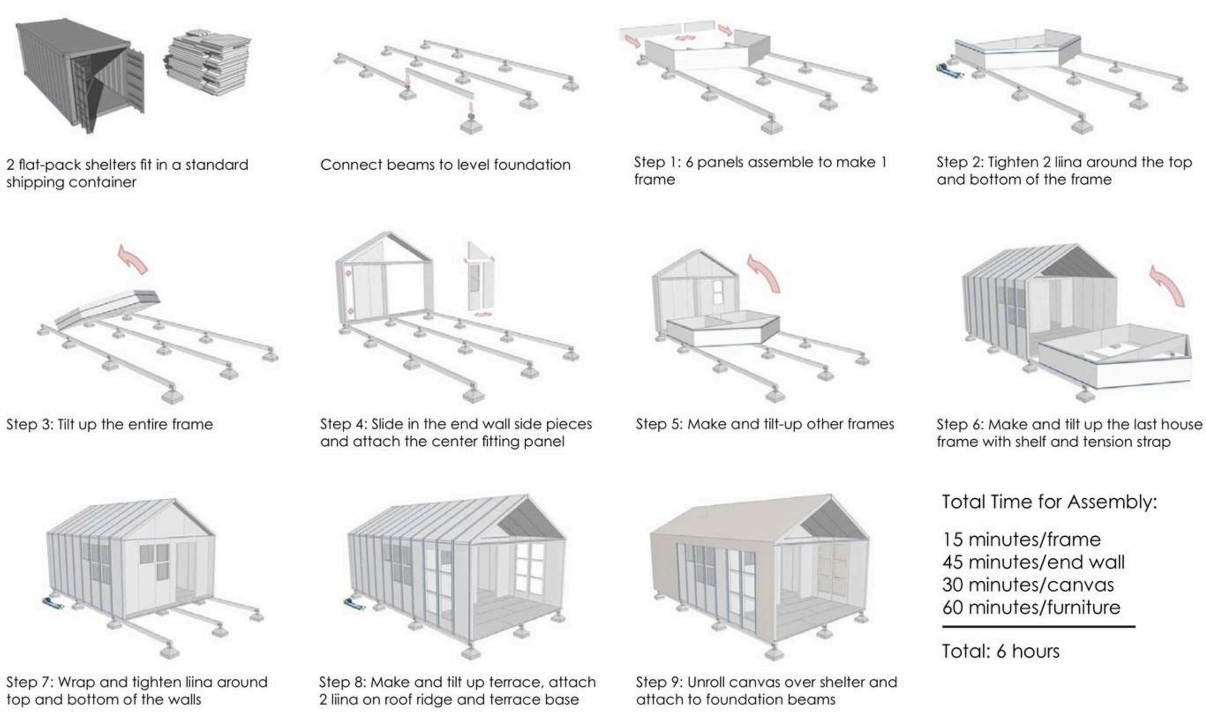

Figure 2.1: Assembly diagram of the shelter, Liina team

The Liina Transitional Shelter's design prioritizes simplicity and **ease of assembly in disaster** zones. It utilizes standard nylon cargo straps and hollow core panels made from LVL frames and birch plywood. These panels are insulated with cellulose fiber and manufactured in dimensions that minimize waste, facilitate easy handling, and efficient shipping. The building assembly starts by creating a five-sided frame using panels connected with dowels. A cargo strap tightens the frame, driving dowels into adjacent panels and compressing gaskets for an airtight seal. The frame is then joined to others, forming parallel sections secured with the same method. A loft and end walls provide stability, and a tarpaulin offers weather protection. Extensive testing ensured the safety and durability of this simple yet unconventional system, leading to minor design refinements (Hudert 2019).

Glænø Stapel: Efficient Timber Shelter with Reciprocal Frames

The Glænø Stapel project (figure 2.2) in Denmark demonstrates a sustainable and innovative approach to agricultural building design. Challenging conventional methods that rely on prefabricated steel or timber trusses, the project utilized **locally sourced**, **lower-quality wood** to create an **optimized timber structure**.

Figure 2.2: Glænø Stapel

With inspiration from **reciprocal frames** (RFs), the design prioritized simplicity and **ease of construction**, employing **reversible connections** and **minimizing** the need for **heavy machinery**. Through meticulous **design iterations**, the **wood quantity** was optimized, resulting in a slender and elegant structure despite the use of lower-grade materials. The Glænø Stapel project demonstrates the feasibility of achieving structurally sound timber shelter using locally sourced, lower-quality wood, highlighting (Hudert 2019).

Timber-Cork Modular: a Lightweight Temporary Housing

(Barreca 2022) proposed a **timber-cork** modular system (figure 2.3) intended for **lightweight temporary housing**, emphasizing **adaptability** and sustainability. The system utilizes a sequence of **modular timber portal frames**, constructed from spruce boards linked by hinges, facilitating the interchangeability of both structural elements and walls. This modular design allows for versatile configurations, catering to **diverse scenarios**.

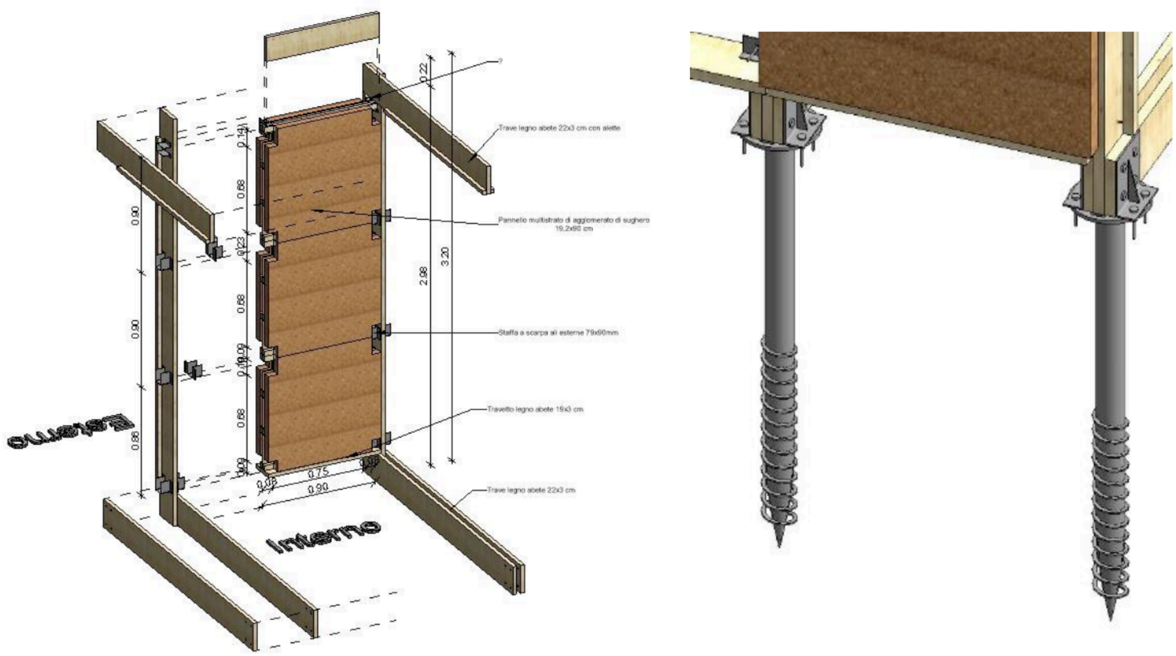

Figure 2.3: Structural design of the basic module, featuring (a) a shear wall and (b) screw foundations.

The structural system uses the platform frame concept, characterized by a lightweight load-bearing framework comprising solid timber uprights and crosspieces, mechanically connected to the internal frame. This design prioritizes **ease of assembly** and **disassembly** while maintaining **structural integrity**.

Haiti's 5-Hour Emergency Shelter: an Open Source Interlocking Solution

Pieter Stoutjesdijk has designed an emergency shelter (figure 2.4) made from **digitally fabricated** components that can be **quickly assembled** in Haiti after the 2010 earthquake. This **cost-effective** design uses **interlocking pieces** (figure 2.5), requiring no additional materials, and can be easily manufactured and distributed. The design promotes **mass customization** and **personalization**. The shelter is adapted to Haiti's tropical climate with an undulating roof for shade and rainwater collection, and large ceilings and windows for ventilation.

Figure 2.4: Haiti's 5-Hour Emergency Shelter, an emergency shelter that assembles in 5 hours

Each component of the shelter features custom joinery, ensuring a precise fit with adjacent pieces. This interlocking design extends to the framework, flooring, roof, and walls, allowing for seamless assembly without additional fasteners (Azzarello 2013).

Figure 2.5: Haiti's 5-Hour Emergency Shelter, each section has a different kind of interlocking part

Table 2.1 outlines the design and optimization objectives identified in the reviewed timber shelters and structures. In addition to the examples mentioned above, other structures as well as Origami Cave by Lava Architects, Minami-Sanriku by Shoichi Haryu Architect & Associates, Pop-up Chapel, and Paper Log House by Shigeru Ban Architects are presented.

	Design and Optimisation Objectives							
Shelter/ Structure	Ease of Transport	Ease or speed of Assembly/ Manufacture	Structural Performance	Local Sourcing	Ease of Disassembly	Material/Cost Efficiency	Adaptability/ Personlisation	Climate-Responsiveness
The Liina Shelter	*	*	*	*				
Glænø Stapel		*	*	*	*	*		
TimberCork Modular	*	*	*		*	*	*	
Haiti's Shelter	*	*				*	*	*
Minami-Sanriku				*				
Origami Cave	*	*		*		*	*	
Pop-up chapel		*						
Paper Log House		*		*	*	*		

Table 2.1: Design and optimization objectives identified in the review of existing timber shelters and structures

This thesis focuses on a case study that explores **structural performance**, **material cost** and **efficiency**, and **local sourcing**. Other objectives, while valuable, are beyond the scope of this research and are recommended for future studies. The following section will discuss timber structures and their optimization methods.

Timber Structure

This chapter aims to address three sub-sections.

First, it examines the specific properties of timber and the limitations associated with it. Second, the chapter explores joinery structure, including its static and dynamic behavior. Finally, it investigates the process of Computer Numerical Control (CNC) on timber shelter production and design. Based on the findings of this section, the respective structural, material, and geometric properties for modeling the case study will be defined.

Timber Properties

"Out of all the natural materials wood has the most balanced characteristics and can be relatively easily worked (Binding, 1975). "

Wood is composed of cellulose and lignin, as shown in (figure 2.6). The cellulose fibers, which are long, provide strength along the grain of the wood, whereas lignin acts as a binder for these fibers, offering shear strength and facilitating the transfer of loads between fibers that are not continuous. In this structure, fiber represents the most robust component (McMullin 2017).

Timber is anisotropic, meaning that it exhibits varying material properties depending on its direction. The properties are strongest along the grain and weakest when measured perpendicular to it. Additionally, timber strength varies significantly by species, which can substantially impact the structural design and calculations. The anisotropic property of timber is dealt with by focusing on the direction of the load(Paul and Jonathan 2017). Timber shows ductile properties when compressed and brittle characteristics under tension and shear, with both failure modes potentially occurring at the same time (van de Kuilen and Sandhaas 2013).

Timber materials are made up of either sawn lumber or engineered (manufactured) wood products. Engineered lumber encompasses materials such as glued laminated timber, structural composite lumber, I-joists, and structural panels (McMullin 2017).

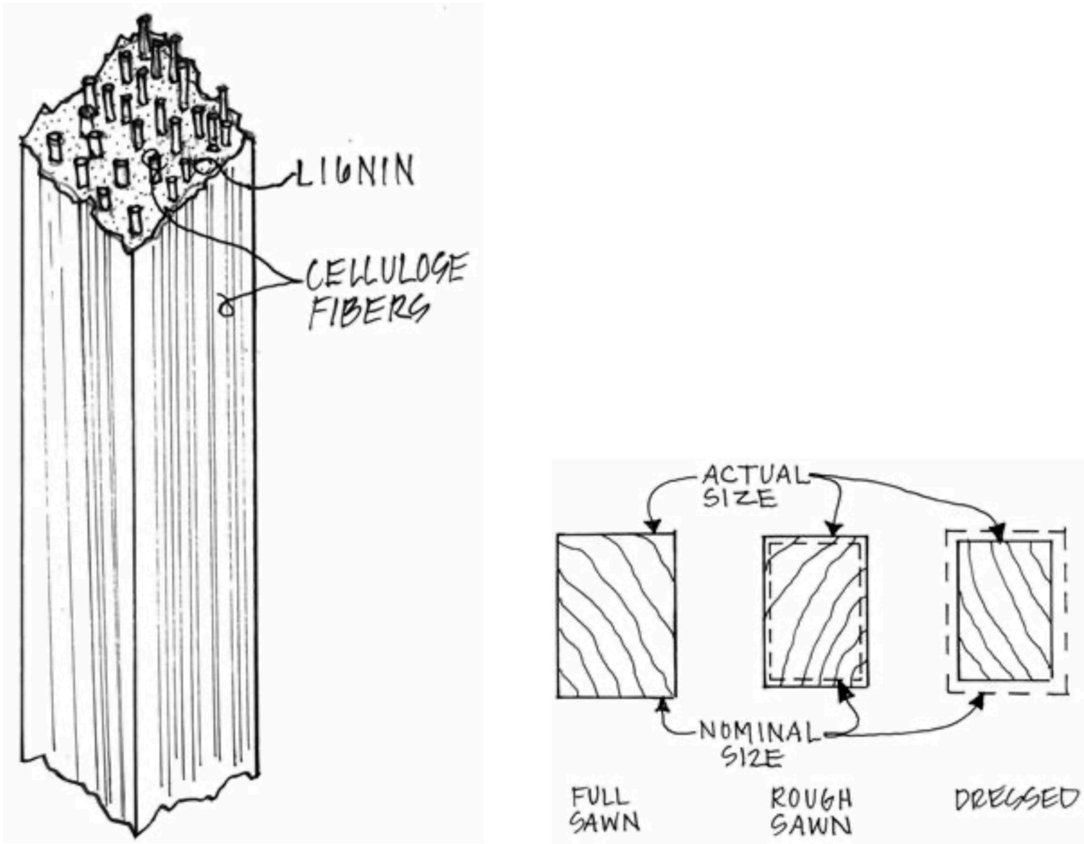

Figure 2.6: a) Conceptual Drawing of timber b) Type of Solid Sawn Lumber

General limitations of timber and Discontinuities

Despite the numerous merits of timber as a building material, it's essential to acknowledge certain structural limitations it poses (Voulpiotis, Köhler et al. 2021). Being a biological material, timber can have considerable defects and physical variations, and is susceptible to disease, infestation, and decay. This limits the predictability of the mechanical behavior of timber, which leads to justifications for the absence of design guidelines specifically related to wood-wood joints. The primary challenges faced by joinery structures include moisture sensitivity, natural defects, fire vulnerability, degradation of connections, and a lack of design guidelines (van Nimwegen and Latteur 2023). All construction materials exhibit some form of imperfections. In the case of timber, typical irregularities include knots, splits, checks, and shakes, as illustrated in figure 2.7. These irregularities are not considered defects but rather discontinuities. The reference design values for timber already consider these characteristics. For instance, heavy timber beams often contain large discontinuities but still maintain substantial overall strength (McMullin 2017).

Figure 2.7: Natural Imperfections of Wood

The stress-strain curve in timber differs based on the type of load and the direction of the load relative to the wood's grain. For bending loads, the stress - strain curve is linear up to the proportional limit, beyond which strain increases at a faster rate than stress until the point of failure, as illustrated in (figure 2.8). In tension along the wood fibers, stress and strain increase linearly until approximately strain of 0.5 to1 percent, followed by sudden failure typically before reaching 2 percent strain, with minimal nonlinear behavior shown in (figure 2.8). Under compression parallel to the grain, stress and strain grow linearly to around strain of 0.5 to 1%, reaching a proportional limit Comparable to the yielding seen in steel, with compression strength gradually decreasing as strain increases, as depicted in (figure 2.8). Compression perpendicular to the grain initially shows a linear increase and then stabilizes at its ultimate capacity without further degradation, as the wood densifies, as shown in Figure x. While timber design generally remains within the linear section of these stress-strain curves, understanding the full curves is useful for gauging potential reserve capacity (McMullin 2017).

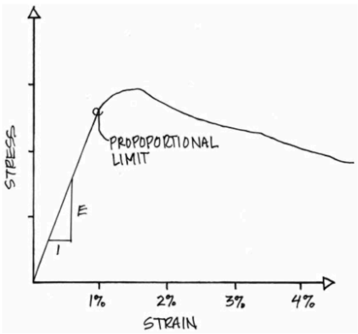

Figure 2.27 Compression parallel to grain stress–strain curve

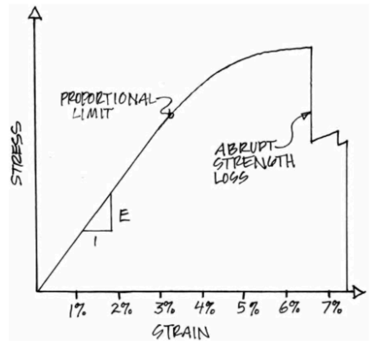

Figure 2.25 Bending stress–strain curve

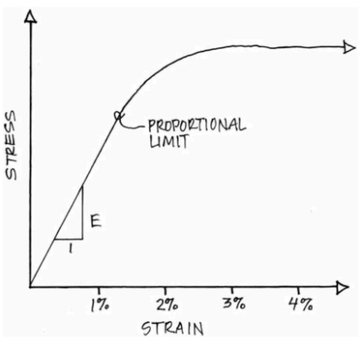

Figure 2.28 Compression perpendicular to grain stress–strain curve

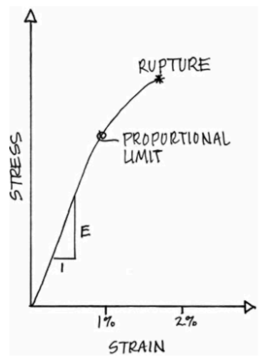

Figure 2.26 Tension stress–strain curve

Figure 2.8: Stress - Strain Curve in Timber in Different Loading Conditions

Timber materials are made up of either sawn lumber or engineered (manufactured) wood products. Solid sawn lumber is produced by milling harvested trees, while engineered wood consists of smaller pieces of wood bonded together with adhesive. Sawn lumber is available in three size categories: full or rough sawn, and dressed, as depicted in (Figure 2.6) Dressed lumber, which is the most commonly used type, is typically what you would purchase at a lumber yard. Engineered wood products offer significantly enhanced strength and stiffness, contributing to the sustainability of timber by enabling the construction of longer spans and taller structures. These products include GLT, structural composite lumber , I-beams, and structural panels, as illustrated in figure. (McMullin 2017).

Timber Systems

The Common timber structure systems can be categorized as (Kolb 2008 ; McMullin 2017):

- log construction
- Timber-frame construction
- Light bearing wall: Balloon and platform frame construction
- Panel construction
- Frame construction
- Solid timber construction

Although each of these systems offers unique benefits, this research utilizes timber frame construction as the structural focus for the case study.

Timber Frame

Timber framing has been in use for over two thousand years. Its development was gradual, as it depended on the availability of tools and the growing skill of laborers to carry out the work. Early timber frames were initially stabilized by burying posts in the ground, but this led to rapid decay. To prevent this, carpenters adapted the structures to stand on stone foundations, making the frames more rigid with diagonal bracing and stronger joinery.

In numerous timber-frame structures, the structural framework that bears the load is left exposed. These types of buildings are common in East Asia (van Nimwegen 2023) ,across Eastern and Central Europe, as well as in England, northern Germany, Denmark, the Netherlands. In colder climates, the timber frames are often arranged in a tight grid of rectangles and squares, with windows seamlessly integrated into this grid. Historically, timber-frame construction developed in areas where wood was scarce enough that it could not be used for solid log construction. This method also accommodates shorter hardwood components. Today, the traditional visible timber-frame is rarely used in new constructions. Modern building materials and methods have replaced the classical timber-frame setups, though carpenters are still familiar with traditional techniques like struts and angle braces. Timber-frame buildings are still cost-effective for certain applications like agricultural or simple utility buildings, now typically with the timber hidden behind cladding. Advances in machine assembly and wood drying technologies have made timber-frame construction a viable economic choice.

Connections in timber-frame construction, such as mortise and tenon and oblique dado joints, are less expensive than those made from preformed metal or steel, particularly as the closely placed timber members bear lower loads. The primary load in timber-frame buildings is transferred directly through the contact points between timber pieces (Kolb 2008). This conclusion shows that Lock n Load should preferably provide an environment that can facilitate the process of design and optimization, effectively integrating all three approaches: analytical, numerical, and experimental.

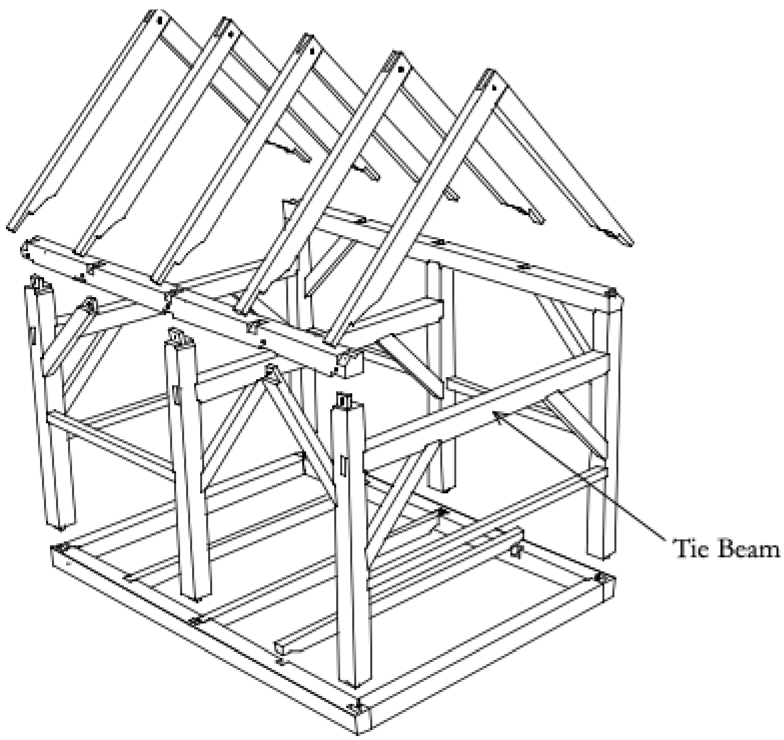

Figure 1-2 American Timber Frame (Redrawn from Sobon and Schroeder, 1984)

Figure 2.9: American Timber Frame

Timber frame walls are integral structural components that utilize a rigid framework of timber sections to transfer loads within both internal and external walls. The bottom plate, also known as the sole plate or sill, forms the base of the timber-frame wall, securing it to the floor construction. It is typically laid on its broader side to optimize support. The placement of the bottom plate varies based on the floor type: resting continuously on concrete slabs or masonry plinths, or at specific points on timber joist floors. Studs, the principal vertical members of the wall, direct structural loads downwards to the foundation. These elements are essential for the framework, sometimes doubled to support greater loads or accompanied by cripple studs to reinforce openings. The spacing of studs typically ranges from 800 to 1200 mm, influenced by the architectural layout and structural requirements. Structural considerations for studs include potential buckling and bending due to lateral forces, with particular attention to the weakening effects at joint connections. Inclined bracing within the wall plane is essential for providing the necessary stiffness in timber-frame structures. These braces transfer horizontal forces, like those from wind, from the top and bottom plates to the foundation. Braces are typically installed in pairs since they are only capable of handling compressive forces, functioning as struts. Rails provide lateral support to sheathing or cladding and are crucial in preventing stud buckling in taller walls. While generally non-structural, rails become necessary around door and window openings where they function as lintels and sills.The top plate and head binder align and stabilize the studs at the upper limits of the wall. The head binder additionally supports the load from upper floors and roof structures, distributing these forces to the studs below. This arrangement is critical for maintaining the integrity and stability of the wall.Timber-frame construction utilizes various joints and fasteners to enhance structural integrity. Halving joints are commonly employed at connections between bottom plates and head binders, while mortise and tenon joints are predominantly used for studs, braces, and rails. Modern construction often supplements traditional wooden pegs with nails, screws, and close-tolerance bolts (Kolb 2008).

Wood joining techniques in timber buildings are shaped by cultural and environmental factors. Joints serve not only a structural role, but also contribute significantly to the architectural expression and embody the conceptual aspects of the timber design (Hudert 2019). Wood construction typically requires joining numerous building components in various ways. Historically, construction methods such as mortise and tenon, dovetail, dowel, split ring, and shear plate joints were employed to connect wooden components. Modern connectors now include nails, bolts, lag screws, truss plates, timber rivets, and engineered metal plate connectors (McMullin 2017). . Despite the advancements in connection technology, traditional joints remain effective and add a unique aesthetic to exposed wood projects (van Nimwegen 2023). This thesis primarily focuses on the **pegged mortise and tenon (PMT)** joinery connection, utilized in the GO case study. This specific connection formed the basis for the development of the tool.

Manufacturing of Timber Structure with Computer Numerical Control Production

In Eastern tradition, a master builder oversaw material selection, construction, and joint design. Conversely, Western cultures developed a divide between design and execution, persisting today. The rise of industrial methods and power tools further marginalized traditional joinery in the West (Hudert 2019). The adaptation of CNC machines for wood required specialized software. Despite challenges, they've become popular due to advancements in technology. They fall into two categories: stationary machines, where the workpiece is secured, and run machines, where the machine positions the workpiece (Tannert 2008). CNC machining uses computers to control tools, which requires coded instructions and G-code is a software programming language used to control a CNC machine. G-code, or geometric code, provides CNC machines with location instructions in a 3D coordinate system (X, Y, Z), along with parameters like speed, angle, and feed rate. M-code, short for machine code, handles non-movement functions, such as program termination. Together, they form the language of CNC machining (Roschlia 2023).

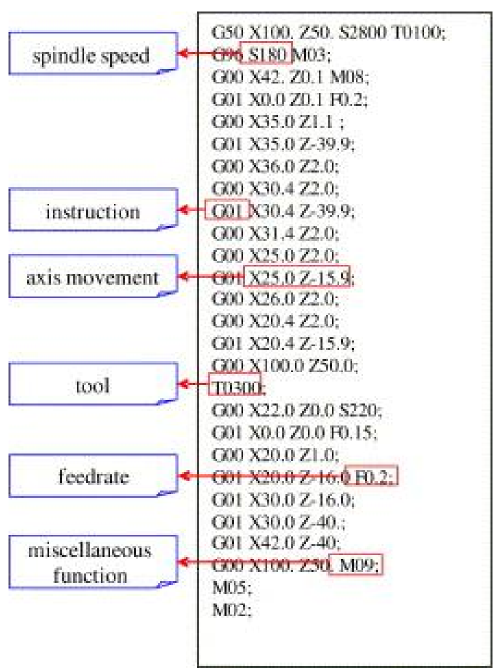

Figure 2.10: Elements in the G-code control formats

However, CNC machines can be programmed using methods beyond G-code, such as STEP-NC, which offers a more integrated and feature-based approach, but G-code remains the dominant language (Shin 2007). In CNC manufacturing, the general sequence is to design a part in CAD software, generate toolpaths and machining instructions in CAM software, and finally, output those instructions as G-code that controls the CNC machine (Lati 2021).

Timber Structure Optimization

Structural optimization involves designing material assemblies to sustain loads in the most effective manner. The goal is to determine the optimal structure that meets specified performance criteria, such as minimal weight, maximum stiffness, or enhanced resistance to buckling. This process necessitates clear definitions of "best" based on the objectives of the structure. Optimization must operate under various constraints, including limits on material quantities, allowable stresses, permissible displacements, and specific geometric configurations, to provide a viable and well-defined solution (Christensen 2008).

The design process should incorporates structural optimization and broader criteria into several main stages:

1. **Function**: Identifies the purpose and essential requirements of the product.
2. **Conceptual Design**: Determines the basic construction type, such as choosing between truss, suspension, or arch designs for a bridge.
3. **Optimization**: Refines the design within the defined constraints to enhance performance, often focusing on the efficiency of material use.
4. **Details**: Addresses market, social, and aesthetic considerations.

These steps ensure that the final product is not only structurally effective but also functional, economically viable, and aesthetically suitable. The traditional approach to the optimization step in design is iterative and intuitive. It involves proposing a design, assessing its compliance with requirements, and revising it as necessary. If a design fails to meet specifications like stress levels or is suboptimal (e.g., too heavy), it is revised and reassessed in a continual loop. This iterative process often employs computer-based methods such as the Finite Element Method (FEM) or Multi-Body Dynamics (MBD) to improve the accuracy and efficiency of design evaluations. However, these methods do not fundamentally change the iterative nature of the process. In contrast, mathematical design optimization takes a systematic approach by formulating a specific mathematical problem where design requirements are constraints, making the process more automatic and less reliant on iterative revisions (Christensen 2008; Haftka 2012) .

Structural optimization problems might appear straightforward to set up but can involve complex elements. They are typically presented as:

Determine the vector χ to minimize the function $f(\chi)$, while ensuring that $g(\chi)$ does not exceed zero.

Here, $f(\chi)$ represents the scalar objective function, χ is a vector with *n* components, and $g(\chi)$ comprises *m* constraint components. Such challenges are known as mathematical programming problems. The formulation simplifies in common presentations to:

$$\text{minimize } f(\chi) \text{ such that } g(\chi)\leq 0$$

or more succinctly:

$$\text{minimize } f(\chi) \mid g(\chi)\leq 0$$

This representation means that each element of the vector $g(\chi)$ must individually satisfy the condition ≤0. Although the notation may vary, the underlying principle remains that minimizing $f(\chi)$ is equivalent to maximizing -ƒ, and $g(\chi)\leq 0$ corresponds to $-g(\chi)\geq 0$. This equivalence is crucial in formulating optimization problems effectively.

Structural optimization problems can be categorized into three main types (figure x) based on the geometric aspects they address: **size**, **shape**, and **topology** optimization.

Size optimization focuses on scenarios where the overall layout of the structure is predefined, but the dimensions of specific components are not fixed figure x.

Shape optimization deals with optimizing the specific contours or forms within a given domain figure x.

Topology optimization extends to determining the number and configuration of voids within a domain, as well as how these voids connect. This form of optimization offers extensive freedom in modifying the structure's topology to meet specific criteria and objectives (Bendsøe 2004; Querin 2017).

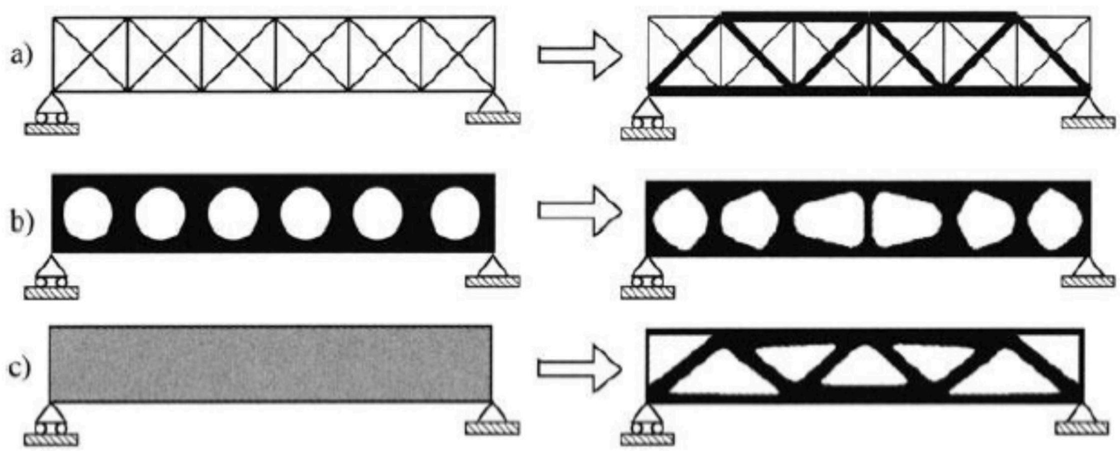

Figure 2.11: a: Size, b: Shape, c: Topology optimization

Various methods and tools are utilized for structural optimizations, with the most commonly employed being Linear Programming, Sequential Linear Programming, Genetic Algorithms, Newton's Method, the Lagrange Multiplier Rule, and Gradient-Based Optimization(Bendsøe 2004; Banichuk 2010).

Literature Review: Analysis, Simulation, and Optimization of Timber Structures

One of the earliest attempts to optimize timber frame structures was made by (Topping1984), who introduced the use of **sequential linear programming** for this purpose. In their study, the design variables include **member cross-sectional properties** and **joint coordinates**, with the objective of **minimizing weight**. (Stanić 2016) presented an **cost optimization** of cross-laminated timber plates with stiffening ribs using enhanced assumed strain **FEM**. This method avoids shear locking in thin plates and meets **Eurocode 5 constraints** on **deflections**, **stresses**, and **eigenfrequency**. **Gradient optimization** yields a cost-efficient timber plate design, demonstrated with numerical examples.

(Pech 2019) developed a new optimization method that considers mechanical property distributions and stress states in wooden boards. After reconstructing knots and determining stiffness, beams are analyzed with an **FEM** to find optimal configurations. To handle complexity, **metaheuristic algorithms** and a **performance-approximating** metamodel were used, **reducing maximum deflection** by **15%–20%** compared to traditional GLT beam production.

(JELUŠIČ 2018) introduced an optimal design approach for timber beams with non-uniform cross-sections using **multiparametric mixed-integer nonlinear programming (MINLP)** along with **response surface optimization (RSO)**. The optimization model incorporates Eurocode specifications and uses FEM to evaluate design performance based on input parameters which contains the **cost objective function**.

(Kravanja 2021) optimized a one-story timber structure with glued laminated timber frames and steel purlins, rails, and façade columns using mixed-integer nonlinear programming. The objective was to **minimize** the **cost of material** while adhering to **Eurocode** standards. The Modified **Outer-Approximation/Equality-Relaxation algorithm** and a **multi-level strategy** were used, resulting in optimal material use and frame configuration.

Some studies specifically concentrate on enhancing timber connections. The design of timber structures heavily relies on the performance of the joints. Joint strength is a key determinant of overall structural strength, while joint stiffness affects the structure's deformation. Furthermore, the size of timber members is often chosen based on the characteristics of the connectors used in the joints (Leichti 2000). The analysis of timber connections is typically done using analytical, experimental, or numerical methods (Fang 2020). Table 2.2 presents the detailing objectives, key findings, and optimization parameters for different types of joints, which were examined through numerical, experimental, and analytical analyses.

Nearly all of the studies summarized in Table 2.2, which performed physical test validations, demonstrated trends consistent with their numerical and analytical simulations. Additionally, various types of loading conditions are presented in this literature review. This diversity ensures that the numerical FEA and analytical models can provide reasonable estimates that are consistent with actual testing under different loading conditions.

Table 2.2: Review of Geometrical optimization of timber Joinery studies with different methods of analysis: Parameters ,Methodologies and Key Findings

	Type of Joint	Objective(s)	Analyzing Method	Optimization parameters	Key Findings
(Hu and Chen 2021)	MT joints	1.Withdrawal load capacity (WRL) 2.Bending load capacity (BLC)	1.FEM) with response surface method 2.Experimental	1 Tenon length(L) 2. Tenon width (W) 3. Tenon thickness(T)	1. L has a greater effect on WRL followed by W. 2. T has a greater effect on BLC followed by L. 3. (w < l < 2w) ratio is recommended
(Eckelman, Erdil et al. 2006)	MT joints	Bending moment capacities (BMC)	Experiment with specimens	1.Diameter(D) 2. Distance from longitudinal axis of tenon to lower edge of stretcher (W), Fs, Fns = BMC 3. Keeping or removing shoulders	1. Close-fitting shoulders greatly increase the strength of the joints 2. The formulas below are obtained: $Fs = 0.934 \times \frac{2w}{D1.66} \times Fns$ 3. When shoulders are contributed, and T is withdrawal strength of the T in tension $FS = 0.894 \times w \times T$
(Wielinga 2023)	Dovetail, arrow and yin yang joints	Yield Strength in tension, shear, compression	FEM (Linear Elastic)	1. Total width wt [mm] 2. Width dovetail head $w1$ [mm] 3. Width dovetail neck $w2$ [mm] 4. Total height ht [mm] 5. Height dovetail $h1$ [mm] 6. Filet radius $fr1$ [mm] 7. Dovetail angle a	1. The contact area has a large impact on the strength of the connection for both tension and shear. 2. The dovetail was optimal in both tension and shear. 3. The dovetail under tension has the most optimal force path 4. A larger width and filet radii lead to higher shear capacity of the dovetail and arrow joint. 5. The yin yang performed the worst under both tension and shear
(Kasal, Smardzewski et al. 2016)	MT joint	1. Stiffness 2. Moment Capacity	FEM (Nonlinear orthotropic)	1. Tenon length(L) 2. Tenon width (W) 3. Tenon thickness(T)	1. Tenon width increases joint stiffness 2. Tenon length boosts moment resistance. 3. Optimal sizes identified for L /T-shaped joints.

(Kaijima, Xuereb Conti et al. 2016)	Topologically Interlocking Joineries	Stiffness	FEM (Orthotropic)	1. Height (HT) 2. Width at the bottom (WB)	1. Adjusting HT and WB significantly improves its stiffness 2. HT has a higher impact on the stiffness
(Kaijima, Xuereb Conti et al. 2015)	Basara Splice and Shihou-Ari Splice	Stiffness in pulling out tension, bending, and self-weight	FEM (Orthotropic)	1.Dovetail angle 2. Dovetail position	1. Dovetail angle for Basara and dovetail position for Shihou-Ari were identified as influential in joint stiffness. 2. Increasing surface friction might be more critical than geometric parameters in improving the stiffness
(Láng and Fodor 2007)	Notched cross-halved joints	Stiffness	FEM (Anisotropic)	1. Gap distance 2. Contacting domain	Configuration of the joint provides added lateral stiffness and stability, which could be beneficial in structures under dynamic loads
(Wilczyński and Warmbier 2003)	MT joints	1. Bending strength 2. Stiffness	Analytical (regression functions)	1. Tenon length(L) 2. Tenon width (W) 3. Tenon thickness(T)	1.The bending strength and stiffness rise as the tenon size increases. 2.The tenon (L) has the greatest impact on joint strength, while the influence of tenon (W) is less significant, and the effect of tenon (T) is minimal. 3. The joint stiffness primarily depends on the tenon (W), with the effects of tenon (L) and (T) being less significant.
(Moradei, Brütting et al. 2018)	Traditional Japanese and Chinese interlocking timber joints	1.Structural Capacity 2. Stiffness	FEM	Cross-sectional Properties	The study highlighted the direct correlation between the geometry of the joint's cross-section with the capacity and stiffness of the member.
(Guan, Kitamori et al. 2008)	Nuki joint	Local failure	1. FEM (nonlinear) 2. Experimental validation	wedge size	In cases where wedges are too large, the resulting contact stresses on the column can surpass the timber's critical stress limit, potentially causing localized damage to the column.

Chapter Conclusion and Discussion

- The review of existing timber shelters reveals a range of optimization objectives. The most frequently observed objective was **ease of assembly**, **manufacturing**, and in some cases, **disassembly**. Working with **available resources** or **tools**, **material** and **cost efficiency** were also common objectives. **Structural Performance** is a crucial goal in designing shelters intended for relatively longer duration of use. In addition, **Adaptability**, **Customization**, and **Climate-Responsiveness** were also mentioned as design objectives in some cases.

  Understanding the design objectives for emergency timber shelters reveals the key areas where Lock n Load can provide support to designers. **To maintain a manageable research scope, Lock n Load will prioritize structural performance, material cost-efficiency, and local sourcing.**

- The review also underscored the significant role of **geometry optimization** in enhancing the **structural performance** of timber structure and connections.

  Consequently, the main variables in the case study were chosen from geometrical variables. This also leads to the conclusion that "Lock n Load" should be able to support **geometrical input** and **output**.

- To ensure accurate structural design in an automated process, "Lock n Load" requires a comprehensive material library encompassing the diverse properties of different timber types. This includes not only **mechanical properties** but also crucial factors like **grading**, **moisture content**, and other **relevant characteristics**. By incorporating this detailed information, designers using "Lock n Load" can effectively **differentiate between various qualities** of timber within the same species, enabling more informed and precise design choices. **The case study should define what properties are critical and necessary**.

- It was observed that **analytical**, **numerical**, and **experimental** methods all demonstrated effectiveness in optimizing timber elements.

This conclusion shows that Lock n Load should preferably provide an environment that can facilitate the process of design and optimization, effectively integrating all three approaches: analytical, numerical, and experimental.

- In the review of optimization studies focused on global structural performance, the primary objectives were typically **weight**, **cost minimization** and **material efficiency**. While **structural performance** often served as a **constraint** in these optimizations, there were also instances where it was the central objective itself.

  Based on this finding, in the case study, weight optimization was adopted as the primary objective function for optimizing the frame structure.

- However, in the optimization of joints, as their nature dictates, the primary objective in all cases was to **enhance structural performance**, such as **strength**, **stiffness**, **ductility**, and **energy dissipation**, through iterative modifications of **geometry variables**.
  Consequently, in the case study, the primary objective of the optimization process was to enhance the load-bearing capacity of the joints.

- The review of simulation and optimization of timber joints highlighted the complexities inherent in designing with wood, particularly in the area of **material modeling**. Additionally, many numerical lead simulation studies in the literature have demonstrated the critical importance of selecting appropriate material models to achieve more realistic simulations.

  In the modeling of the joints in the case study, this conclusion led to special attention being given to the material model for refining and validating the simulation results.

- Most of the literature studies on optimizing joints and timber structures focus on common joints and elements used in **Timber Frame** systems. Therefore, a timber frame can be a good option for a case study, as the existing literature can provide methods and insights for design and optimization.
- To facilitate the automated transition from timber shelter design to CNC fabrication, **"Lock n Load" must have the capability to convert design outputs into G-code**, the

programming language used by CNC machines. The case study should explore how this conversion is achieved.

These findings informed the definition and design of the case study's objectives and the chosen methods for design and optimization.

"By applying appropriate tools and techniques to a good piece of timber, a woodworker's imagination is limited only by the nature of his material- a material that often seems to have a life of its own"

Norwegian Wood: Tradition of Building, Jerri Holan

Case Study

A case study focusing on timber frame construction was conducted to further investigate design and optimization methods for timber structures. Timber frame was selected due to its long history of use and widespread familiarity in many regions globally. Additionally, there exists a substantial body of literature on timber frame design, optimization, and construction, making it a suitable system for a case study aimed at establishing a digital framework for **automation** of design and optimization.

Preliminary Design

The initial step in designing the timber frame involved defining the building's footprint. To facilitate transportation and assembly, a maximum element length of 2 meters was established. Three columns in a row were positioned along both lengths of the building, resulting in a 4 by 2 meter timber frame shelter (figure 3.1).

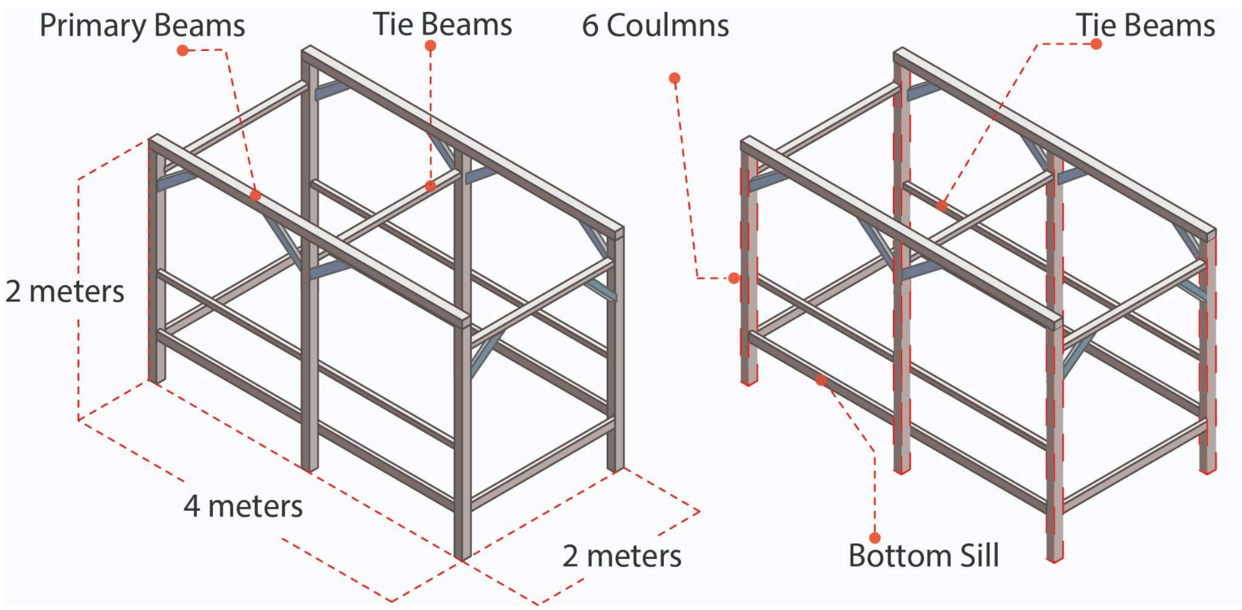

Figure 3.1: Footprint and Overall Shape of the Shelter

The columns serve to support two primary beams that span the length of the building. It's important to note that this represents just one specific configuration for a timber frame system. While this example demonstrates support from two sides, alternative designs exist where the frame could be supported from four sides or other variations, depending on the structural requirements and architectural intent.

Design and Optimization of Timber Frame

This research designs the structure of the timber frame according to Eurocode 5 (EN 1995-1-1), with a focus on optimizing member cross-sectional properties (figure 3.2). The primary goal of the optimization was to reduce the weight of the frames. A Python script was created to perform the iterations, which can be found in the appendix. In this stage, the structure was assumed to be completely rigid.

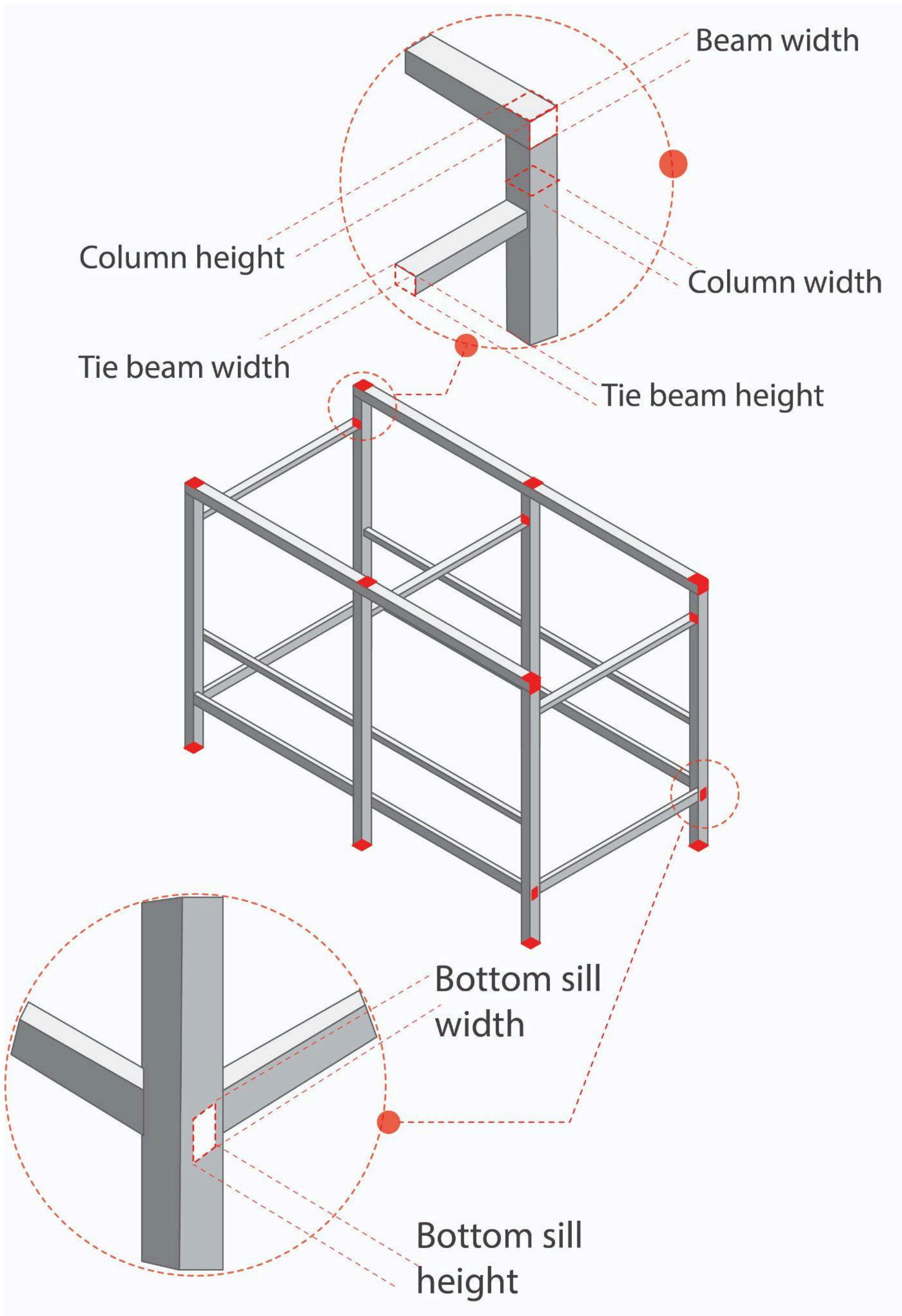

Figure 3.2: Cross-sectional Variables in Optimisation of the Timber Frame

The same cross-sectional properties are used in each iteration for the columns and beams in the frame. For practical purposes, the length of both the columns and beams in the frame has been set to a constant value of 2 meters. The governing load combinations for both ULS and SLS (respectively Equation 3.1, and 3.2) were assumed based on the most demanding load scenarios recommended in (EN 1990 6.4.3.2) for a shelter in the Green Village in Delft, the Netherlands. The more detailed load calculation can be found in the appendix. In this study, weight is used as the primary objective function to simplify the design problem while optimizing timber frames. This simplification helps in formulating the algorithm. The design variables include modifications to the members' cross-sectional dimensions, width (w) and thickness (t). The objective function is subject to both equality and inequality design and dimensioning constraints. In the objective function, C represents the weight of the material, and ρ denotes the density of the timber as detailed in Equation 3.3.

$$\sum_{j\geq 1} \gamma G.j\ .\ Gk.j\ +\ \gamma Q.1.\ Qk.1\ +\ \sum_{j\geq 1} \gamma Q.i\ .\psi 0.i\ .\ Qk.1$$

Equation 3.1: ULS Load Combination

$$\sum_{j\geq 1} Gk.j\ +\ Qk.1\ +\ \sum_{j\geq 1} \psi 0.i\ .\ Qk.i$$

Equation 3.2: SLS Load Combination

$$C\ =\ (t\ .\ w)\ .\ \rho$$

Equation 3.3

The dimensioning equations for the timber frame are established based on formulas from the Eurocode. **For Ultimate Limit State (ULS)** considerations, these equations account for the cross-sectional resistances of columns and beams under **axial compression force**, **bending moment**, **shear force**, and **buckling**. Additionally, for **Serviceability Limit State (SLS)** considerations, the equations address the **deflections** of the beam.

In this design approach, the **compressive stress** for the column ($\sigma_{c,o,d}$) in the timber's rectangular cross-sections must not exceed the design compressive strength ($f_{c,o,d}$), as outlined in Equations 3.4 and 3.5 . Specifically, Equation calculates $\sigma_{c,o,d}$ where N_{ED} is the design axial compressive force and A is the cross-sectional area. The modification factor k_{mod} adjusts for the impact of load duration and moisture content. The term ($f_{c,og}$) refers to the characteristic compressive strength of timber, and y_M is a partial factor accounting for the material properties.

$$\sigma_{c,o,d} \leq f_{c,o,d} \qquad \text{Equation 3.4}$$

$$\frac{N_{ED}}{A} \leq k_{mod} \cdot \frac{f_{c,o,d}}{y_M} \qquad \text{Equation 3.5}$$

The **bending stress** about the y-axis ($\sigma_{m,y,d}$), in the beam should not exceed the design bending strength ($f_{m,y,d}$) as specified in Equations 3.6 and 3.7. In these formulas, ($M_{y,ED}$) represents the bending moment around the y-axis, w_y denotes the section modulus about the y-axis, and $f_{m,g,k}$ is the characteristic bending strength of the swan timber.

$$\sigma_{m,y,d} \leq f_{m,y,d} \qquad \text{Equation 3.6}$$

$$\frac{M_{y,ED}}{w_y} \leq K_{mod} \cdot \frac{f_{m,g,k}}{y_M} \qquad \text{Equation 3.7}$$

The design **shear stress** for the beam, τ_d, must be less than or equal to the design shear strength, $f_{v,d}$ as outlined in Equations 3.8 and 3.9. In these equations, v_{ED} is the design shear force, while b and h represent the width and height (depth) of the cross-section, respectively. The term $f_{v,g,k}$ refers to the characteristic shear strength of timber, and k_{cr} is a factor that accounts for the potential cracking of the timber.

$$\tau_d \leq f_{v,d} \qquad \text{Equation 3.8}$$

$$\frac{3}{2} \cdot \frac{v_{ED}}{b_{ef.h}} \leq k_{mod} \cdot \frac{f_{v,g,k}}{y_M} \qquad \text{Equation 3.9}$$

$$b_{ef} = k_{cr} \cdot b \qquad \text{Equation 3.10}$$

Columns of the timber frame are evaluated for **compressive** and **buckling resistance**. This assessment occurs in two contexts: for buckling about the y-axis, which is within the plane of the frame, and for buckling about the z-axis. These checks are detailed in the respective equations 3.11 to 3.16 provided in the documentation.

$$\sigma_{c,o,d} \leq k_c \cdot f_{c,o,d}$$ *Equation 3.11*

$$\frac{N_{ED}}{A} \leq k_c \cdot k_{mod} \cdot \frac{f_{c,o,g,k}}{y_M}$$ *Equation 3.12*

$$k_c = \frac{1}{k+\sqrt{k^2 - \lambda_{rel}^2}}$$ *Equation 3.13*

$$k = 0.5.[1 + \beta_c(\lambda_{rel} - 0.3) + \lambda_{rel}^2]$$ *Equation 3.14*

$$\lambda_{rel} = \frac{\lambda}{\pi} \cdot \sqrt{\frac{f_{c,o,g,k}}{E_{o,g,05}}}$$ *Equation 3.15*

$$\lambda = \frac{L_{ef}}{i}$$ *Equation 3.16*

For **SLS design** in timber framing, various deformations of the beam are considered:

- w_c is the precamber.
- w_{inst} is the instantaneous deformation.
- w_{creep} is the creep deformation.
- w_{fin} is the final deformation: $w_{inst} + w_{creep}$.
- $w_{net.fin}$ is the net final deformation: $w_{inst} + w_{creep} - w_c$.

According to EN 1995-1-1, for a fixed beam, there are recommended limits for these deformations. These limits specify the maximum allowable deformations that should not be exceeded to ensure the structural integrity and functionality of the beam over time.

w_{inst}	$w_{net.fin}$	w_{fin}
L/300 to L/500	L/250 to L/350	L/150 to L/300

Creep, or the gradual deformation of a material under constant stress, is another consideration when designing timber structures. Eurocode 5 provides a framework to account for this time-dependent behavior.

The additional deformation caused by the permanent weight of the structure (dead load) is calculated as:

$$w_{creep,g} = w_{inst,g} \cdot k_{def}$$ *Equation 3.16*

For leading variable action the creep deformation is:

$$w_{creep,lead} = w_{inst,lead} \cdot k_{def} \cdot \psi_{Lead}$$ *Equation 3.17*

For accompany variable action, the calculation is similar:

$$w_{creep,acmp} = w_{inst,acmp} \cdot k_{def} \cdot \psi_{acmp}$$ *Equation 3.18*

Finally the final deformation is calculated by :

$$w_{fin} = w_{inst} + w_{creep,g} + w_{creep,lead} + w_{creep,acmp}$$ *Equation 3.19*

The results of frame cross-sectional optimisation

Three predominant wood species commonly found in the Netherlands and other parts of Western Europe were utilized in the optimization and design process: **DouglasFir, European Spruce, European Larch**. Table 3.1 shows the material properties of three species used in the cross-sectional optimization. The timber elements were optimized by iterating through a range of cross-sectional dimensions, with widths of 95, 100, 115, 125, 138, 150, and 175 mm, and thicknesses of 100, 110, 115, 120, 125, 130, 135, 140, 145, 150, 155, 160, and 165 mm.

Table 3.1: Material Properties of three species used in the Cross-Sectional Optimisation

	Douglas fir	European spruce	European Larch
y_M	1.3	1.3	1.3
ρ (Kg/m3)	550	440	610
$f_{m,g,k}$ (N/mm3)	86	63	91
$f_{v,g,k}$ (N/mm3)	8.2	5.3	9
$f_{c,o,d}$ (N/mm3)	42	35	45
E (kN/mm3)	12.17	9.7	11.2

The results (Figure 3.3, 3.4, 3.5, appendix) indicates that for most "Unacceptable" cross sections, the Serviceability Limit State (SLS) was governing failure criteria, indicating that deflections exceeded allowable limits, potentially leading to serviceability issues such as excessive sagging. Bending utilization emerged as another critical factor leading to design failure, also marked as "Unacceptable." This indicates that the selected sections were insufficient to bear the applied loads, necessitating resizing or reinforcement. Both factors were optimized by increasing the beam's thickness. As the beam and column thicknesses were kept equal in each iteration, the column never reached its failure point and, therefore, did not govern the structure's dimensions. The similarity in cross-sectional dimensions for columns and beams reduces the likelihood of buckling or compression strength surpassing acceptable limits. Table 3.2 presents the most optimal cross-sections in terms of weight that meet the structural requirements outlined in Eurocode 5. While Larch was stronger, Douglas Fir offered comparable strength with smaller dimensions, due to its lower density and resulting lighter weight, which reduced the overall load on the shelter. Spruce, although requiring a slightly larger cross-section, still maintained a lower weight due to its lower density compared to the other two options.

Table 3.2: The Optimal Dimensions and their Corresponding Utilization Factors and Weight

Species	Weight (kg)	Width (mm)	Thickness (mm)	Bending Utilisation (%)	Shear Utilisation (%)	SLS Utilisation (%)	Compression Utilisation (%)	Buckling Utilisation Y (%)	Buckling Utilisation Z (%)	Final Utilisation factor (%)
DouglasFir[1]	**12.54**	95	120	37.94%	23.88%	97.23%	4.18%	5.10%	7.22%	97.23%
Spruce[2]	**10.87**	95	130	44.13%	34.10%	95.95%	4.63%	5.28%	8.29%	95.95%
Larch[3]	**14.49**	95	125	33.05%	20.88%	93.47%	3.75%	4.79%	7.35%	93.47%

As illustrated in (Figure 3.3, 3.4, 3.5, appendix), varying the width-to-thickness ratio of timber elements can greatly enhance the structural performance of timber frame components. Therefore, identifying the optimal width-to-thickness ratio could be a valuable area for further optimization. The cross sections mentioned in the table 3.2 will be utilized in the next chapter to design the optimal timber joints.

[1] Pseudotsuga Menziesii
[2] European or Norway Spruce (Picea abies)
[3] European Larch (Picea abies)

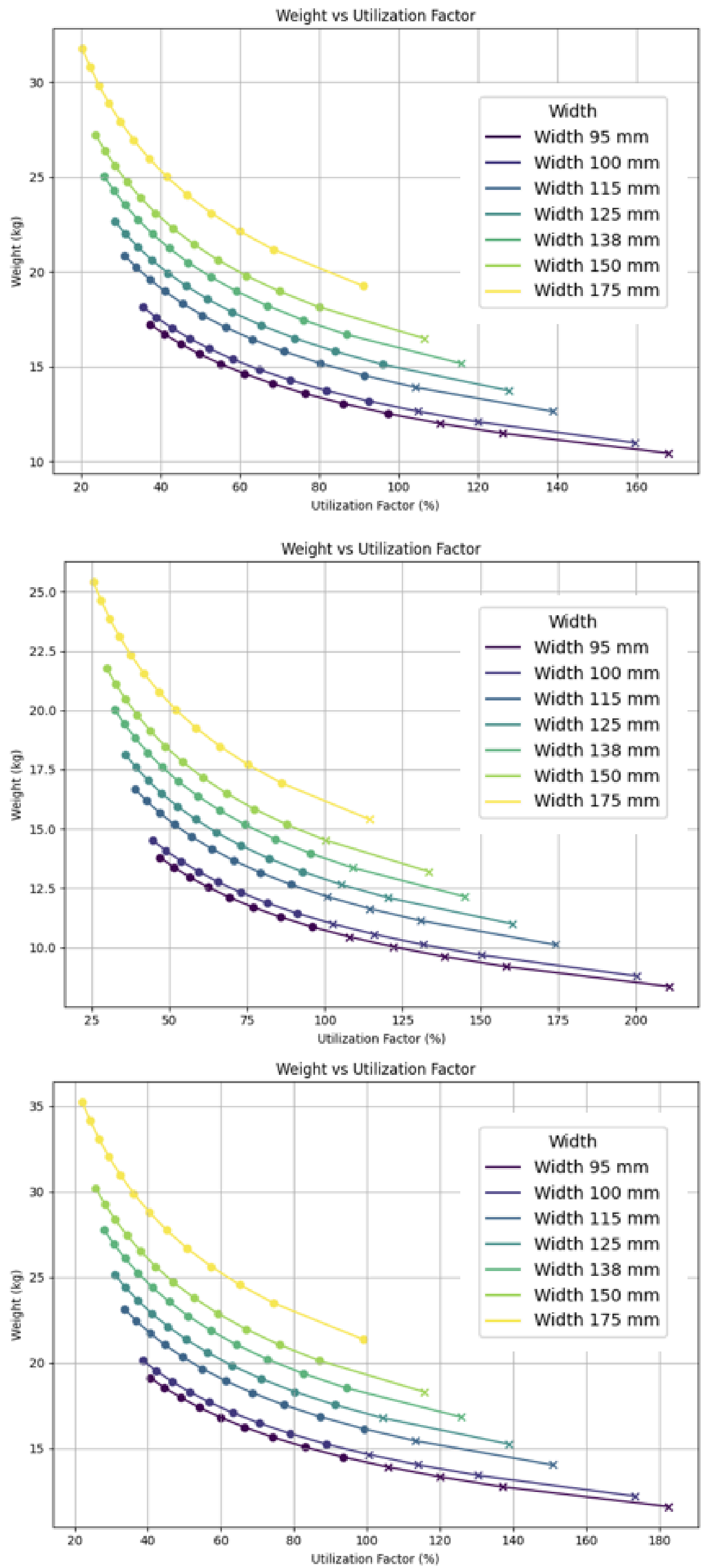

Figure 3.3: Weight to Utilization Factor, from top to bottom, Douglas Fir, Spruce, Larch

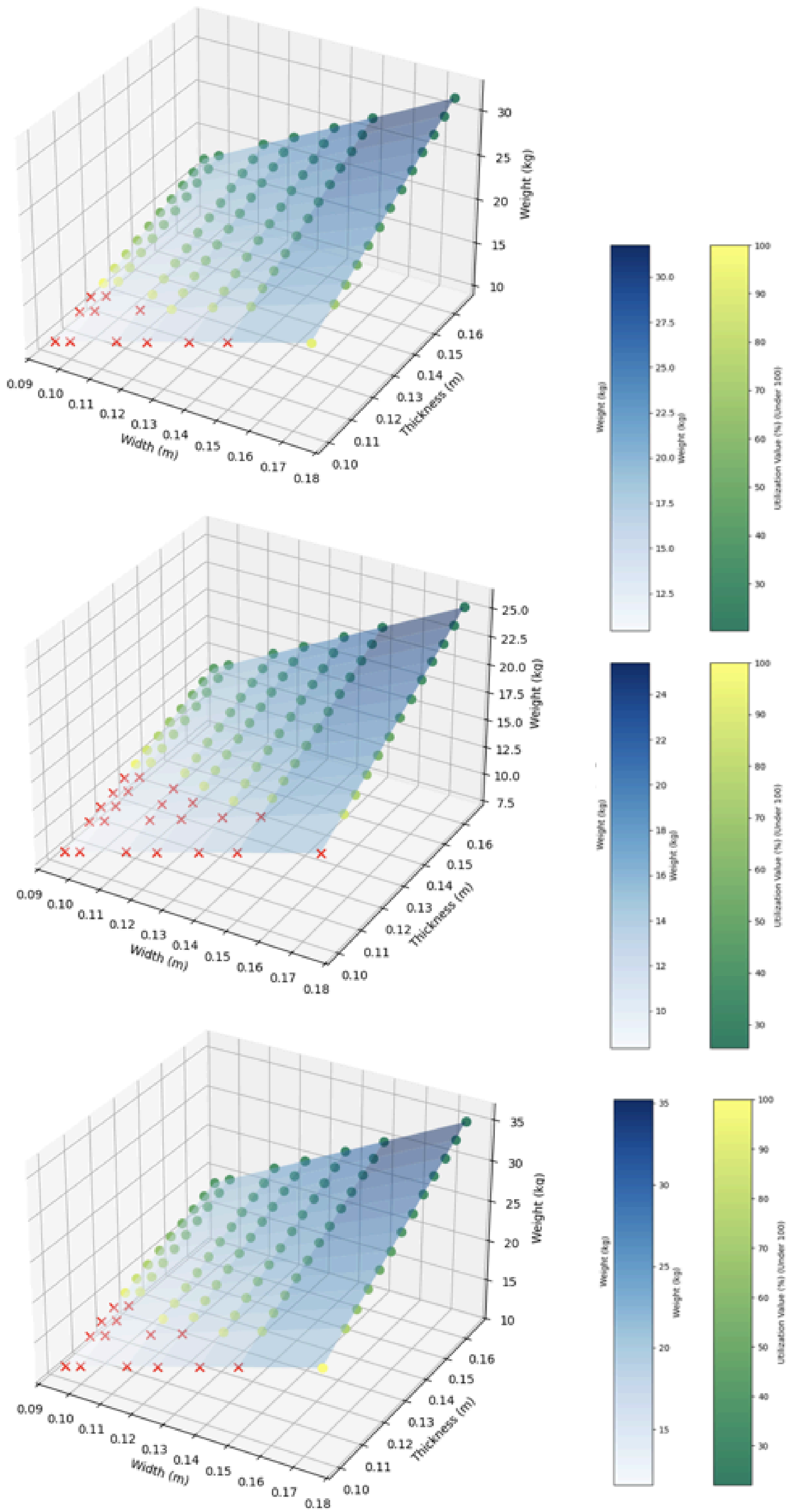

Figure 3.4: Dimensions, Weight, Utilization Factor, from top to bottom, Douglas Fir, Spruce, Larch

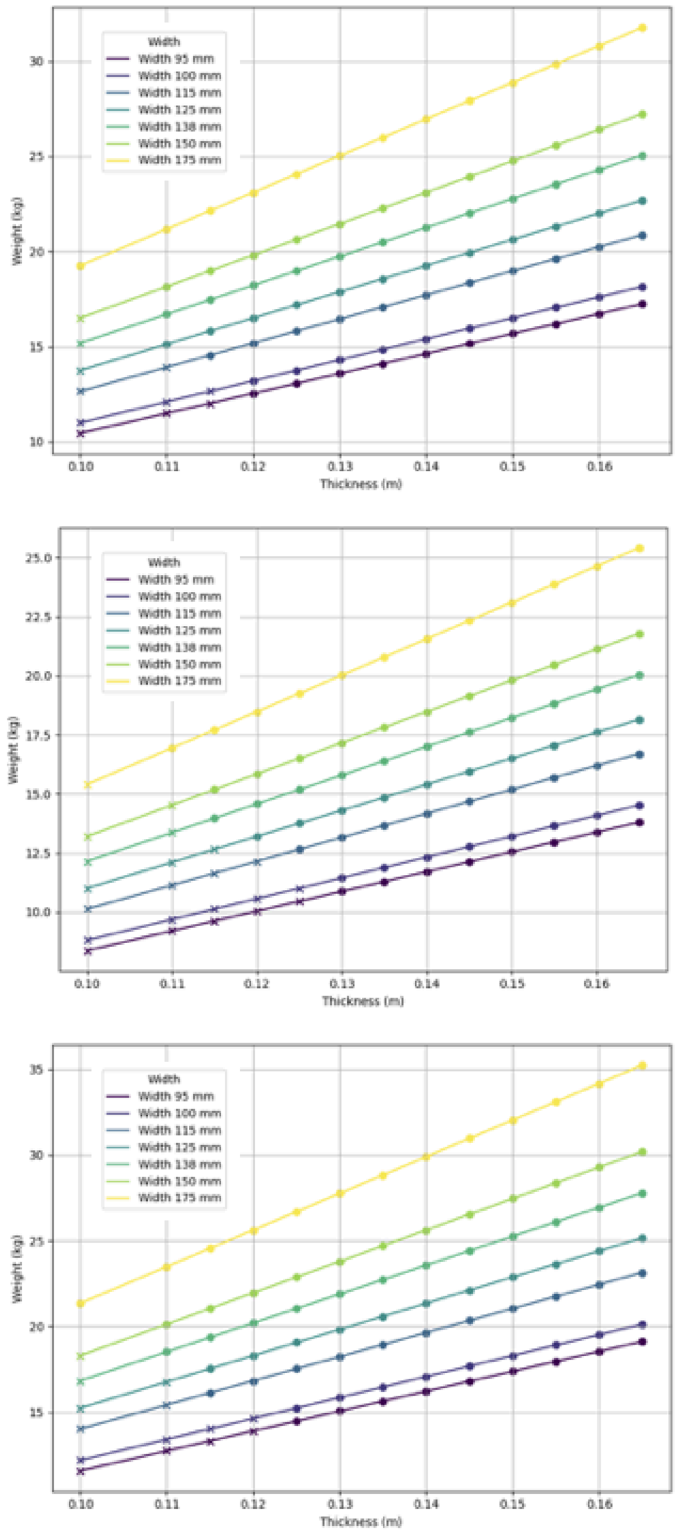

Figure 3.5: Dimensions, Weight, Unacceptable Utilization is shown by cross mark, from top to bottom, Douglas Fir, Spruce, Larch

Design and Optimization of the connections

Timber framing involves the use of large, widely spaced timbers that are connected with all-wood joints. In timber frame design in order to withstand Unprecedented events,such as seismic events, ductility is a key factor in determining performance. This is especially true for the connections within the frame. Ductility allows a structure to exhibit nonlinear behavior, preventing sudden failures. In timber frames, ductile joints enable the structure to yield without collapsing, redistributing forces within the frame to enhance its resilience during such events (Schmidt 1999; Schmidt and Miller 2004). The timber frame system analyzed in this case study required four types of joints: **Pegged Mortise and Tenon joints**, **Scarf joints**, **Gooseneck joints**, and blind mortise and tenon joints (Figure 3.6). Two of these joint types (Pegged Mortise and Tenon and Scarf Joint) were optimized.

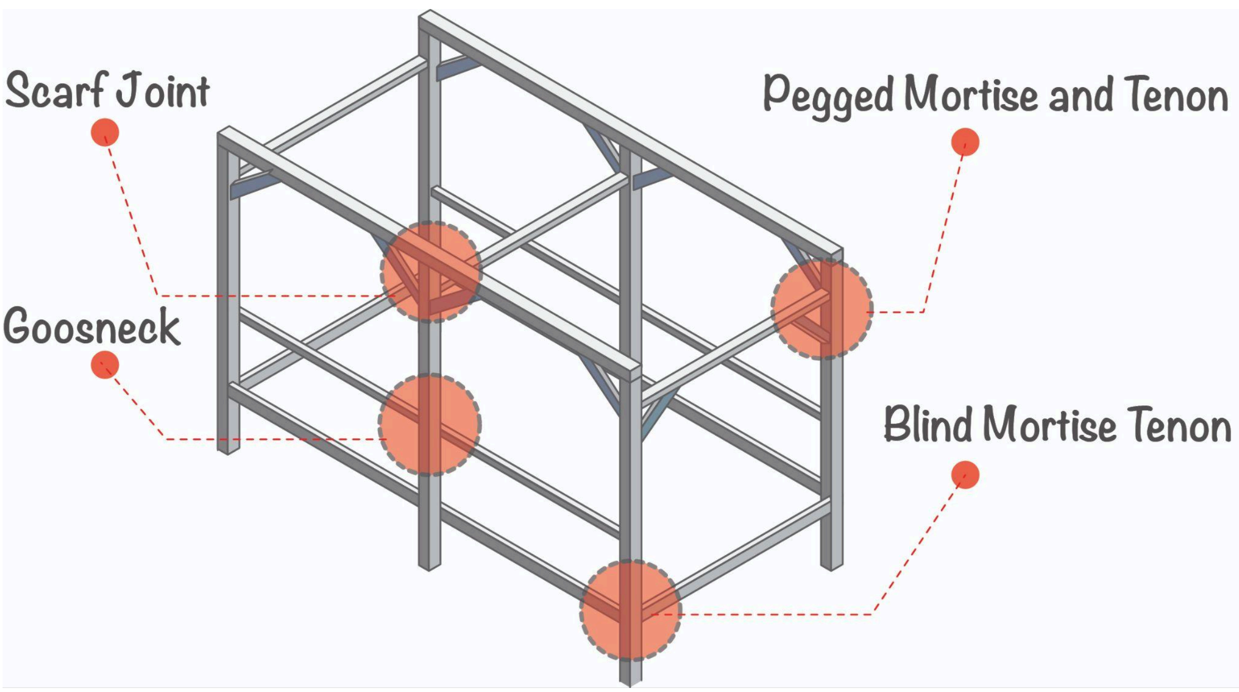

Figure 3.6: The Position and type of Joints in the timber structure

Pegged Mortise and Tenon (PMT)

The PMT method is one of the oldest construction techniques, dating back to ancient times (Benson 1997). In timber-frame construction, pegs secure the tenon inside the mortise which provides a semi-rigid connection between frame members. A common use of the mortise and tenon connection is to join a beam to a post in a heavy timber structure, (as shown in figure 3.7) (Schmidt 1997).

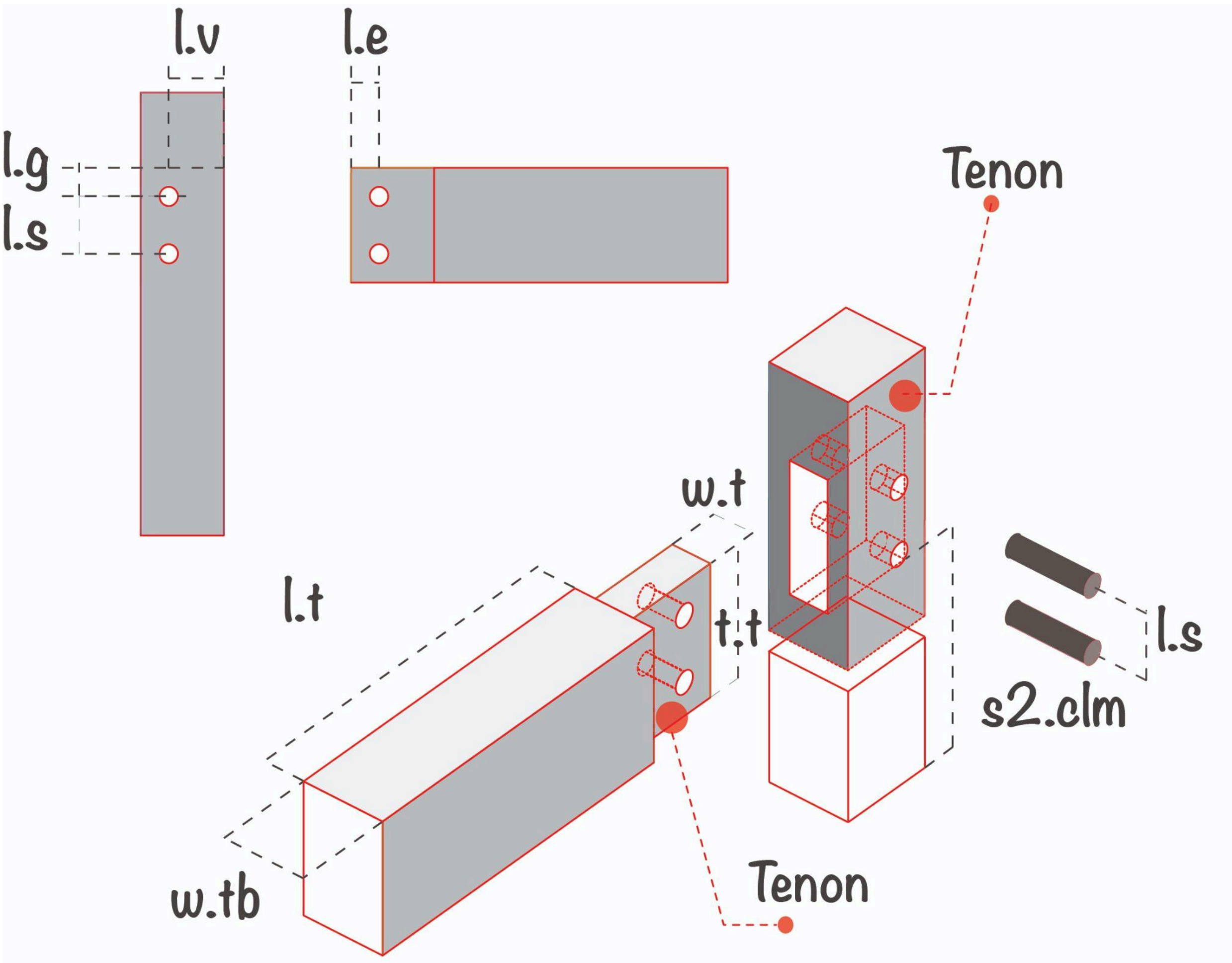

Figure 3.7: A drawing of Pegged Mortise and Tenon with Dimensional Details

Standard mortise and tenon joints are capable of effectively transmitting shear and compressive forces from the beam to the post through direct wood-to-wood contact. However, under wind loads or other similar conditions, the joint may be subjected to tensile forces that try to pull the tenon out of the mortise. In such cases, the connection forces must be transferred between the mortise and tenon using wooden pegs (Schmidt and Miller 2004). Peg sizes and wood species are similar between the United States, United Kingdom, and Asian timber framing practices. However, in Japan, square pegs are more commonly used instead of round ones (Brown 1995). The overall strength of the connection depends on various factors, including the bending and shear strengths of the peg, as well as the dowel bearing strength of the peg within the frame (Schmidt 1999). Peg failure is the preferred failure mode due to the ductility it displayed before reaching ultimate failure. By prioritizing peg failures, joints can be repaired after extreme loading events simply by replacing the damaged pegs (Schmidt and Miller 2004).

Figure 3.8: A Pegged Mortise and Tenon joint connecting a Beam to a Post

K. W. Johansen proposed a yield model in 1949 to predict the capacity of symmetrical steel-dowelled timber connections, considering various potential failure modes such as bearing failure and dowel moment yielding. H. J. Larsen expanded this model in 1973 to include additional failure modes for single and double shear connections. This method forms the foundation of the NDS (AFPA, 1991), European Yield Model (EYM) and underpins design codes such as (BS EN 1996-1 2004a) and (BS 5268 2002). However, steel-dowelled connections differ significantly from timber-pegged connections, making Johansen's bearing failure modes inapplicable to traditional timber joints. This is due to the similar bearing stiffness between the pegs and the connection material, as well as differences in the shear-to-bending stiffness ratio between timber pegs and steel dowels (Shanks, J. and P. Walker 2009). The analytical method for pegged mortise-and-tenon joints in (Schmidt and Mackay 1997) applies the European Yield Model, focusing on failure modes under tension load . MacKay tested typical U.S. carpentry connections and introduced additional yield modes specific to U.S. timber-pegged connections, which also account for tenon relish failure. (Schmidt and MacKay 1997) identified a third failure mode in joints. Two failures were mode Vd, and one was a single flexural hinge (IIIs), forming at the dowel's center due to localized crushing in the mortise member, allowing the dowel to rotate. The (Schmidt 1999)'s study found that Mode IV failure is not applicable to timber frame joints, and Mode IIIs, which happens in joints with thin side members like metallic plates, is unlikely in MT connections due to the significant localized crushing required in the mortise member. Their review identified five potential failure modes in traditional timber frame construction. Modes Im and Is are the two currently recognized in the NDS for timber frame joints. Three additional modes include peg bearing failure (mode Id), shear and bending failure (mode Vd) in pegs, and peg bending failure with a one flexural hinge. Mode Vd is mainly a shear failure, with fractures near ultimate loads caused by bending. Figure 3.9 illustrates five failure modes for timber frame joints under tension.

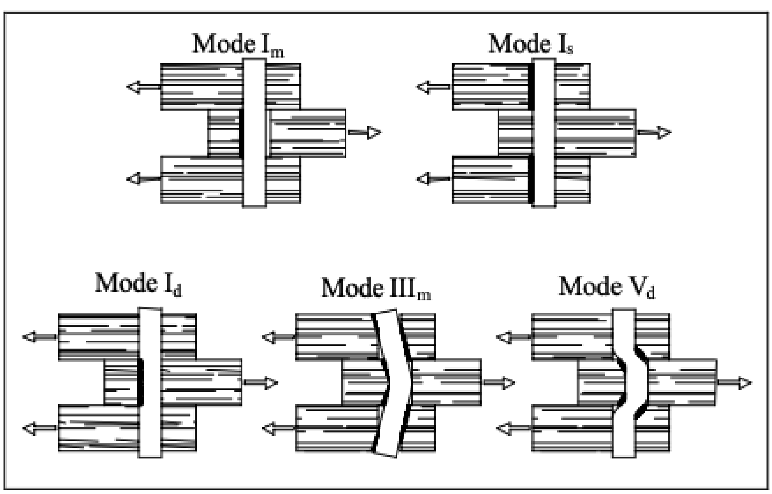

Figure 3.9: Proposed Failure Modes by Schmidt

(Shanks and Walker 2009) expanded the analytical model for pegged mortise-and-tenon tension joints by incorporating the elasto-plastic behavior and energy dissipation of the peg. However, Shanks' model did not incorporate the tenon relish failure mode introduced by Schmidt, as this failure mode has not been observed in tests on U.K. connections. The connection capacities proposed by U.S. research are not directly applicable to U.K. , as U.S. timber joints are often made from wood with low bearing strength and use relatively stiff oak pegs.

Detailing Requirements and equation for PMT

The preferred failure mode in most design situations is the failure of the fastener, rather than the timber. The NDS outlines minimum detailing requirements to ensure this preference. Similarly, tests on MT joints with wooden dowels have shown that they can be ductile when proper spacing, end distance, and edge distance are maintained (Schmidt 1999). The goal of the minimum spacing requirements is to ensure localized failure of connection inside or around the fastener. This is favored over the failure of the base material, such as mortise splitting or tension failure in the tenon relish, which results in a sudden, brittle collapse, causing structural unserviceability and making repairs challenging. Previous tests (Kessel 1990; Kessel 1996; Schmidt 1997; Schmidt 1999; Schmidt and Miller 2004; Shanks and Walker 2009) have shown that peg failure can exhibit some ductility before losing load-carrying capacity. The minimum spacing requirements for pegged and bolted connections are determined by the joint configuration, bolt diameter, material breadth, and fastener aspect ratio, which impacts the connection's mechanics.

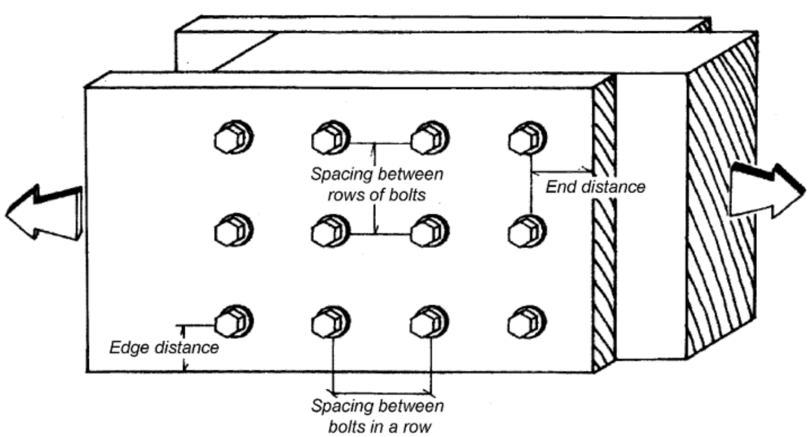

Figure 3.10: Drawing shows spacing dimensions around the bolts

In the absence of comprehensive guidelines for wood-wood connections in building codes, one viable approach for determining appropriate spacing and peg geometry involves employing the concept of an equivalent steel bolt. This method entails analyzing the wood connection by drawing parallels to a steel bolt connection.(Schmidt and MacKay 1997; Schmidt 1999) developed an analytical model (figure 3.11) for determining spacing requirements for timber frame joints using wooden pegs, based on the concept of an equivalent steel bolt. They reported that a comparison between experimental and analytical work demonstrates that specifying minimum end, edge, and spacing distance for pegs ensures that a brittle failure of the connected members will not happen before significant deformation of the joint after yield. However, the end and edge distances calculated with this equivalent steel bolt method tend to be more conservative compared to the minimum values observed in physical tests. The proposed design process is as follows: the designer first establishes the required load capacity for the joint. Then, the size and number of pegs needed to support this load are calculated using the five failure modes and a safety factor. The strength of a single peg is then substituted into the four EYM equations for double shear connections with a steel bolt. The largest diameter from the EYM equations is used as the equivalent steel bolt for the joint design (Equation 3.19). In pegged mortise and tenon joints, if the tenon plug experiences shear failure (also known as relish failure), the joint will fail suddenly and without warning. To prevent this type of brittle failure, it's crucial to maintain a minimum distance between the edge of the wood and the peg. This ensures that the surrounding wood material fails first, forming "yield hinges" in the pegs. This type of failure is more gradual and predictable, allowing the joint to deform before it completely break(Shanks, Chang et al. 2008)

Mode I_m
$$Z = \frac{D\, t_m\, F_{em}}{4K_{\theta}}$$

Mode I_s
$$Z = \frac{D\, t_s\, F_{es}}{2K_{\theta}}$$

Mode III_s
$$Z = \frac{k_3\, D\, t_s\, F_{em}}{1.6\, K_{\theta}\left(2 + R_e\right)}$$

Mode IV
$$Z = \frac{D^2}{1.6\, K_{\theta}} \sqrt{\frac{2\, F_{em}\, F_{es}}{3(1 + R_e)}}$$

Equation 3.19, Z represents capacity of Steel Bolt in tension and D is the diameter of the bolt

The capacity of a timber frame joint in double shear is determined by the lowest value among three different equations. This model categorizes bearing failure into three categories according to material strength under steel load. Two modes consider the strength of tenon and peg, while the third focuses on the mortise. Additionally, another mode is calculated by the shear span-to-diameter ratio of peg and mortise or tenon.

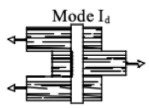

$$P_{Im} = \frac{n\,D\,t_m\,F_{ed}}{2.0} \qquad (4\text{-}6)$$

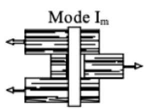

$$P_{Im} = \frac{n\,D\,t_m\,F_{em}}{2.0} \qquad (4\text{-}7)$$

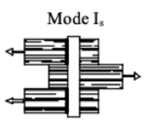

$$P_{Is} = \frac{2\,n\,D\,t_s\,F_{es}}{2.0} \qquad (4\text{-}8)$$

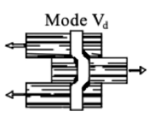

$$P_{Vd} = \frac{2\,n\,A_d\,\tau_c}{2.0} = \frac{n\,\pi\,D^2\,\tau_c}{4} \qquad (4\text{-}9)$$

n = number of fasteners
D = diameter of fastener
F_{ed} = peg dowel bearing strength
F_{em} = tenon dowel bearing strength
F_{es} = mortise dowel bearing strength
t_m = thickness of tenon,
t_s = thickness of mortise cheeks
A_d = area of the dowel
τ_c = shear capacity of the dowel

Figure 3.11: Equivalent Steel Bolt Method

Geometry Optimisation of PMT Joints Using Equivalent Steel Bolt Method

A Python script (Appendix), utilizing the equivalent steel bolt method, was developed to determine the peg diameter yielding the highest tension capacity while adhering to spacing constraints. The script generates edging, end, spacing, and perpendicular-to-grain edge distances, providing essential data for the spacing requirements and geometry configuration of a PMT joint. Spacing requirements for Douglas Fir timber were sourced from (Schmidt 1999). However, due to the absence of a specific factor for edge distance perpendicular to the grain, the NDS value of 1.5 was adopted. The cross-section dimensions were aligned with the results from the frame cross-sectional optimization for Douglas Fir conducted in the previous section. The minimum required load capacity was derived from the load calculations presented earlier (Appendix). The iteration steps range from 12.5 millimeters to 25 millimeters, with each step incrementing by approximately 5 millimeters. Traditionally, the tenon thickness to mortise thickness ratio is 1/3 to prevent weakening of the mortised stock. This study, however, examines this ratio using the equivalent steel bolt method to determine the optimal ratio for maximum capacity. Ten diameter values and ten thickness ratios ranging from 1/8 to 12/8 were used for the thickness ratio optimization iteration process.

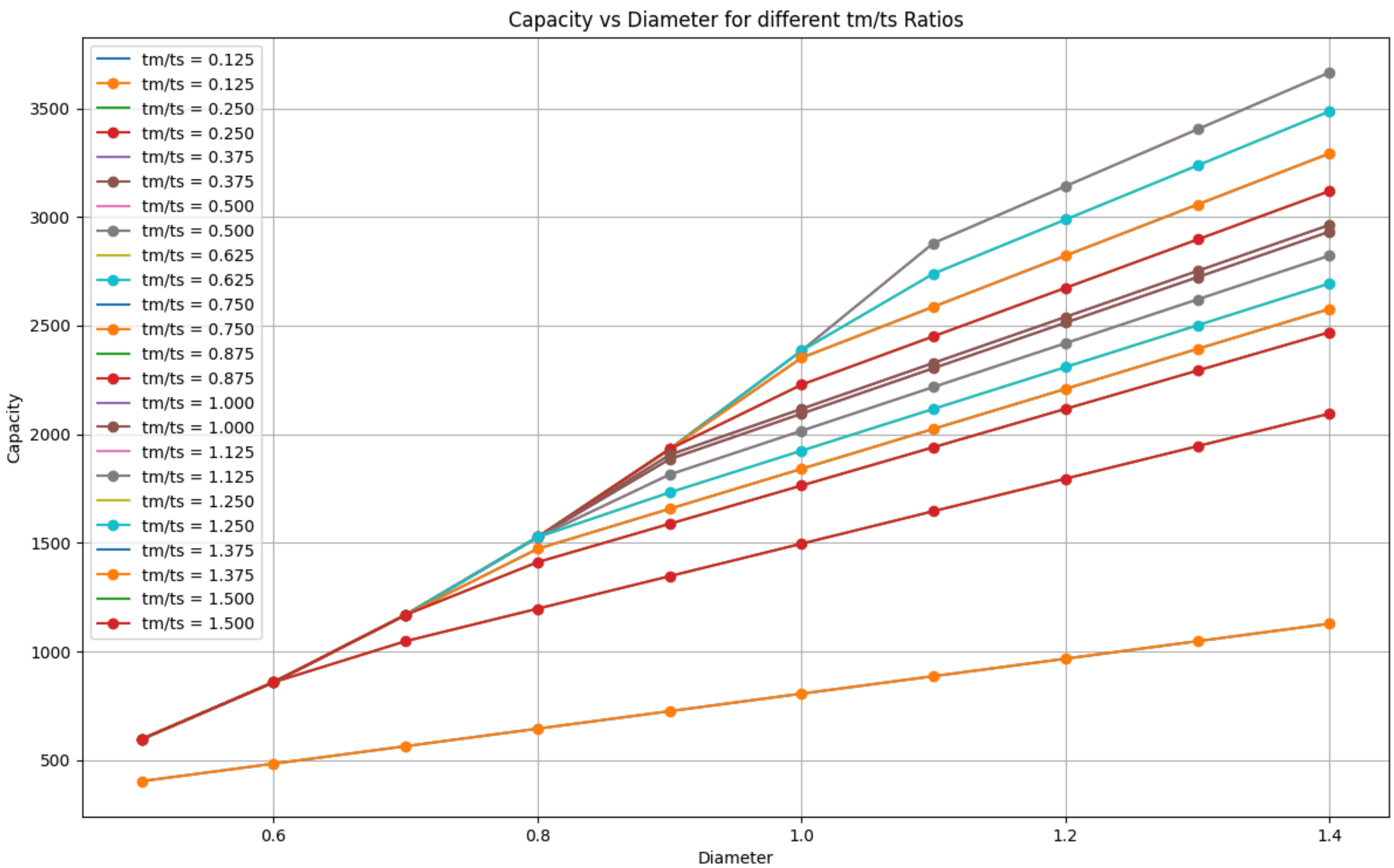

Figure 3.12: The tenon to mortise thickness Ratio compared to capacity

Based on the graph represented in figure 3.12, a tm/ts ratio of approximately 0.5 appears to be optimal for maximizing capacity across different diameter ranges. At this ratio, the capacity curves for different diameters tend to be closer together and higher overall compared to lower ratios. While higher ratios might show slightly better capacity for some specific diameter ranges, a ratio of 0.5 seems to provide a good balance of strength and efficiency across a wider range of peg sizes. While the results align with traditional rules of thumb regarding the tenon-to-mortise thickness ratio, it's crucial to remember that tension might not be the primary concern in tenon design.

Bending and shear failures can govern tenon performance. Therefore, further analysis considering these failure modes is necessary to determine the optimal tm/ts ratio for overall joint strength and stability. Therefore, further investigation is necessary to examine how the tenon-to-mortise thickness ratio influences joint capacity when subjected to shear loading.

The abrupt shift in the graph's trajectory is attributed to a change in the predominant failure modes. Initially, for all ratios, mode vd exhibits the lowest value, thereby governing the failure. Consequently, the trend line for all ratios remains consistent at the outset, as tm/ts is not factored into mode vd. Subsequently, the trend undergoes a change with a uniform slope, as one of the modes Im, Is, or Id consistently governs, maintaining a constant ratio while other variables remain unchanged.

FIgure 3.13 and table 3.3 presents the optimal peg diameter that yields the highest capacity while maintaining acceptable spacing, based on the input variables. The green row in table 3.3 highlights the most optimal result, with the full results available in Appendix. The table showcases 4 selected thresholds from a total of 30 steps in the iteration.

Diameter(mm)	L.e(mm)	L.s(mm)	L.v(mm)	L.g(mm)	Joint capacity(kN)	Joint Status
16.51	22.21	27.76	16.66	16.66	4.48	Not Acceptable
16.764	22.9	28.62	17.17	17.17	4.62	Acceptable
26.416	56.85	71.07	42.64	42.64	11.47	Acceptable
26.67	57.95	72.44	43.46	43.46	11.69	Not Acceptable

Table 3.3: The Optimal Dimensions and their Corresponding Utilization Factors and Weight

The results highlight the significant impact of optimizing joint geometry configuration, particularly in relation to peg diameter. It appears that even a moderate adjustment of 60% in peg diameter can lead to a substantial 150% increase in joint capacity. This underscores the importance of careful consideration of geometric parameters when designing timber connections to achieve optimal structural performance.

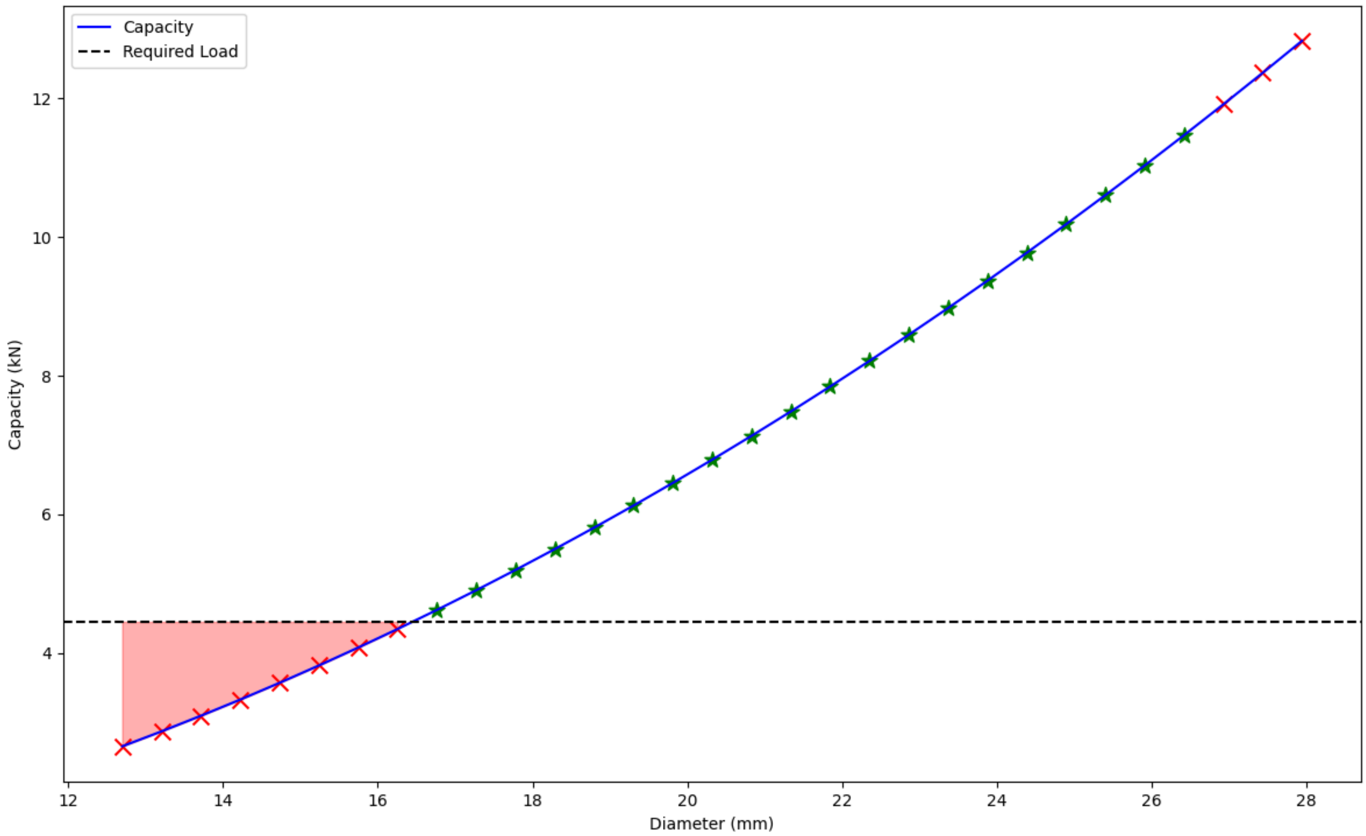

Figure 3.13: optimisation results for PMT joint based on Steel Equivalent Method, green stars and red crosses indicate acceptable and unacceptable spacing around the peg or required load bearing capacity

Geometry Optimisation of PMT Joints Using Numerical Model

While the equivalent steel bolt method provides a conservative estimate for ductile failure spacing requirements, an FEM model was developed to refine these analytical predictions. Furthermore, given the FEM software's capacity to handle intricate geometries, the model was employed in an optimization loop to assess the impact of complex shapes on PMT joint capacity.

FEM setup

To establish and validate the initial FEM, a study by (Miller 2004) was utilized. This research details both numerical and experimental approaches for conducting strength-based analyses on pegged PMT joints. Following Miller's methodology, a three-dimensional FEM was constructed with the objective of accurately predicting the 5% offset yield load of mortise and tenon joints subjected to tension. The 5% offset yield load, as defined by (ASTM D5764-23), Standard Test Methods for Evaluating Dowel-Bearing Strength of Wood and Wood-Based Products, involves identifying the initial linear portion of the load-deflection curve. Subsequently, a line parallel to this initial segment is offset by 5% of the peg diameter along the deflection axis. The intersection of this offset line with the load-deflection curve establishes the yield load. Upon successful validation, the FEM model was further utilized to predict yield loads for PMT joints exhibiting diverse geometrical properties, extending beyond the scope of the physical tests reported by (Miller 2004) . The finite element modeling was conducted by ANSYS 2023 R2, a commercially available software program. The analyses were performed on an ASUS ROG G513 laptop with an AMD Ryzen 7 processor, running the Microsoft Windows 10 operating system.

Model's detail

To accurately model the physical model done by (Miller 2004), a FEM that replicates tenison testing (figure 3.14.a) was developed. To accurately replicate the physical testing conducted by Miller (2004), a FEM (figure 3.14.b) simulating the tension test configuration was developed. The dimensions of the PMT joint are presented in Table 3.4. The peg, mortise, and tenon were partitioned into three subvolumes which let us define a different mechanical properties and geometry for each. Each subvolume was assigned a flexible stiffness behavior.

Table 3.4: the geometrical details of the FEM

Geometry of FEM	Dimensions
Distance of tenon’s end to center of the peg (Lv)	7.62 cm
Depth of tenon from the center of peg (le)	7.62 cm
Tenon thickness	4.826 cm
Gap between the mortise and tenon	0.127 cm
Peg diameter	5.08 cm

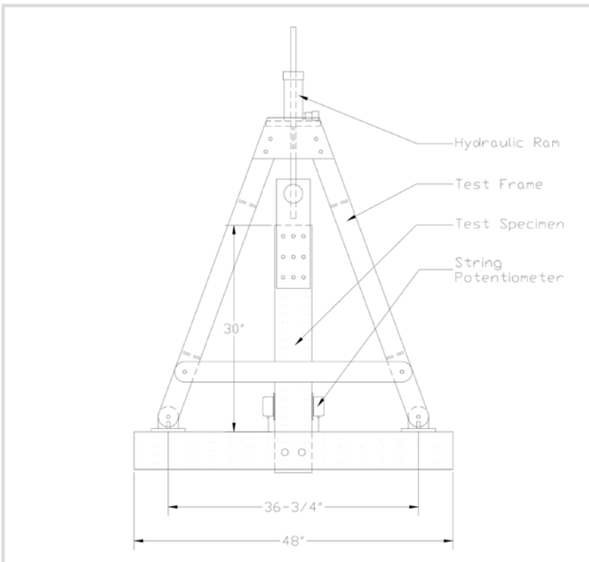

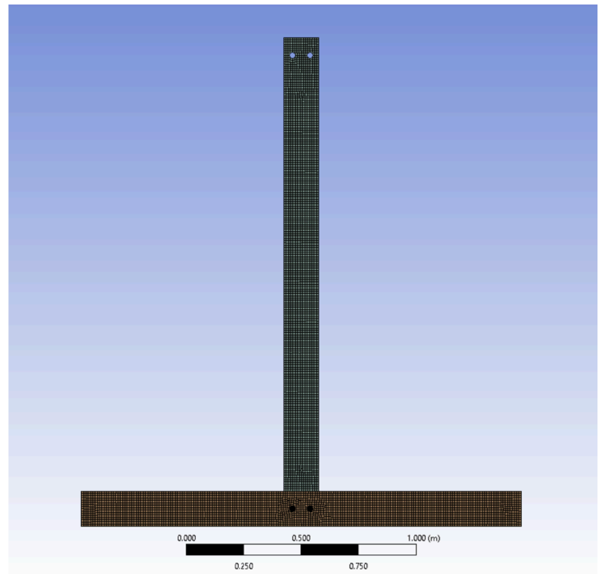

Figure 3.14: a)Tension Testing Apparatus from Schmidt and MacKay (1997), b) Developed FEM model

Material Model

Although (Miller 2004) mentioned the material properties and values in their report, new values for some of these values have been performed and some values updated based on more recent sources to achieve a higher accuracy. Formula by (Yang 2005) is used to calculate shear moduli:

$$G = \frac{E}{2(1+V)}$$

The orthotropic material properties of Douglas Fir were simulated by assigning **orthotropic elasticity** in the elastic region, and Orthotropic stress and strain limits.

Although simulating the plastic behavior of the timber was not the primary interest of this, a **bilinear stress-strain relation** was used to facilitate the determination of the yield load. Plasticity of the material was modeled by assigning **bilinear isotropic hardening**. The **Hill yield criterion** was assigned to determine when yielding occurs based on the applied stresses and the material's anisotropic yield strengths. Given that Douglas fir is an orthotropic material, the FEA model employed the "Hill Yield Criterion" to account for the material's plasticity. The Hill criterion is particularly suitable for orthotropic materials, as it provides a framework for predicting yield behavior under multiaxial loading conditions. Based on (Miller 2004)'s report on physical tests on Douglas Fir, the tangent stiffness perpendicular to the grain was half of MOE. Moreover, when the material was loaded perpendicular to the grain direction, the tangent stiffness approached plastic behavior and could be assumed to be close to 0.1E. Due to the minimal difference in values between the radial and tangential directions, the same elastic modulus E (mean value) was applied to both for simplicity. Similarly, a single Poisson's ratio μ was utilized for both the radial-longitudinal and tangential-longitudinal planes.

Table 3.5: the material properties of the FEM

Parameter	Value	Unit
E_x	16500	MPa
$E_{y} = E_{z}$	960	MPa
$G_{xy} = G_{xz}$	810	MPa
G_{yz}	350	MPa
$V_{xy\ (LR\ or\ LT)}$	0.37	
$V_{yz\ (RT\ or\ TR)}$	0.38	
$V_{xz\ (TL or\ RL)}$	0.032	
$\delta_{u,c}$	0.0001	MPa
$f_{t,0}$	57	MPa
$f_{c,0}$	36.9	MPa
$f_{t,90}$	1.8	MPa
$f_{c,90}$	7.2	MPa
f_v	6.9	MPa
f_{roll}	9.7	MPa

Contact

Four bonded contact regions (Figure 3.15) were defined: two for each peg in contact with the mortise, and one for the tenon. No contact interaction was defined between the face of the tenon and the mortise, as the loading was assumed to be purely tensile, with the pegs primarily responsible for stress transfer.

Meshing

The Hex Dominant meshing method, incorporating quad and tri elements, was employed for all subvolumes. Specific contact typing and face sizing was applied to both contact and target surfaces within each interaction to facilitate the generation of a finer mesh at the contact interfaces.

A **mesh refinement study** (Table 3.6) was conducted to ensure the accuracy of the finite element analysis. Three levels of mesh refinement were evaluated, with the results demonstrating a convergence in the predicted structural response. The maximum difference in calculated values between the finest and coarsest meshes was less than 3%. Consequently, the intermediate mesh density was selected for subsequent analyses, providing a balance between computational efficiency and solution accuracy.

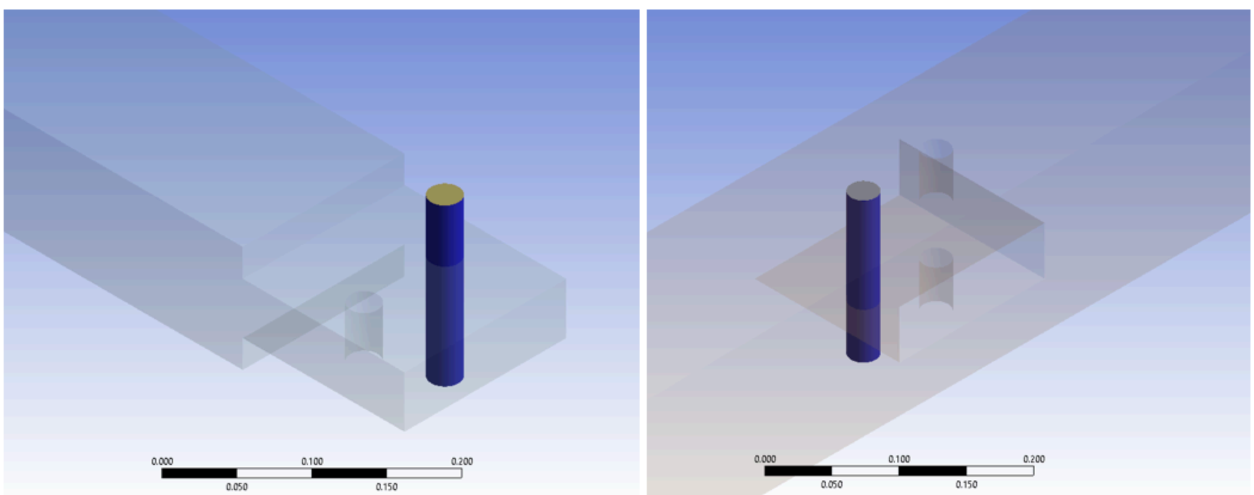

Figure 3.15: Four bonded contact regions a)the contact region between tenon and pegs, b) the contact region between mortise and pegs

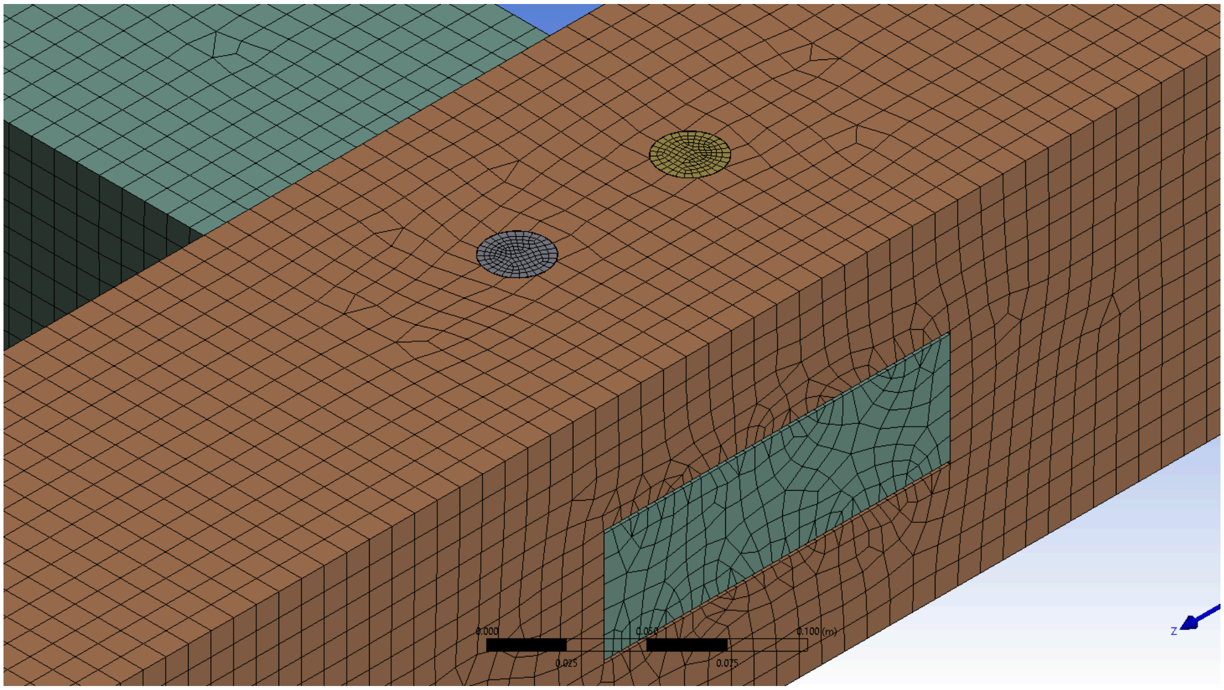

Figure 3.16: Meshing quality and properties of the FEM

Force (N)	Deflection (mm)	Force (N)	Deflection (mm)	Force (N)	Deflection (mm)
0	0	0	0	0	0
8207,5	1	8340,5	1	8504,8	1
15507	2	15856	2	16288	2
21820	3	22321	3	23048	3
27866	4	28482	4	29469	4
33722	5	34476	5	35717	5
39434	6	40356	6	41845	6
45053	7	46142	7	47868	7
50600	8	51838	8	53787	8
56085	9	57453	9	59603	9
61508	10	62977	10	65326	10
	N = 32821		N = 150826		N = 521064
	E = 8698		E = 41016		E = 131451

Table 3.6: the mesh refinement results

Boundary and Loading Condition

A bearing load was applied to the end face of the tenon, acting in the longitudinal direction (parallel to the grain) of the tenon. Given that the focus of the analysis was on the macroscopic load-deflection response, convergence was assessed by examining the applied load and the corresponding deflection at a node located away from the peg region. Two fixed supports were applied to the cross-section of the mortise model to more accurately replicate the boundary conditions employed in the physical tests conducted by .

Validating FEA setup

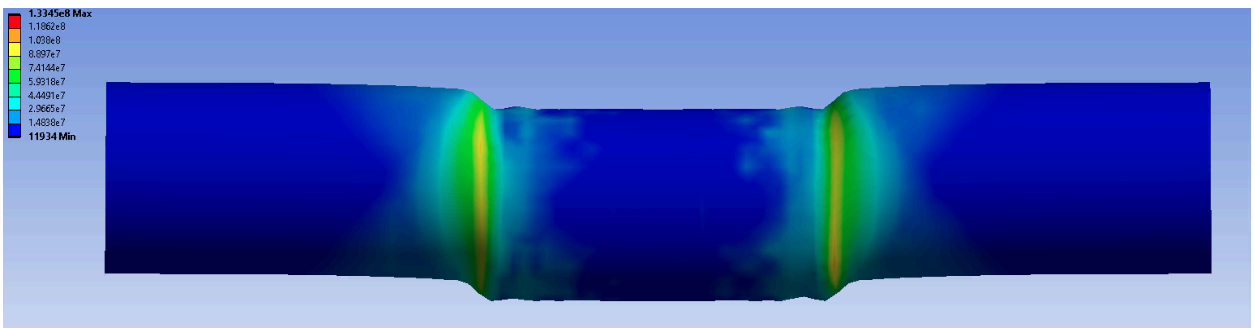

Figure 3.17: Plastic deformation of the peg model

Validation ensures the FEA model accurately reflects real-world behavior. While any model is an approximation, validation confirms it meets its purpose. Using commercial software like Ansys, we assume the underlying numerical methods are sound, focusing on whether our model setup captures the real-life model adequately. An iterative process of reviewing results and adjusting the model setup was undertaken to ensure reasonable deformation behavior. Upon observing the formation of four hinges in the peg (Figure 3.18), further refinement was performed to enhance the accuracy of the results.

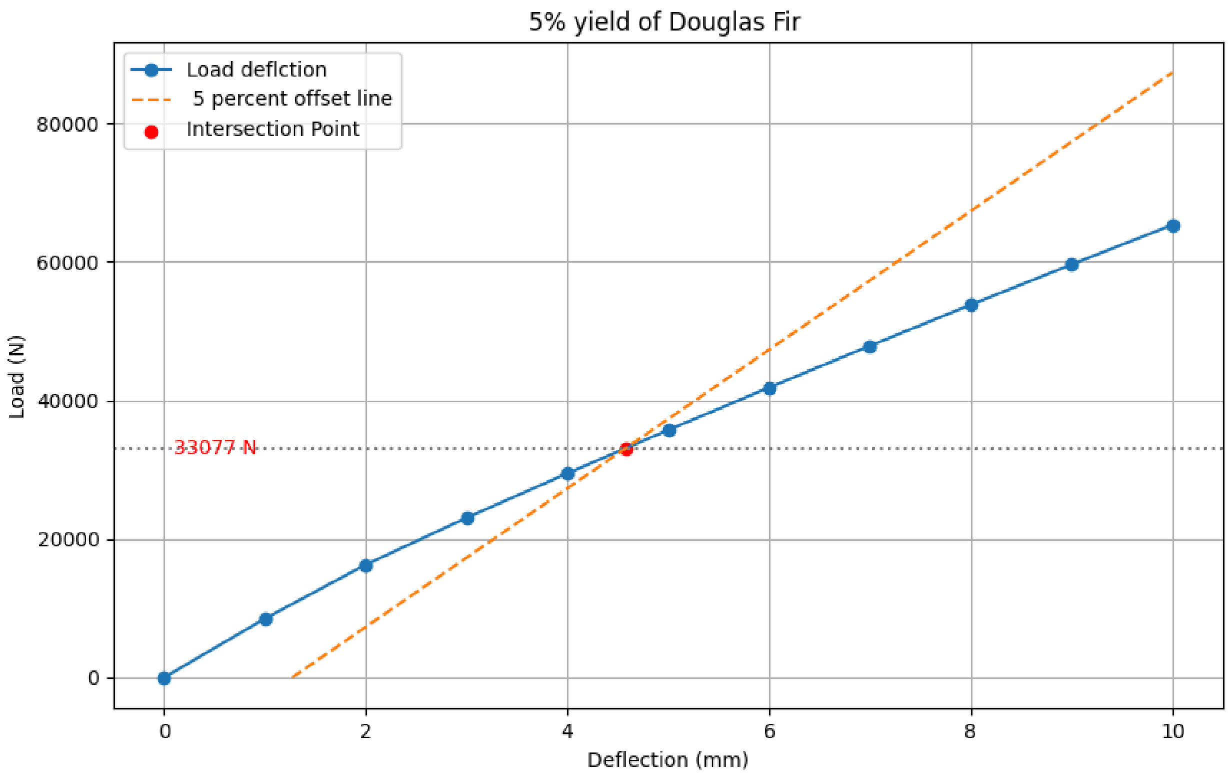

Figure 3.18: the validation result for 5% offset yield mode

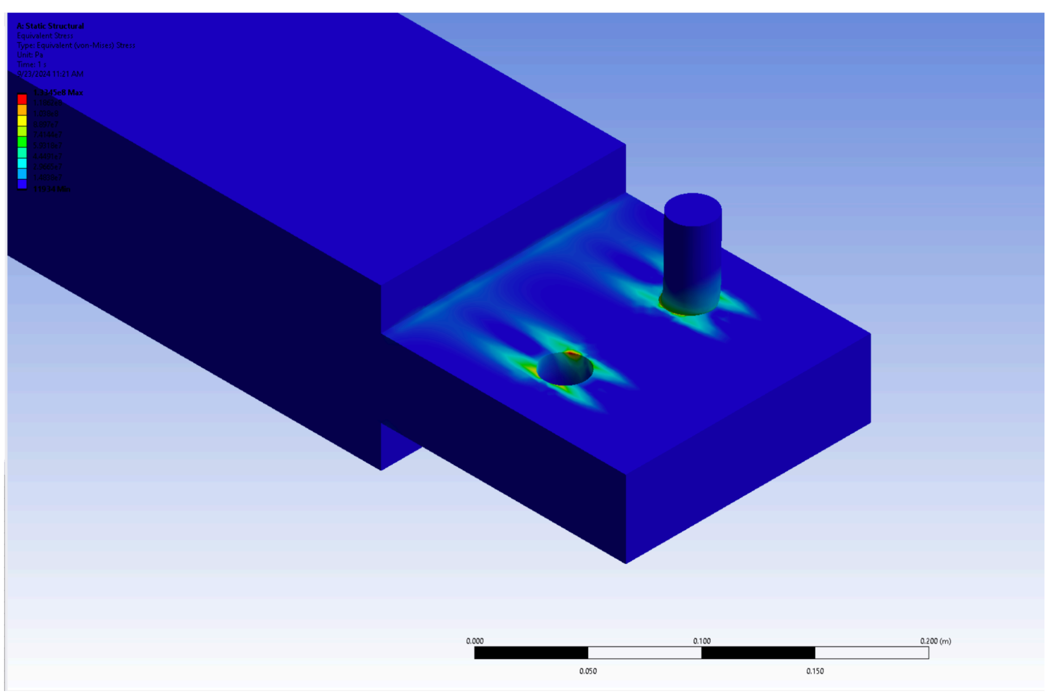

Figure 3.19: the plastic deformation of the peg model in the tenon

The 5% yield method was applied to the load-deflection graph generated by the finite element model. Results (table 3.7 ,and figure 3.18) indicated that the model was capable of predicting the mean value results obtained from the 5% yield method of physical testing, with an accuracy of 25%. The model developed in this study exhibited slightly higher accuracy compared to the one developed by (Miller 2004), and additionally, demonstrated increased plasticity. This enhanced performance can be attributed to the more detailed plasticity model explained earlier in the thesis. This higher plasticity can be beneficial in the optimization process. As the 5% yield increases, it may fail to intersect with the line, and higher plasticity aids in modeling the yield value more accurately.

Table 3.7: the Comparison of the result for 5% offset yield mode of physical, and the FEM and numerical model developed by Miller

Physical Yield load (N)	Modeled Yield load(N)	Ratio	Modeled Yield load by Miller (N)
26,244	33,077	1.25	33539

Optimization Loop

To examine how the placement of pegs affects joint performance, 25 different scenarios were created, with each scenario representing a unique arrangement of pegs within the mortise-tenon joint. These arrangements were methodically designed to cover a wide range of positions, enabling a thorough analysis of how changes in geometry impact load deflection and stress distribution. The specifics of these scenarios are detailed in Table 3.8. Each scenario was analyzed using FEM, allowing for the assessment of mechanical responses under simulated loading conditions. This systematic approach ensures that the study captures the subtle details of joint performance across various geometries, ultimately leading to the identification of the best arrangements for improved structural strength. The location of the pegs within the joint is determined by two factors: 'y', representing the peg's distance from the tenon's side edge, and 'h', representing its distance from the tenon's bottom edge (figure 3.20). In this analysis, we assume a consistent peg diameter of 1 inch and symmetrical placement of the left and right pegs.

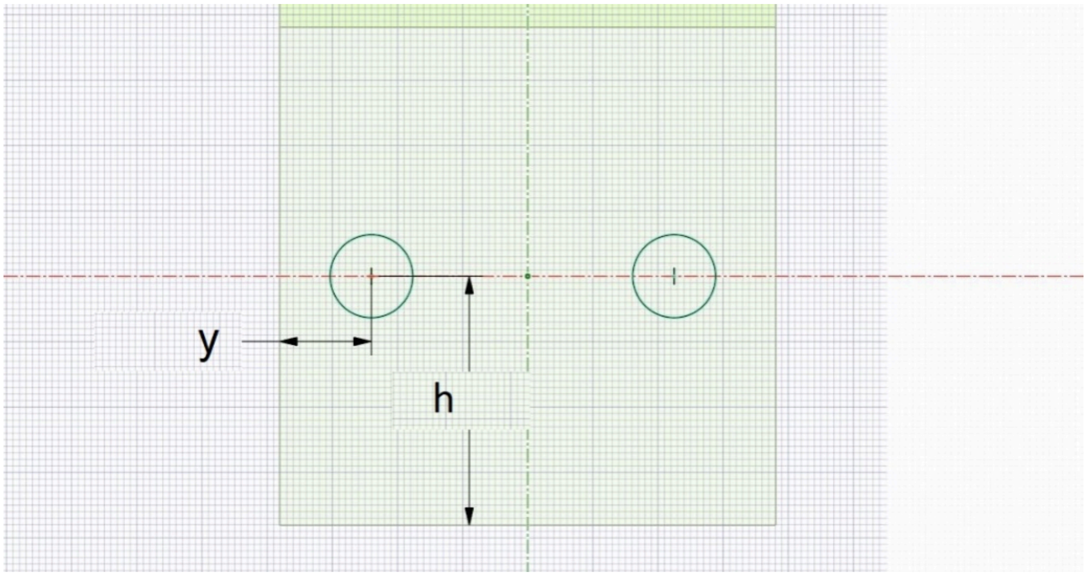

Figure 3.20: the plastic deformation of the peg model

Case Number	y (mm)	h (mm)	Case Number	y (mm)	h (mm)
1	25	76.2	14	35	101.6
2	30	76.2	15	35	127
3	35	76.2	16	35	50.8
4	40	76.2	17	35	25.4
5	45	76.2	18	40	101.6
6	25	101.6	19	40	127
7	25	127	20	40	50.8
8	25	50.8	21	40	25.4
9	25	25.4	22	45	101.6
10	30	101.6	23	45	127
11	30	127	24	45	50.8
12	30	50.8	25	45	25.4
13	30	25.4			

Table 3.8: Details of variations in the optimisation loop

After the model was validated, it was used as the basis for optimizing the joint geometries. The validated FEA model was used to create data for all 25 cases, which allowed for a thorough analysis of how different peg placements affect how the joint performs. The outputs included load deflection, stress distribution, and failure modes, which were systematically recorded and analyzed.

Methodology - Data Collection

Gathering data was a key part of this study, as it gave us important information about how well the mortise-tenon joints performed with different peg placements. We collected a full set of results for each of the 25 different peg configurations. These results focused on key measurements like the amount of force applied, the highest stress levels in the pegs, tenon, and mortise. This information was essential for understanding how the placement of the pegs affected the overall strength and stability of the joints.

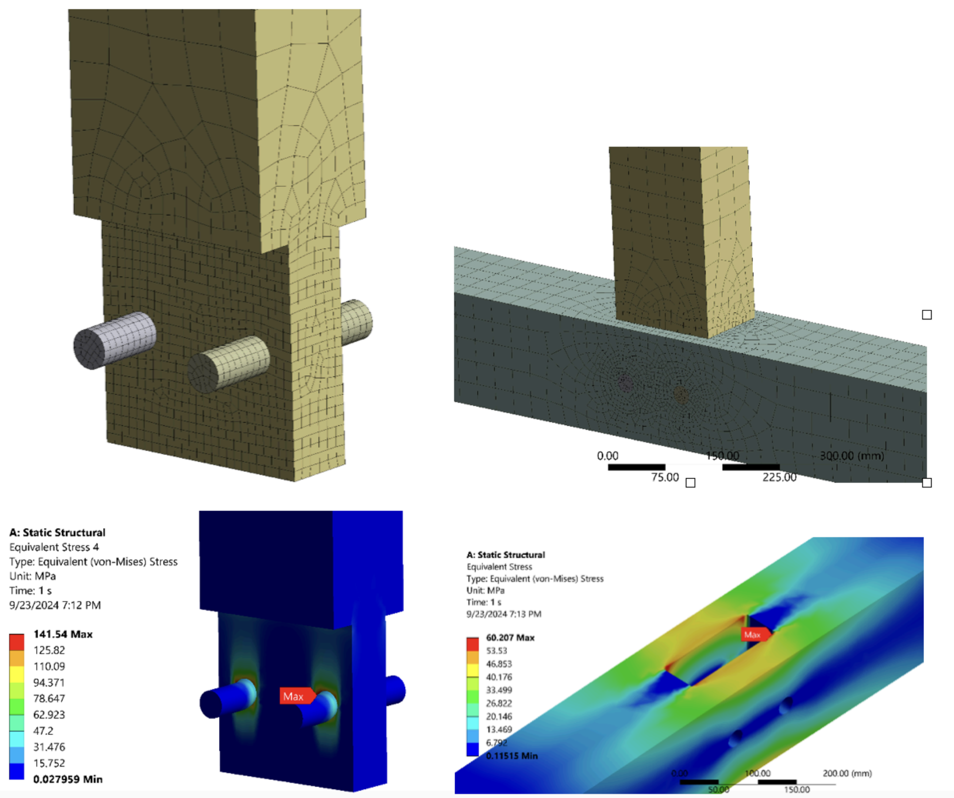

Figure 3.21: Results of the FEA of one the optimization cases (Case 2)

The FEA simulations were carried out in 21 incremental steps, allowing close examination of how the joint responded as it was gradually deflected by 10 mm. This step-by-step increase in deflection helped us understand how the joint behaved under growing loads, and it captured the important shift from elastic (reversible) to plastic (permanent) deformation. By carefully controlling the deflection in smaller increments, we ensured that the stress distribution and force responses were precisely recorded at different loading stages. All the data gathered was systematically organized and stored in an Excel spreadsheet, which acted as a central database for further analysis. This organized approach made it easy to access and efficiently work with the data, including visualizing it in helpful ways. The Excel file had separate columns for each of the 25 different joint configurations, detailing the corresponding force values and stress measurements for the pegs, tenon, and mortise.

This dataset is crucial for upcoming optimization analyses, as it enables us to pinpoint the best peg placements for improved joint performance. By examining the connection between peg location and stress distribution, the study aims to offer practical insights to enhance mortise-tenon joint design. The data analysis was performed using MATLAB (appendix), a powerful computational tool that simplified the processing and visualization of the finite element analysis (FEA) results. The main goal of the analysis was to calculate the yield load for each of the 25 peg configurations using the established 5% offset method, a common technique for determining yield points in load-deflection curves. To begin the analysis, a MATLAB script was developed to load the data collected from the FEA simulations. The data was efficiently organized by the script, and key metrics such as applied force and corresponding deflection values were extracted for each case. Once the data was loaded, the analysis focused on calculating the yield load, which is critical for understanding the performance limits of the mortise-tenon joints. To determine the yield load for each case, a line was drawn parallel to the initial linear portion of the load-deflection curve, starting at an offset of 0.5 mm. The intersection of this offset line with the curve indicated the yield load. Yield loads were calculated for all 25 cases. MATLAB code was used to generate plots visualizing the results, including load-deflection curves for each configuration with highlighted yield points. These plots allowed for easy comparison between different peg placements and their impact on stress distribution within the joint. The visualizations helped identify trends and patterns in the data, contributing to the understanding of how peg positioning affects joint performance and informing design optimization for mortise-tenon joints. Overall, the MATLAB data analysis was instrumental in converting raw simulation data into useful insights, supporting the study's goal of improving joint performance through informed design choices.

Results - Presentation of Data and Analysis of Data

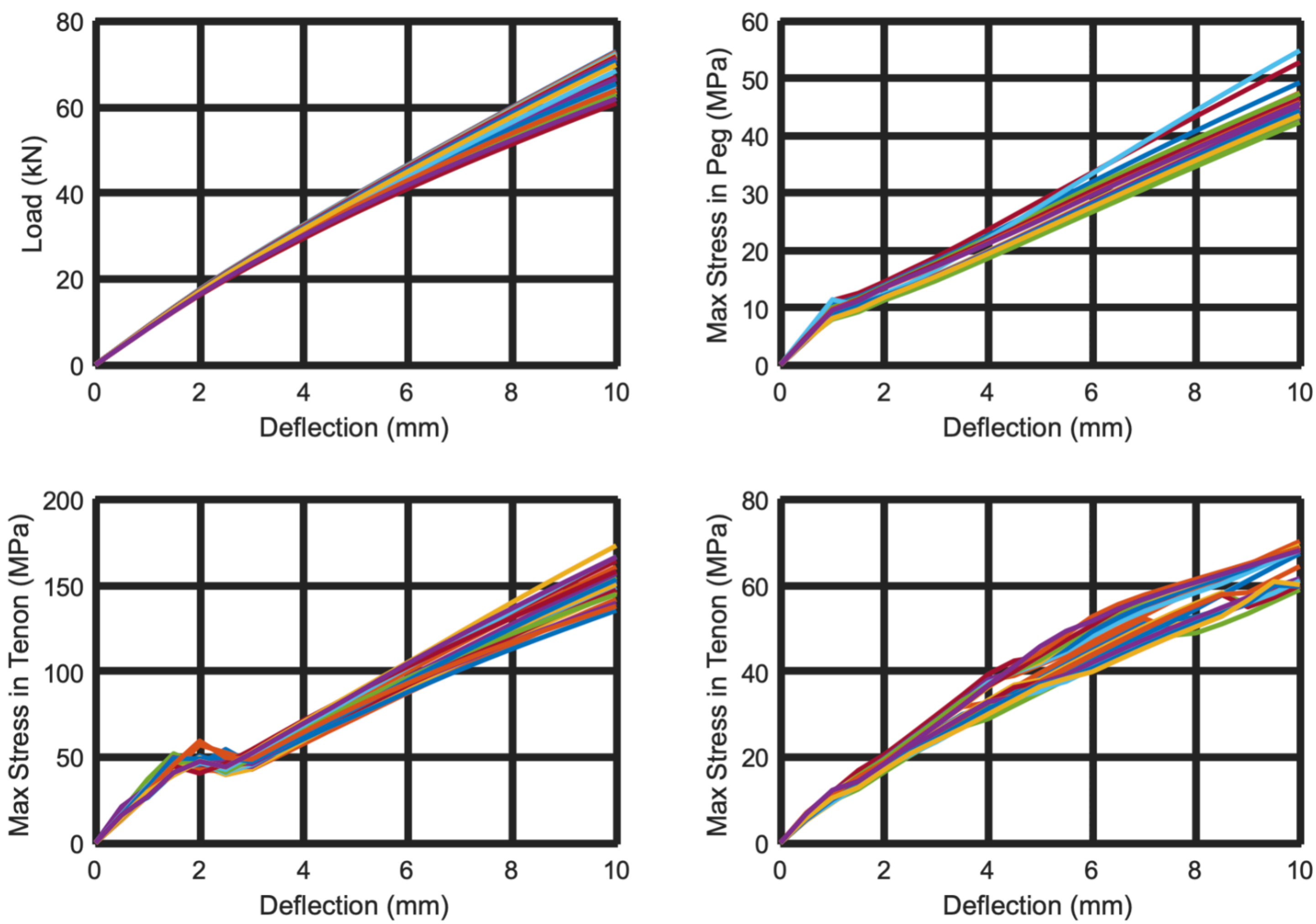

Figure 3.22: load and corresponding maximum stress in each elements vs deflection

This study visualized the results of Finite Element Method (FEM) simulations on 25 different mortise-tenon joint designs. Graphs were used to demonstrate how forces and stresses varied across these designs, providing a comprehensive view of the joints' behavior. One key finding was that the placement of the peg significantly influenced the mechanical response of the joint. Load-deflection curves showed how different peg positions affected the joint's strength and stiffness. Some configurations were clearly stronger and more rigid than others. Furthermore, visualizations of the maximum stress on different joint components (peg, tenon, and mortise) revealed how design choices impacted stress distribution. This allowed for the identification of configurations that minimized stress concentrations, which is crucial for improving the joint's durability and longevity. In essence, these visual representations effectively captured the complex relationship between the joint's geometry and its performance under load. By highlighting the impact of peg placement on both force distribution and stress concentrations, this study provides valuable insights for optimizing the design of mortise-tenon joints.

The analysis does not solely focus on maximizing the yield load. A crucial aspect of the study is the consideration of stress levels in the mortise and tenon. The design constraint stipulates that the pegs must fail before the mortise or tenon, which serves to protect the integrity of the primary structural components. Therefore, the optimal peg configuration must strike a balance between achieving a high yield load and keeping stress levels within safe limits.

Analysis of the data revealed clear trends in how different peg placements affected both the strength and stress distribution within the mortise-tenon joint. Each of the 25 configurations was assessed based on its yield load (the maximum force it could withstand before permanent deformation, calculated using the 5% offset method) and the highest stress levels observed in the peg, mortise, and tenon components during loading.

Yield Load Variation: As shown in Figure 3.22, there was significant variation in yield load across the different configurations. Some peg positions clearly resulted in a stronger joint, indicating that specific geometries are better at distributing forces. For example, placing the peg near the edges of the mortise (cases 7, 9, 11, 13, 15) generally led to lower yield loads. This is likely due to less efficient load transfer and higher bending stresses caused by stress concentration in those areas.

In contrast, the strongest configurations were those with pegs positioned towards the center of the allowable area. This is likely because having more material around the peg allows for better stress distribution, reducing stress concentrations and increasing the load the joint can withstand before yielding.

Stress Distribution

In addition to analyzing yield load, this study carefully examined the maximum stress levels within the mortise and tenon components (figure 3.24). This analysis revealed that certain peg configurations, particularly those where the peg was positioned close to the edges of the mortise (Cases 7 and 9), led to higher stress concentrations in either the mortise or the tenon. Similarly, almost all configurations with an "h" value of 50.8 mm (Cases 16, 20, and 24) showed elevated stress levels in the tenon. These findings emphasize the importance of considering both yield load and stress distribution when optimizing joint design. While a high yield load is desirable, it's equally important to ensure that stress concentrations remain within safe limits to prevent the joint from failing prematurely.

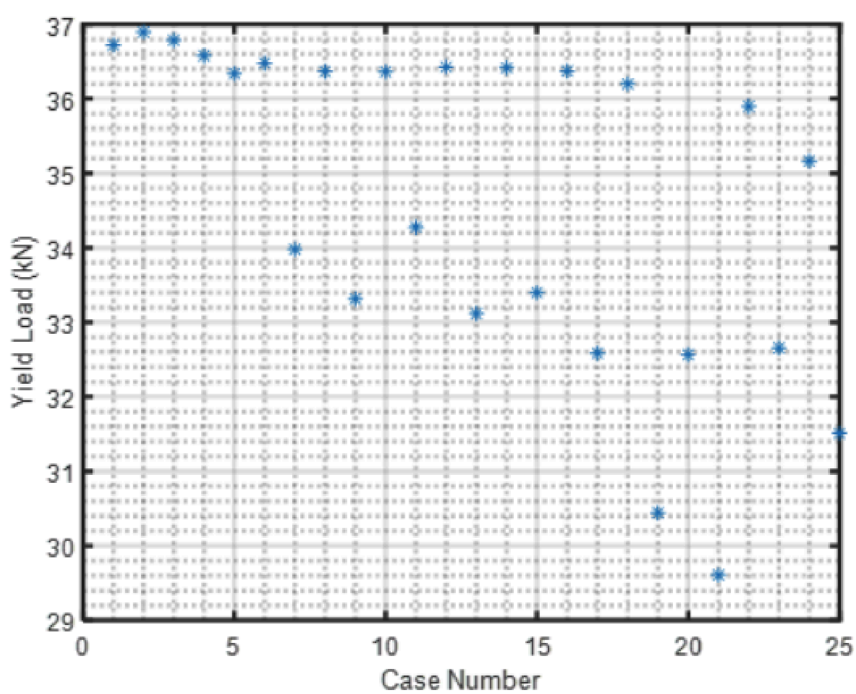

Figure 3.23: case numbers and their corresponding yield load

The ultimate goal of this study was to pinpoint the optimal peg configuration that maximizes yield load while keeping stress levels within acceptable limits. A systematic evaluation of all 25 configurations revealed several promising candidates that exhibited a good balance between high yield strength and low stress concentrations in the mortise and tenon. Cases 1, 2, 3, 4, 5, 6, 8, 10, 12, 14, 16, and 18 demonstrated the highest yield loads, with less than a 3% difference between them. However, when considering maximum stress values in the tenon, Cases 2, 11, 15, and 23 showed the lowest values.

Taking both factors into account, configuration number 2 emerged as the best overall performer. It exhibited a high yield load combined with minimal stress on the tenon, making it the optimal choice among the 25 configurations tested.

Effect of Peg Stress Values

This study found a strong link between how much force a mortise-tenon joint can handle before permanently deforming (yield load) and the highest stress levels in the pegs. Joints with higher yield loads generally had lower peak stress in the pegs. This is because of how stress concentrates and spreads within the joint. Stress concentration happens when external forces cause stress to build up in specific areas of a material. In mortise-tenon joints, the pegs, which transfer load between the tenon and mortise, can create high-stress zones around where they're inserted. This is due to the peg's shape disrupting the material's continuity, causing stress to increase locally. When pegs have high stress concentrations, the whole joint is weaker. High peg stress can cause early failure, as the material might yield or break at these stress points before the entire joint reaches its maximum load capacity. Therefore, designing peg configurations that minimize stress concentration is vital for improving the joint's overall strength and performance.

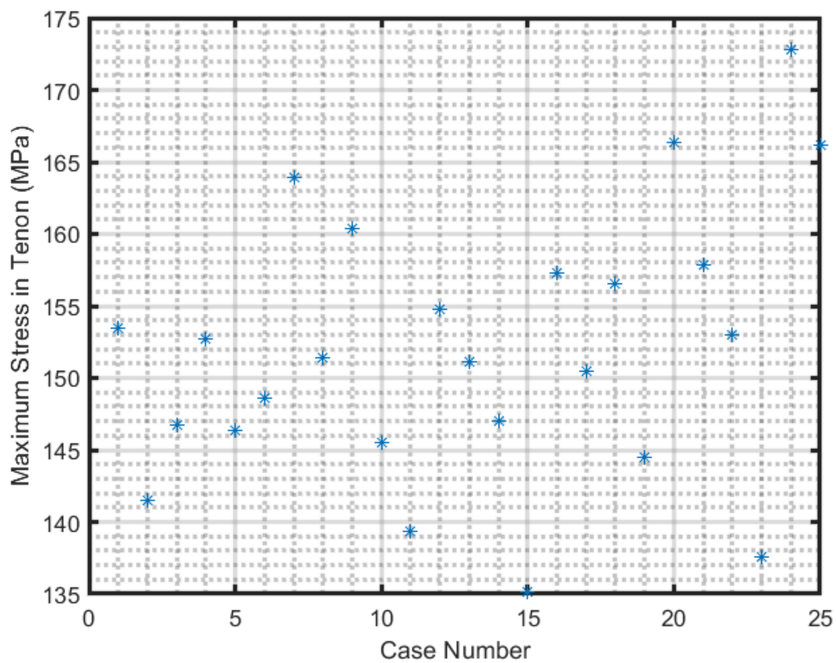

Figure 3.24: case numbers and their corresponding maximum stress in the tenon

Conversely, effective stress distribution plays a vital role in maximizing the yield load of mortise-tenon joints. Stress distribution refers to how applied forces are spread across the joint and its components. A well-distributed stress profile allows the joint to withstand higher loads without reaching critical stress levels that could lead to failure. In configurations where stress is evenly distributed, the load is shared more effectively among the pegs, mortise, and tenon. This distribution reduces the likelihood of localized stress peaks, allowing the joint to endure greater external forces. As a result, the yield load increases, enhancing the joint's total capacity to withstand loads.

The analysis underscored the inherent trade-offs in joint design. While it is desirable to maximize yield load, achieving this goal often involves compromises in other performance metrics. For example, configurations that positioned pegs too far from the mortise edges (15, 23) might yield lower stress concentrations but also resulted in reduced yield loads.

Understanding these trade-offs is essential for making informed design decisions. The study emphasizes the need for a holistic approach to joint design, where multiple factors are considered simultaneously. Designers must weigh the benefits of higher yield loads against the potential risks associated with elevated stress levels in the mortise and tenon.

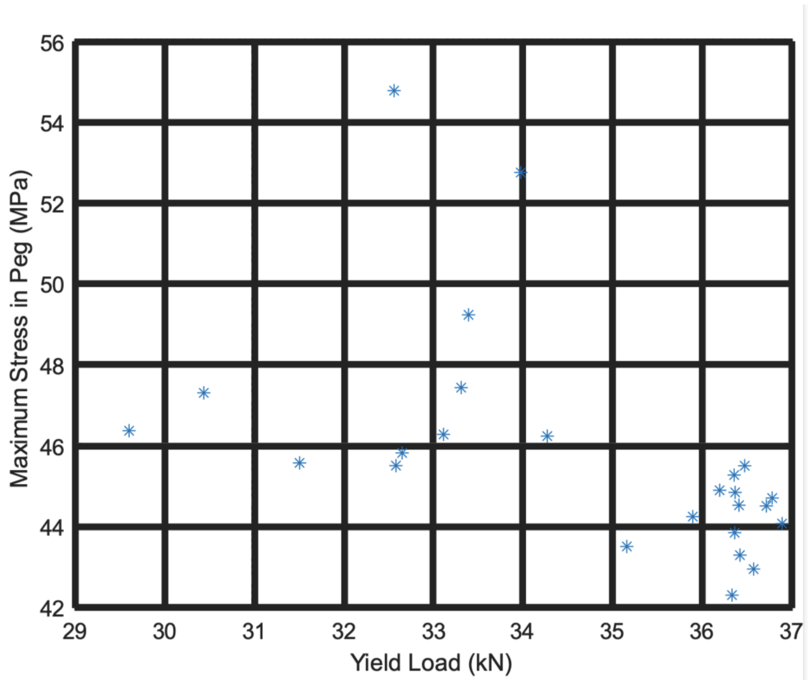

Figure 3.25: Yield load - maximum stress in the pegs

Developing Connection Design Methods Based on Rule of Thumb and Carpenters Recommendation

After optimizing the pegged mortise and tenon joint and finalizing its geometry, three additional joint categories were designed: Scarf, Blind Mortise Tenon, and Gooseneck joints. These designs were based on established carpentry practices and the recommendations of experienced carpenters, drawing upon generations of knowledge in timber framing.

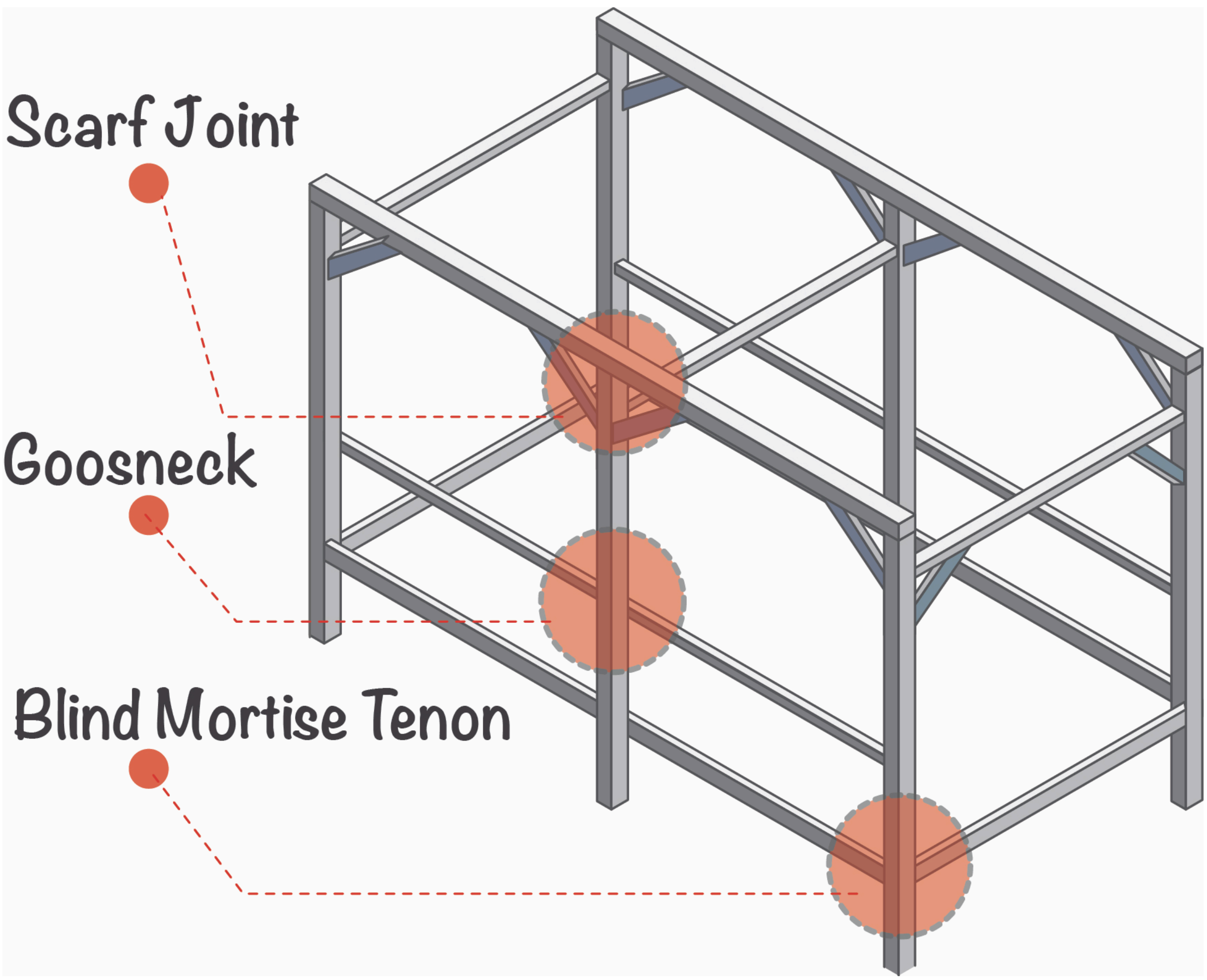

Figure 3.26: The Position and type of Joints in the timber structure

Scarf joint

Scarf joints, also known as splice joints (Figure X), are used to connect two members end-to-end (Hewett 1980). This technique is particularly useful when the required length of a member exceeds the available material. Considered the strongest method for lengthening timber without glue (Thelandersson 2003), the scarf joint employs a pair of matching angled cuts that are secured together with pegs (Branco 2015).

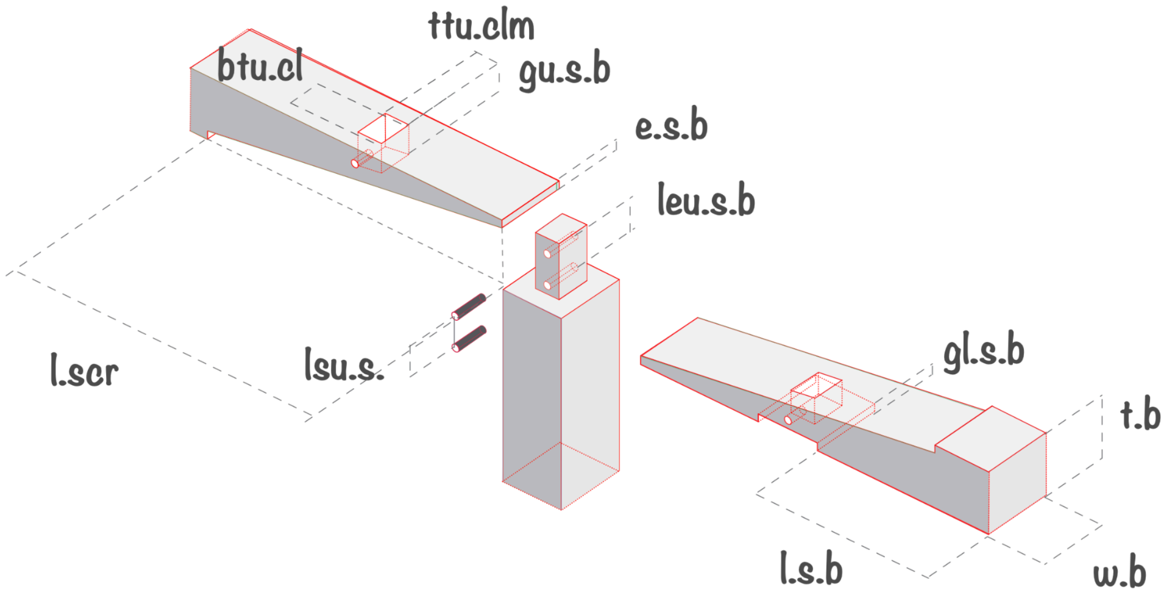

Figure 3.27: the Scarf joint details used in the case study

Based on (Fountain 2009), to achieve structurally sound and aesthetically pleasing scarf joints in timber framing, the following design recommendations are proposed (figure 28) :

- **Length:** The scarf joint's overall length should be three times the height (or depth) of the timber members being joined. This ensures sufficient surface area for load transfer and a visually balanced joint.
- **Abutment Height:** The height of the abutments at each end of the scarf should be one-sixth of the timber's height. This dimension can be rounded to the nearest 1/16th or 1/8th of an inch to simplify layout.
- **Centerline Positioning:** When a scarf joint is located near a knee brace, its centerline should be offset 5 1/2 inches from the brace's bearing point on the adjacent post. This strategic offset prevents interference between the brace's tenon and the upper section of the scarf, facilitating a clean and efficient construction process.

These recommendations, derived from established carpentry practices and a focus on proportionality, provide a framework for designing robust and visually harmonious scarf joints in timber frame structures.

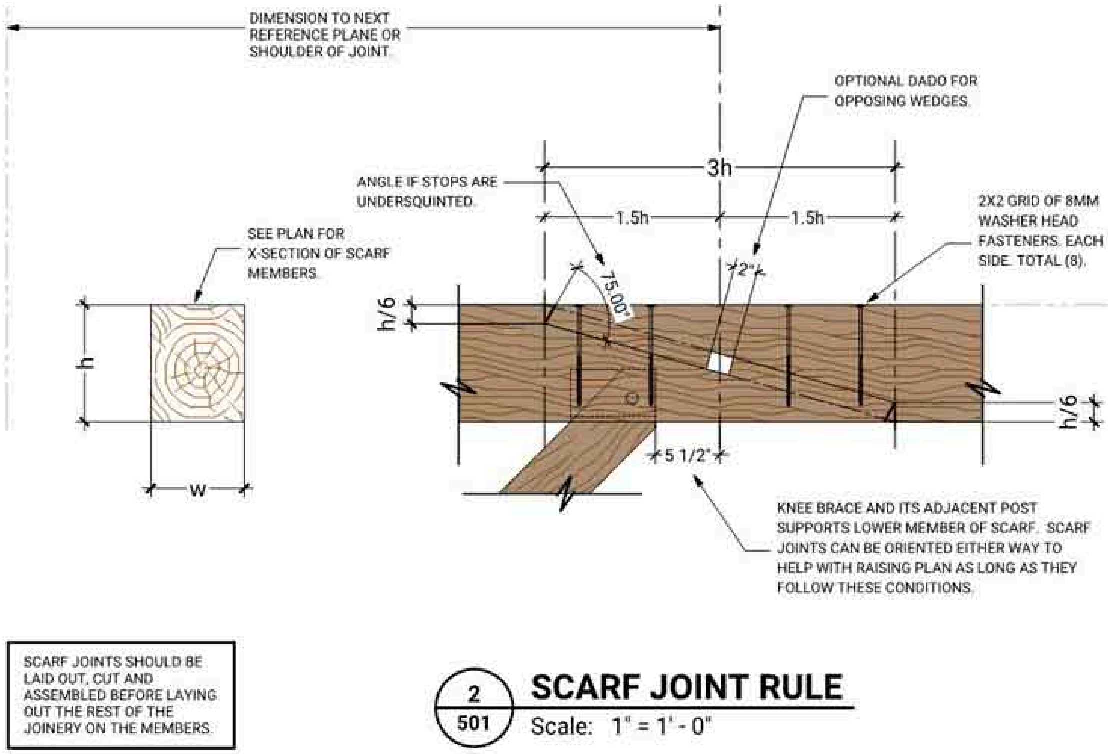

Figure 3.28: the Scarf joint rule of thumbs detailing

Gooseneck Joint

Due to the lack of established design guidelines for gooseneck joints (Figure 3.29), a Finite Element Method (FEM) analysis was conducted to determine the optimal geometric configuration for this specific joint type. The same meshing details and material properties used in the analysis of the Pegged Mortise and Tenon (PMT) joint were applied to ensure consistency and comparability. For this analysis, the gooseneck joint was subjected to a pure tension force to evaluate its performance under tensile loading. This FEM-based approach allowed for a detailed investigation of the joint's behavior and the identification of the most efficient geometric ratios for maximizing its strength and stability.

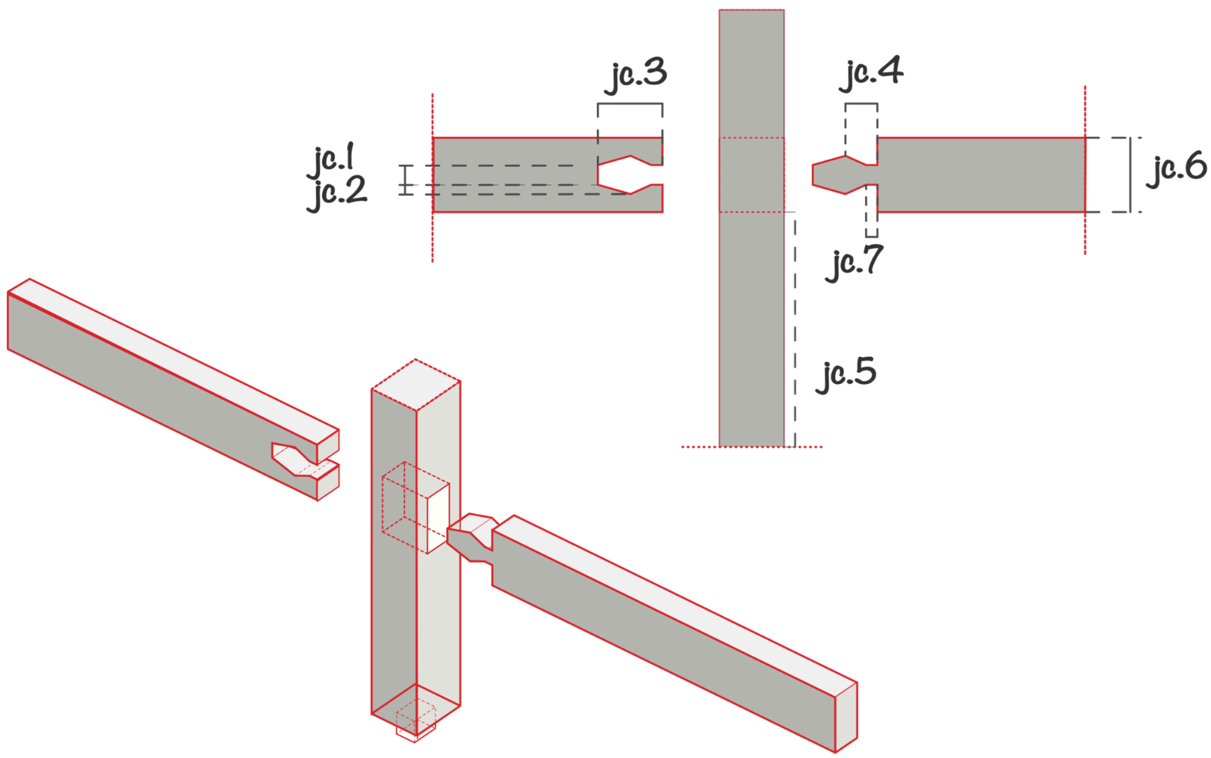

Figure 3.29: the Scarf joint drawing with variables used in optimisation

The variables of the optimization loop are shown in the table 3.9. Figure 3.30 presents the results of finite element analysis (FEA) conducted on 25 distinct joint geometries. The analysis involved applying a 5 mm displacement to the end of each joint and measuring the resulting tensile force and stress distribution. The results clearly demonstrate that variations in joint geometry significantly influence both the magnitude of tensile force and the stress concentration. This finding underscores the importance of the optimization process in identifying a geometry that minimizes stress while maximizing tensile force. The optimal geometry, as determined through this process, exhibits distinct characteristics that differentiate it from the other configurations. Figure 3.31 illustrates the yield strength of the structure for each of the analyzed cases.

jc.4 (in)	jc.1 (in)	jc.2 (in)	jc.4 (in)
Case 1	2.5	1.8	0.8
Case 2	2.5	2.1	0.9125
Case 3	2.5	2.4	1.025
Case 4	2.5	2.7	1.1375
Case 5	2.5	3	1.25
Case 6	3.875	1.8	0.9125
Case 7	3.875	2.1	1.025
Case 8	3.875	2.4	1.1375
Case 9	3.875	2.7	1.25
Case 10	3.875	3	0.8
Case 11	5.25	1.8	1.025
Case 12	5.25	2.1	1.1375
Case 13	5.25	2.4	1.25
Case 14	5.25	2.7	0.8
Case 15	5.25	3	0.9125
Case 16	6.625	1.8	1.1375
Case 17	6.625	2.1	1.25
Case 18	6.625	2.4	0.8
Case 19	6.625	2.7	0.9125
Case 20	6.625	3	1.025
Case 21	8	1.8	1.25
Case 22	8	2.1	0.8
Case 23	8	2.4	0.9125
Case 24	8	2.7	1.025
Case 25	8	3	1.1375

Table 3.9: the variables of the optimisation loop of the Scarf joint

Notably, cases 6 through 25 exhibit nearly identical yield strength values. This observation suggests that, with the exception of cases 1 to 6, where the geometric parameter `jc4` is minimized, the yield strength remains relatively consistent across the range of geometries. This finding highlights the influence of jc4 on the structural performance. Figure 3.32 presents the maximum principal stress observed in both the male and female components of the joint.

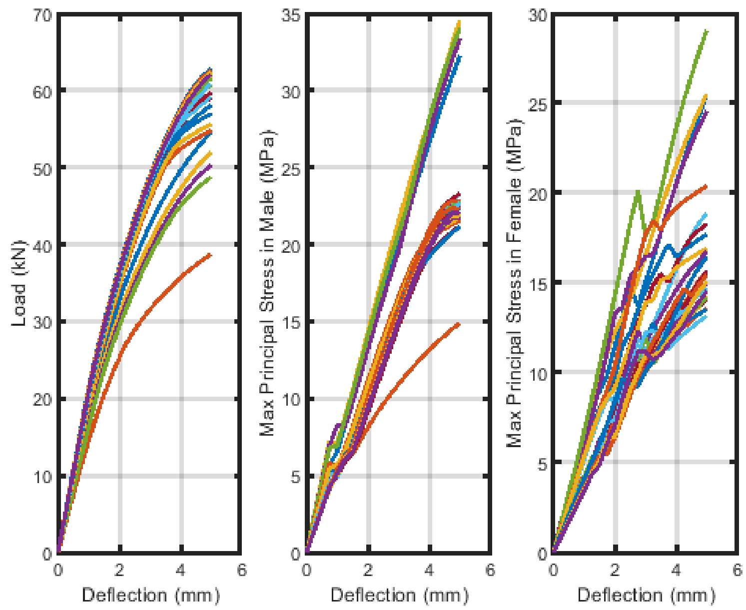

Figure 3.30: the variation of stress and yield loads - deflection with different case numbers

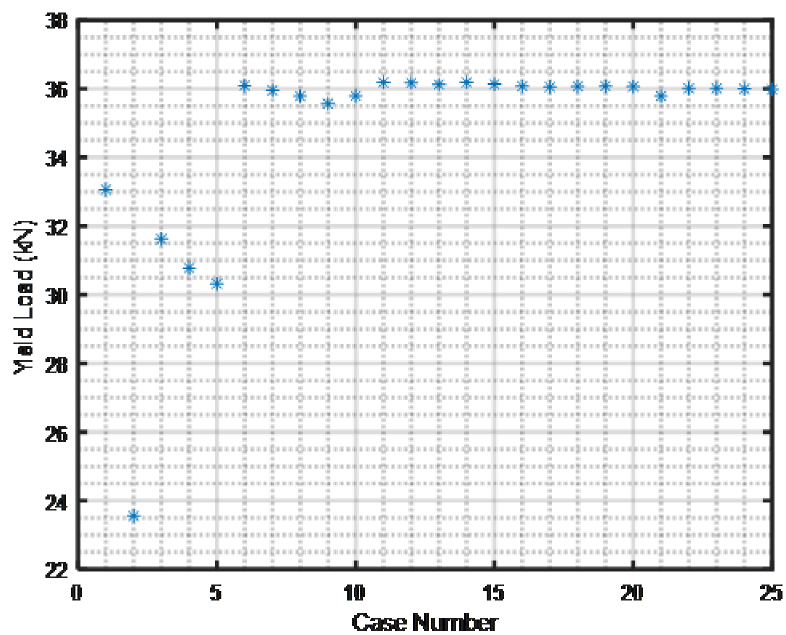

Figure 3.31: case numbers and their corresponding yield load

Among the cases exhibiting the highest yield strength, cases 13 and 15 demonstrate the lowest principal stress in both the male and female components, as illustrated in Figure [Figure number].

Figure [Figure number] presents the maximum von Mises stress for each case. Notably, case 15 exhibits the lowest total von Mises stress across both the male and female components.

Based on the analysis of both principal stress and von Mises stress, alongside yield strength, case 15 emerges as the optimal geometry due to its superior performance across these critical metrics. This case effectively minimizes stress concentrations while maintaining high yield strength, making it the most suitable choice for the intended application.

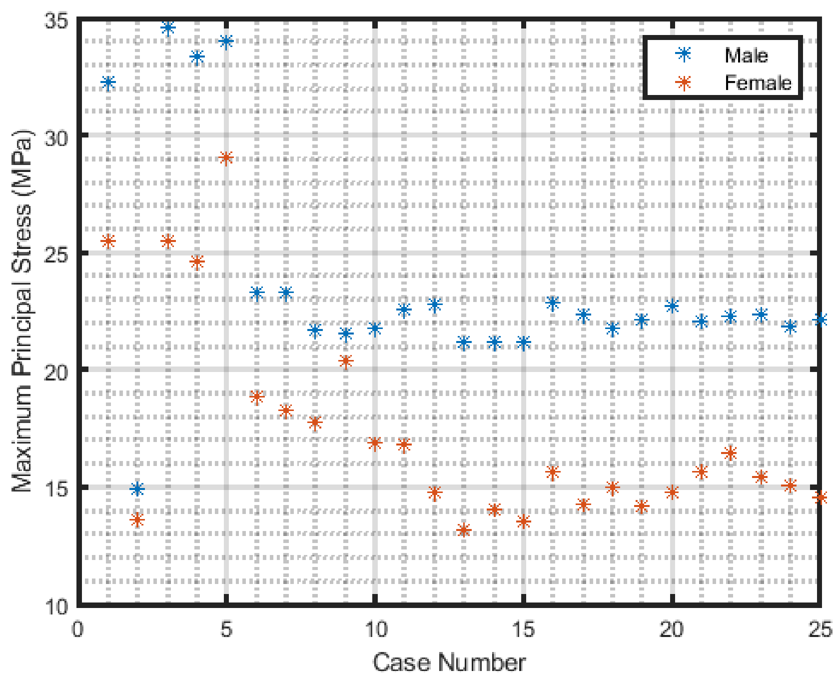

Figure 3.32: case numbers and their corresponding maximum principal stress

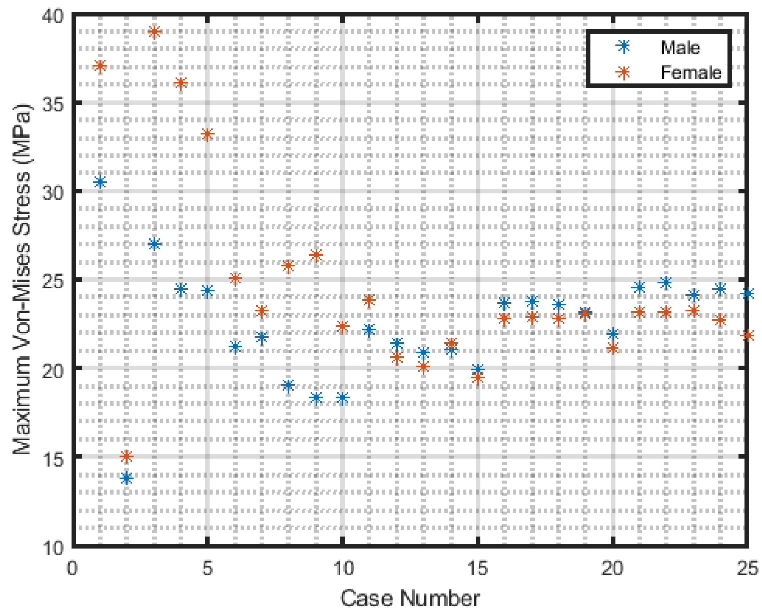

Figure 3.33: the Scarf joint drawing with variables used in optimisation

Final Design

Having determined the footprint, cross-sectional properties, and joint details, the final structural design is illustrated in Figure 3.34.

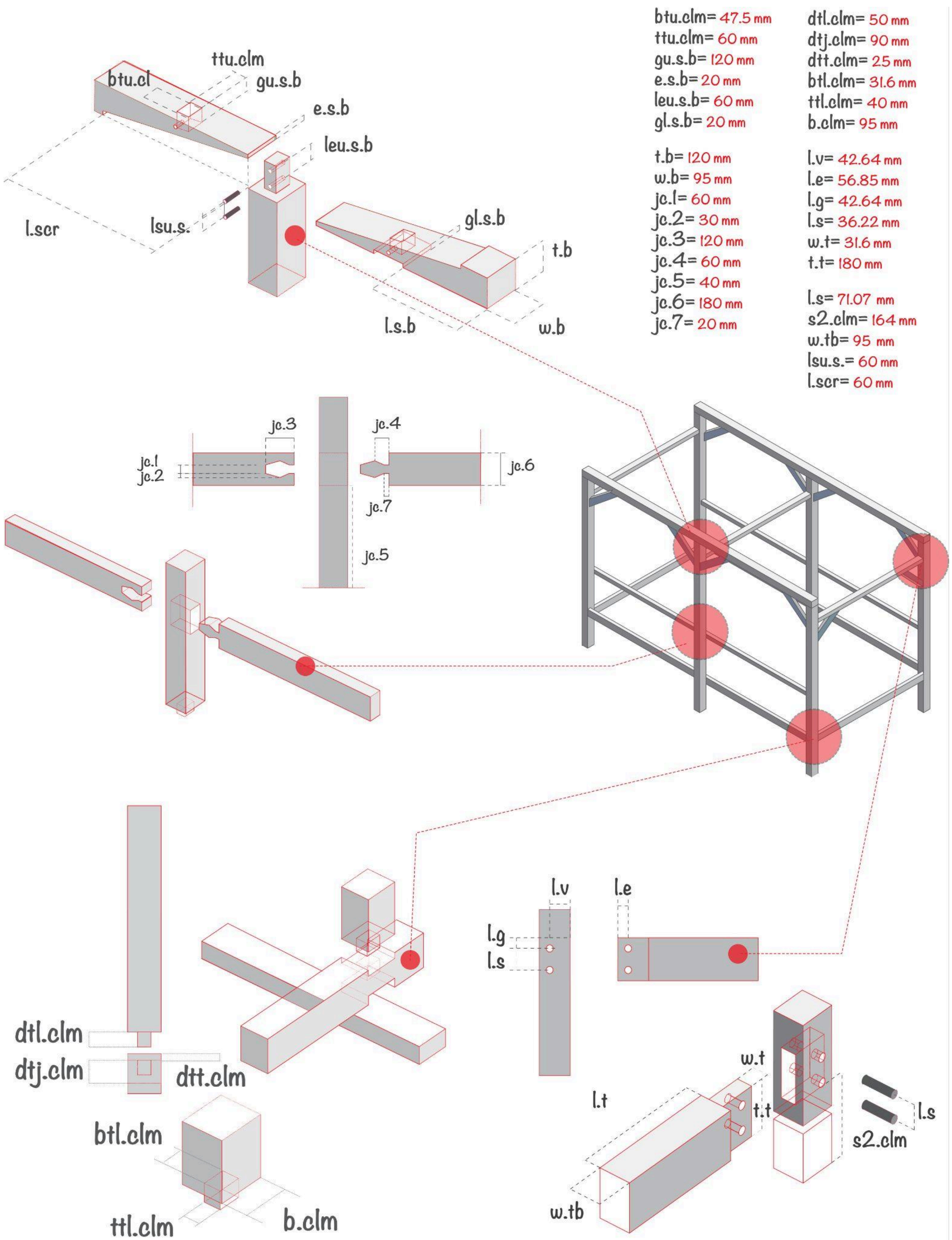

Figure 3.34: the final structural design

Conclusion and Discussion of Case-Study

- The preliminary design and layout chosen for this specific timber frame inherently restricts the potential for automation to the parameters defined within this particular system. This observation underscores a crucial consideration in the development of 'Lock n Load': **the initial layout of any structural system fundamentally constrains the scope of design automation to the variables explicitly established within that system.** Consequently, the first and pivotal step in automating any design process is the deliberate selection of both the structural system itself and its specific variation.
- In this case study, a simplified approach was initially taken, assuming **rigid connections** between primary beams and columns, and simply supported connections for eaves beams and joists. However, for the finite element method (FEM) analysis, a more realistic representation was adopted, considering the connections as semi-rigid. This highlights a crucial insight for the development of 'Lock n Load': **the ability to define connections with varying stiffness based on their analyzed behavior is essential. This flexibility will allow for more accurate modeling and simulation of real-world structures, leading to improved design and performance predictions**.
- Prior to initiating any structural computations, it is imperative to define the material properties of the timber used in the design. Therefore, in developing 'Lock n Load,' **incorporating a material library would be advantageous for designers, enabling them to readily access and utilize pre-defined material properties**. It's also critical to ensure that within the 'Lock n Load' workflow, **the input of material properties be provided before any structural calculations.**
- A load calculator can significantly simplify the design process for designers, particularly by automating the input of environmental factors. Since load calculations also rely on geometry variables, it's essential that within the development of 'Lock n Load,' **the load calculation method is executed only after the user has finalized the geometry and material output. This ensures accurate and relevant load calculations based on the specific design parameters provided by the user**.
- Safety and modification factors should be generated through an interaction between the built-in computation component and the selected material type. **This approach ensures**

that both the specific element material type and its designated service class are taken into account when determining appropriate safety and modification factors.

- Cross-sectional optimization of timber elements was found to be effective in achieving significantly lower utilization factors while maintaining approximately the same overall weight.
- In analytical analyses of timber joints, unlike other elements in timber structures, the applicable methods can be restricted to specific types of timber. Therefore, in the development of Lock and Load, **it is crucial to clearly specify which types of timber each specific method is suitable for**.
- In the analytical case study, the focus was solely on the tensile capacity of the joint. However, it is recognized that joints can be subjected to other types of loading, such as shear and bending, which also warrant analysis. Therefore, it's important that Lock and Load be **equipped to handle and provide for different types of loading that a building might experience**.
- In the analytical optimization of the PMT joint, a tm/ts ratio of approximately **0.5** was found to be optimal for maximizing capacity. This **aligns with the findings of (Hu 2021)**, who recommended a width-to-length ratio **(w < l < 2w)** for optimal joint performance. However still the effect of shear and bending should be examined.
- Optimizing the geometry of PMT joints resulted in an approximate **10% reduction** in stress on the base materials and a **17% increase in yield load**. Although the initial simulation stages were validated using physical experiments, **further validation is required to confirm the accuracy of the FEM optimization loop results**.
- This study utilized FEM analysis to determine an optimal geometric ratio of **jc.4 : jc.1 : jc.2 = 5.25 : 3 : 0.9125** for **gooseneck** joints in timber structures under tensile loading. This finding offers valuable guidance for designing such joints, but further research is needed to assess the impact of different timber species, joint sizes, and loading conditions, including bending moment and stiffness optimization, on this optimal ratio.
- Given the discrepancy between FEM and analytical model results, **"Lock n Load" should empower designers with the flexibility to customize variable values within the platform.**

- To automate Eurocode-based structural design, the system must generate the following load outputs: **ULS** (**instantaneous, medium-term, permanent**), **SLS**, and four **creep** and **deflection factors.**

" Technology is best when it brings people together."

Matt Mullenweg

Lock n Load

This section introduces Lock n Load and its purpose. Lock n Load is a digital web-based tool designed to simplify, improve, and integrate the process of delivering, designing, optimizing, and assembling timber shelters for emergency use after disasters. This tool aims to benefit shelter-seekers, shelter designers, and other key stakeholders involved in the supply chain.

Front-End Functionality

Lock and Load is composed of four key components: the **Designer Panel**, the **Shelter-seekers panel**, the **CNC interface**, and the **Timber providers network** (figure 4.1).

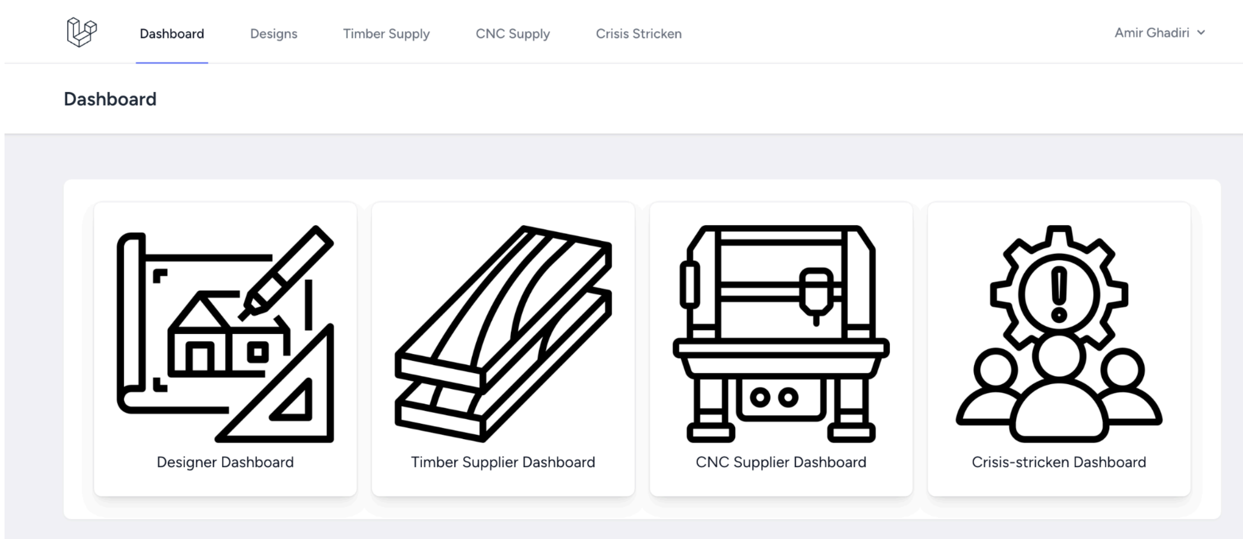

Figure 4.1: the homepage of Lock n Load

Designer Dashboard

When users access the designer dashboard, they can create a new timber frame design block. However, the case study's findings highlighted a key constraint: automating the design process across different structural systems necessitates a unique, **built-in** automation method for each system and its variations, at least within the scope of the methods explored in this thesis. Currently, the website administrators control how a structural system is designed, and only one type of timber frame is supported. However, users can still create their own custom designs within these limitations, as explained below.

When users begin the timber frame design process, they have the option to either select a pre-existing material from the library or create a new material block with custom properties (figure 4.3). These material properties (figure 4.4) will be used as inputs for subsequent calculations.

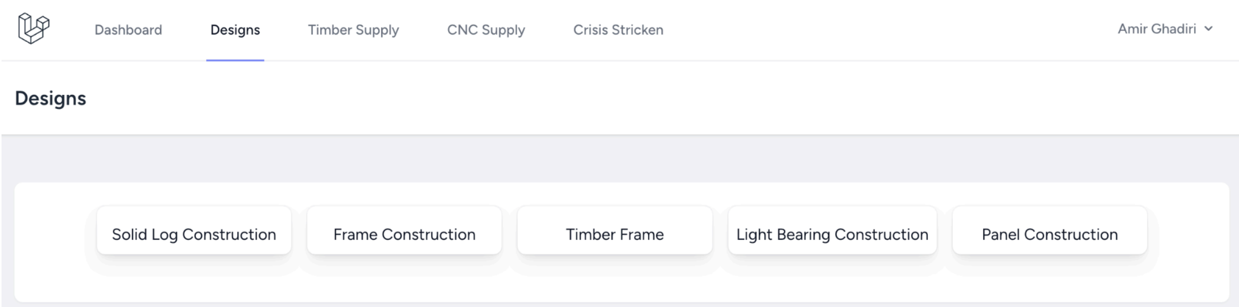

Figure 4.2: they have the option to utilize a built-in timber frame design module, lock n Load currently only supports one type of timber frame

It is crucial that the system obtains material property inputs during the initial design stages to enable accurate dead load calculations.

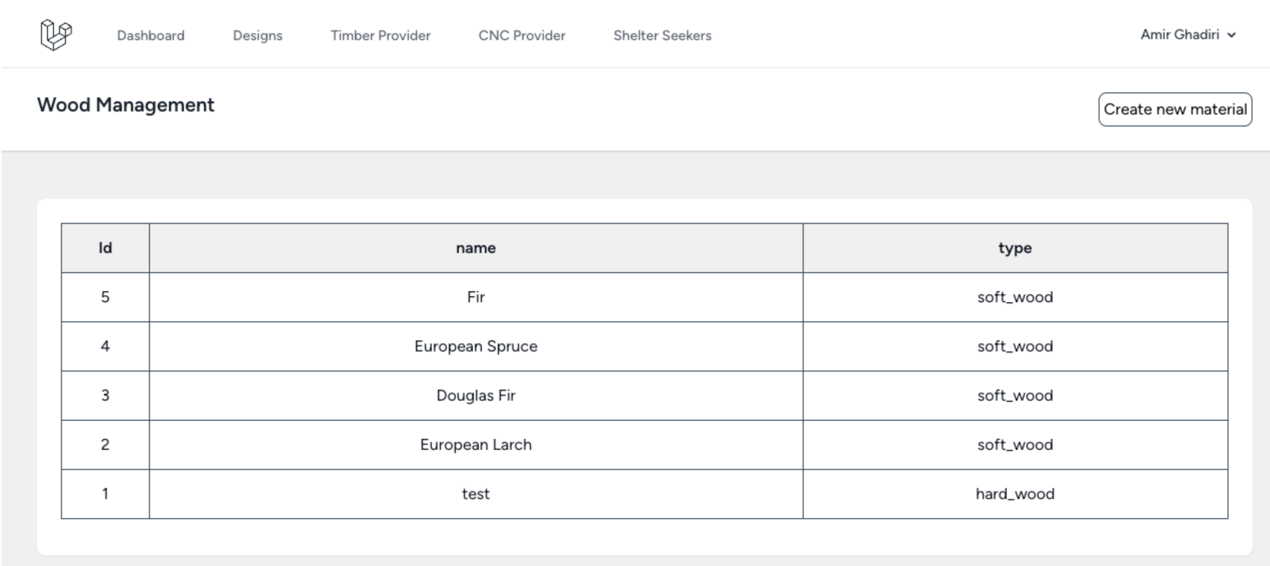

Id	name	type
5	Fir	soft_wood
4	European Spruce	soft_wood
3	Douglas Fir	soft_wood
2	European Larch	soft_wood
1	test	hard_wood

Figure 4.3: they have the option to utilize a built-in timber frame design module, lock n Load currently only supports one type of timber frame

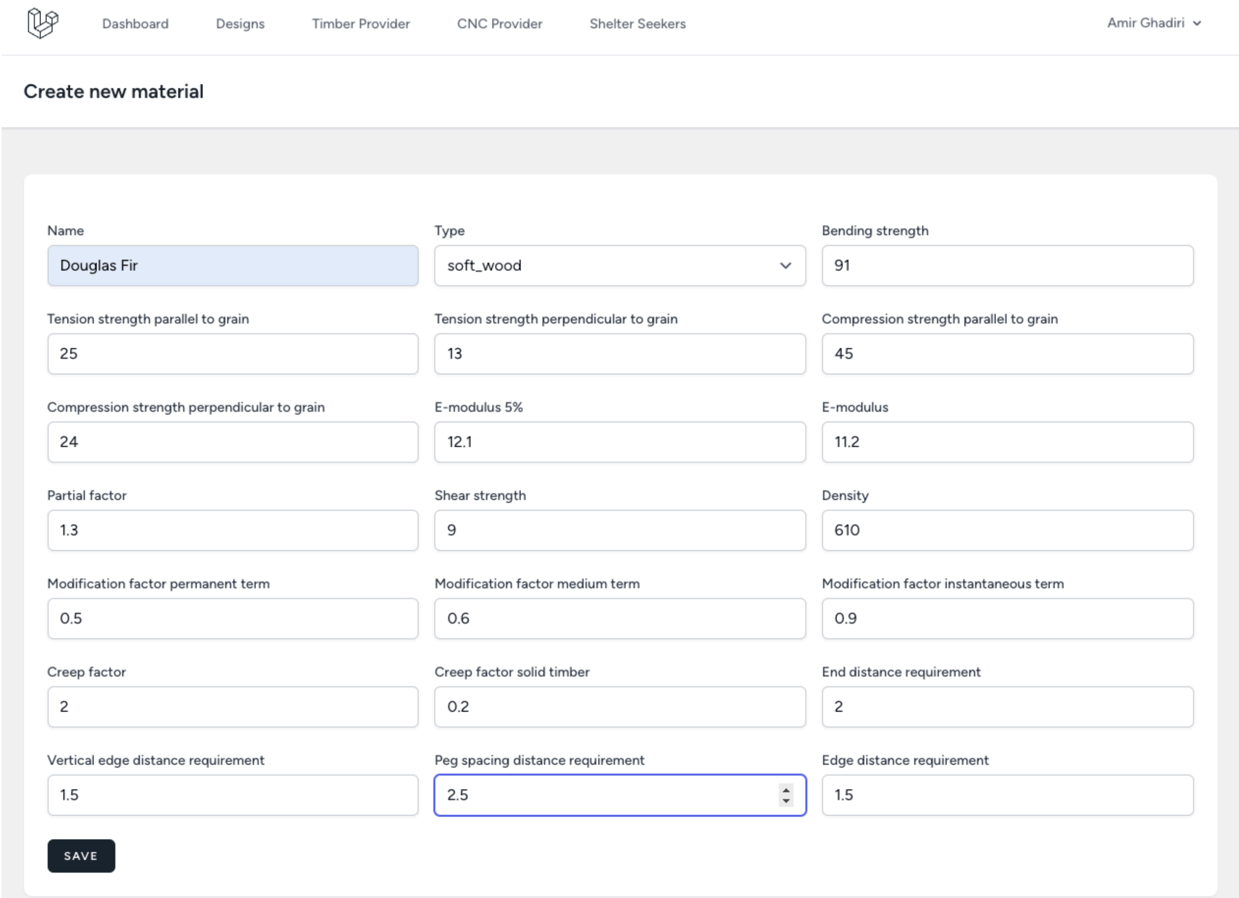

Figure 4.4: Material properties in one timber material block

Once the material properties have been selected, the user proceeds to input the predefined geometry variables for the structure, which include height, width, length, number of columns, and slab thickness (figure 4.5). This section empowers designers to further customize the timber shelter's dimensions according to their specific needs and preferences. Finalizing footprint inputs before load computation is essential, as the building's size and geometry directly influence the final load calculations.

After defining the material and geometry of the structure, the next crucial step is to determine the loads acting upon it. This tool offers users the flexibility to either manually input load values or utilize a built-in load calculator. Accurately calculating load combinations is essential in structural design. It ensures that structures can safely withstand various loads throughout their lifespan without unnecessary over-design. However, navigating the complexities of load combination requirements in standards like Eurocode can be challenging even for experienced designers.

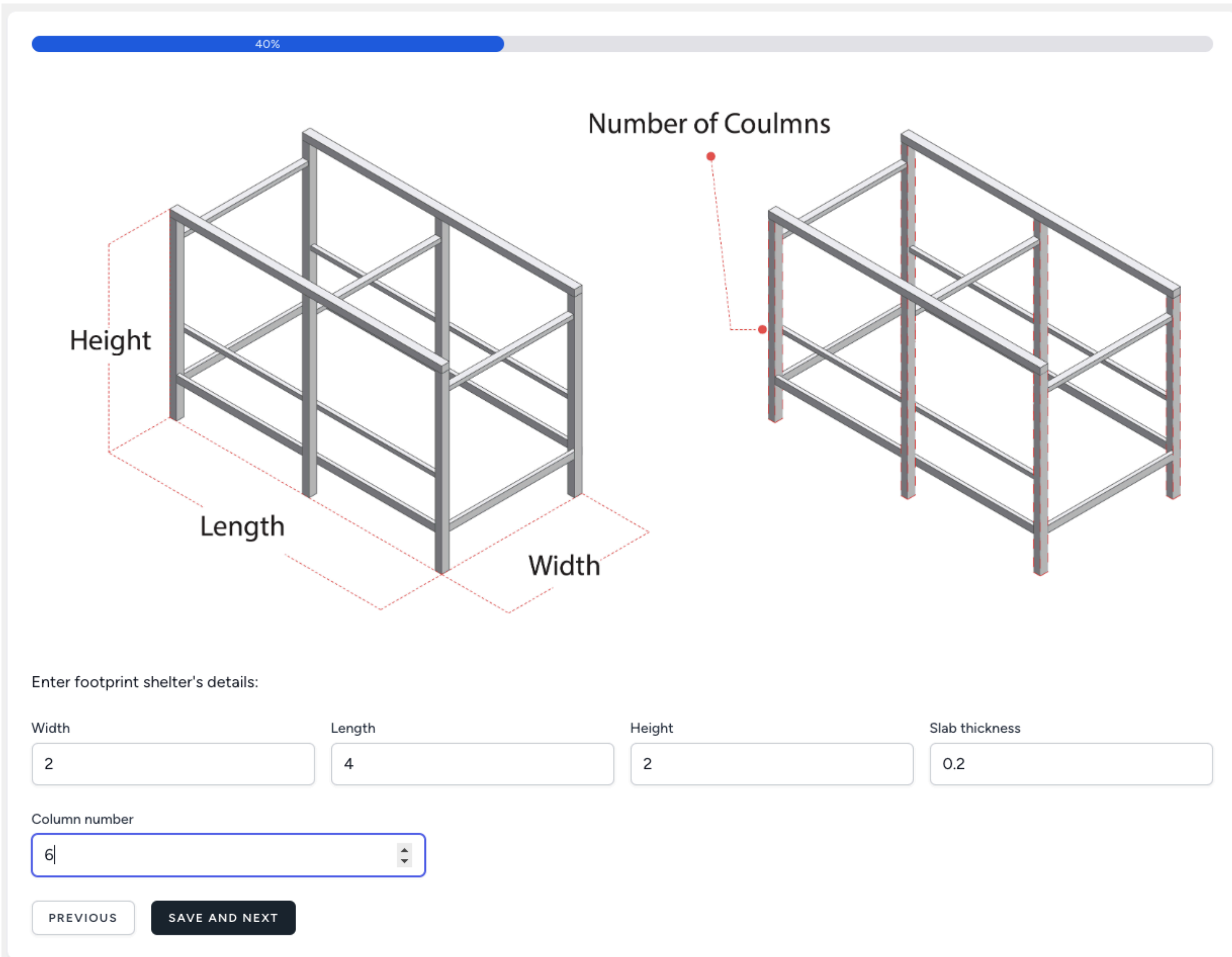

Figure 4.5: shelter footprint inputs

To address this, a Python-based load calculator script, detailed in Annex , has been integrated into the tool. This script simplifies the process of generating load combinations based on (EN 1990 6.10.) It assists designers in:

- **Optimizing and verifying new designs:** By accurately calculating the combined effects of various loads.

- **Checking the suitability of existing designs:** For specific locations and load conditions.

The load calculator generates load combinations for both **Ultimate Limit State** (ULS) and **Serviceability Limit State** (SLS) design scenarios. It considers **permanent**, **medium-term**, and **instantaneous** actions, providing the necessary factors for calculating combination values, **frequent values**, and **quasi-permanent** values of variable actions. This information is crucial for determining different types of deflection, including creep and net final deformation (illustrated in Figure 4.6).

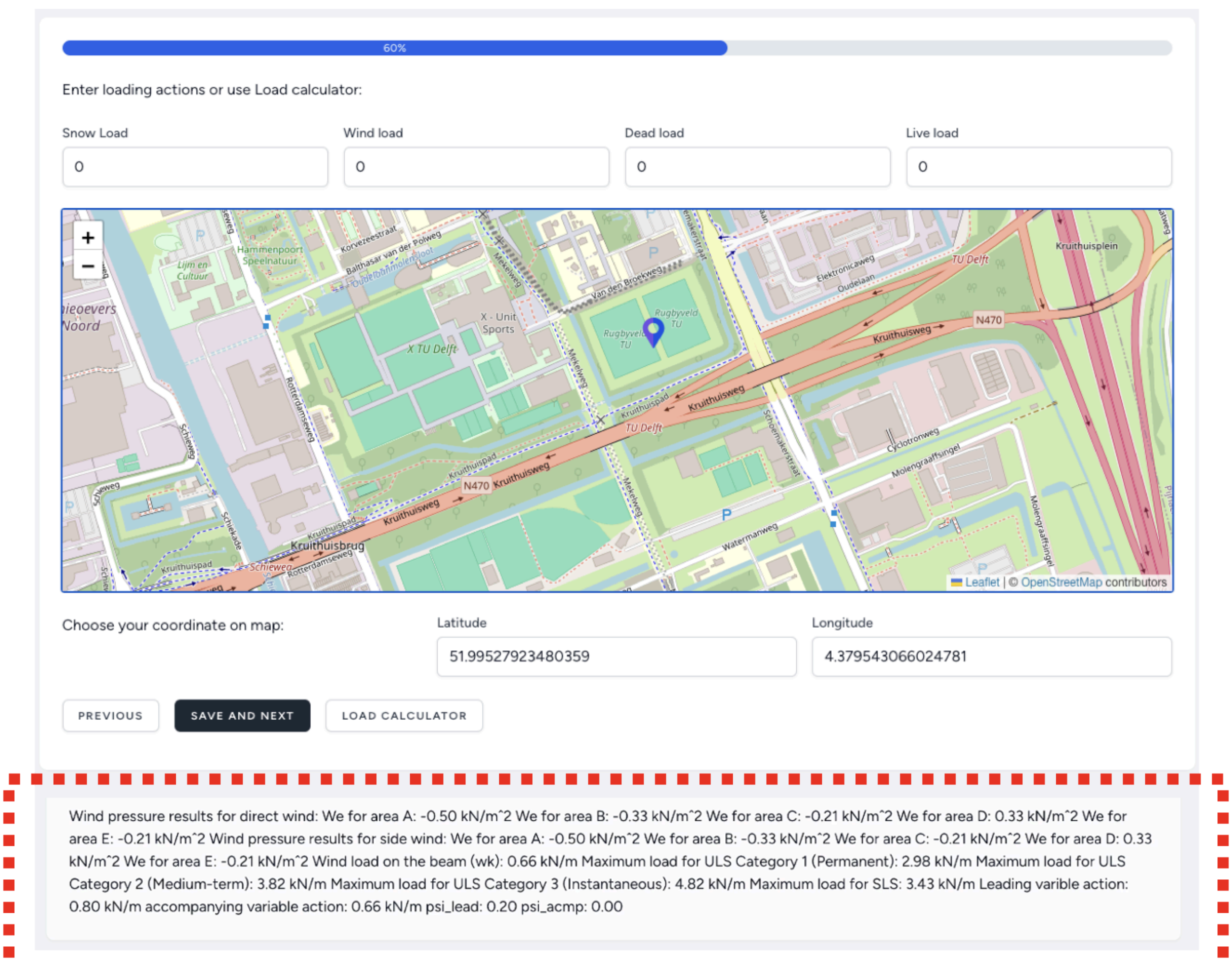

Figure 4.6: Load calculation outputs

By automating these calculations, the tool streamlines the design process, reduces the risk of errors, and ensures compliance with Eurocode requirements. This allows designers to focus on other critical aspects of structural design, confident that the load combinations are accurately and efficiently determined.

Once the loads on the structure have been determined, the next step involves defining the dimensions of its key supporting elements: primary beams, columns, bottom sills, and tie beams. Each of these elements is characterized by two key variables: width and thickness.

To facilitate this process, the tool offers users two distinct approaches:

1. **Direct Input:** Users with prior knowledge or specific dimensional requirements can directly input the desired width and thickness for each element. This allows for full control over the structural design (figure 4.7).

2. **Optimization:** Alternatively, users can leverage the built-in optimizer to determine the optimal dimensions for each element. This feature automatically calculates the most efficient width and thickness values based on the load calculations and predefined design constraints. This approach can help optimize material usage and structural performance (figure 4.8).

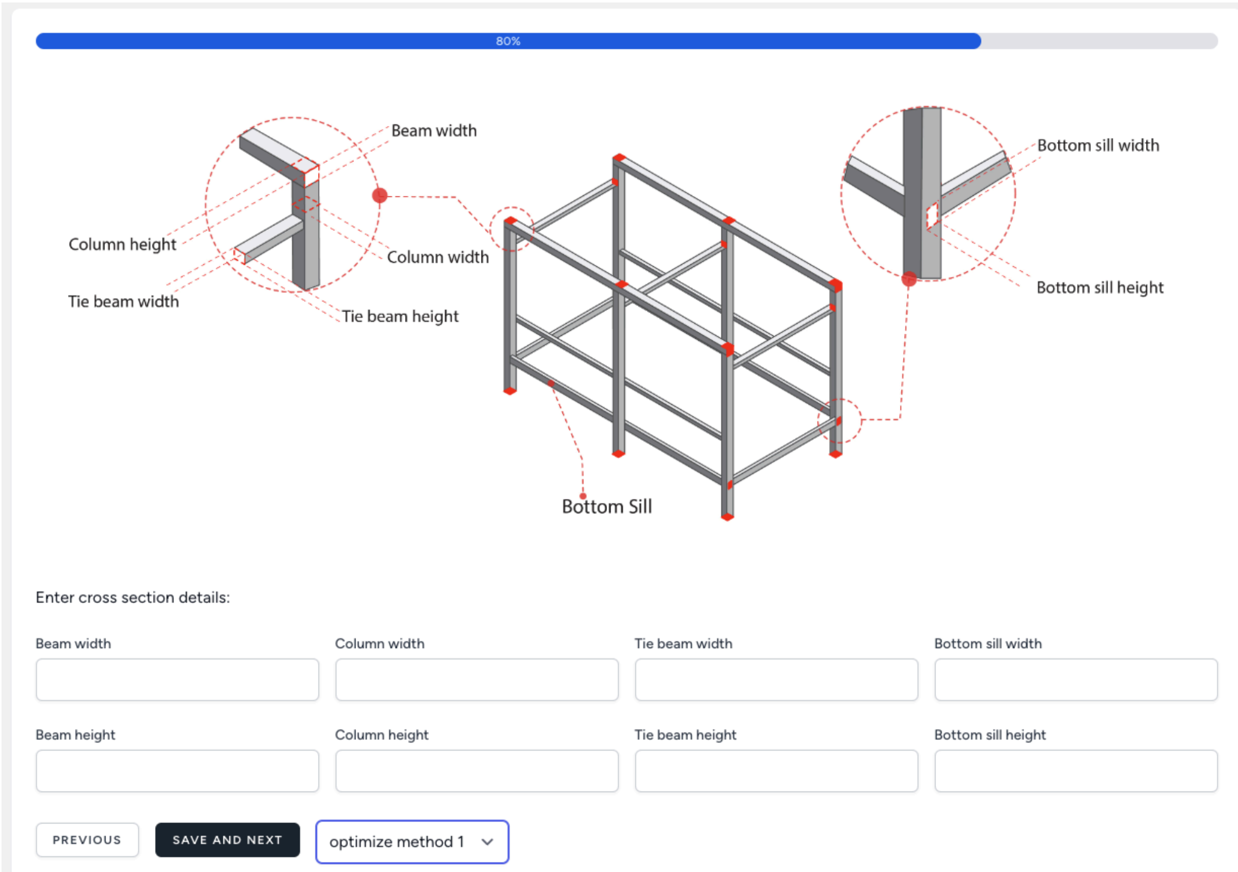

Figure 4.7: Manual inputs for cross-sectional design

bending_status : Acceptable, bending_utilisation : 26.27%, buckling_status_in_plane : Acceptable, buckling_status_out_of_plane : Acceptable, buckling_utilisation_in_plane : 2.98%, buckling_utilisation_out_of_plane : 11.13%, compression_status : Acceptable, compression_utilisation : 2.85%, final_utilisation : 86.75%, final_utilisation_status : Acceptable, length : 2.00 m, shear_status : Acceptable, shear_utilisation : 19.79%, sls_status : Acceptable, sls_utilisation : 86.75%, thickness : 149 mm, weight : 11.82 kg, width : 65 mm,

bending_status : Acceptable, bending_utilisation : 26.99%, buckling_status_in_plane : Acceptable, buckling_status_out_of_plane : Acceptable, buckling_utilisation_in_plane : 3.06%, buckling_utilisation_out_of_plane : 11.28%, compression_status : Acceptable, compression_utilisation : 2.88%, final_utilisation : 90.34%, final_utilisation_status : Acceptable, length : 2.00 m, shear_status : Acceptable, shear_utilisation : 20.06%, sls_status : Acceptable, sls_utilisation : 90.34%, thickness : 147 mm, weight : 11.66 kg, width : 65 mm,

bending_status : Acceptable, bending_utilisation : 27.74%, buckling_status_in_plane : Acceptable, buckling_status_out_of_plane : Acceptable, buckling_utilisation_in_plane : 3.14%, buckling_utilisation_out_of_plane : 11.44%, compression_status : Acceptable, compression_utilisation : 2.92%, final_utilisation : 94.13%, final_utilisation_status : Acceptable, length : 2.00 m, shear_status : Acceptable, shear_utilisation : 20.33%, sls_status : Acceptable, sls_utilisation : 94.13%, thickness : 145 mm, weight : 11.50 kg, width : 65 mm,

bending_status : Acceptable, bending_utilisation : 28.52%, buckling_status_in_plane : Acceptable, buckling_status_out_of_plane : Acceptable, buckling_utilisation_in_plane : 3.23%, buckling_utilisation_out_of_plane : 11.60%, compression_status : Acceptable, compression_utilisation : 2.97%, final_utilisation : 98.14%, final_utilisation_status : Acceptable, length : 2.00 m, shear_status : Acceptable, shear_utilisation : 20.62%, sls_status : Acceptable, sls_utilisation : 98.14%, thickness : 143 mm, weight : 11.34 kg, width : 65 mm,

bending_status : Unacceptable, bending_utilisation : 133.90%, buckling_status_in_plane : Acceptable, buckling_status_out_of_plane : Acceptable, buckling_utilisation_in_plane : 24.76%, buckling_utilisation_out_of_plane : 23.39%, compression_status : Acceptable, compression_utilisation : 6.33%, final_utilisation : 1013.75%, final_utilisation_status : Unacceptable, length : 2.00 m, shear_status : Acceptable, shear_utilisation : 44.00%, sls_status : Unacceptable, sls_utilisation : 1013.75%, thickness : 65 mm, weight : 5.31 kg, width : 67 mm,

bending_status : Unacceptable, bending_utilisation : 142.54%, buckling_status_in_plane : Acceptable, buckling_status_out_of_plane : Acceptable, buckling_utilisation_in_plane : 27.09%, buckling_utilisation_out_of_plane : 24.13%, compression_status : Acceptable, compression_utilisation : 6.53%, final_utilisation : 1113.40%, final_utilisation_status : Unacceptable, length : 2.00 m, shear_status : Acceptable, shear_utilisation : 45.40%, sls_status : Unacceptable, sls_utilisation : 1113.40%, thickness : 63 mm, weight : 5.15 kg, width : 67 mm,

bending_status : Unacceptable, bending_utilisation : 152.04%, buckling_status_in_plane : Acceptable, buckling_status_out_of_plane : Acceptable, buckling_utilisation_in_plane : 29.74%, buckling_utilisation_out_of_plane : 24.92%, compression_status : Acceptable, compression_utilisation : 6.74%, final_utilisation : 1226.54%, final_utilisation_status : Unacceptable, length : 2.00 m, shear_status : Acceptable, shear_utilisation : 46.89%, sls_status : Unacceptable, sls_utilisation : 1226.54%, thickness : 61 mm, weight : 4.99 kg, width : 67 mm,

Figure 4.8: cross-sectional options generated by iteration

Currently, Lock n Load features a weight optimization tool, similar to the one developed in the case study. This tool generates a variety of cross-sectional options for structural elements, each with its corresponding utilization factors for bending, shear, buckling, compression, and deflection, along with its respective weight. This allows users to assess the structural performance of various cross-sections while considering their weight. By providing these key performance indicators, the tool enables users to make informed decisions about the optimal cross-section for their design, balancing structural efficiency with weight minimization.

Lock n Load is designed to be adaptable to a wide range of user preferences and design approaches. By offering both manual input and automated optimization capabilities, it caters to users with varying levels of expertise and different design philosophies. This flexibility empowers users to tailor the structural design process to their specific needs.

For instance, experienced engineers who prefer hands-on control can directly input their chosen dimensions for each structural element. Conversely, users who seek efficiency or wish to explore optimal solutions can utilize the automated optimization feature to determine the most efficient dimensions based on predefined constraints and loading conditions. This dual approach ensures that Lock n Load remains a versatile and accessible tool for a broad user base.

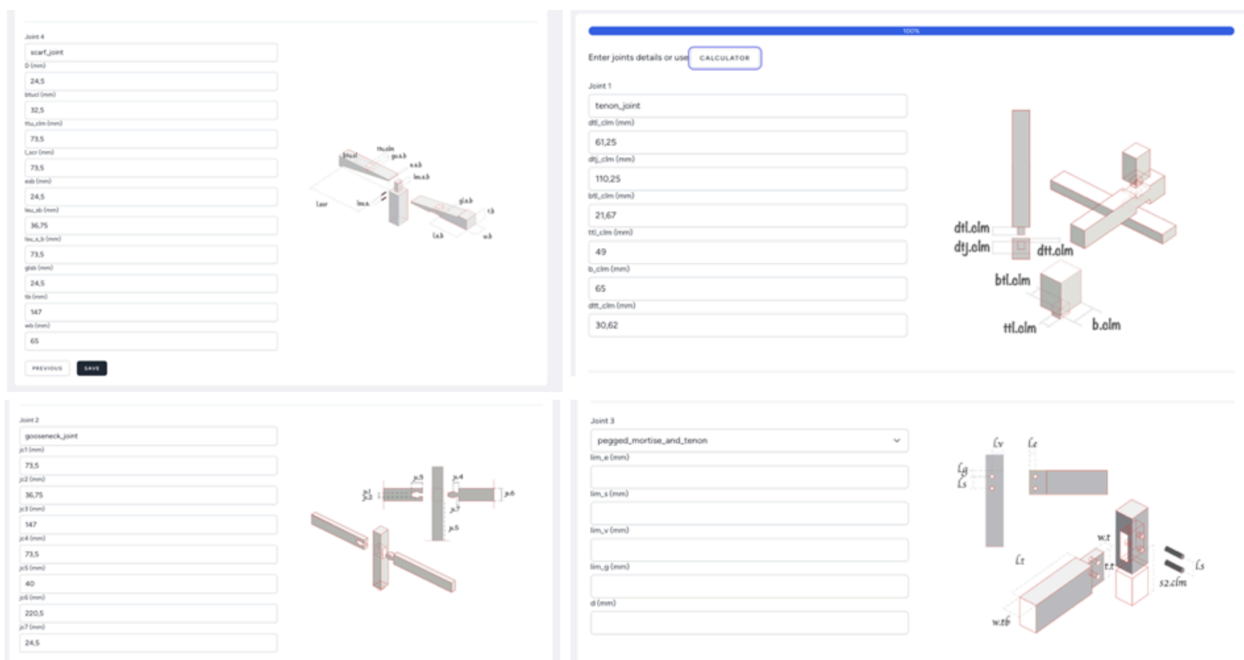

Figure 4.9: joint detail inputs

After determining the cross-sectional dimensions of the structural elements, the next stage in Lock n Load involves defining the connections between them. The system currently offers four families of joint types for users to choose from, providing a range of established connection design methods (figure 4.9).

However, recognizing the need for flexibility and customization, Lock n Load also allows expert users to define new joint types and integrate their own analytical methods through a dedicated

API. This feature empowers users to expand the system's capabilities by incorporating specialized or innovative connection design approaches, making them accessible to other designers.

This thesis demonstrates this functionality by incorporating the "equivalent steel bolt" method for the design and optimization of PMT joints, developed gooseneck joint method, and scarf joint. Furthermore, a material-specific method was developed and implemented specifically for Douglas Fir timber. This exemplifies how Lock n Load can be extended to accommodate diverse joint design methodologies and cater to the specific requirements of different materials.

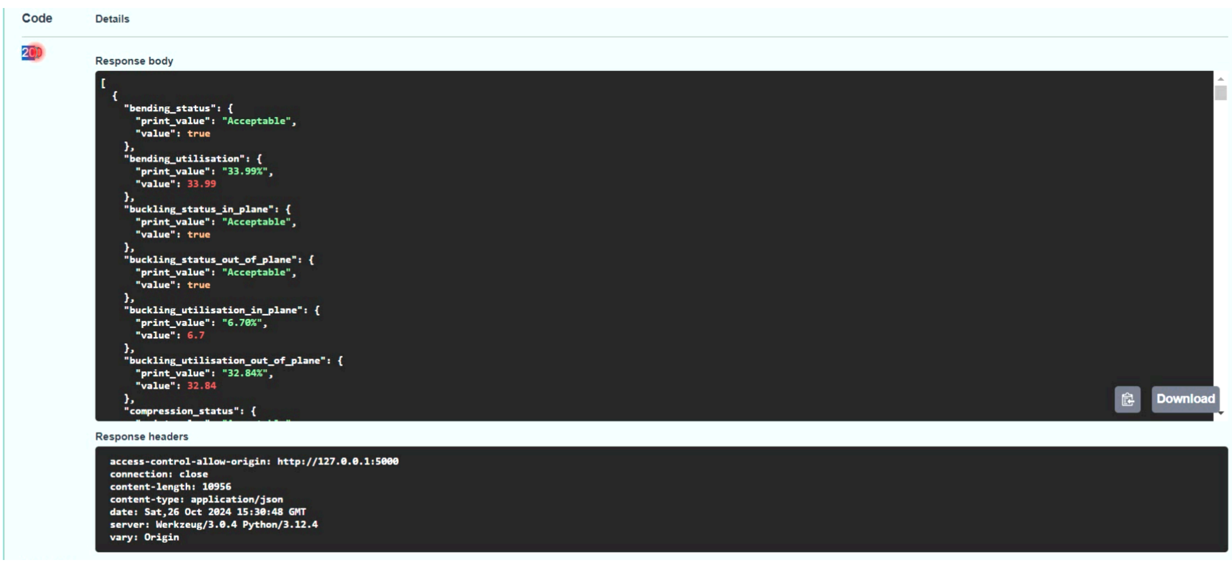

Figure 4.10: API Input panel for developing methods

Once all the geometric details for each of the four joints within the structural frame have been specified, Lock n Load generates a comprehensive report detailing both the structural performance and design specifics (figure 4.11). This report is structured in "**design blocks**", each providing a detailed breakdown of the individual components: beams, columns, tie beams, and joints. Within each block, users can find information on the chosen dimensions, materials, and connection details, along with an assessment of the element's structural performance, including utilization factors and deflections. Furthermore, the report provides an overall assessment of the entire structure's performance, considering the combined effects of all elements and the specific loading conditions at the design location. This holistic evaluation allows users to verify the adequacy of their design and ensure it meets all safety and serviceability requirements. This output is then saved as a distinct design block within the design library, making it readily available for future reference.

Figure 4.11: data set in one block of design

Timber and CNC Provider

Lock n Load incorporates the crucial role of timber providers in the construction process by allowing them to actively participate in the platform. Timber providers can register on the system and create a "supply point" by specifying their location on a map (figure 4.12). They can also indicate their delivery radius, specifying how far they are willing to transport timber to CNC fabricators. This information is then displayed to shelter-seekers, enabling them to choose a provider based on proximity and availability. Furthermore, timber providers can specify the types of timber they currently have in stock from the material library. To ensure accuracy, they can access a database of timber properties to verify the characteristics of their stock. This material selection feature plays a crucial role in matching shelter-seekers with suitable shelter designs based on the locally available timber. This localized approach promotes resource efficiency and reduces transportation costs and environmental impact.

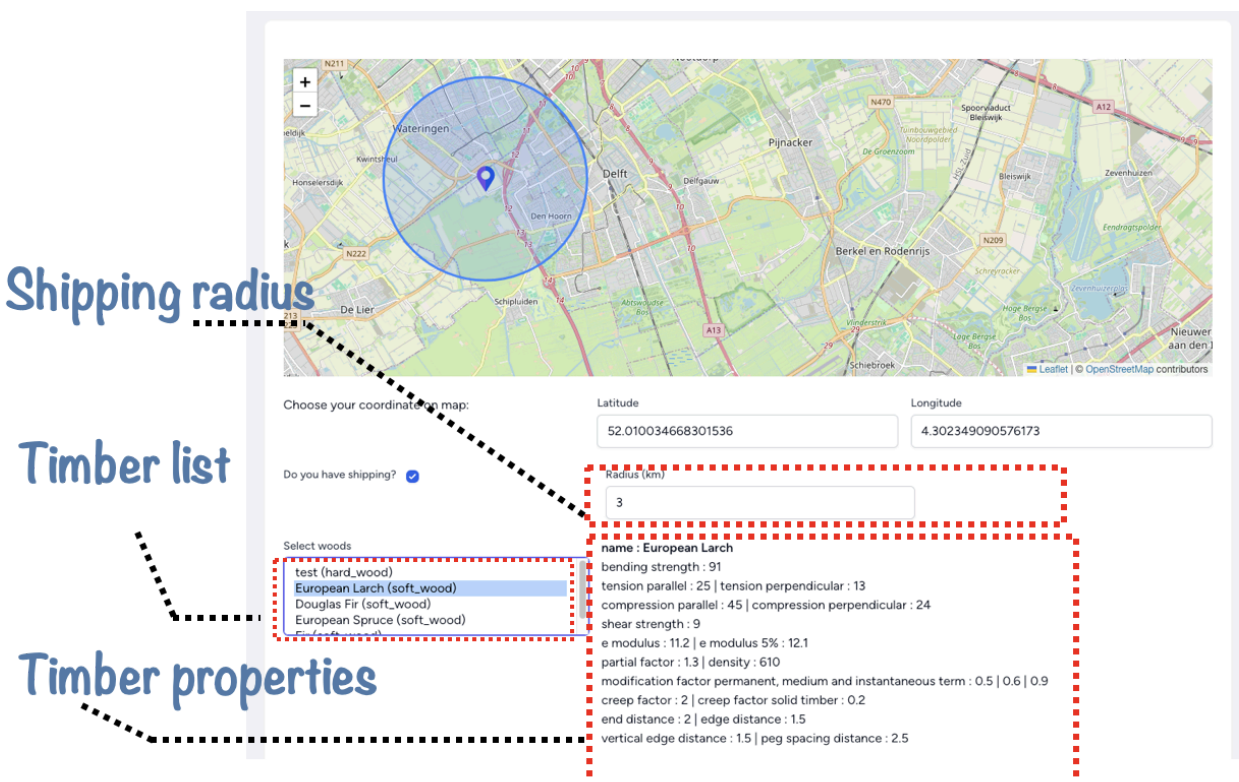

Figure 4.12: timber supplier panel

In the Lock n Load workflow, after timber is sourced from a provider, it is shipped to a CNC fabricator for cutting and fabrication of the structural elements. Similar to timber providers, CNC fabricators can register on the platform and specify their location, enabling the calculation of transportation distances for both timber providers and shelter-seekers (figure 4.12). This location information is crucial for several reasons:

- **Efficient logistics:** Timber providers can determine the shipping distance to various CNC fabricators, facilitating efficient logistics.
- **Accessibility for shelter-seekers:** Shelter-seekers can identify CNC fabricators within a reasonable distance for receiving their ready-to-assemble structural components. CNC providers can also specify their delivery radius for these finished elements.
- **Localized supply chain:** By connecting shelter-seekers with local timber providers and CNC fabricators, Lock n Load promotes a localized and sustainable supply chain, minimizing transportation distances and associated costs and environmental impact.

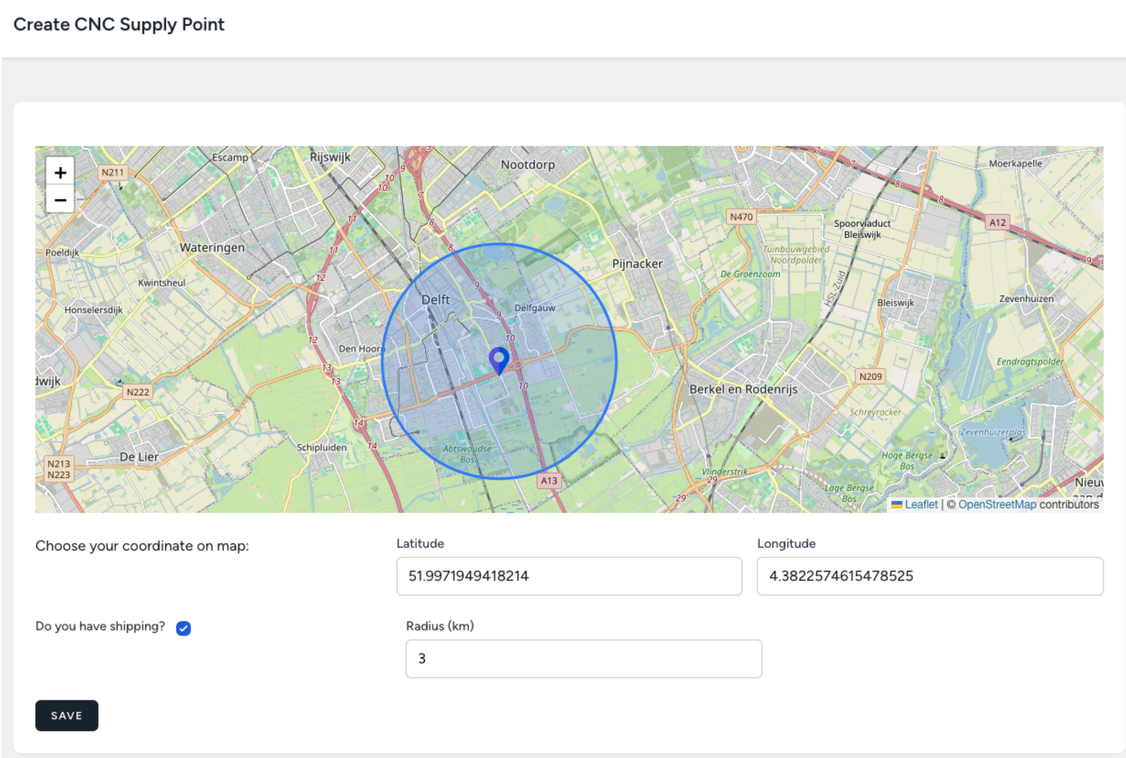

Figure 4.13: CNC supplier panel

This system ensures a streamlined and transparent process, connecting all stakeholders and facilitating efficient collaboration between timber providers, CNC fabricators, and shelter-seekers.

Shelter-Seekers panel

Lock n Load streamlines the process of obtaining a customized timber shelter by guiding shelter-seekers through a series of steps. Upon entering the shelter-seeker panel, users are prompted to define their desired shelter dimensions (maximum and minimum height, width, and length). This customization allows for shelters tailored to individual needs and facilitates the selection of suitable designs from the available options (figure 4.14).

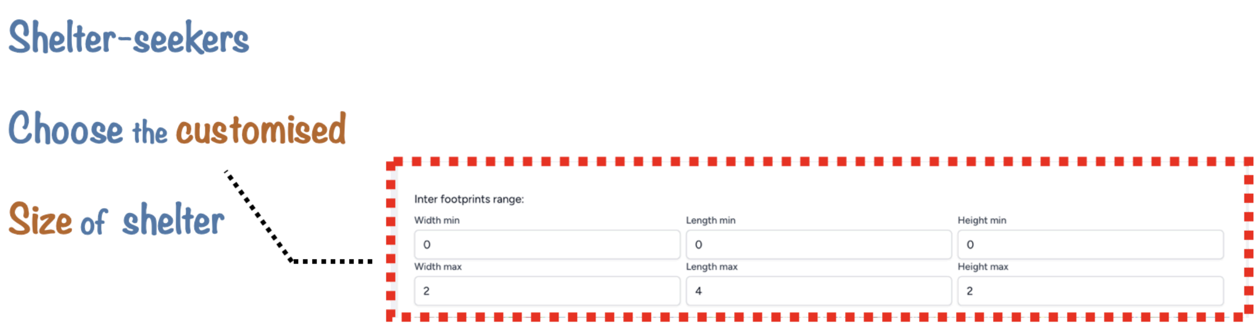

Figure 4.14: size inputs from shelter-seekers

Next, shelter-seekers specify their location on a map. This triggers the "load verifier" tool, which analyzes the structural design library database and environmental load data to identify shelter designs capable of withstanding the specific conditions at that location (figure 4.15).

The filtered designs are then presented to the user, who can proceed to select a timber provider and the desired timber species. This further refines the available options, ensuring that the chosen shelter can be constructed using locally sourced materials. Subsequently, shelter-seekers can select a CNC fabricator based on proximity and delivery radius to ensure efficient processing and delivery of the prefabricated components (figure 4.16).

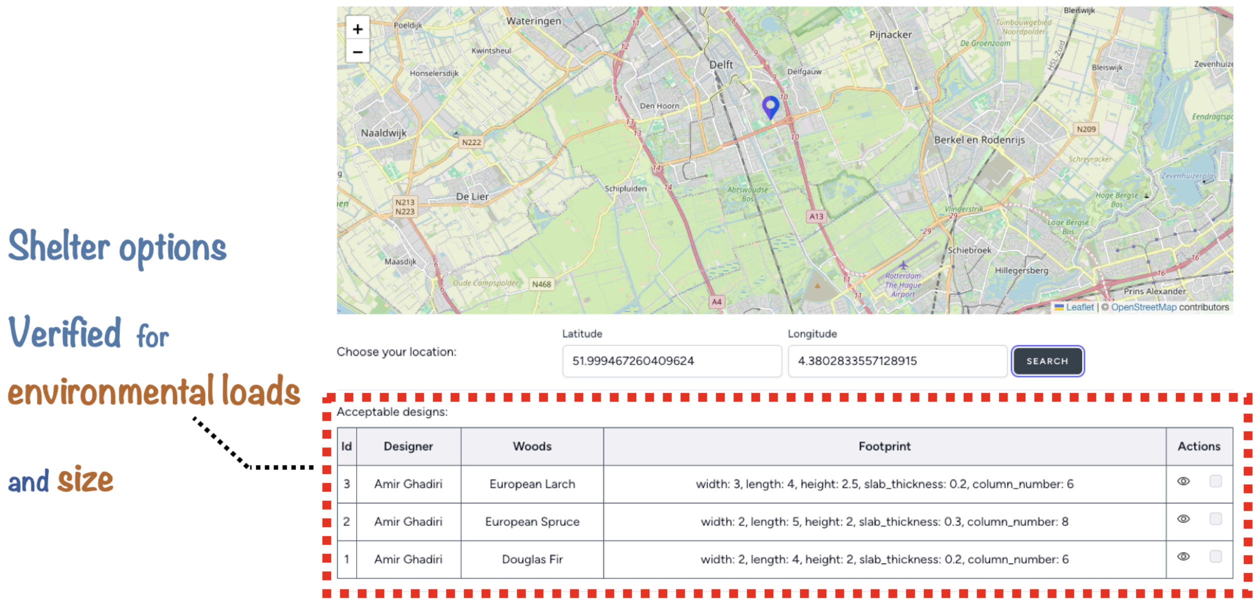

Figure 4.15: filtered design blocks based on environmental loads and sizing constraints

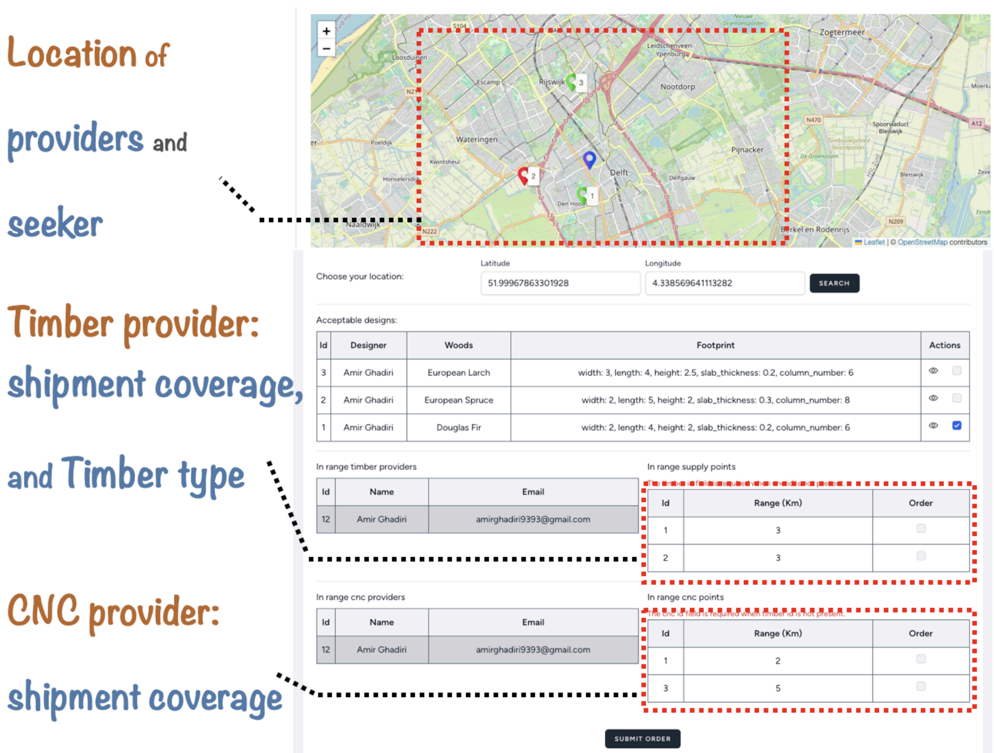

Figure 4.16: CNC and timber provider selection inputs

Once the order is submitted, Lock n Load automatically generates the necessary G-code instructions for the CNC fabrication process and sends them to the chosen provider. Simultaneously, the timber provider receives an order for the required timber, initiating the material supply chain. This automated workflow ensures seamless coordination between all stakeholders and facilitates the efficient delivery of customized timber shelters (figure 4.17).

Figure 4.17: G-code generated and sent to CNC-provider order box

How Lock n Load Works: The Technical Details

Lock n Load employs a scalable web development architecture, utilizing **Laravel** for its **backend** framework and **JavaScript** for its **front-end** development. Specifically, **PHP** is used as the programming language for developing the backend within the Laravel framework.

To ensure a well-organized and maintainable codebase, the **Model-View-Controller (MVC) architectural pattern** is employed. This pattern separates the application into three interconnected components:

- **Model:** Handles data logic and interaction with the database.
- **View:** Manages the presentation layer and user interface.
- **Controller:** Acts as an intermediary between the Model and View, handling user requests and business logic.

This separation of concerns offers several advantages:

- **Improved code organization:** MVC promotes a clear and structured codebase, making it easier to understand, navigate, and maintain.
- **Enhanced testability:** Individual components (models, views, and controllers) can be tested independently, facilitating thorough testing and debugging.
- **Increased scalability and extensibility:** The modular nature of MVC simplifies the process of adding new features or modifying existing ones, enhancing the platform's scalability and adaptability to future needs.

By leveraging the Laravel framework and adhering to the MVC pattern, Lock n Load benefits from a robust and well-structured foundation, ensuring its maintainability, scalability, and future-proofing.

While Laravel and JavaScript provide the foundation for the web application, **Python** plays a crucial role in powering the core structural design and analysis capabilities.

Specifically, Python is used to develop and implement the structural design methods and perform the necessary computations. This includes algorithms for:

- **Structural analysis:** Calculating stresses, deflections, and other critical performance parameters.
- **Optimization:** Determining optimal cross-sectional dimensions and joint configurations.
- **Load verification:** Assessing the structural adequacy of designs under specific loading conditions.
- **G-code generation:** Generating CNC fabrication instructions.

To seamlessly integrate these Python-based functionalities into the web platform, a dedicated **API** was developed using **Flask**, a lightweight Python web framework. This **API** allows the Laravel backend to communicate with the Python modules, enabling efficient data exchange and execution of the structural design processes.

Backend framework of Lock n Load

The backend of Lock n Load is built on a robust and versatile architecture, primarily utilizing PHP within the Laravel framework. To manage user data and interactions, a **CRUD** (Create, Read, Update, Delete) system was implemented in **PHP**, enabling efficient handling of user information within the database. However, for certain functionalities, such as displaying material properties from the database, **jQuery** is employed to enhance the user interface and data presentation.

The design process within Lock n Load involves multiple layers, including footprint definition, cross-section selection, and joint design. To manage this **multi-step process**, design data is temporarily stored in a session rather than being immediately saved to the database. This approach ensures data integrity and allows for modifications throughout the design process until the finalization stage. The session mechanism, alongside managing user login data, also securely stores this temporary design information.

For location-based functionalities, Lock n Load integrates **OpenStreetMap**. The **JavaScript API** provided by OpenStreetMap enables the retrieval of various geographical data, including latitude and longitude coordinates, which are crucial for determining user location, provider proximity, and transportation distances.

Integration with the **Python-based** structural analysis modules is achieved through a dedicated **API** developed using **Flask**. When specific Python functionalities are required, such as structural calculations or G-code generation, the Laravel backend communicates with the Flask API via **POST requests**. These requests include validated input data, and the API returns a **JSON** response containing the results ("**print value**" and "**value**") as depicted in Figure 4.18. Error handling is implemented to ensure data integrity, with the API returning a non-200 OK status code in case of invalid input.

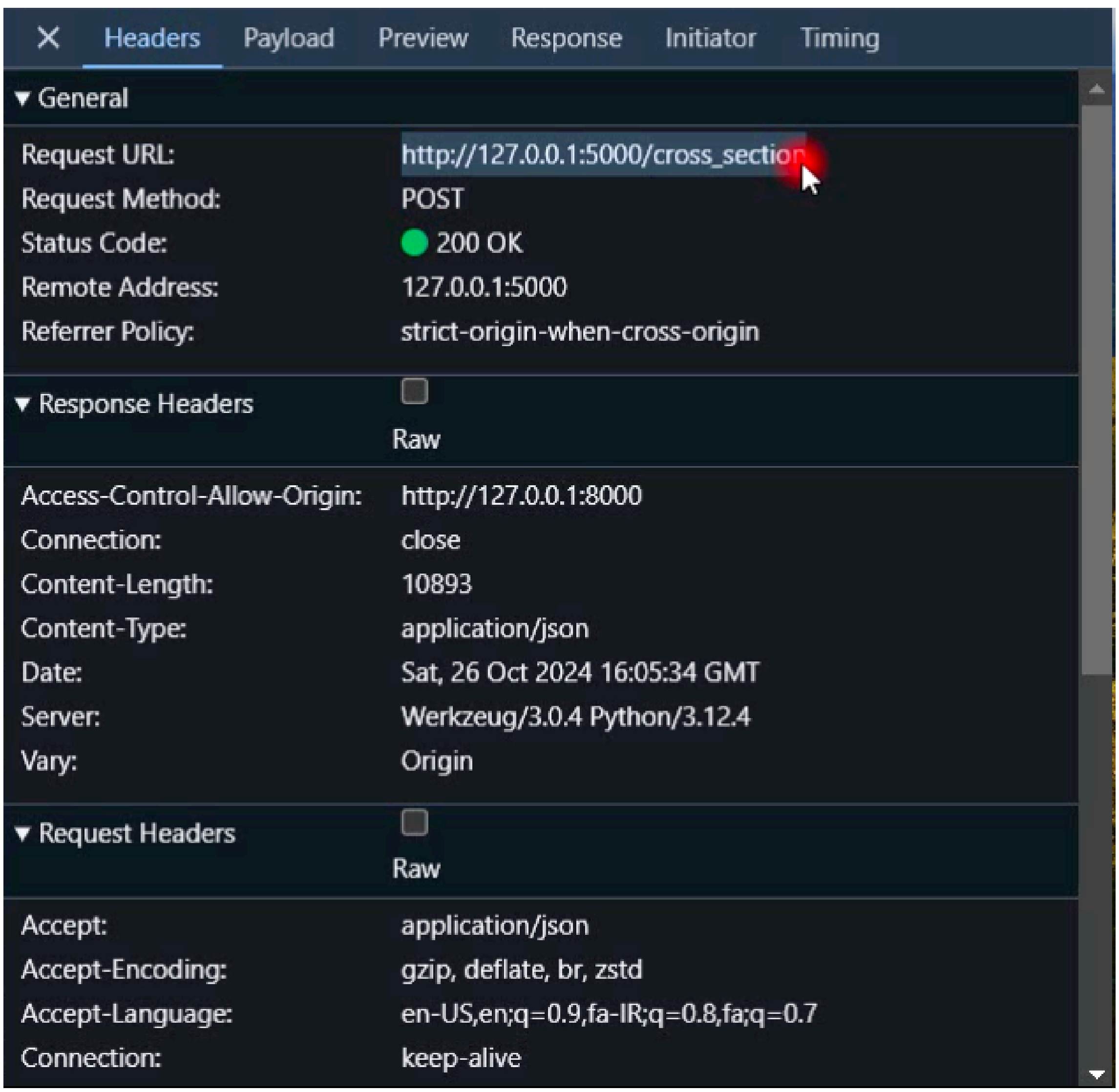

Figure 4.18: API communication panel with Flask URL

To facilitate the selection of suitable providers, Lock n Load utilizes **jQuery** to send shelter-seeker location data to the CNC and timber provider APIs. This enables the system to filter and display providers whose shipment radius covers the seeker's location, as illustrated in figure 4.19. This dynamic filtering ensures that users are presented with relevant and accessible options for material supply and fabrication.

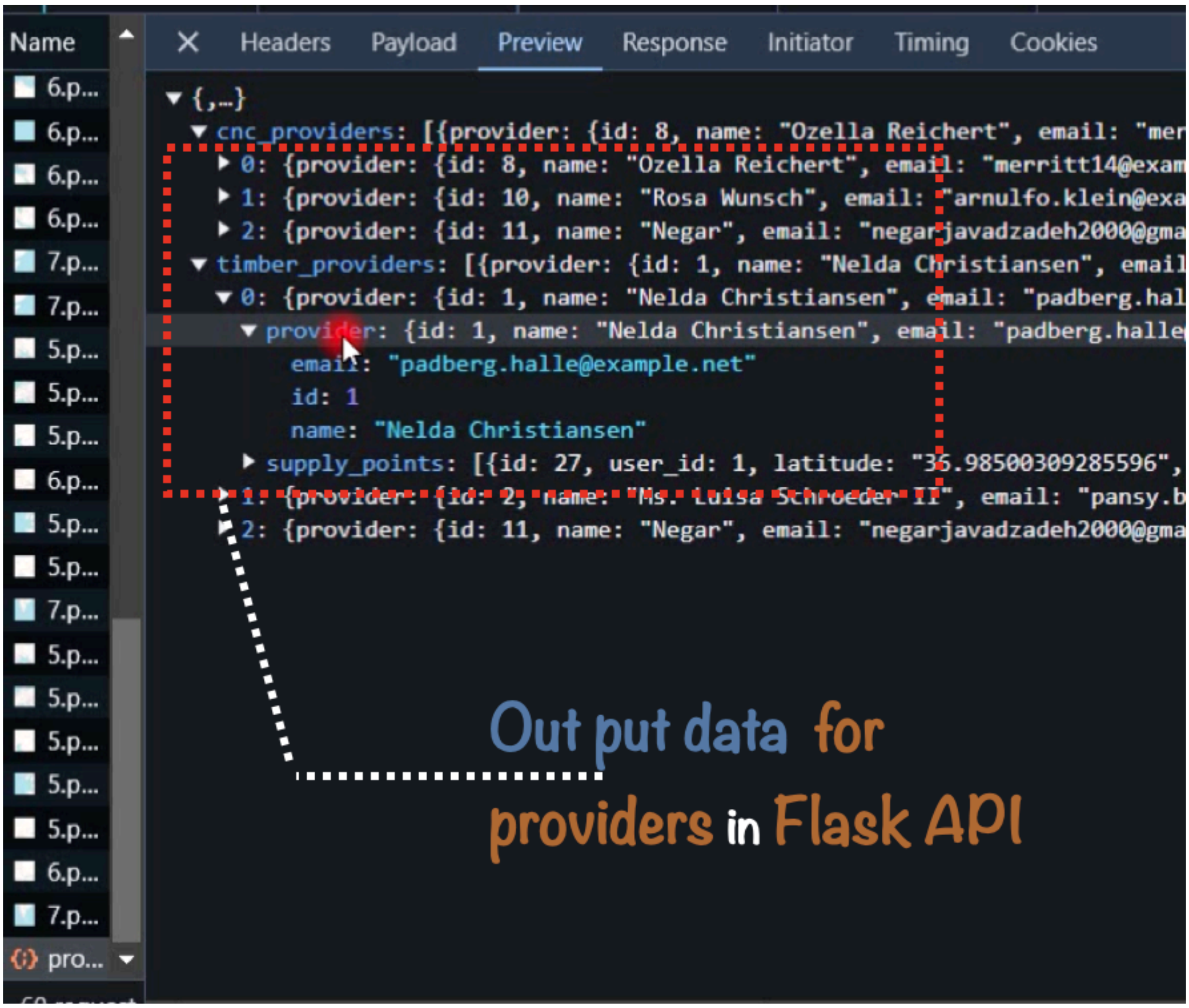

Figure 4.19: Output providers ID form FLASK API

Load Calculator

To automate the process of load combination alongside the values and factors mentioned above, load combinations according to Eurocode also include five components of the characteristic load value: **snow**, **wind**, **dead**, **seismic**, and **live** actions. However, in this tool, seismic loads are not covered, though it is recommended that they be considered in the future development. To calculate wind action, three main functions were defined: **wind pressure calculator**, the **peak wind velocity pressure calculator**, and the **wind load calculator on elements**. The peak wind velocity calculator includes several sub-functions that compute necessary values and factors which are: **Turbulence Intensity** (*Iv*), **Turbulence factor** (*kl*), **Terrain facto**r (*kr*), **Roughness factor** (*cr*), **Roughness Length** (*z0*). **The fundamental value of the basic wind velocity (*vb.0*)**, which is location-specific, is obtained from external online sources (as of the time of writing this thesis, © 2001–2024 Dlubal Software GmbH). The wind pressure calculator computes the wind pressure on the external surfaces of the shelter (***we***) by multiplying the peak wind velocity by the external pressure coefficient for the five different wind action zones defined in EN-1991-1-4.

The mechanism of calculating three actions of snow, live, and dead actions are similar. First the total effect of these actions is calculated on the shelter, then based on the vertical or horizontal nature of the elements the computing for load distribution is done. To calculate the snow load, the primary required value is the **characteristic snow load** (s_g). This value is multiplied by the snow load **shape coefficient**, **exposure coefficient**, and **thermal coefficient**, which are constant in our case due to the flat-roofed timber structure. To calculate the dead and live loads, the slab thickness must be specified by the users, and the timber density is obtained from the material database. For the live load calculation, Category A for floors with an area load (q_k) of 1.5 kN/m² is considered.

The calculator is developed in python (appendix), and defines several functions to calculate different types of loads on a structure according to Eurocode standards. Here's a breakdown of each function:

- **peak_wind_velocity_calculator**: This function calculates the peak wind velocity pressure based on parameters like basic wind velocity, height above ground, terrain factor, and turbulence factors, as defined in EN 1991-1-4. It calculates the mean wind velocity and turbulence intensity before ultimately determining the peak wind velocity pressure.
- **wind_pressure_calculator**: This function calculates the wind pressure on external surfaces using the peak wind velocity pressure and external pressure coefficients from EN 1991-1-4.
- **wind_load_on_elements**: This function calculates the wind load on individual structural elements by multiplying the wind pressure with the element's area.
- **snow_load**: This function calculates the snow load on a flat roof based on the characteristic ground snow load and various coefficients from EN 1991-1-3.
- **dead_load**: This function calculates the dead load of a structural element based on its material density, thickness, and area.
- **live_load**: This function calculates the live load on a floor using the specified area load and the floor area.

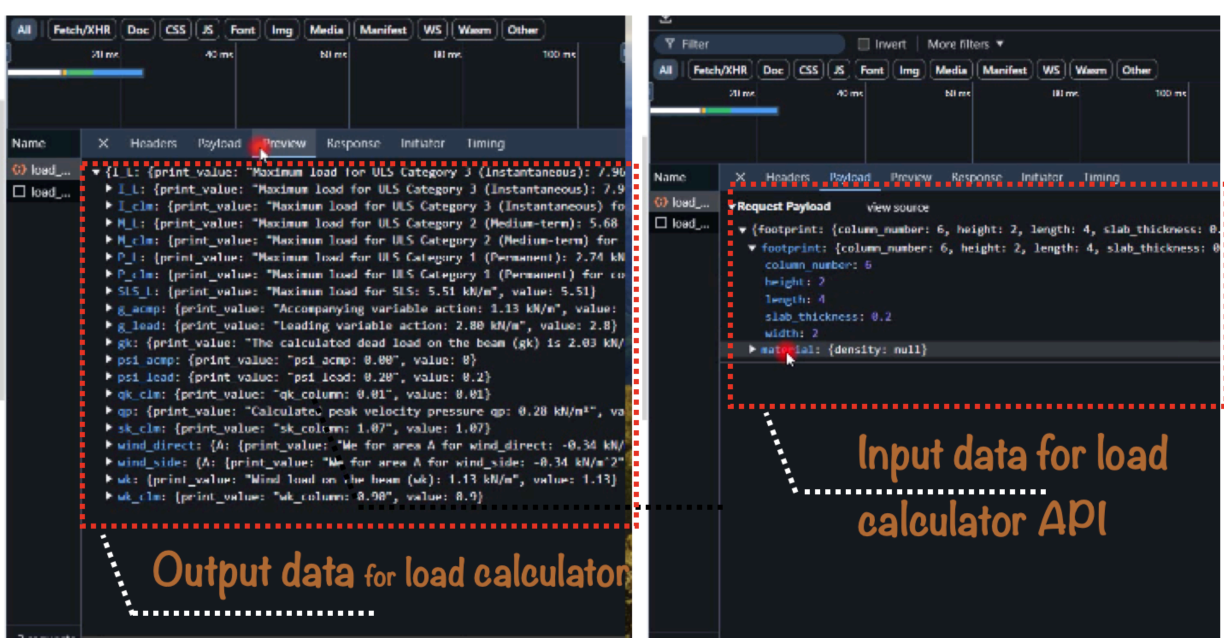

Figure 4.20: Output providers ID form FLASK API

Integration with Lock n Load:

This Python code is integrated with the Lock n Load platform through a Flask API. When a user inputs design parameters and location information, the Laravel backend sends a request to the Flask API, which executes the relevant Python functions to calculate the loads. The results are then returned to the backend in JSON format, allowing the platform to display the load values and proceed with the structural design process (figure 4.20).

Automated G-code Generation for CNC Milling of "Lock n Load" Joints

This section details the development of a Python-based (appandix) G-code generator for PMT joints and tie beams, however the G-CODE generator does not provide G-codes for other elements. For the PMT joint, a secure woodworking joint characterized by a through mortise, a mating tenon, and perpendicular peg holes for reinforcement. The generator aims to automate the CNC milling process for this joint, enhancing precision and efficiency in fabrication.

Joint Design and Parameters

The "Lock n Load" joint, as illustrated in the accompanying diagram, consists of:

- **Mortise:** A rectangular cavity that passes entirely through the first workpiece.
- **Tenon:** A protruding rectangular section on the second workpiece, sized to fit snugly into the mortise.
- **Peg holes:** Two perpendicular holes drilled through both the mortise and tenon, accommodating cylindrical pegs for added strength and stability.

The Python script allows for customization of the following parameters:

- **Mortise:** Width, height, and depth.
- **Tenon:** Width, height, and length.
- **Peg holes:** Diameter and depth.
- **Milling:** Tool diameter, feed rate, spindle speed, and step-down depth per pass.

G-code Generation Algorithm

The Python script employs a modular approach, defining functions for key milling operations:

- `mill_pocket()`: Generates G-code for milling rectangular pockets, incorporating multiple passes with a specified step-down depth to ensure complete material removal.
- `drill_hole()`: Generates G-code for drilling holes, with the option to include drilling cycles (e.g., G81) if supported by the CNC machine.

The main G-code generation function orchestrates these operations, first milling the mortise and tenon pockets, then drilling the peg holes through both workpieces. The generated G-code adheres to standard conventions, including:

- **G21:** Units in millimeters.
- **G17:** XY plane selection.
- **G90:** Absolute coordinates.
- **F:** Feed rate specification.
- **S:** Spindle speed specification.

Assumptions and Limitations

The current implementation operates under these assumptions:

- Workpiece origin (X0, Y0, Z0) is set at the top-left corner.
- A flat end mill is used for milling operations.
- The CNC machine has a safe Z clearance height defined.
- Basic G-code commands and potentially drilling cycles are supported.

Limitations include:

- Simplified toolpath strategies.
- No optimization for tool changes or material properties.
- Reliance on consistent workpiece setup and fixturing.

ASSUMPTION:
The workpiece origin (X0, Y0, Z0) is set at the top-left corner of the workpiece.

- The tool is a flat end mill suitable for cutting the workpiece material.
- The CNC machine has a safe Z clearance height for rapid moves.
- The machine supports basic G-code commands and potentially drilling cycles (e.g., G81).
- **Single Pass:** The `mill_rectangle` function only makes a single pass around the perimeter of the mortise and tenon. This would leave a lot of material in the middle. You would need multiple passes with progressively deeper cuts or a wider tool to fully clear the material.
- **No Pockets:** It doesn't account for creating the actual "pocket" of the mortise. It just cuts a shallow perimeter. Proper milling would involve clearing out the entire area within the mortise.
- **Drilling Only:** The `drill_hole` function only drills straight down. To create proper peg holes, you'd likely need to use a drilling cycle (like a G81 or similar) that handles pecking or retracting to clear chips.

Structural Optimizer and verifier

The weight optimization module in Lock n Load aims to provide users with the most weight-efficient cross-sections for their structural elements while ensuring that all design requirements are met. This is achieved through an evaluation of a range of possible cross-sectional dimensions, considering various load cases and design code provisions. Python code can be found in the appendix.

Workflow:

1. **Input Parameters:** The optimizer takes as input the material properties (strength, modulus of elasticity, density, etc.), loading conditions (forces, moments, etc.), and geometric constraints (length of the element). These parameters can either be user-defined or automatically retrieved from previous design steps within Lock n Load.

2. **Dimension Iteration:** The code iterates through a predefined range of widths and thicknesses for the cross-section. For each combination, it calculates the cross-sectional properties such as area, moment of inertia, and section modulus.

3. **Structural Analysis:** For each cross-section, the code performs structural analysis checks according to Eurocode 5:

   - **Bending Stress:** Calculates the maximum bending stress and compares it to the allowable bending strength of the material.
   - **Shear Stress:** Calculates the maximum shear stress and compares it to the allowable shear strength.
   - **Deflection:** Calculates the instantaneous and final deflections and compares them to the allowable limits for serviceability limit states (SLS).
   - **Compression:** Calculates the compressive stress and compares it to the allowable compressive strength.
   - **Buckling:** Checks for buckling failure in both the major and minor axes of the column, considering the slenderness ratio and instability factors.
4. **Utilization Calculation:** For each check, a utilization factor is calculated as the ratio of the applied stress/deflection to the allowable stress/deflection. This provides a measure of how much of the element's capacity is being utilized.

5. **Acceptability Check:** The code verifies whether each utilization factor is less than 100%. If any check fails, the cross-section is deemed unacceptable.

6. **Weight Calculation:** The weight of the element is calculated based on its volume and material density.

7. **Result Compilation:** The results, including weight, dimensions, utilization factors, and status (acceptable/unacceptable), are compiled for all considered cross-sections.

8. **Output:** The results are sorted by weight and presented to the user. This allows the user to select the lightest cross-section that satisfies all design requirements.

Code Structure and integration with Flask API:

The provided Python code effectively implements this workflow. It defines functions for calculating various loads, stresses, and utilization factors. The `main` function iterates through the dimensions, performs the structural analysis, and compiles the results.

The Python code for weight optimization in Lock n Load is seamlessly integrated into the platform through a combination of API endpoints and data exchange mechanisms. This integration allows the web application, built with Laravel and JavaScript, to leverage the computational power of Python for structural analysis and optimization (figure 4.21).

Figure 4.21: Output for structural verifier form FLASK API

Here's a breakdown of the integration process:

1. **Flask API:** The Python code, including the optimization algorithms and structural analysis functions, is exposed as a RESTful API using Flask, a lightweight Python web framework. This API defines specific endpoints that can be accessed by the Lock n Load backend.

2. **API Endpoints:** Each endpoint corresponds to a specific functionality, such as calculating loads, performing structural checks, or running the optimization algorithm. These endpoints accept input data in JSON format, which includes parameters like material properties, loading conditions, and geometric constraints.

3. **Request Handling:** When a user initiates the weight optimization process within the Lock n Load web interface, the JavaScript frontend sends an API request to the Flask backend. This request contains the necessary input data for the optimization process.

4. **Data Processing:** The Flask API receives the request, parses the JSON data, and executes the corresponding Python code. This involves running the optimization algorithm, performing structural analysis checks, and calculating utilization factors.

5. **Response Generation:** Once the calculations are complete, the Flask API generates a JSON response containing the optimization results. This includes the optimized cross-section dimensions, weight, utilization factors, and status (acceptable/unacceptable).

6. **Data Exchange:** The JSON response is sent back to the Laravel backend, which then processes the data and displays it to the user in a user-friendly format within the web interface.

7. **Visualization and User Interaction:** The frontend utilizes JavaScript to visualize the optimization results, potentially through graphs, tables, or interactive displays. Users can then interact with these visualizations, explore different options, and make informed decisions about their design.

User Input/Output Flow

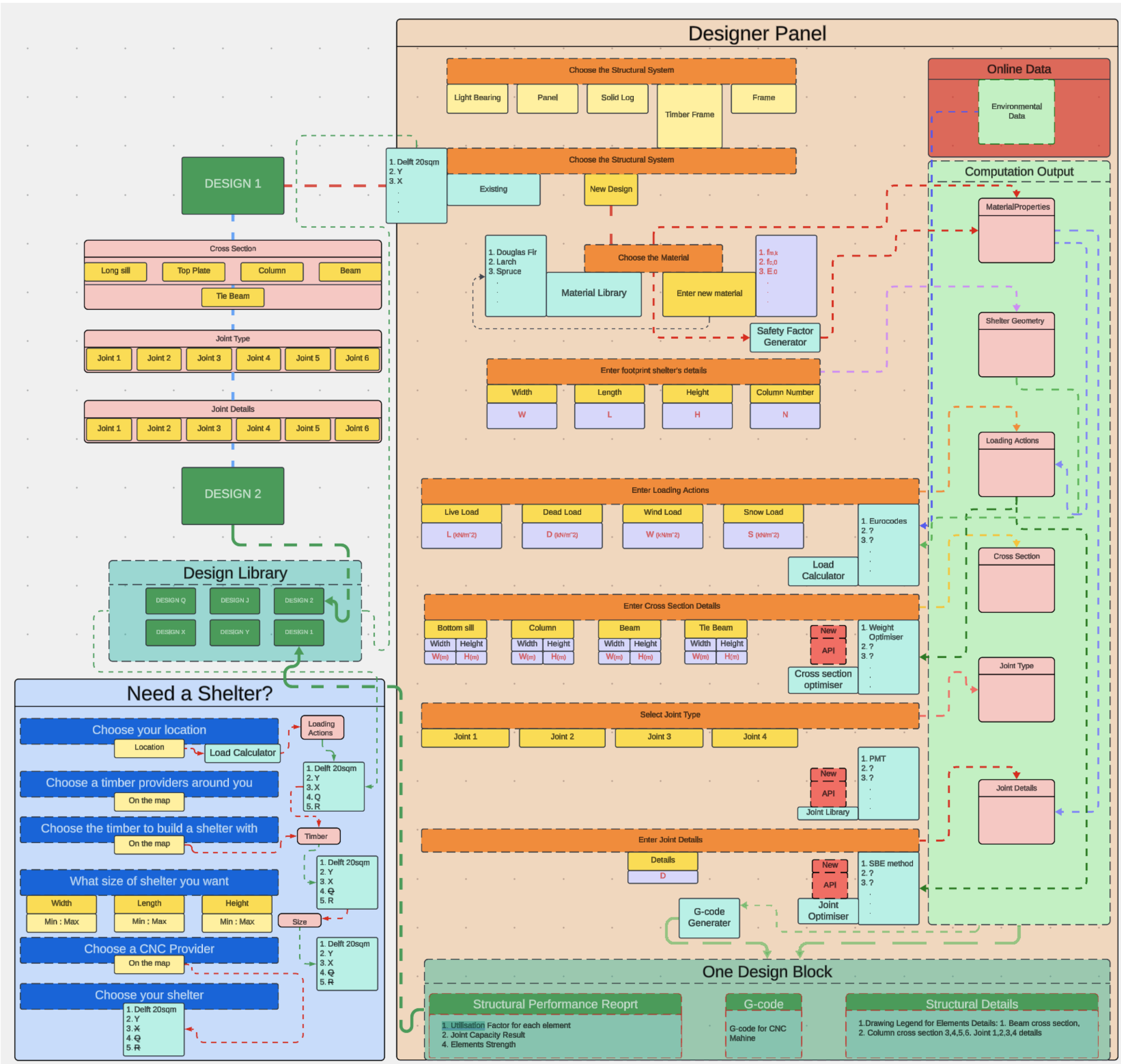

Conclusion and Future Recommendation

This research explored the development of "Lock n Load," a digital tool designed to revolutionize post-disaster timber shelter delivery. The core research question asked whether such a tool could simplify, improve, and integrate the processes of design, optimization, assembly, and delivery of these shelters, benefiting disaster victims, designers, and the entire supply chain. This research conclusively demonstrates that the answer is a resounding **yes**.

Lock n Load empowers **shelter designers** through dynamic, in-built features. Automated structural optimization, connection design tools, load calculators, and an extensive design library streamline the design process. Furthermore, an API allows **experts** to contribute to an evolving ecosystem of design methods, fostering ongoing innovation and refinement within the platform. The result is a more efficient workflow and a chain of continuous improvement in shelter design.

For those **seeking shelter**, Lock n Load dramatically **simplifies** the process. By answering a few basic questions about their needs and location, individuals can submit an order for a safe, customized, and readily obtainable shelter. This ease of access ensures that critical needs are met **quickly** and **efficiently** in the aftermath of a disaster.

The benefits extend throughout the **supply chain**. Lock n Load seamlessly **connects** designers and shelter seekers with timber providers and CNC fabricators. Orders and fabrication instructions are transmitted digitally, eliminating the need for direct communication between parties and ensuring a **smooth** and **coordinated flow** of materials and production.

The key to Lock n Load's success lies in its **web-based** platform. By leveraging the **accessibility** and **interconnected** nature of the internet, the tool unites all stakeholders within a single, **user-friendly** environment. This online foundation facilitates **seamless interaction** and information exchange, creating a dynamic and responsive system. Moreover, it positions Lock n Load for **future development**, **expansion**, and **adaptation** to evolving needs and technological advancements.

Research Limitations

1. While Lock n Load effectively addresses structural considerations, it currently lacks comprehensive integration of climate responsiveness and other crucial contextual factors. Although this limitation falls outside the initial scope of the research, the inherent challenge of merging climate-sensitive design with structural optimization necessitates a more sophisticated, multi-objective approach. Developing a linear framework that seamlessly considers both aspects presents a significant hurdle in achieving truly holistic and optimized shelter designs.

Future Recommendation:

To overcome this limitation, future development should prioritize the integration of climate-responsive design principles within Lock n Load. This could involve:

- **Developing a climate data integration module:** This module would allow users to input specific location data (e.g., temperature, humidity, rainfall, wind patterns) and receive design recommendations that optimize shelter performance in those conditions.
- **Expanding the material library with climate-specific options:** Including materials with varying thermal properties, moisture resistance, and durability would allow for tailored solutions based on climate considerations.
- **Incorporating passive design strategies:** The tool could suggest design features that maximize natural ventilation, solar gain, and shading to improve thermal comfort and reduce energy consumption.
- **Developing a "climate-responsive design score"**: This score would evaluate the overall climate performance of a shelter design, helping users understand and optimize its suitability for the intended environment.

2. Lock n Load currently restricts the addition of new structural systems and design methods to the administrator. This centralized control limits the platform's flexibility and

scalability, potentially hindering the rapid expansion and diversification of available shelter designs. Relying solely on administrator input creates a bottleneck and may not fully leverage the collective expertise of the broader engineering community.

Future Recommendation:

To address this, Lock n Load should evolve into a parametric platform that empowers users to define and contribute their own structural systems and design methods. This could be achieved by:

- **Integrating parametric modeling tools:** Allowing users to create parametric models of their structural systems would enable greater design flexibility and optimization.
- **Developing a user-friendly interface for defining structural systems:** This interface would allow users to input parameters such as materials, geometry, connections, and loading conditions to create custom structural systems

3. Lock n Load currently lacks direct integration with Finite Element Analysis (FEA) software. This limits the platform's ability to perform detailed structural analysis and optimization, potentially leading to conservative designs or requiring users to rely on external FEA tools, disrupting the streamlined workflow.

Future Recommendation:

- Automate FEA simulations: The integration could automate the process of generating FEA models from Lock n Load designs, significantly reducing the time and expertise required for analysis.
- Offer varying levels of FEA fidelity: Provide options for different levels of analysis detail, allowing users to balance accuracy with computational cost depending on their needs.

4. Lock n Load currently lacks a robust system for comparing and evaluating the advantages of different design methods. This makes it difficult for designers to objectively assess which approach is best suited for a particular context. This limitation stems from the inherent subjectivity and complexity of timber structure design, particularly in joinery and timber framing, where numerous factors influence optimal solutions.

Future Recommendation:

- Developing a standardized set of performance metrics: These metrics could include structural efficiency, material usage, cost, construction time, environmental impact, and aesthetic considerations.
- Creating a comparative analysis tool: This tool would allow designers to input design parameters and receive a comparative analysis of different methods based on the chosen metrics.
- Incorporating a weighting system: Allow designers to assign weights to different performance metrics based on their priorities, generating customized rankings of design methods.
- Developing a visual comparison tool: Generate visual representations of different design options, highlighting key differences and trade-offs.

Reflection

Relation between my Graduation Project Topic and Building Technology

Building technology, as its name implies, serves as a crucial bridge between technology and architecture, introducing innovative methods and possibilities within the architectural domain. My graduation project embodies this same spirit, forging a connection between the tradition of timber construction and a novel digital tool aimed at its enhancement. This endeavor has allowed me to apply a range of skills and methodologies acquired during my studies in Building Technology, including structural design, material science, simulation, coding, and programming.

Influence of Research on Design/Recommendations and Vice Versa

Although I have always been an advocate of incorporating timber in design, my thesis project highlighted the complexities of utilizing timber as a structural material. The extensive research I conducted, ranging from examining the work of traditional carpenters to modern structural engineers, revealed that while timber is an intriguing and versatile material, it also presents significant challenges. This realization profoundly influenced my design approach, prompting me to adhere to the inherent limitations of timber and embrace the simplicity of traditional construction methods. This is evident in my thesis through the deliberate choice to employ a classic timber frame system, rather than adopting the more futuristic and intricate interlocking systems that are currently trending in timber design.

Assessment of the Value of the Way of Working (approach, used methods, used methodology)?

This thesis did not follow a single, straightforward methodology. Initially, I was somewhat lost, focusing solely on timber connections as the most interesting aspect for me. This narrow focus prevented me from adequately addressing the research questions I had defined. Consequently, I had to postpone my graduation. During the extended time, I embarked on a new path, engaging in a broader literature review and conducting a case study. This revised approach proved beneficial to the project, allowing me to design the foundation of the tool based on the case study findings. Developing "Lock n Load" grounded in a real structural design experience gave me a clearer understanding of the design process itself. With this clarity, I could then concentrate my efforts on automating this process.

How do you assess the academic and societal value, scope and implication of your graduation project, including ethical aspects?

The academic value of my project lies primarily in its novel approach to simplifying the provision of emergency shelter for everyone involved in the supply chain, not just the shelter seekers themselves. Particular attention was given to streamlining the design process and integrating it seamlessly with the supply chain. Additionally, from a societal perspective, my thesis aims to empower individuals to actively participate in providing shelter to those in need. This is how "Lock n Load" fosters a sense of community and shared responsibility.

How do you assess the value of the transferability of your project results?

Considering that my primary focus in developing "Lock n Load" was to empower users to create their own designs and methods, I believe this project has at least attempted to establish a platform that encourages exploration and adaptability to various contexts. For instance, I see no reason why this shelter-providing platform, with appropriate modifications and considerations, couldn't be utilized for different types of structures in diverse situations. Furthermore, although the tool primarily focuses on structural optimization, I envision future projects adapting a similar approach to optimize other aspects of building design, such as environmental sustainability or social impact.

Personal Reflection

The most crucial soft skill I developed during this thesis was learning to aim for what's achievable. Initially, I was overly ambitious, envisioning a project that would encompass every possible aspect. This led to setbacks and ultimately, I had to postpone my graduation. Subsequently, I shifted my focus from creating a grand project to developing a genuinely useful one. I learned numerous techniques and skills throughout this thesis. Notably, structural design, which had previously been outside my comfort zone and not a strength of mine, became an area where I made significant progress. Initially, I struggled with some of the fundamental concepts, but I persevered and learned a great deal.

While I've always possessed strong coding skills, working on a project of this scale and with multiple coding languages involved truly solidified my confidence in my ability to code.

Additionally, I believe the most challenging aspect of this thesis was learning how to work with Finite Element Analysis software, specifically Ansys. This is a skill not typically taught in architecture schools, adding another layer of complexity to the project. Working with timber specifically made the FEM simulation process more challenging, as timber can exhibit less predictable behavior under various conditions.To address this issue, I had to seek out specialized literature focusing on specific types of timber. I believe the final results demonstrate a good validation performance.

Future research should focus on developing a tool that empowers users to define structural systems beyond the administrative constraints of the current site. This limitation arose from my limited expertise in web design, particularly in backend development. However, even small components of this project could be improved, particularly the non-structural aspects of the existing system.

Ultimately, I believe "Lock n Load" can address, or at least partially resolve, the problem statement raised at the outset. It has the potential to streamline the process of designing and delivering shelters, which was the primary objective of this project.

Appendix :

Matlab codes for optimisation of PMT

```
clc
clear

%% Reading the data
A = xlsread('Optimisation.xlsx');
v = linspace(0,10,size(A,1));

Force_index = 1:4:97;
Peg_index = 2:4:98;
Tenon_index = 3:4:99;
Mortise_index = 4:4:100;

F = A(:,Force_index);
sigma_Peg = A(:,Peg_index);
sigma_Tenon = A(:,Tenon_index);
sigma_Mortise = A(:,Mortise_index);

%% Finding the Yield Forces
N = 200;
x = linspace(0,8,N);
G = zeros(N,length(F));
X0 = zeros(1,length(F));
Y0 = zeros(1,length(F));

for i = 1:length(F)
  m = (F(2,i)-F(1,i))/(v(2)-v(1));
  G(:,i) = m*(x-0.5);
```

```
    [X0(i),Y0(i)] = intersections(x,G(:,i),v,F(:,i));

end


%% Plots
figure
subplot(2,2,1)
plot(v,F/1000,'LineWidth',2)
xlabel('Deflection (mm)')
ylabel('Load (kN)')
grid on
set(gca,'Linewidth',2)

subplot(2,2,2)
plot(v,sigma_Peg,'LineWidth',2)
xlabel('Deflection (mm)')
ylabel('Max Stress in Peg (MPa)')
grid on
set(gca,'Linewidth',2)

subplot(2,2,3)
plot(v,sigma_Tenon,'LineWidth',2)
xlabel('Deflection (mm)')
ylabel('Max Stress in Tenon (MPa)')
grid on
set(gca,'Linewidth',2)

subplot(2,2,4)
plot(v,sigma_Mortise,'LineWidth',2)
xlabel('Deflection (mm)')
ylabel('Max Stress in Tenon (MPa)')
```

```
grid on
set(gca,'Linewidth',2)

plot(Y0/1000,'*')
xlabel('Case Number')
ylabel('Yield Load (kN)')
grid on
grid minor
set(gca,'Linewidth',2)

plot(max(sigma_Tenon),'*')
xlabel('Case Number')
ylabel('Maximum Stress in Tenon (MPa)')
grid on
grid minor
set(gca,'Linewidth',2)

figure
plot(Y0/1000,max(sigma_Peg),'*')
xlabel('Yield Load (kN)')
ylabel('Maximum Stress in Peg (MPa)')
grid on
set(gca,'Linewidth',2)
```

FEM optimisation loop results of PMT joints

Force (N)	Max Stress in Peg (MPa)	Max Stress in Tenon (MPa)	Max Stress in Mortise (MPa)	Force (N)	Max Stress in Peg (MPa)	Max Stress in Tenon (MPa)	Max Stress in Mortise (MPa)	Force (N)	Max Stress in Peg (MPa)	Max Stress in Tenon (MPa)	Max Stress in Mortise (MPa)	Force (N)
0	0	0	0	0	0	0	0	0	0	0	0	0
4493,7	4,3237	18,574	5,536	4474,5	4,373	13,322	5,4289	4452,9	4,1532	13,399	5,2438	4435,8
8939	8,6111	30,595	9,6275	8899,3	8,1765	27,292	9,7861	8858,1	8,3818	27,427	9,319	8823,1
13312	10,156	46,597	13,768	13258	9,615	41,685	14,534	13195	9,6075	41,774	13,452	13142
17532	11,596	47,261	18,116	17464	11,45	46,266	19,131	17383	11,496	45,332	17,711	17315
21541	13,159	42,98	22,239	21470	13,061	46,143	23,502	21372	13,054	39,536	21,767	21295
25322	14,952	46,868	26,118	25250	14,882	42,715	27,624	25140	14,853	42,947	25,595	25051
28986	16,947	54,414	29,868	28910	16,893	50,235	31,606	28782	16,838	51,228	27,659	28677
32581	19,031	62,045	31,904	32500	18,964	57,728	32,658	32357	18,945	59,571	31,047	32230
36121	21,149	70,241	35,212	36038	21,064	65,152	36,129	35879	21,117	67,543	34,369	35729
39617	23,283	78,419	38,557	39529	23,166	72,466	39,509	39353	23,312	75,317	37,602	39180
43075	25,432	86,378	41,834	42981	25,277	79,932	42,839	42787	25,502	83,109	40,773	42589
46500	27,584	94,217	45,046	46397	27,395	87,241	46,051	46184	27,696	90,738	43,864	45963
49893	29,722	101,94	48,171	49781	29,521	94,375	49,173	49548	29,884	98,161	46,877	49303
53259	31,854	109,48	51,251	53138	31,64	101,47	52,229	52884	32,056	105,47	48,088	52612
56601	33,98	116,99	51,423	56467	33,744	108,41	49,828	56191	34,202	112,62	50,743	55891
59915	36,105	124,45	52,552	59769	35,836	115,23	52,189	59467	36,33	119,61	51,267	59139
63204	38,218	131,85	54,335	63041	37,912	121,98	54,348	62713	38,442	126,49	53,547	62356
66467	40,321	139,12	56,447	66285	39,975	128,64	56,427	65930	40,541	133,28	55,673	65544
69704	42,416	146,32	58,416	69501	42,025	135,14	58,361	69114	42,626	140,02	57,719	68699
7,29E+04	44,498	153,45	60,235	7,27E+04	44,06	141,54	60,207	72268	44,693	146,71	59,613	7,18E+04
Case 1				Case 2				Case 3				Case 4

Force (N)	Max Stress in Peg (MPa)	Max Stress in Tenon (MPa)	Max Stress in Mortise (MPa)	Force (N)	Max Stress in Peg (MPa)	Max Stress in Tenon (MPa)	Max Stress in Mortise (MPa)	Force (N)	Max Stress in Peg (MPa)	Max Stress in Tenon (MPa)	Max Stress in Mortise (MPa)	Force (N)
0	0	0	0	0	0	0	0	0	0	0	0	0
4435,8	4,416	18,339	5,4783	4416,5	4,6099	18,345	5,339	4478,7	4,3381	18,38	5,818	4392,8
8823,1	8,0863	27,912	9,9711	8784,5	7,9238	36,907	9,7578	8908,1	8,9412	27,695	10,215	8737,1
13142	9,4364	42,511	13,461	13085	9,2086	51,886	12,503	13265	10,767	42,466	14,32	13004
17315	11,271	46,404	17,729	17244	11,254	45,381	16,475	17467	12,246	46,262	17,872	17105
21295	12,931	44,11	21,796	21208	12,891	45,527	20,261	21462	13,932	41,129	20,495	20984
25051	14,743	44,331	25,635	24944	14,662	45,622	23,832	25233	15,773	45,363	23,989	24618
28677	16,724	52,723	27,766	28548	16,6	53,372	26,909	28880	17,774	53,227	27,323	28122
32230	18,745	61,353	31,193	32080	18,582	61,249	28,835	32456	19,843	60,889	30,557	31529
35729	20,784	69,845	34,557	35557	20,583	68,614	31,91	35976	21,961	68,053	33,768	34862
39180	22,834	78,101	37,852	38986	22,593	75,899	34,926	39446	24,123	75,3	35,278	38117
42589	24,897	86,166	41,075	42374	24,61	83,256	37,901	42875	26,29	83,016	38,234	41297
45963	26,953	94,068	44,255	45726	26,624	90,558	40,746	46267	28,456	90,809	41,34	44404
49303	28,999	101,72	47,337	49043	28,632	97,715	43,488	49625	30,616	98,491	44,685	47433
52612	31,034	109,26	50,352	52329	30,632	104,84	45,548	52954	32,774	105,96	48,005	50382
55891	33,055	116,75	49,861	55584	32,619	111,95	48,184	56254	34,926	113,33	51,285	53274
59139	35,062	124,16	51,157	58807	34,588	119,03	48,797	59525	37,062	120,55	54,552	56120
62356	37,053	131,44	53,392	61997	36,533	126,03	50,903	62769	39,183	127,69	57,816	58917
65544	39,031	138,63	55,519	65152	38,462	132,9	53,328	65984	41,296	134,74	61,031	61654
68699	40,993	145,72	57,497	68274	40,384	139,67	56,121	69170	43,4	141,71	64,211	64333
7,18E+04	42,935	152,71	59,302	71363	42,29	146,33	58,895	7,23E+04	45,492	148,62	67,33	66971
Case 4				Case 5				Case 6				Case 7

Force (N)	Max Stress in Peg (MPa)	Max Stress in Tenon (MPa)	Max Stress in Mortise (MPa)	Force (N)	Max Stress in Peg (MPa)	Max Stress in Tenon (MPa)	Max Stress in Mortise (MPa)	Force (N)	Max Stress in Peg (MPa)	Max Stress in Tenon (MPa)	Max Stress in Mortise (MPa)
0	0	0	0	0	0	0	0	0	0	0	0
4392,8	5,4298	15,569	6,1068	4455,8	4,3786	19,105	5,7174	4323,1	4,8962	15,112	7,0019
8737,1	11,211	30,371	11,833	8862,6	8,3306	26,327	10,732	8595,2	9,9982	30,399	11,821
13004	12,479	43,169	16,861	13201	9,7021	40,509	13,609	12794	11,541	44,806	15,586
17105	14,475	47,381	20,53	17385	11,91	50,51	17,909	16836	13,891	42,312	19,618
20984	16,64	48,975	25,076	21368	13,652	45,853	21,177	20667	16,012	41,896	24,153
24618	18,798	50,062	29,697	25122	15,519	48,773	24,873	24259	17,968	49,482	28,548
28122	21,133	58,994	34,364	28750	17,479	56,639	28,433	27690	19,922	57,856	33,068
31529	23,581	68,043	39,239	32307	19,479	64,317	31,913	31023	21,967	66,62	37,751
34862	26,061	76,937	42,335	35809	21,493	71,786	35,326	34268	24,073	75,202	38,891
38117	28,54	85,587	43,313	39260	23,521	79,491	36,456	37423	26,213	83,532	41,424
41297	31,017	93,965	46,463	42669	25,578	87,134	39,507	40489	28,358	91,681	43,867
44404	33,49	102,1	49,008	46043	27,649	94,433	42,542	43461	30,534	99,759	46,798
47433	35,977	110,18	51,554	49383	29,716	101,63	45,525	46325	32,737	107,72	49,902
50382	38,449	118,23	54,229	52689	31,776	108,9	48,439	49123	34,897	115,59	52,844
53274	40,879	126,1	56,543	55962	33,82	116,11	51,207	51866	37,029	123,34	55,942
56120	43,295	133,85	58,742	59207	35,844	123,29	54,333	54558	39,142	130,94	58,949
58917	45,691	141,52	60,942	62419	37,861	130,37	57,599	57208	41,241	138,41	61,862
61654	48,069	149,05	63,633	65600	39,858	137,4	60,911	59816	43,323	145,82	64,694
64333	50,42	156,51	66,254	68746	41,852	144,4	64,137	62380	45,385	153,17	67,444
66971	52,752	163,93	68,836	7,19E+04	43,834	151,36	67,311	64900	47,426	160,4	70,128
Case 7				Case 8				Case 9			

Force (N)	Max Stress in Peg (MPa)	Max Stress in Tenon (MPa)	Max Stress in Mortise (MPa)	Force (N)	Max Stress in Peg (MPa)	Max Stress in Tenon (MPa)	Max Stress in Mortise (MPa)	Force (N)	Max Stress in Peg (MPa)	Max Stress in Tenon (MPa)	Max Stress in Mortise (MPa)	Force (N)
0	0	0	0	0	0	0	0	0	0	0	0	0
4457,7	4,2277	13,727	5,5399	4379,9	5,2155	21,062	6,5802	4441,1	4,3519	15,155	5,7203	4298,5
8866	8,8218	28,147	10,213	8710,4	9,6626	32,196	12,116	8834,1	8,0874	30,65	10,138	8545,9
13204	10,672	42,934	13,919	12969	11,859	44,737	15,403	13159	9,5824	41,204	13,342	12723
17388	12,155	48,292	18,327	17072	13,945	45,679	19,778	17336	11,761	47,012	17,562	16742
21370	13,825	40,945	22,025	20962	16,159	47,409	24,271	21316	13,515	43,636	21,575	20553
25127	15,69	47,449	25,867	24610	18,192	48,176	28,718	25067	15,328	47,986	25,35	24124
28759	17,716	52,507	29,569	28124	20,249	55,827	33,263	28689	17,268	56,289	28,982	27541
32318	19,825	60,211	33,184	31532	22,36	63,586	37,994	32238	19,272	64,479	32,532	30850
35820	21,97	67,887	36,727	34855	24,516	70,821	40,001	35731	21,29	72,104	34,112	34069
39270	24,123	75,113	37,858	38095	26,654	78,327	42,129	39172	23,3	79,732	37,332	37198
42680	26,294	82,456	41,057	41251	28,769	85,515	45,443	42567	25,314	87,446	40,496	40222
46055	28,458	89,849	44,201	44312	30,869	92,227	49,225	45925	27,351	95,153	43,608	43126
49395	30,616	97,199	47,287	47288	32,882	98,694	52,766	49248	29,388	102,72	46,671	45951
52705	32,762	104,55	50,31	50202	34,855	104,81	55,642	52537	31,417	110,23	49,686	48711
55986	34,893	111,68	53,159	53060	36,786	110,87	57,945	55793	33,435	117,67	52,559	51411
59236	37,001	118,64	55,736	55863	38,718	116,97	59,965	59019	35,435	125,07	55,247	54065
62457	39,085	125,52	58,181	58601	40,614	122,82	61,95	62215	37,42	132,45	57,803	56671
65647	41,162	132,29	55,317	61279	42,505	128,43	63,916	65375	39,391	139,9	55,595	59223
68804	43,22	138,96	57,521	63911	44,373	133,97	65,876	68498	41,345	147,38	58,538	61724
7,19E+04	45,262	145,53	59,795	66497	46,226	139,34	67,798	71577	43,28	154,74	61,448	64190
Case 10				Case 11				Case 12				Case 13

Force (N)	Max Stress in Peg (MPa)	Max Stress in Tenon (MPa)	Max Stress in Mortise (MPa)	Force (N)	Max Stress in Peg (MPa)	Max Stress in Tenon (MPa)	Max Stress in Mortise (MPa)	Force (N)	Max Stress in Peg (MPa)	Max Stress in Tenon (MPa)	Max Stress in Mortise (MPa)	Force (N)
0	0	0	0	0	0	0	0	0	0	0	0	0
4298,5	4,8098	15,389	6,362	4440,5	4,2315	14,423	5,5082	4342,6	5,0281	14,507	5,8259	4415,1
8545,9	9,8372	31,229	10,945	8832,8	8,7988	29,403	10,151	8635,3	10,406	29,489	10,432	8780,7
12723	11,357	41,875	14,95	13156	10,569	45,304	13,449	12853	11,822	45,07	15,147	13081
16742	13,715	46,548	19,383	17332	12,064	45,299	17,663	16909	13,879	45,701	19,01	17237
20553	15,764	40,56	23,944	21306	13,732	44,507	21,687	20730	15,914	54,434	23,271	21197
24124	17,662	48,474	28,299	25056	15,584	46,662	25,472	24335	18,019	45,89	27,615	24937
27541	19,624	56,52	32,717	28679	17,576	54,435	29,116	27789	20,242	53,05	32,084	28545
30850	21,627	64,587	37,23	32228	19,665	62,312	32,673	31141	22,578	60,371	36,611	32079
34069	23,731	72,493	39,564	35724	21,773	69,721	36,164	34408	24,911	67,477	40,142	35556
37198	25,849	80,381	41,686	39169	23,88	77,065	37,381	37591	27,232	74,111	42,509	38984
40222	27,983	88,153	44,444	42572	25,996	84,398	40,552	40682	29,562	80,883	45,011	42369
43126	30,122	95,625	48	45935	28,108	91,792	43,665	43678	31,877	87,73	49,126	45713
45951	32,238	102,93	51,214	49265	30,208	99,051	46,731	46598	34,16	94,264	52,289	49023
48711	34,317	110,1	53,811	52564	32,3	106,19	49,731	49453	36,408	100,68	55,119	52298
51411	36,356	117,19	56,066	55831	34,373	113,22	52,577	52248	38,624	106,87	57,493	55539
54065	38,379	124,21	58,195	59067	36,426	120,14	55,185	54977	40,796	112,78	59,633	58749
56671	40,385	131,09	60,276	62273	38,472	126,95	57,672	57643	42,939	118,54	61,66	61925
59223	42,364	137,84	62,877	65444	40,507	133,64	54,836	60256	45,061	124,17	63,803	65065
61724	44,322	144,48	65,48	68573	42,526	140,33	57,05	62821	47,158	129,69	66,48	68156
64190	46,267	151,08	68,005	71652	44,515	146,99	59,859	65344	49,228	135,15	69,083	71196
Case 13				Case 14				Case 15				Case 16

Force (N)	Max Stress in Peg (MPa)	Max Stress in Tenon (MPa)	Max Stress in Mortise (MPa)	Force (N)	Max Stress in Peg (MPa)	Max Stress in Tenon (MPa)	Max Stress in Mortise (MPa)	Force (N)	Max Stress in Peg (MPa)	Max Stress in Tenon (MPa)	Max Stress in Mortise (MPa)	Force (N)
0	0	0	0	0	0	0	0	0	0	0	0	0
4415,1	4,1999	15,48	5,3726	4278,1	4,728	16,355	6,215	4414,7	4,2073	19,128	5,6343	4260,5
8780,7	8,5581	28,953	9,8165	8506,3	9,6717	33,049	11,454	8780,3	8,6556	32,275	10,364	8473,5
13081	9,9519	42,16	13,463	12656	11,288	42,491	15,601	13077	10,48	49,631	14,394	12560
17237	12,015	56,927	17,723	16645	13,643	49,474	18,799	17228	12,045	47,002	18,986	16445
21197	13,686	52,408	21,772	20422	15,645	42,043	23,107	21183	13,699	47,322	21,876	20063
24937	15,498	47,7	25,584	23966	17,576	49,752	27,275	24915	15,548	45,973	25,682	23479
28545	17,511	55,825	29,25	27347	19,491	57,964	31,665	28516	17,563	54,548	29,316	26776
32079	19,619	64,767	32,828	30623	21,492	65,797	36,2	32043	19,664	63,256	32,812	29988
35556	21,756	71,811	34,098	33805	23,553	73,539	40,019	35516	21,803	71,759	33,786	33114
38984	23,913	79,86	37,321	36891	25,63	81,192	41,965	38938	23,935	80,096	37,142	36147
42369	26,075	87,961	40,49	39856	27,736	88,722	46,217	42319	26,071	88,373	39,054	39096
45713	28,25	95,991	43,602	42725	29,809	96,089	50,7	45660	28,226	96,381	41,889	41968
49023	30,401	103,94	46,667	45509	31,856	103,23	53,758	48966	30,374	104,16	44,594	44763
52298	32,525	111,77	49,68	48229	33,857	110,22	56,267	52240	32,507	111,88	47,219	47497
55539	34,623	119,51	52,58	50892	35,831	117,14	58,412	55483	34,62	119,56	49,768	50168
58749	36,708	127,19	55,252	53504	37,78	124,03	60,451	58694	36,709	127,21	52,203	52774
61925	38,779	134,77	57,759	56060	39,704	130,81	62,49	61871	38,791	134,78	54,697	55322
65065	40,831	142,39	58,202	58564	41,606	137,48	64,536	65005	40,847	142,18	57,099	57823
68156	42,847	149,91	61,262	61024	43,562	144,04	66,591	68090	42,88	149,44	59,397	60276
71196	44,833	157,28	64,313	63445	45,495	150,51	69,171	71116	44,885	156,51	61,514	62688
Case 16				Case 17				Case 18				Case 19

Force (N)	Max Stress in Peg (MPa)	Max Stress in Tenon (MPa)	Max Stress in Mortise (MPa)	Force (N)	Max Stress in Peg (MPa)	Max Stress in Tenon (MPa)	Max Stress in Mortise (MPa)	Force (N)	Max Stress in Peg (MPa)	Max Stress in Tenon (MPa)	Max Stress in Mortise (MPa)	Force (N)
0	0	0	0	0	0	0	0	0	0	0	0	0
4260,5	4,7943	14,875	6,2237	4337,7	5,6814	16,565	5,5006	4192,2	4,9294	15,97	6,2669	4391,1
8473,5	9,999	30,441	10,879	8629,8	11,37	33,115	9,4999	8333,7	9,6702	32,411	11,671	8734,3
12560	11,53	46,332	15,61	12805	10,369	39,514	13,267	12353	11,377	44,702	14,545	13007
16445	13,684	47,986	19,441	16790	12,377	46,602	17,437	16175	13,534	40,43	18,668	17136
20063	15,748	41,175	23,912	20530	14,23	42,695	20,645	19731	15,594	46,108	22,94	21064
23479	17,797	49,06	28,431	24060	16,663	51,076	23,476	23077	17,534	54,19	27,347	24773
26776	19,95	57,495	33,048	27498	19,291	59,95	26,869	26294	19,547	62,787	31,82	28352
29988	22,144	65,809	36,608	30877	22,009	68,382	30,186	29418	21,633	71,294	36,453	31855
33114	24,355	73,822	39,638	34204	24,814	76,771	33,473	32450	23,779	79,315	39,812	35303
36147	26,574	81,589	42,552	37485	27,643	85,229	35,86	35378	25,963	87,208	43,56	38702
39096	28,809	88,849	46,216	40728	30,471	93,711	37,529	38213	28,155	94,963	47,153	42058
41968	31,005	96,085	50,53	43934	33,298	101,99	40,452	40964	30,312	102,51	50,602	45375
44763	33,167	102,85	53,659	47106	36,092	110,16	43,214	43634	32,415	109,81	54,212	48655
47497	35,286	109,34	56,41	50244	38,868	118,41	45,91	46239	34,464	116,98	56,93	51904
50168	37,364	115,63	58,758	53350	41,615	126,56	48,614	48790	36,479	123,98	59,138	55118
52774	39,403	121,6	60,866	56427	44,334	134,66	51,12	51289	38,464	130,93	61,086	58297
55322	41,414	127,48	62,865	59471	47,019	142,83	53,462	53734	40,462	137,76	62,977	61435
57823	43,398	133,31	64,792	62476	49,658	150,84	55,795	56130	42,457	144,51	64,846	64525
60276	45,357	138,98	66,672	65439	52,248	158,71	58,061	58485	44,42	151,2	66,698	67564
62688	47,295	144,51	68,513	68352	54,778	166,33	60,959	60801	46,359	157,86	68,537	70535
Case 19				Case 20				Case 21				Case 22

Force (N)	Max Stress in Peg (MPa)	ss in Tenon	Max Stress in Mortise (MPa)	Force (N)	Max Stress in Peg (MPa)	Max Stress in Tenon (MPa)	Max Stress in Mortise (MPa)	Force (N)	Max Stress in Peg (MPa)	Max Stress in Tenon (MPa)	Max Stress in Mortise (MPa)
0	0	0	0	0	0	0	0	0	0	0	0
4391,1	4,2778	15,827	5,4581	4285,2	4,6254	14,638	6,0425	4364,8	4,3333	14,666	5,8155
8734,3	8,7261	32,208	10,076	8520,3	9,664	29,75	11,205	8681,9	8,0868	29,717	10,455
13007	10,454	49,178	13,495	12670	11,188	45,429	15,296	12929	9,6165	39,264	12,904
17136	12,02	48,818	17,8	16653	13,414	59,291	18,795	17028	11,753	47,466	17,033
21064	13,662	49,792	21,162	20428	15,269	49,666	23,052	20921	13,551	44,034	20,787
24773	15,481	47,166	24,294	23981	17,187	48,633	27,487	24582	15,408	52,507	23,756
28352	17,472	55,106	27,691	27383	19,205	56,645	32,021	28113	17,355	61,724	26,682
31855	19,548	63,044	30,996	30676	21,286	64,478	36,652	31570	19,361	70,531	29,925
35303	21,648	70,621	34,198	33866	23,389	72,029	41,112	34975	21,38	79,187	33,144
38702	23,746	78,31	36,839	36959	25,518	79,355	44,239	38332	23,415	87,839	36,367
42058	25,848	86,367	38,248	39965	27,615	86,245	48,387	41645	25,459	96,497	38,201
45375	27,947	94,466	40,56	42887	29,718	92,853	52,576	44921	27,513	105	39,755
48655	30,041	102,32	43,305	45735	31,799	99,254	55,441	48160	29,564	113,6	42,524
51904	32,12	109,96	46,006	48505	33,824	105,39	57,637	51365	31,614	122,46	45,234
55118	34,191	117,49	48,631	51201	35,827	111,27	59,512	54535	33,649	131,24	47,83
58297	36,245	124,87	51,124	53828	37,891	116,8	61,322	57667	35,665	139,83	50,248
61435	38,282	132,21	53,438	56400	39,924	122,14	63,11	60758	37,664	148,29	52,668
64525	40,293	139,28	55,665	58918	41,924	127,35	64,908	63804	39,641	156,64	56,437
67564	42,277	146,22	59,907	61389	43,885	132,53	66,702	66795	41,586	164,79	60,769
70535	44,232	153,02	59,693	63816	45,809	137,57	68,497	69721	43,494	172,78	60,021
Case 22				Case 23				Case 24			

Load Calculator Inputs in Green village, Delft

Load combination

$g_{.k}$	Permanent load
$q_{.k}$	Live load
$s_{.k}$	Snow load
$w_{.k}$	Wind load

Permanent load

	Per area	Applied on one element
Roof	1.1 kN/mˆ2	-
Walls	4.5 kN/mˆ2	4.4 kN/m
Beams	later	1.38 kN/m
Columns	later	2.76 kN
Floor	0.9 kN/mˆ2	-

Snow load

	Applied on one elements
Sk	0.56 kN/mˆ2
Beams	1.7 kN/m
Columns	1.4 kN

Material properties, Values, Variables used in the optimisation of timber frames

	Douglas fir	European spruce	European Larch
y.m	1.3	1.3	1.3
ρ (Kg/m3)[4]	550	440	610
fm.k (N/mm3)	86	63	91
fv.k (N/mm3)	8.2	5.3	9
fc.k (N/mm3)	42	35	45
E (kN/mm3)	12.17	9.7	11.2
$k_{.mod.p}$	0.5	0.5	0.5
$k_{.mod.m}$	0.65	0.65	0.65
$k_{.mod.i}$	0.90	0.90	0.90
$k_{.def}$	2	2	2
$P_{.L}$ (kN/m)	2.96	2.96	2.96
$M_{.L}$(kN/m)	7.44	7.44	7.44
$I_{.L}$(kN/m)	5.66	5.66	5.66
$SLS_{.L}$ (kN/m)	5.18	5.18	5.18
g_k (kN/m)	1.38	1.38	1.38
$g_{.lead}$ (kN/m)	2	2	2
$g_{.acm}$ (kN/m)	1.4	1.4	1.4
psi.lead	0	0	0
psi.acmp	0.2	0.2	0.2
$B_{.c}$	0.2	0.2	0.2

[4] Air-dried (around 12-15% moisture content)

P.clm	3.1	3.4	2.9
M.clm	7.1	8.6	8.3
I.clm	6.1	7.2	7

Optimisation results for timber frame Douglas Fir

Weight (kg)	Width (mm)	Thickness (mm)	Bending Util (%)	Bending Status	Shear Util (%)	Shear Status	SLS Util (%)	SLS Status	Compression Util (%)	Compression Status	Buckling Util Y (%)	Buckling Status Y	Buckling Util Z (%)	Buckling Status Z	Final Util (%)	Final Status
10.45	95	100	54.64%	Acceptable	28.65%	Acceptable	168.01 %	Unacceptable	5.02%	Acceptable	7.97%	Acceptable	8.66%	Acceptable	168.01 %	Unacceptable
11.00	100	100	51.91%	Acceptable	27.22%	Acceptable	159.61 %	Unacceptable	4.77%	Acceptable	7.57%	Acceptable	7.57%	Acceptable	159.61 %	Unacceptable
11.50	95	110	45.16%	Acceptable	26.05%	Acceptable	126.23 %	Unacceptable	4.56%	Acceptable	6.27%	Acceptable	7.87%	Acceptable	126.23 %	Unacceptable
12.02	95	115	41.31%	Acceptable	24.91%	Acceptable	110.47 %	Unacceptable	4.36%	Acceptable	5.63%	Acceptable	7.53%	Acceptable	110.47 %	Unacceptable
12.10	100	110	42.90%	Acceptable	24.75%	Acceptable	119.92 %	Unacceptable	4.33%	Acceptable	5.95%	Acceptable	6.88%	Acceptable	119.92 %	Unacceptable
12.54	95	120	37.94%	Acceptable	23.88%	Acceptable	97.23%	Acceptable	4.18%	Acceptable	5.10%	Acceptable	7.22%	Acceptable	97.23%	Acceptable
12.65	100	115	39.25%	Acceptable	23.67%	Acceptable	104.95 %	Unacceptable	4.14%	Acceptable	5.35%	Acceptable	6.58%	Acceptable	104.95 %	Unacceptable
12.65	115	100	45.14%	Acceptable	23.67%	Acceptable	138.79 %	Unacceptable	4.14%	Acceptable	6.58%	Acceptable	5.35%	Acceptable	138.79 %	Unacceptable
13.06	95	125	34.97%	Acceptable	22.92%	Acceptable	86.02%	Acceptable	4.01%	Acceptable	4.66%	Acceptable	6.93%	Acceptable	86.02%	Acceptable
13.20	100	120	36.05%	Acceptable	22.68%	Acceptable	92.37%	Acceptable	3.97%	Acceptable	4.85%	Acceptable	6.31%	Acceptable	92.37%	Acceptable
13.58	95	130	32.33%	Acceptable	22.04%	Acceptable	76.47%	Acceptable	3.86%	Acceptable	4.29%	Acceptable	6.66%	Acceptable	76.47%	Acceptable
13.75	100	125	33.22%	Acceptable	21.78%	Acceptable	81.72%	Acceptable	3.81%	Acceptable	4.43%	Acceptable	6.06%	Acceptable	81.72%	Acceptable
13.75	125	100	41.53%	Acceptable	21.78%	Acceptable	127.69 %	Unacceptable	3.81%	Acceptable	6.06%	Acceptable	4.43%	Acceptable	127.69 %	Unacceptable
13.91	115	110	37.30%	Acceptable	21.52%	Acceptable	104.28 %	Unacceptable	3.77%	Acceptable	5.18%	Acceptable	4.86%	Acceptable	104.28 %	Unacceptable

14.11	95	135	29.98%	Acceptable	21.22%	Acceptable	68.29%	Acceptable	3.72%	Acceptable	3.98%	Acceptable	6.41%	Acceptable	68.29%	Acceptable
14.30	100	130	30.71%	Acceptable	20.94%	Acceptable	72.65%	Acceptable	3.67%	Acceptable	4.08%	Acceptable	5.82%	Acceptable	72.65%	Acceptable
14.55	115	115	34.13%	Acceptable	20.58%	Acceptable	91.26%	Acceptable	3.60%	Acceptable	4.65%	Acceptable	4.65%	Acceptable	91.26%	Acceptable
14.63	95	140	27.88%	Acceptable	20.47%	Acceptable	61.23%	Acceptable	3.58%	Acceptable	3.71%	Acceptable	6.19%	Acceptable	61.23%	Acceptable
14.85	100	135	28.48%	Acceptable	20.16%	Acceptable	64.87%	Acceptable	3.53%	Acceptable	3.78%	Acceptable	5.61%	Acceptable	64.87%	Acceptable
15.12	125	110	34.32%	Acceptable	19.80%	Acceptable	95.94%	Acceptable	3.47%	Acceptable	4.76%	Acceptable	4.03%	Acceptable	95.94%	Acceptable
15.15	95	145	25.99%	Acceptable	19.76%	Acceptable	55.11%	Acceptable	3.46%	Acceptable	3.48%	Acceptable	5.97%	Acceptable	55.11%	Acceptable
15.18	115	120	31.34%	Acceptable	19.72%	Acceptable	80.32%	Acceptable	3.45%	Acceptable	4.22%	Acceptable	4.46%	Acceptable	80.32%	Acceptable
15.18	138	100	37.61%	Acceptable	19.72%	Acceptable	115.66%	Unacceptable	3.45%	Acceptable	5.49%	Acceptable	3.62%	Acceptable	115.66%	Unacceptable
15.40	100	140	26.48%	Acceptable	19.44%	Acceptable	58.17%	Acceptable	3.40%	Acceptable	3.52%	Acceptable	5.41%	Acceptable	58.17%	Acceptable
15.67	95	150	24.28%	Acceptable	19.10%	Acceptable	49.78%	Acceptable	3.35%	Acceptable	3.27%	Acceptable	5.77%	Acceptable	49.78%	Acceptable
15.81	115	125	28.89%	Acceptable	18.94%	Acceptable	71.06%	Acceptable	3.32%	Acceptable	3.85%	Acceptable	4.28%	Acceptable	71.06%	Acceptable
15.81	125	115	31.40%	Acceptable	18.94%	Acceptable	83.96%	Acceptable	3.32%	Acceptable	4.28%	Acceptable	3.85%	Acceptable	83.96%	Acceptable
15.95	100	145	24.69%	Acceptable	18.77%	Acceptable	52.36%	Acceptable	3.29%	Acceptable	3.30%	Acceptable	5.22%	Acceptable	52.36%	Acceptable
16.20	95	155	22.74%	Acceptable	18.49%	Acceptable	45.12%	Acceptable	3.24%	Acceptable	3.10%	Acceptable	5.59%	Acceptable	45.12%	Acceptable
16.45	115	130	26.71%	Acceptable	18.21%	Acceptable	63.17%	Acceptable	3.19%	Acceptable	3.54%	Acceptable	4.12%	Acceptable	63.17%	Acceptable
16.50	100	150	23.07%	Acceptable	18.15%	Acceptable	47.29%	Acceptable	3.18%	Acceptable	3.11%	Acceptable	5.05%	Acceptable	47.29%	Acceptable
16.50	125	120	28.84%	Acceptable	18.15%	Acceptable	73.90%	Acceptable	3.18%	Acceptable	3.88%	Acceptable	3.69%	Acceptable	73.90%	Acceptable
16.50	150	100	34.60%	Acceptable	18.15%	Acceptable	106.41%	Unacceptable	3.18%	Acceptable	5.05%	Acceptable	3.11%	Acceptable	106.41%	Unacceptable
16.70	138	110	31.09%	Acceptable	17.93%	Acceptable	86.90%	Acceptable	3.14%	Acceptable	4.31%	Acceptable	3.29%	Acceptable	86.90%	Acceptable
16.72	95	160	21.34%	Acceptable	17.91%	Acceptable	41.02%	Acceptable	3.14%	Acceptable	2.94%	Acceptable	5.41%	Acceptable	41.02%	Acceptable
17.05	100	155	21.61%	Acceptable	17.56%	Acceptable	42.86%	Acceptable	3.08%	Acceptable	2.94%	Acceptable	4.88%	Acceptable	42.86%	Acceptable

17.08	115	135	24.77%	Acceptable	17.53%	Acceptable	56.41%	Acceptable	3.07%	Acceptable	3.28%	Acceptable	3.96%	Acceptable	56.41%	Acceptable
17.19	125	125	26.58%	Acceptable	17.42%	Acceptable	65.38%	Acceptable	3.05%	Acceptable	3.54%	Acceptable	3.54%	Acceptable	65.38%	Acceptable
17.24	95	165	20.07%	Acceptable	17.36%	Acceptable	37.40%	Acceptable	3.04%	Acceptable	2.81%	Acceptable	5.25%	Acceptable	37.40%	Acceptable
17.46	138	115	28.44%	Acceptable	17.15%	Acceptable	76.05%	Acceptable	3.00%	Acceptable	3.88%	Acceptable	3.15%	Acceptable	76.05%	Acceptable
17.60	100	160	20.28%	Acceptable	17.01%	Acceptable	38.97%	Acceptable	2.98%	Acceptable	2.80%	Acceptable	4.73%	Acceptable	38.97%	Acceptable
17.71	115	140	23.03%	Acceptable	16.91%	Acceptable	50.58%	Acceptable	2.96%	Acceptable	3.06%	Acceptable	3.82%	Acceptable	50.58%	Acceptable
17.88	125	130	24.57%	Acceptable	16.75%	Acceptable	58.12%	Acceptable	2.93%	Acceptable	3.26%	Acceptable	3.41%	Acceptable	58.12%	Acceptable
18.15	100	165	19.07%	Acceptable	16.50%	Acceptable	35.53%	Acceptable	2.89%	Acceptable	2.67%	Acceptable	4.59%	Acceptable	35.53%	Acceptable
18.15	150	110	28.60%	Acceptable	16.50%	Acceptable	79.95%	Acceptable	2.89%	Acceptable	3.97%	Acceptable	2.83%	Acceptable	79.95%	Acceptable
18.22	138	120	26.12%	Acceptable	16.44%	Acceptable	66.93%	Acceptable	2.88%	Acceptable	3.51%	Acceptable	3.02%	Acceptable	66.93%	Acceptable
18.34	115	145	21.47%	Acceptable	16.32%	Acceptable	45.53%	Acceptable	2.86%	Acceptable	2.87%	Acceptable	3.69%	Acceptable	45.53%	Acceptable
18.56	125	135	22.78%	Acceptable	16.13%	Acceptable	51.90%	Acceptable	2.82%	Acceptable	3.02%	Acceptable	3.28%	Acceptable	51.90%	Acceptable
18.98	115	150	20.06%	Acceptable	15.78%	Acceptable	41.12%	Acceptable	2.76%	Acceptable	2.70%	Acceptable	3.57%	Acceptable	41.12%	Acceptable
18.98	138	125	24.07%	Acceptable	15.78%	Acceptable	59.22%	Acceptable	2.76%	Acceptable	3.21%	Acceptable	2.90%	Acceptable	59.22%	Acceptable
18.98	150	115	26.17%	Acceptable	15.78%	Acceptable	69.97%	Acceptable	2.76%	Acceptable	3.57%	Acceptable	2.70%	Acceptable	69.97%	Acceptable
19.25	175	100	29.66%	Acceptable	15.55%	Acceptable	91.21%	Acceptable	2.72%	Acceptable	4.33%	Acceptable	2.44%	Acceptable	91.21%	Acceptable
19.25	125	140	21.19%	Acceptable	15.55%	Acceptable	46.53%	Acceptable	2.72%	Acceptable	2.82%	Acceptable	3.16%	Acceptable	46.53%	Acceptable
19.61	115	155	18.79%	Acceptable	15.27%	Acceptable	37.27%	Acceptable	2.67%	Acceptable	2.56%	Acceptable	3.45%	Acceptable	37.27%	Acceptable
19.73	138	130	22.26%	Acceptable	15.17%	Acceptable	52.65%	Acceptable	2.66%	Acceptable	2.95%	Acceptable	2.78%	Acceptable	52.65%	Acceptable
19.80	150	120	24.03%	Acceptable	15.12%	Acceptable	61.58%	Acceptable	2.65%	Acceptable	3.23%	Acceptable	2.59%	Acceptable	61.58%	Acceptable
19.94	125	145	19.75%	Acceptable	15.02%	Acceptable	41.88%	Acceptable	2.63%	Acceptable	2.64%	Acceptable	3.06%	Acceptable	41.88%	Acceptable
20.24	115	160	17.63%	Acceptable	14.79%	Acceptable	33.89%	Acceptable	2.59%	Acceptable	2.43%	Acceptable	3.34%	Acceptable	33.89%	Acceptable

20.49	138	135	20.64%	Acceptable	14.61%	Acceptable	47.01%	Acceptable	2.56%	Acceptable	2.74%	Acceptable	2.68%	Acceptable	47.01%	Acceptable
20.62	125	150	18.46%	Acceptable	14.52%	Acceptable	37.83%	Acceptable	2.54%	Acceptable	2.49%	Acceptable	2.95%	Acceptable	37.83%	Acceptable
20.62	150	125	22.15%	Acceptable	14.52%	Acceptable	54.48%	Acceptable	2.54%	Acceptable	2.95%	Acceptable	2.49%	Acceptable	54.48%	Acceptable
20.87	115	165	16.58%	Acceptable	14.34%	Acceptable	30.90%	Acceptable	2.51%	Acceptable	2.32%	Acceptable	3.24%	Acceptable	30.90%	Acceptable
21.18	175	110	24.51%	Acceptable	14.14%	Acceptable	68.53%	Acceptable	2.48%	Acceptable	3.40%	Acceptable	2.22%	Acceptable	68.53%	Acceptable
21.25	138	140	19.19%	Acceptable	14.09%	Acceptable	42.15%	Acceptable	2.47%	Acceptable	2.55%	Acceptable	2.58%	Acceptable	42.15%	Acceptable
21.31	125	155	17.28%	Acceptable	14.05%	Acceptable	34.29%	Acceptable	2.46%	Acceptable	2.35%	Acceptable	2.86%	Acceptable	34.29%	Acceptable
21.45	150	130	20.48%	Acceptable	13.96%	Acceptable	48.43%	Acceptable	2.44%	Acceptable	2.72%	Acceptable	2.39%	Acceptable	48.43%	Acceptable
22.00	125	160	16.22%	Acceptable	13.61%	Acceptable	31.17%	Acceptable	2.38%	Acceptable	2.24%	Acceptable	2.77%	Acceptable	31.17%	Acceptable
22.01	138	145	17.89%	Acceptable	13.60%	Acceptable	37.94%	Acceptable	2.38%	Acceptable	2.39%	Acceptable	2.50%	Acceptable	37.94%	Acceptable
22.14	175	115	22.43%	Acceptable	13.53%	Acceptable	59.97%	Acceptable	2.37%	Acceptable	3.06%	Acceptable	2.12%	Acceptable	59.97%	Acceptable
22.28	150	135	18.99%	Acceptable	13.44%	Acceptable	43.25%	Acceptable	2.35%	Acceptable	2.52%	Acceptable	2.30%	Acceptable	43.25%	Acceptable
22.69	125	165	15.25%	Acceptable	13.20%	Acceptable	28.43%	Acceptable	2.31%	Acceptable	2.13%	Acceptable	2.68%	Acceptable	28.43%	Acceptable
22.77	138	150	16.72%	Acceptable	13.15%	Acceptable	34.27%	Acceptable	2.30%	Acceptable	2.25%	Acceptable	2.41%	Acceptable	34.27%	Acceptable
23.10	175	120	20.60%	Acceptable	12.96%	Acceptable	52.78%	Acceptable	2.27%	Acceptable	2.77%	Acceptable	2.04%	Acceptable	52.78%	Acceptable
23.10	150	140	17.66%	Acceptable	12.96%	Acceptable	38.78%	Acceptable	2.27%	Acceptable	2.35%	Acceptable	2.22%	Acceptable	38.78%	Acceptable
23.53	138	155	15.66%	Acceptable	12.73%	Acceptable	31.06%	Acceptable	2.23%	Acceptable	2.13%	Acceptable	2.33%	Acceptable	31.06%	Acceptable
23.92	150	145	16.46%	Acceptable	12.51%	Acceptable	34.90%	Acceptable	2.19%	Acceptable	2.20%	Acceptable	2.15%	Acceptable	34.90%	Acceptable
24.06	175	125	18.98%	Acceptable	12.44%	Acceptable	46.70%	Acceptable	2.18%	Acceptable	2.53%	Acceptable	1.95%	Acceptable	46.70%	Acceptable
24.29	138	160	14.69%	Acceptable	12.33%	Acceptable	28.24%	Acceptable	2.16%	Acceptable	2.03%	Acceptable	2.26%	Acceptable	28.24%	Acceptable
24.75	150	150	15.38%	Acceptable	12.10%	Acceptable	31.53%	Acceptable	2.12%	Acceptable	2.07%	Acceptable	2.07%	Acceptable	31.53%	Acceptable
25.02	175	130	17.55%	Acceptable	11.96%	Acceptable	41.51%	Acceptable	2.10%	Acceptable	2.33%	Acceptable	1.88%	Acceptable	41.51%	Acceptable

25.05	138	165	13.82%	Acceptable	11.95%	Acceptable	25.75%	Acceptable	2.09%	Acceptable	1.93%	Acceptable	2.19%	Acceptable	25.75%	Acceptable
25.57	150	155	14.40%	Acceptable	11.71%	Acceptable	28.57%	Acceptable	2.05%	Acceptable	1.96%	Acceptable	2.01%	Acceptable	28.57%	Acceptable
25.99	175	135	16.27%	Acceptable	11.52%	Acceptable	37.07%	Acceptable	2.02%	Acceptable	2.16%	Acceptable	1.81%	Acceptable	37.07%	Acceptable
26.40	150	160	13.52%	Acceptable	11.34%	Acceptable	25.98%	Acceptable	1.99%	Acceptable	1.86%	Acceptable	1.94%	Acceptable	25.98%	Acceptable
26.95	175	140	15.13%	Acceptable	11.11%	Acceptable	33.24%	Acceptable	1.95%	Acceptable	2.01%	Acceptable	1.75%	Acceptable	33.24%	Acceptable
27.23	150	165	12.71%	Acceptable	11.00%	Acceptable	23.69%	Acceptable	1.93%	Acceptable	1.78%	Acceptable	1.89%	Acceptable	23.69%	Acceptable
27.91	175	145	14.11%	Acceptable	10.73%	Acceptable	29.92%	Acceptable	1.88%	Acceptable	1.89%	Acceptable	1.69%	Acceptable	29.92%	Acceptable
28.88	175	150	13.18%	Acceptable	10.37%	Acceptable	27.02%	Acceptable	1.82%	Acceptable	1.78%	Acceptable	1.63%	Acceptable	27.02%	Acceptable
29.84	175	155	12.35%	Acceptable	10.03%	Acceptable	24.49%	Acceptable	1.76%	Acceptable	1.68%	Acceptable	1.58%	Acceptable	24.49%	Acceptable

Optimisation results for timber frame, European Spruce

Weight (kg)	Width (mm)	Thickness (mm)	Bending Util (%)	Bending Status	Shear Util (%)	Shear Status	SLS Util (%)	SLS Status	Compression Util (%)	Compression Status	Buckling Util Y (%)	Buckling Status Y	Buckling Util Z (%)	Buckling Status Z	Final Util (%)	Final Status
8.36	95	100	74.59%	Acceptable	44.33%	Acceptable	210.80%	Unacceptable	6.02%	Acceptable	9.91%	Acceptable	10.78%	Acceptable	210.80%	Unacceptable
8.80	100	100	70.86%	Acceptable	42.11%	Acceptable	200.26%	Unacceptable	5.72%	Acceptable	9.41%	Acceptable	9.41%	Acceptable	200.26%	Unacceptable
9.20	95	110	61.64%	Acceptable	40.30%	Acceptable	158.38%	Unacceptable	5.47%	Acceptable	7.77%	Acceptable	9.80%	Acceptable	158.38%	Unacceptable
9.61	95	115	56.40%	Acceptable	38.55%	Acceptable	138.60%	Unacceptable	5.24%	Acceptable	6.97%	Acceptable	9.38%	Acceptable	138.60%	Unacceptable
9.68	100	110	58.56%	Acceptable	38.28%	Acceptable	150.46%	Unacceptable	5.20%	Acceptable	7.38%	Acceptable	8.56%	Acceptable	150.46%	Unacceptable
10.03	95	120	51.80%	Acceptable	36.94%	Acceptable	121.99%	Unacceptable	5.02%	Acceptable	6.30%	Acceptable	8.99%	Acceptable	121.99%	Unacceptable
10.12	100	115	53.58%	Acceptable	36.62%	Acceptable	131.67%	Unacceptable	4.97%	Acceptable	6.62%	Acceptable	8.19%	Acceptable	131.67%	Unacceptable
10.12	115	100	61.61%	Acceptable	36.62%	Acceptable	174.14%	Unacceptable	4.97%	Acceptable	8.19%	Acceptable	6.62%	Acceptable	174.14%	Unacceptable
10.45	95	125	47.74%	Acceptable	35.46%	Acceptable	107.93%	Unacceptable	4.82%	Acceptable	5.75%	Acceptable	8.63%	Acceptable	107.93%	Unacceptable
10.56	100	120	49.21%	Acceptable	35.09%	Acceptable	115.89%	Unacceptable	4.77%	Acceptable	5.99%	Acceptable	7.85%	Acceptable	115.89%	Unacceptable
10.87	95	130	44.13%	Acceptable	34.10%	Acceptable	95.95%	Acceptable	4.63%	Acceptable	5.28%	Acceptable	8.29%	Acceptable	95.95%	Acceptable
11.00	100	125	45.35%	Acceptable	33.69%	Acceptable	102.53%	Unacceptable	4.58%	Acceptable	5.46%	Acceptable	7.53%	Acceptable	102.53%	Unacceptable
11.00	125	100	56.69%	Acceptable	33.69%	Acceptable	160.21%	Unacceptable	4.58%	Acceptable	7.53%	Acceptable	5.46%	Acceptable	160.21%	Unacceptable
11.13	115	110	50.92%	Acceptable	33.29%	Acceptable	130.83%	Unacceptable	4.52%	Acceptable	6.42%	Acceptable	6.02%	Acceptable	130.83%	Unacceptable

11.29	95	135	40.93%	Acceptable	32.84%	Acceptable	85.68%	Acceptable	4.46%	Acceptable	4.88%	Acceptable	7.99%	Acceptable	85.68%	Acceptable
11.44	100	130	41.93%	Acceptable	32.39%	Acceptable	91.15%	Acceptable	4.40%	Acceptable	5.01%	Acceptable	7.24%	Acceptable	91.15%	Acceptable
11.64	115	115	46.59%	Acceptable	31.84%	Acceptable	114.50%	Unacceptable	4.33%	Acceptable	5.76%	Acceptable	5.76%	Acceptable	114.50%	Unacceptable
11.70	95	140	38.05%	Acceptable	31.66%	Acceptable	76.82%	Acceptable	4.30%	Acceptable	4.54%	Acceptable	7.70%	Acceptable	76.82%	Acceptable
11.88	100	135	38.88%	Acceptable	31.19%	Acceptable	81.39%	Acceptable	4.24%	Acceptable	4.63%	Acceptable	6.97%	Acceptable	81.39%	Acceptable
12.10	125	110	46.85%	Acceptable	30.63%	Acceptable	120.37%	Unacceptable	4.16%	Acceptable	5.90%	Acceptable	4.96%	Acceptable	120.37%	Unacceptable
12.12	95	145	35.48%	Acceptable	30.57%	Acceptable	69.15%	Acceptable	4.15%	Acceptable	4.25%	Acceptable	7.44%	Acceptable	69.15%	Acceptable
12.14	115	120	42.79%	Acceptable	30.52%	Acceptable	100.77%	Unacceptable	4.14%	Acceptable	5.21%	Acceptable	5.52%	Acceptable	100.77%	Unacceptable
12.14	138	100	51.35%	Acceptable	30.52%	Acceptable	145.11%	Unacceptable	4.14%	Acceptable	6.82%	Acceptable	4.44%	Acceptable	145.11%	Unacceptable
12.32	100	140	36.15%	Acceptable	30.08%	Acceptable	72.98%	Acceptable	4.09%	Acceptable	4.31%	Acceptable	6.72%	Acceptable	72.98%	Acceptable
12.54	95	150	33.15%	Acceptable	29.55%	Acceptable	62.46%	Acceptable	4.01%	Acceptable	3.99%	Acceptable	7.19%	Acceptable	62.46%	Acceptable
12.65	115	125	39.43%	Acceptable	29.30%	Acceptable	89.16%	Acceptable	3.98%	Acceptable	4.75%	Acceptable	5.30%	Acceptable	89.16%	Acceptable
12.65	125	115	42.86%	Acceptable	29.30%	Acceptable	105.34%	Unacceptable	3.98%	Acceptable	5.30%	Acceptable	4.75%	Acceptable	105.34%	Unacceptable
12.76	100	145	33.70%	Acceptable	29.04%	Acceptable	65.69%	Acceptable	3.94%	Acceptable	4.03%	Acceptable	6.49%	Acceptable	65.69%	Acceptable
12.96	95	155	31.05%	Acceptable	28.60%	Acceptable	56.61%	Acceptable	3.88%	Acceptable	3.77%	Acceptable	6.96%	Acceptable	56.61%	Acceptable
13.16	115	130	36.46%	Acceptable	28.17%	Acceptable	79.26%	Acceptable	3.83%	Acceptable	4.36%	Acceptable	5.09%	Acceptable	79.26%	Acceptable
13.20	100	150	31.49%	Acceptable	28.08%	Acceptable	59.34%	Acceptable	3.81%	Acceptable	3.79%	Acceptable	6.28%	Acceptable	59.34%	Acceptable
13.20	125	120	39.37%	Acceptable	28.08%	Acceptable	92.71%	Acceptable	3.81%	Acceptable	4.79%	Acceptable	4.55%	Acceptable	92.71%	Acceptable

13.20	150	100	47.24%	Acceptable	28.08%	Acceptable	133.51%	Unacceptable	3.81%	Acceptable	6.28%	Acceptable	3.79%	Acceptable	133.51%	Unacceptable
13.36	138	110	42.43%	Acceptable	27.74%	Acceptable	109.03%	Unacceptable	3.77%	Acceptable	5.35%	Acceptable	4.03%	Acceptable	109.03%	Unacceptable
13.38	95	160	29.14%	Acceptable	27.71%	Acceptable	51.46%	Acceptable	3.76%	Acceptable	3.58%	Acceptable	6.74%	Acceptable	51.46%	Acceptable
13.64	100	155	29.49%	Acceptable	27.17%	Acceptable	53.78%	Acceptable	3.69%	Acceptable	3.59%	Acceptable	6.07%	Acceptable	53.78%	Acceptable
13.66	115	135	33.81%	Acceptable	27.13%	Acceptable	70.78%	Acceptable	3.68%	Acceptable	4.03%	Acceptable	4.90%	Acceptable	70.78%	Acceptable
13.75	125	125	36.28%	Acceptable	26.95%	Acceptable	82.03%	Acceptable	3.66%	Acceptable	4.37%	Acceptable	4.37%	Acceptable	82.03%	Acceptable
13.79	95	165	27.40%	Acceptable	26.87%	Acceptable	46.93%	Acceptable	3.65%	Acceptable	3.41%	Acceptable	6.54%	Acceptable	46.93%	Acceptable
13.97	138	115	38.82%	Acceptable	26.54%	Acceptable	95.42%	Acceptable	3.60%	Acceptable	4.80%	Acceptable	3.86%	Acceptable	95.42%	Acceptable
14.08	100	160	27.68%	Acceptable	26.32%	Acceptable	48.89%	Acceptable	3.57%	Acceptable	3.40%	Acceptable	5.88%	Acceptable	48.89%	Acceptable
14.17	115	140	31.44%	Acceptable	26.16%	Acceptable	63.46%	Acceptable	3.55%	Acceptable	3.75%	Acceptable	4.73%	Acceptable	63.46%	Acceptable
14.30	125	130	33.54%	Acceptable	25.92%	Acceptable	72.92%	Acceptable	3.52%	Acceptable	4.01%	Acceptable	4.20%	Acceptable	72.92%	Acceptable
14.52	100	165	26.03%	Acceptable	25.52%	Acceptable	44.58%	Acceptable	3.47%	Acceptable	3.24%	Acceptable	5.71%	Acceptable	44.58%	Acceptable
14.52	150	110	39.04%	Acceptable	25.52%	Acceptable	100.30%	Unacceptable	3.47%	Acceptable	4.92%	Acceptable	3.45%	Acceptable	100.30%	Unacceptable
14.57	138	120	35.66%	Acceptable	25.43%	Acceptable	83.98%	Acceptable	3.45%	Acceptable	4.34%	Acceptable	3.70%	Acceptable	83.98%	Acceptable
14.67	115	145	29.31%	Acceptable	25.26%	Acceptable	57.12%	Acceptable	3.43%	Acceptable	3.51%	Acceptable	4.57%	Acceptable	57.12%	Acceptable
14.85	125	135	31.10%	Acceptable	24.96%	Acceptable	65.11%	Acceptable	3.39%	Acceptable	3.71%	Acceptable	4.04%	Acceptable	65.11%	Acceptable
15.18	115	150	27.38%	Acceptable	24.41%	Acceptable	51.60%	Acceptable	3.32%	Acceptable	3.30%	Acceptable	4.41%	Acceptable	51.60%	Acceptable
15.18	138	125	32.86%	Acceptable	24.41%	Acceptable	74.30%	Acceptable	3.32%	Acceptable	3.96%	Acceptable	3.55%	Acceptable	74.30%	Acceptable

15.18	150	115	35.72%	Acceptable	24.41%	Acceptable	87.78%	Acceptable	3.32%	Acceptable	4.41%	Acceptable	3.30%	Acceptable	87.78%	Acceptable
15.40	175	100	40.49%	Acceptable	24.06%	Acceptable	114.43%	Unacceptable	3.27%	Acceptable	5.38%	Acceptable	2.96%	Acceptable	114.43%	Unacceptable
15.40	125	140	28.92%	Acceptable	24.06%	Acceptable	58.38%	Acceptable	3.27%	Acceptable	3.45%	Acceptable	3.90%	Acceptable	58.38%	Acceptable
15.69	115	155	25.65%	Acceptable	23.63%	Acceptable	46.76%	Acceptable	3.21%	Acceptable	3.12%	Acceptable	4.27%	Acceptable	46.76%	Acceptable
15.79	138	130	30.38%	Acceptable	23.47%	Acceptable	66.05%	Acceptable	3.19%	Acceptable	3.63%	Acceptable	3.41%	Acceptable	66.05%	Acceptable
15.84	150	120	32.80%	Acceptable	23.40%	Acceptable	77.26%	Acceptable	3.18%	Acceptable	3.99%	Acceptable	3.16%	Acceptable	77.26%	Acceptable
15.95	125	145	26.96%	Acceptable	23.23%	Acceptable	52.55%	Acceptable	3.16%	Acceptable	3.23%	Acceptable	3.76%	Acceptable	52.55%	Acceptable
16.19	115	160	24.07%	Acceptable	22.89%	Acceptable	42.51%	Acceptable	3.11%	Acceptable	2.96%	Acceptable	4.14%	Acceptable	42.51%	Acceptable
16.39	138	135	28.17%	Acceptable	22.61%	Acceptable	58.98%	Acceptable	3.07%	Acceptable	3.36%	Acceptable	3.29%	Acceptable	58.98%	Acceptable
16.50	125	150	25.19%	Acceptable	22.46%	Acceptable	47.47%	Acceptable	3.05%	Acceptable	3.04%	Acceptable	3.64%	Acceptable	47.47%	Acceptable
16.50	150	125	30.23%	Acceptable	22.46%	Acceptable	68.35%	Acceptable	3.05%	Acceptable	3.64%	Acceptable	3.04%	Acceptable	68.35%	Acceptable
16.70	115	165	22.63%	Acceptable	22.19%	Acceptable	38.76%	Acceptable	3.01%	Acceptable	2.82%	Acceptable	4.01%	Acceptable	38.76%	Acceptable
16.94	175	110	33.46%	Acceptable	21.88%	Acceptable	85.98%	Acceptable	2.97%	Acceptable	4.22%	Acceptable	2.69%	Acceptable	85.98%	Acceptable
17.00	138	140	26.20%	Acceptable	21.80%	Acceptable	52.88%	Acceptable	2.96%	Acceptable	3.12%	Acceptable	3.17%	Acceptable	52.88%	Acceptable
17.05	125	155	23.59%	Acceptable	21.74%	Acceptable	43.02%	Acceptable	2.95%	Acceptable	2.87%	Acceptable	3.52%	Acceptable	43.02%	Acceptable
17.16	150	130	27.95%	Acceptable	21.60%	Acceptable	60.77%	Acceptable	2.93%	Acceptable	3.34%	Acceptable	2.92%	Acceptable	60.77%	Acceptable
17.60	125	160	22.14%	Acceptable	21.06%	Acceptable	39.11%	Acceptable	2.86%	Acceptable	2.72%	Acceptable	3.41%	Acceptable	39.11%	Acceptable
17.61	138	145	24.42%	Acceptable	21.05%	Acceptable	47.60%	Acceptable	2.86%	Acceptable	2.92%	Acceptable	3.06%	Acceptable	47.60%	Acceptable

17.71	175	115	30.62%	Acceptable	20.93%	Acceptable	75.24%	Acceptable	2.84%	Acceptable	3.78%	Acceptable	2.58%	Acceptable	75.24%	Acceptable
17.82	150	135	25.92%	Acceptable	20.80%	Acceptable	54.26%	Acceptable	2.82%	Acceptable	3.09%	Acceptable	2.81%	Acceptable	54.26%	Acceptable
18.15	125	165	20.82%	Acceptable	20.42%	Acceptable	35.66%	Acceptable	2.77%	Acceptable	2.59%	Acceptable	3.31%	Acceptable	35.66%	Acceptable
18.22	138	150	22.82%	Acceptable	20.34%	Acceptable	43.00%	Acceptable	2.76%	Acceptable	2.75%	Acceptable	2.96%	Acceptable	43.00%	Acceptable
18.48	175	120	28.12%	Acceptable	20.05%	Acceptable	66.22%	Acceptable	2.72%	Acceptable	3.42%	Acceptable	2.47%	Acceptable	66.22%	Acceptable
18.48	150	140	24.10%	Acceptable	20.05%	Acceptable	48.65%	Acceptable	2.72%	Acceptable	2.87%	Acceptable	2.71%	Acceptable	48.65%	Acceptable
18.82	138	155	21.37%	Acceptable	19.69%	Acceptable	38.97%	Acceptable	2.67%	Acceptable	2.60%	Acceptable	2.86%	Acceptable	38.97%	Acceptable
19.14	150	145	22.47%	Acceptable	19.36%	Acceptable	43.79%	Acceptable	2.63%	Acceptable	2.69%	Acceptable	2.62%	Acceptable	43.79%	Acceptable
19.25	175	125	25.91%	Acceptable	19.25%	Acceptable	58.59%	Acceptable	2.61%	Acceptable	3.12%	Acceptable	2.37%	Acceptable	58.59%	Acceptable
19.43	138	160	20.06%	Acceptable	19.07%	Acceptable	35.43%	Acceptable	2.59%	Acceptable	2.46%	Acceptable	2.77%	Acceptable	35.43%	Acceptable
19.80	150	150	20.99%	Acceptable	18.72%	Acceptable	39.56%	Acceptable	2.54%	Acceptable	2.53%	Acceptable	2.53%	Acceptable	39.56%	Acceptable
20.02	175	130	23.96%	Acceptable	18.51%	Acceptable	52.09%	Acceptable	2.51%	Acceptable	2.86%	Acceptable	2.28%	Acceptable	52.09%	Acceptable
20.04	138	165	18.86%	Acceptable	18.50%	Acceptable	32.30%	Acceptable	2.51%	Acceptable	2.35%	Acceptable	2.69%	Acceptable	32.30%	Acceptable
20.46	150	155	19.66%	Acceptable	18.11%	Acceptable	35.85%	Acceptable	2.46%	Acceptable	2.39%	Acceptable	2.45%	Acceptable	35.85%	Acceptable
20.79	175	135	22.22%	Acceptable	17.83%	Acceptable	46.51%	Acceptable	2.42%	Acceptable	2.65%	Acceptable	2.19%	Acceptable	46.51%	Acceptable
21.12	150	160	18.45%	Acceptable	17.55%	Acceptable	32.59%	Acceptable	2.38%	Acceptable	2.27%	Acceptable	2.37%	Acceptable	32.59%	Acceptable
21.56	175	140	20.66%	Acceptable	17.19%	Acceptable	41.70%	Acceptable	2.33%	Acceptable	2.46%	Acceptable	2.12%	Acceptable	41.70%	Acceptable
21.78	150	165	17.35%	Acceptable	17.02%	Acceptable	29.72%	Acceptable	2.31%	Acceptable	2.16%	Acceptable	2.30%	Acceptable	29.72%	Acceptable

22.33	175	145	19.26%	Acceptable	16.60%	Acceptable	37.54%	Acceptable	2.25%	Acceptable	2.31%	Acceptable	2.04%	Acceptable	37.54%	Acceptable
23.10	175	150	18.00%	Acceptable	16.04%	Acceptable	33.91%	Acceptable	2.18%	Acceptable	2.17%	Acceptable	1.97%	Acceptable	33.91%	Acceptable
23.87	175	155	16.85%	Acceptable	15.53%	Acceptable	30.73%	Acceptable	2.11%	Acceptable	2.05%	Acceptable	1.91%	Acceptable	30.73%	Acceptable
24.64	175	160	15.82%	Acceptable	15.04%	Acceptable	27.94%	Acceptable	2.04%	Acceptable	1.94%	Acceptable	1.85%	Acceptable	27.94%	Acceptable
25.41	175	165	14.87%	Acceptable	14.58%	Acceptable	25.47%	Acceptable	1.98%	Acceptable	1.85%	Acceptable	1.79%	Acceptable	25.47%	Acceptable

Optimisation results for timber frame, European Larch

Weight (kg)	Width (mm)	Thickness (mm)	Bending Util (%)	Bending Status	Shear Util (%)	Shear Status	SLS Util (%)	SLS Status	Compression Util (%)	Compression Status	Buckling Util Y (%)	Buckling Status Y	Buckling Util Z (%)	Buckling Status Z	Final Util (%)	Final Status
11.59	95	100	51.64%	Acceptable	26.11%	Acceptable	182.57%	Unacceptable	4.68%	Acceptable	8.42%	Acceptable	9.19%	Acceptable	182.57%	Unacceptable
12.20	100	100	49.05%	Acceptable	24.80%	Acceptable	173.44%	Unacceptable	4.45%	Acceptable	8.00%	Acceptable	8.00%	Acceptable	173.44%	Unacceptable
12.75	95	110	42.68%	Acceptable	23.73%	Acceptable	137.16%	Unacceptable	4.26%	Acceptable	6.56%	Acceptable	8.35%	Acceptable	137.16%	Unacceptable
13.33	95	115	39.04%	Acceptable	22.70%	Acceptable	120.04%	Unacceptable	4.07%	Acceptable	5.86%	Acceptable	7.99%	Acceptable	120.04%	Unacceptable
13.42	100	110	40.54%	Acceptable	22.55%	Acceptable	130.31%	Unacceptable	4.04%	Acceptable	6.23%	Acceptable	7.27%	Acceptable	130.31%	Unacceptable
13.91	95	120	35.86%	Acceptable	21.75%	Acceptable	105.65%	Unacceptable	3.90%	Acceptable	5.28%	Acceptable	7.66%	Acceptable	105.65%	Unacceptable
14.03	100	115	37.09%	Acceptable	21.57%	Acceptable	114.04%	Unacceptable	3.87%	Acceptable	5.57%	Acceptable	6.96%	Acceptable	114.04%	Unacceptable
14.03	115	100	42.66%	Acceptable	21.57%	Acceptable	150.82%	Unacceptable	3.87%	Acceptable	6.96%	Acceptable	5.57%	Acceptable	150.82%	Unacceptable
14.49	95	125	33.05%	Acceptable	20.88%	Acceptable	93.47%	Acceptable	3.75%	Acceptable	4.79%	Acceptable	7.35%	Acceptable	93.47%	Acceptable
14.64	100	120	34.07%	Acceptable	20.67%	Acceptable	100.37%	Unacceptable	3.71%	Acceptable	5.01%	Acceptable	6.67%	Acceptable	100.37%	Unacceptable
15.07	95	130	30.55%	Acceptable	20.08%	Acceptable	83.10%	Acceptable	3.60%	Acceptable	4.38%	Acceptable	7.07%	Acceptable	83.10%	Acceptable

15.25	100	125	31.40%	Acceptable	19.84%	Acceptable	88.80%	Acceptable	3.56%	Acceptable	4.55%	Acceptable	6.40%	Acceptable	88.80%	Acceptable
15.25	125	100	39.24%	Acceptable	19.84%	Acceptable	138.75 %	Unacceptable	3.56%	Acceptable	6.40%	Acceptable	4.55%	Acceptable	138.75 %	Unacceptable
15.43	115	110	35.25%	Acceptable	19.60%	Acceptable	113.31 %	Unacceptable	3.52%	Acceptable	5.42%	Acceptable	5.06%	Acceptable	113.31 %	Unacceptable
15.65	95	135	28.33%	Acceptable	19.34%	Acceptable	74.20%	Acceptable	3.47%	Acceptable	4.03%	Acceptable	6.81%	Acceptable	74.20%	Acceptable
15.86	100	130	29.03%	Acceptable	19.08%	Acceptable	78.94%	Acceptable	3.42%	Acceptable	4.16%	Acceptable	6.15%	Acceptable	78.94%	Acceptable
16.13	115	115	32.25%	Acceptable	18.75%	Acceptable	99.16%	Acceptable	3.36%	Acceptable	4.84%	Acceptable	4.84%	Acceptable	99.16%	Acceptable
16.23	95	140	26.35%	Acceptable	18.65%	Acceptable	66.53%	Acceptable	3.35%	Acceptable	3.73%	Acceptable	6.56%	Acceptable	66.53%	Acceptable
16.47	100	135	26.92%	Acceptable	18.37%	Acceptable	70.49%	Acceptable	3.30%	Acceptable	3.82%	Acceptable	5.93%	Acceptable	70.49%	Acceptable
16.77	125	110	32.43%	Acceptable	18.04%	Acceptable	104.24 %	Unacceptable	3.24%	Acceptable	4.98%	Acceptable	4.14%	Acceptable	104.24 %	Unacceptable
16.81	95	145	24.56%	Acceptable	18.00%	Acceptable	59.88%	Acceptable	3.23%	Acceptable	3.47%	Acceptable	6.34%	Acceptable	59.88%	Acceptable
16.84	115	120	29.62%	Acceptable	17.97%	Acceptable	87.28%	Acceptable	3.22%	Acceptable	4.36%	Acceptable	4.64%	Acceptable	87.28%	Acceptable
16.84	138	100	35.55%	Acceptable	17.97%	Acceptable	125.68 %	Unacceptable	3.22%	Acceptable	5.80%	Acceptable	3.65%	Acceptable	125.68 %	Unacceptable
17.08	100	140	25.03%	Acceptable	17.71%	Acceptable	63.21%	Acceptable	3.18%	Acceptable	3.54%	Acceptable	5.71%	Acceptable	63.21%	Acceptable
17.38	95	150	22.95%	Acceptable	17.40%	Acceptable	54.09%	Acceptable	3.12%	Acceptable	3.25%	Acceptable	6.13%	Acceptable	54.09%	Acceptable
17.54	115	125	27.30%	Acceptable	17.25%	Acceptable	77.22%	Acceptable	3.09%	Acceptable	3.96%	Acceptable	4.45%	Acceptable	77.22%	Acceptable
17.54	125	115	29.67%	Acceptable	17.25%	Acceptable	91.23%	Acceptable	3.09%	Acceptable	4.45%	Acceptable	3.96%	Acceptable	91.23%	Acceptable
17.69	100	145	23.33%	Acceptable	17.10%	Acceptable	56.89%	Acceptable	3.07%	Acceptable	3.30%	Acceptable	5.52%	Acceptable	56.89%	Acceptable
17.96	95	155	21.49%	Acceptable	16.84%	Acceptable	49.03%	Acceptable	3.02%	Acceptable	3.06%	Acceptable	5.93%	Acceptable	49.03%	Acceptable
18.24	115	130	25.24%	Acceptable	16.59%	Acceptable	68.65%	Acceptable	2.98%	Acceptable	3.61%	Acceptable	4.28%	Acceptable	68.65%	Acceptable
18.30	100	150	21.80%	Acceptable	16.53%	Acceptable	51.39%	Acceptable	2.97%	Acceptable	3.09%	Acceptable	5.33%	Acceptable	51.39%	Acceptable
18.30	125	120	27.25%	Acceptable	16.53%	Acceptable	80.30%	Acceptable	2.97%	Acceptable	4.01%	Acceptable	3.79%	Acceptable	80.30%	Acceptable
18.30	150	100	32.70%	Acceptable	16.53%	Acceptable	115.62 %	Unacceptable	2.97%	Acceptable	5.33%	Acceptable	3.09%	Acceptable	115.62 %	Unacceptable

18.52	138	110	29.38%	Acceptable	16.34%	Acceptable	94.42%	Acceptable	2.93%	Acceptable	4.51%	Acceptable	3.32%	Acceptable	94.42%	Acceptable
18.54	95	160	20.17%	Acceptable	16.32%	Acceptable	44.57%	Acceptable	2.93%	Acceptable	2.89%	Acceptable	5.74%	Acceptable	44.57%	Acceptable
18.91	100	155	20.42%	Acceptable	16.00%	Acceptable	46.57%	Acceptable	2.87%	Acceptable	2.90%	Acceptable	5.16%	Acceptable	46.57%	Acceptable
18.94	115	135	23.41%	Acceptable	15.97%	Acceptable	61.30%	Acceptable	2.87%	Acceptable	3.33%	Acceptable	4.12%	Acceptable	61.30%	Acceptable
19.06	125	125	25.12%	Acceptable	15.87%	Acceptable	71.04%	Acceptable	2.85%	Acceptable	3.64%	Acceptable	3.64%	Acceptable	71.04%	Acceptable
19.12	95	165	18.97%	Acceptable	15.82%	Acceptable	40.64%	Acceptable	2.84%	Acceptable	2.74%	Acceptable	5.57%	Acceptable	40.64%	Acceptable
19.36	138	115	26.88%	Acceptable	15.63%	Acceptable	82.64%	Acceptable	2.80%	Acceptable	4.03%	Acceptable	3.17%	Acceptable	82.64%	Acceptable
19.52	100	160	19.16%	Acceptable	15.50%	Acceptable	42.34%	Acceptable	2.78%	Acceptable	2.74%	Acceptable	5.00%	Acceptable	42.34%	Acceptable
19.64	115	140	21.76%	Acceptable	15.40%	Acceptable	54.96%	Acceptable	2.76%	Acceptable	3.08%	Acceptable	3.98%	Acceptable	54.96%	Acceptable
19.82	125	130	23.22%	Acceptable	15.26%	Acceptable	63.15%	Acceptable	2.74%	Acceptable	3.33%	Acceptable	3.50%	Acceptable	63.15%	Acceptable
20.13	100	165	18.02%	Acceptable	15.03%	Acceptable	38.61%	Acceptable	2.70%	Acceptable	2.60%	Acceptable	4.85%	Acceptable	38.61%	Acceptable
20.13	150	110	27.03%	Acceptable	15.03%	Acceptable	86.87%	Acceptable	2.70%	Acceptable	4.15%	Acceptable	2.81%	Acceptable	86.87%	Acceptable
20.20	138	120	24.69%	Acceptable	14.98%	Acceptable	72.73%	Acceptable	2.69%	Acceptable	3.63%	Acceptable	3.04%	Acceptable	72.73%	Acceptable
20.34	115	145	20.29%	Acceptable	14.87%	Acceptable	49.47%	Acceptable	2.67%	Acceptable	2.87%	Acceptable	3.84%	Acceptable	49.47%	Acceptable
20.59	125	135	21.53%	Acceptable	14.70%	Acceptable	56.39%	Acceptable	2.64%	Acceptable	3.06%	Acceptable	3.37%	Acceptable	56.39%	Acceptable
21.05	115	150	18.96%	Acceptable	14.38%	Acceptable	44.69%	Acceptable	2.58%	Acceptable	2.68%	Acceptable	3.71%	Acceptable	44.69%	Acceptable
21.05	138	125	22.75%	Acceptable	14.38%	Acceptable	64.35%	Acceptable	2.58%	Acceptable	3.30%	Acceptable	2.92%	Acceptable	64.35%	Acceptable
21.05	150	115	24.73%	Acceptable	14.38%	Acceptable	76.03%	Acceptable	2.58%	Acceptable	3.71%	Acceptable	2.68%	Acceptable	76.03%	Acceptable
21.35	175	100	28.03%	Acceptable	14.17%	Acceptable	99.11%	Acceptable	2.54%	Acceptable	4.57%	Acceptable	2.37%	Acceptable	99.11%	Acceptable
21.35	125	140	20.02%	Acceptable	14.17%	Acceptable	50.56%	Acceptable	2.54%	Acceptable	2.83%	Acceptable	3.25%	Acceptable	50.56%	Acceptable
21.75	115	155	17.76%	Acceptable	13.91%	Acceptable	40.50%	Acceptable	2.50%	Acceptable	2.53%	Acceptable	3.59%	Acceptable	40.50%	Acceptable
21.89	138	130	21.03%	Acceptable	13.82%	Acceptable	57.20%	Acceptable	2.48%	Acceptable	3.01%	Acceptable	2.81%	Acceptable	57.20%	Acceptable

21.96	150	120	22.71%	Acceptable	13.78%	Acceptable	66.91%	Acceptable	2.47%	Acceptable	3.34%	Acceptable	2.57%	Acceptable	66.91%	Acceptable
22.11	125	145	18.67%	Acceptable	13.68%	Acceptable	45.51%	Acceptable	2.45%	Acceptable	2.64%	Acceptable	3.14%	Acceptable	45.51%	Acceptable
22.45	115	160	16.66%	Acceptable	13.48%	Acceptable	36.82%	Acceptable	2.42%	Acceptable	2.39%	Acceptable	3.48%	Acceptable	36.82%	Acceptable
22.73	138	135	19.50%	Acceptable	13.31%	Acceptable	51.08%	Acceptable	2.39%	Acceptable	2.77%	Acceptable	2.70%	Acceptable	51.08%	Acceptable
22.88	125	150	17.44%	Acceptable	13.23%	Acceptable	41.11%	Acceptable	2.37%	Acceptable	2.47%	Acceptable	3.03%	Acceptable	41.11%	Acceptable
22.88	150	125	20.93%	Acceptable	13.23%	Acceptable	59.20%	Acceptable	2.37%	Acceptable	3.03%	Acceptable	2.47%	Acceptable	59.20%	Acceptable
23.15	115	165	15.67%	Acceptable	13.07%	Acceptable	33.57%	Acceptable	2.34%	Acceptable	2.26%	Acceptable	3.37%	Acceptable	33.57%	Acceptable
23.48	175	110	23.17%	Acceptable	12.88%	Acceptable	74.46%	Acceptable	2.31%	Acceptable	3.56%	Acceptable	2.15%	Acceptable	74.46%	Acceptable
23.57	138	140	18.14%	Acceptable	12.84%	Acceptable	45.80%	Acceptable	2.30%	Acceptable	2.57%	Acceptable	2.61%	Acceptable	45.80%	Acceptable
23.64	125	155	16.33%	Acceptable	12.80%	Acceptable	37.26%	Acceptable	2.30%	Acceptable	2.32%	Acceptable	2.93%	Acceptable	37.26%	Acceptable
23.79	150	130	19.35%	Acceptable	12.72%	Acceptable	52.63%	Acceptable	2.28%	Acceptable	2.77%	Acceptable	2.37%	Acceptable	52.63%	Acceptable
24.40	125	160	15.33%	Acceptable	12.40%	Acceptable	33.87%	Acceptable	2.22%	Acceptable	2.20%	Acceptable	2.84%	Acceptable	33.87%	Acceptable
24.41	138	145	16.91%	Acceptable	12.39%	Acceptable	41.22%	Acceptable	2.22%	Acceptable	2.39%	Acceptable	2.52%	Acceptable	41.22%	Acceptable
24.55	175	115	21.20%	Acceptable	12.32%	Acceptable	65.16%	Acceptable	2.21%	Acceptable	3.18%	Acceptable	2.06%	Acceptable	65.16%	Acceptable
24.71	150	135	17.94%	Acceptable	12.25%	Acceptable	46.99%	Acceptable	2.20%	Acceptable	2.55%	Acceptable	2.29%	Acceptable	46.99%	Acceptable
25.16	125	165	14.41%	Acceptable	12.02%	Acceptable	30.89%	Acceptable	2.16%	Acceptable	2.08%	Acceptable	2.76%	Acceptable	30.89%	Acceptable
25.25	138	150	15.80%	Acceptable	11.98%	Acceptable	37.24%	Acceptable	2.15%	Acceptable	2.24%	Acceptable	2.43%	Acceptable	37.24%	Acceptable
25.62	175	120	19.47%	Acceptable	11.81%	Acceptable	57.35%	Acceptable	2.12%	Acceptable	2.87%	Acceptable	1.97%	Acceptable	57.35%	Acceptable
25.62	150	140	16.69%	Acceptable	11.81%	Acceptable	42.14%	Acceptable	2.12%	Acceptable	2.36%	Acceptable	2.20%	Acceptable	42.14%	Acceptable
26.10	138	155	14.80%	Acceptable	11.59%	Acceptable	33.75%	Acceptable	2.08%	Acceptable	2.10%	Acceptable	2.35%	Acceptable	33.75%	Acceptable
26.53	150	145	15.55%	Acceptable	11.40%	Acceptable	37.93%	Acceptable	2.05%	Acceptable	2.20%	Acceptable	2.13%	Acceptable	37.93%	Acceptable
26.69	175	125	17.94%	Acceptable	11.34%	Acceptable	50.74%	Acceptable	2.03%	Acceptable	2.60%	Acceptable	1.89%	Acceptable	50.74%	Acceptable

26.94	138	160	13.89%	Acceptable	11.23%	Acceptable	30.68%	Acceptable	2.01%	Acceptable	1.99%	Acceptable	2.28%	Acceptable	30.68%	Acceptable
27.45	150	150	14.53%	Acceptable	11.02%	Acceptable	34.26%	Acceptable	1.98%	Acceptable	2.06%	Acceptable	2.06%	Acceptable	34.26%	Acceptable
27.75	175	130	16.59%	Acceptable	10.90%	Acceptable	45.11%	Acceptable	1.96%	Acceptable	2.38%	Acceptable	1.82%	Acceptable	45.11%	Acceptable
27.78	138	165	13.06%	Acceptable	10.89%	Acceptable	27.98%	Acceptable	1.95%	Acceptable	1.89%	Acceptable	2.21%	Acceptable	27.98%	Acceptable
28.36	150	155	13.61%	Acceptable	10.67%	Acceptable	31.05%	Acceptable	1.91%	Acceptable	1.94%	Acceptable	1.99%	Acceptable	31.05%	Acceptable
28.82	175	135	15.38%	Acceptable	10.50%	Acceptable	40.28%	Acceptable	1.88%	Acceptable	2.19%	Acceptable	1.75%	Acceptable	40.28%	Acceptable
29.28	150	160	12.77%	Acceptable	10.33%	Acceptable	28.23%	Acceptable	1.85%	Acceptable	1.83%	Acceptable	1.93%	Acceptable	28.23%	Acceptable
29.89	175	140	14.30%	Acceptable	10.12%	Acceptable	36.12%	Acceptable	1.82%	Acceptable	2.02%	Acceptable	1.69%	Acceptable	36.12%	Acceptable
30.20	150	165	12.01%	Acceptable	10.02%	Acceptable	25.74%	Acceptable	1.80%	Acceptable	1.74%	Acceptable	1.87%	Acceptable	25.74%	Acceptable
30.96	175	145	13.33%	Acceptable	9.77%	Acceptable	32.51%	Acceptable	1.75%	Acceptable	1.88%	Acceptable	1.63%	Acceptable	32.51%	Acceptable
32.02	175	150	12.46%	Acceptable	9.45%	Acceptable	29.37%	Acceptable	1.69%	Acceptable	1.76%	Acceptable	1.58%	Acceptable	29.37%	Acceptable
33.09	175	155	11.67%	Acceptable	9.14%	Acceptable	26.61%	Acceptable	1.64%	Acceptable	1.66%	Acceptable	1.53%	Acceptable	26.61%	Acceptable

Optimisation results for PMT Joints based on Equivalent Steel Bolt Method

Diameter(mm)	L.e(mm)	L.s(mm)	L.v(mm)	L.g(mm)	Joint capacity(kN)	Joint Status
12.7	14.69	18.36	11.02	11.02	2.65	Not Acceptable
12.954	14.98	18.73	11.24	11.24	2.76	Not Acceptable
13.208	15.28	19.1	11.46	11.46	2.87	Not Acceptable
13.462	15.57	19.46	11.68	11.68	2.98	Not Acceptable
13.716	15.86	19.83	11.9	11.9	3.09	Not Acceptable

13.97	16.16	20.2	12.12	12.12	3.21	Not Acceptable
14.224	16.48	20.61	12.36	12.36	3.33	Not Acceptable
14.478	17.08	21.35	12.81	12.81	3.45	Not Acceptable
14.732	17.68	22.1	13.26	13.26	3.57	Not Acceptable
14.986	18.3	22.87	13.72	13.72	3.69	Not Acceptable
15.24	18.92	23.65	14.19	14.19	3.82	Not Acceptable
15.494	19.56	24.45	14.67	14.67	3.95	Not Acceptable
15.748	20.21	25.26	15.15	15.15	4.08	Not Acceptable
16.002	20.86	26.08	15.65	15.65	4.21	Not Acceptable
16.256	21.53	26.91	16.15	16.15	4.34	Not Acceptable
16.51	22.21	27.76	16.66	16.66	4.48	Not Acceptable
16.764	22.9	28.62	17.17	17.17	4.62	Acceptable
17.018	23.6	29.5	17.7	17.7	4.76	Acceptable
17.272	24.31	30.38	18.23	18.23	4.9	Acceptable
17.526	25.03	31.28	18.77	18.77	5.05	Acceptable
17.78	25.76	32.2	19.32	19.32	5.2	Acceptable
18.034	26.5	33.12	19.87	19.87	5.35	Acceptable
18.288	27.25	34.06	20.44	20.44	5.5	Acceptable
18.542	28.01	35.02	21.01	21.01	5.65	Acceptable
18.796	28.78	35.98	21.59	21.59	5.81	Acceptable
19.05	29.57	36.96	22.18	22.18	5.97	Acceptable

19.304	30.36	37.95	22.77	22.77	6.13	Acceptable
19.558	31.17	38.96	23.37	23.37	6.29	Acceptable
19.812	31.98	39.98	23.99	23.99	6.45	Acceptable
20.066	32.81	41.01	24.6	24.6	6.62	Acceptable
20.32	33.64	42.05	25.23	25.23	6.79	Acceptable
20.574	34.49	43.11	25.87	25.87	6.96	Acceptable
20.828	35.34	44.18	26.51	26.51	7.13	Acceptable
21.082	36.21	45.27	27.16	27.16	7.31	Acceptable
21.336	37.09	46.36	27.82	27.82	7.48	Acceptable
21.59	37.98	47.47	28.48	28.48	7.66	Acceptable
21.844	38.88	48.6	29.16	29.16	7.84	Acceptable
22.098	39.79	49.73	29.84	29.84	8.03	Acceptable
22.352	40.71	50.88	30.53	30.53	8.21	Acceptable
22.606	41.64	52.05	31.23	31.23	8.4	Acceptable
22.86	42.58	53.22	31.93	31.93	8.59	Acceptable
23.114	43.53	54.41	32.65	32.65	8.78	Acceptable
23.368	44.49	55.61	33.37	33.37	8.98	Acceptable
23.622	45.46	56.83	34.1	34.1	9.17	Acceptable
23.876	46.45	58.06	34.84	34.84	9.37	Acceptable
24.13	47.44	59.3	35.58	35.58	9.57	Acceptable
24.384	48.44	60.56	36.33	36.33	9.78	Acceptable

24.638	49.46	61.82	37.09	37.09	9.98	Acceptable
24.892	50.48	63.1	37.86	37.86	10.19	Acceptable
25.146	51.52	64.4	38.64	38.64	10.4	Acceptable
25.4	52.57	65.71	39.42	39.42	10.61	Acceptable
25.654	53.62	67.03	40.22	40.22	10.82	Acceptable
25.908	54.69	68.36	41.02	41.02	11.04	Acceptable
26.162	55.77	69.71	41.82	41.82	11.25	Acceptable
26.416	56.85	71.07	42.64	42.64	11.47	Acceptable
26.67	57.95	72.44	43.46	43.46	11.69	Not Acceptable
26.924	59.06	73.83	44.3	44.3	11.92	Not Acceptable

Input script optimisation of timber frames

```
from itertools import groupby
import numpy as np
import math as mt
import matplotlib.pyplot as plt
from mpl_toolkits.mplot3d import Axes3D
import matplotlib.colors as mcolors
import csv
def save_results_to_csv(results, filename="results.csv"):
    # Column headers for the CSV
    columns = ['Weight (kg)', 'Width (mm)', 'Thickness (mm)', 'Length (m)',
            'Bending Util (%)', 'Bending Status', 'Shear Util (%)', 'Shear Status',
            'SLS Util (%)', 'SLS Status', 'Compression Util (%)', 'Compression Status',
            'Buckling Util Y (%)', 'Buckling Status Y', 'Buckling Util Z (%)', 'Buckling Status Z',
            'Final Util (%)', 'Final Status']
    # Writing to CSV file
    with open(filename, mode='w', newline='') as file:
        writer = csv.writer(file)
        writer.writerow(columns)  # Write the headers

        # Write the rows
        for result in results:
            writer.writerow([f"{result[0]:.2f}", f"{result[1]*1000:.0f}", f"{result[2]*1000:.0f}", f"{result[3]:.2f}",
                        f"{result[4]:.2f}%", result[5], f"{result[6]:.2f}%", result[7],
                        f"{result[8]:.2f}%", result[9], f"{result[10]:.2f}%", result[11],
                        f"{result[12]:.2f}%", result[13], f"{result[14]:.2f}%", result[15],
                        f"{result[16]:.2f}%", result[17]])

def plot_3d_surface_with_distinct_gradient_markers(results):
   # Convert results to numpy arrays for easier manipulation
    widths = np.array([result[1] for result in results])
    thicknesses = np.array([result[2] for result in results])
    weights = np.array([result[0] for result in results])
    utilizations = np.array([result[16] for result in results])  # Assuming the final utilization factor is at index 17
    # Normalize the utilization values for color mapping
    under_util = utilizations[utilizations < 100]
    if under_util.size > 0:  # Ensure there are under-utilized values
        norm = mcolors.Normalize(vmin=np.min(under_util), vmax=100)
    else:
        norm = mcolors.Normalize(vmin=0, vmax=100)  # Default normalization if no values are under 100
    util_cmap = plt.cm.summer  # Distinct, soft colormap for under-utilization
    # Create grid values for width and thickness
    W, T = np.meshgrid(np.unique(widths), np.unique(thicknesses))
    weight_dict = {(width, thickness): weight for width, thickness, weight in zip(widths, thicknesses, weights)}
    W_flat, T_flat = W.flatten(), T.flatten()
```

```
    Wt_flat = np.array([weight_dict.get((w, t), np.nan) for w, t in zip(W_flat, T_flat)])
    Wt = Wt_flat.reshape(W.shape)

    # Create the 3D plot
    fig = plt.figure(figsize=(12, 8))
    ax = fig.add_subplot(111, projection='3d')
    surface = ax.plot_surface(W, T, Wt, cmap='Blues', edgecolor='none', alpha=0.5)
    # Plotting individual points with selective gradient colors
    for width, thickness, weight, utilization in zip(widths, thicknesses, weights, utilizations):
        if utilization >= 100:
            color = 'red'  # Uniform color for over-utilization
            marker = 'x'
        else:
            color = util_cmap(norm(utilization))  # Gradient color for under-utilization
            marker = 'o'
        ax.scatter(width, thickness, weight, color=color, marker=marker, s=50)
    # Labels and titles
    ax.set_xlabel('Width (m)')
    ax.set_ylabel('Thickness (m)')
    ax.set_zlabel('Weight (kg)')
    ax.set_title('3D Surface Plot of Weight vs Width and Thickness with Selective Gradient Utilization Markers')

    # Colorbar for the under-utilization values
    sm_util = plt.cm.ScalarMappable(cmap=util_cmap, norm=norm)
    sm_util.set_array([])
    cbar_util = plt.colorbar(sm_util, ax=ax, aspect=10)
    cbar_util.set_label('Utilization Value (%) (Under 100)')
    # Colorbar for the surface weight values
    sm_weight = plt.cm.ScalarMappable(cmap='Blues')
    sm_weight.set_array(Wt)
    cbar_weight = plt.colorbar(sm_weight, ax=ax, aspect=10)
    cbar_weight.set_label('Weight (kg)')
    plt.show()
    # Pretty print the range of utilization values
    min_util = np.min(utilizations)
    max_util = np.max(utilizations)
    print(f"Utilization Value Range: {min_util:.2f}% to {max_util:.2f}%")
def plot_results(results):
    plt.figure(figsize=(10, 6))

    # Group results by width
    grouped_results = {}
    for result in results:
        weight, width, thickness, length, util_bend, bend_status, util_shear, shear_status, util_sls, sls_status, util_cmprs,
Compression_status, util_buckl_y, bkl_y_status, util_buckl_z, bkl_z_status, util_final, _ = result
        if width not in grouped_results:
            grouped_results[width] = []
        grouped_results[width].append((thickness, weight, util_final))
```

```
    # Create a colormap
    width_values = sorted(grouped_results.keys())
    colors = plt.cm.viridis(np.linspace(0, 1, len(width_values)))
    width_to_color = dict(zip(width_values, colors))

    # Plot each group
    for width, data in grouped_results.items():
        # Sort data by thickness for continuous lines
        data.sort()
        thicknesses, weights, utilizations = zip(*data)
        color = width_to_color[width]

        # Plot the line connecting the points
        plt.plot(thicknesses, weights, linestyle='-', color=color, label=f'Width {width*1000:.0f} mm')

        # Plot individual points with different markers
        for thickness, weight, utilization in zip(thicknesses, weights, utilizations):
            marker = 'o' if utilization < 100 else 'x'
            plt.scatter(thickness, weight, color=color, marker=marker)

    plt.xlabel('Thickness (m)')
    plt.ylabel('Weight (kg)')
    plt.title('Weight vs. Thickness by Width and Utilisation')
    plt.legend(title='Width', loc='upper left', bbox_to_anchor=(1.05, 1), borderaxespad=0.)
    plt.grid(True)
    plt.tight_layout()
    plt.show()
def main():

    y_m = 1.3  # Partial factor

    # User inputs for material properties and load
    rho = 450
    fm_k = 24
    fv_k = 4
    fc_k = 30
    E = 11.3
    E_0_G_05 = 11.3
    kmod_p = 0.5
    kmod_m = 0.65
    kmod_i = 0.9
    P_L = 2.96
    M_L = 7.44
    I_L = 5.66
    SLS_L = 5.18
    gk = 1.38
    g_lead = 2
    g_acmp = 1.4
    K_def = 2
```

```
psi_lead = 0
psi_acmp = 0.2
B_c = 0.2   #factor for solid timber
P_clm = 3.7
M_clm = 9.2
I_clm = 7
L = 2
L_clm = 2
n_width = 10
# widths = [float(input(f"Enter width {i+1} in mm: ")) / 1000 for i in range(n_width)]
widths = [75, 100, 115, 125, 138, 150, 175, 200, 225, 275,300]
widths = [ x / 1000 for x in widths]
n_thickness = 10
# thicknesses = [float(input(f"Enter thickness {i+1} in mm: ")) / 1000 for i in range(n_thickness)]
thicknesses = [35, 38, 44, 47, 50, 63, 75, 100, 150, 250,300]
thicknesses = [ x / 1000 for x in thicknesses]
# Derived design strength values
fm_d_p = (kmod_p * fm_k) / y_m
fm_d_m = (kmod_m * fm_k) / y_m
fm_d_i = (kmod_i * fm_k) / y_m

fv_d_p = (kmod_p * fv_k) / y_m
fv_d_m = (kmod_m * fv_k) / y_m
fv_d_i = (kmod_i * fv_k) / y_m
fc_d_p = (kmod_p * fc_k) / y_m
fc_d_m = (kmod_m * fc_k) / y_m
fc_d_i = (kmod_i * fc_k) / y_m
# Prepare to collect results
results = []
# Iteration over possible dimensions
for W in widths:
  for T in thicknesses:
    V = L * W * T
    Wt = rho * V
    I_y = (W * 1000) * ((T * 1000)**3) / 12  # Moment of inertia with correct units
    I_z = (T * 1000) * ((W * 1000)**3) / 12  # Moment of inertia with correct units
    # ULS Calculations for beam
    Md_1 = P_L * L**2 / 8
    Md_2 = M_L * L**2 / 8
    Md_3 = I_L * L**2 / 8
    h = T  # Total depth of the beam
    # Shear and Bending stresses for ULS beam
    tau_1 = 3/2 * (P_L * L / 2) / (W * h) / 1000
    tau_2 = 3/2 * (M_L * L / 2) / (W * h) / 1000
    tau_3 = 3/2 * (I_L * L / 2) / (W * h) / 1000
    util_bend = max((Md_1 / I_y) * (h * 1000 / 2) * (10**6) / fm_d_p,
            (Md_2 / I_y) * (h * 1000 / 2) * (10**6) / fm_d_m,
            (Md_3 / I_y) * (h * 1000 / 2) * (10**6) / fm_d_i) * 100
    util_shear = max(tau_1 / fv_d_p, tau_2 / fv_d_m, tau_3 / fv_d_i) * 100
```

```
        # SLS Calculations for deflection
        δ_inst = 5*(1e6) *(SLS_L * L**4) / (384 * E * I_y)
        δ_crp_g = 5*(1e6) *(gk * L**4) * K_def / (384 * E * I_y)
        δ_crp_lead = 5*(1e6) *(g_lead * L**4) * K_def * psi_lead / (384 * E * I_y)
        δ_crp_acmp = 5*(1e6) *(g_acmp * L**4) * K_def * psi_acmp / (384 * E * I_y)
        δ_fin = δ_inst + δ_crp_g + δ_crp_lead + δ_crp_acmp
        util_deflct_inst = δ_inst / (L / 300) * 100
        util_deflct_fin = δ_fin / (L / 150) * 100
        util_sls = max(util_deflct_inst, util_deflct_fin)
        # ULS Calculations for Column Compression
        Strs_c_1 = P_clm / ((W * T)*(1e3))
        Strs_c_2 = M_clm / ((W * T)*(1e3))
        Strs_c_3 = I_clm / ((W * T)*(1e3))
        util_cmprs = max(Strs_c_1 / fc_d_p , Strs_c_2 / fc_d_m , Strs_c_3/ fc_d_i ) * 100
        # ULS Calculations for Column Buckling
        L_y = L_clm     # Buckling lengths
        L_Z = L_clm

        i_y = (I_y / (W * T* (1e12)))**(1/2) #Radius of inertia
        i_z = (I_z / (W * T* (1e12)))**(1/2)

        sln_rtio_y = L_y/i_y       #Slenderness ratio
        sln_rtio_z = L_Z/i_z

        sln_rel_y = (((sln_rtio_y/ mt.pi)) * (((fc_k/ E_0_G_05 )*(10))**(1/2)))/100   #Relative slenderness ratio
        sln_rel_z = (((sln_rtio_z/ mt.pi)) * (((fc_k/ E_0_G_05 )*(10))**(1/2)))/100
        k_y = 0.5 * (1 + B_c * (sln_rel_y - 0.3) + (sln_rel_y **2))   #Instability factor
        k_z = 0.5 * (1 + B_c * (sln_rel_z - 0.3) + (sln_rel_z **2))
        k_c_y = 1 / (k_y + mt.sqrt((k_y**2) - (sln_rel_y **2)))      #Buckling reduction coefficient
        k_c_z = 1 / (k_z + mt.sqrt((k_z**2) - (sln_rel_z **2)))
        util_buckl_y = (Strs_c_1/ ((k_c_y) * (fc_d_m))) * 100   #Utilization in plane
        util_buckl_z = (Strs_c_1/ ((k_c_z) * (fc_d_m) )) * 100  #Utilization out of plane
        # Acceptability checks
        bend_status = "Acceptable" if util_bend < 100 else "Unacceptable"
        shear_status = "Acceptable" if util_shear < 100 else "Unacceptable"
        sls_status = "Acceptable" if util_sls < 100 else "Unacceptable"
        Compression_status = "Acceptable" if util_cmprs < 100 else "Unacceptable"
        bkl_y_status = "Acceptable" if util_buckl_y < 100 else "Unacceptable"
        bkl_z_status = "Acceptable" if util_buckl_z < 100 else "Unacceptable"
        util_final = max(util_bend,util_shear, util_sls, util_cmprs, util_buckl_y, util_buckl_z)
        final_status = "Acceptable" if util_final < 100 else "Unacceptable"
        results.append((Wt, W, T, L, util_bend, bend_status, util_shear, shear_status, util_sls, sls_status, util_cmprs,
Compression_status, util_buckl_y, bkl_y_status, util_buckl_z, bkl_z_status, util_final, final_status ))
    # Sort results by weight and print final summary
    results.sort()  # Default sort by first element which is weight
    for result in results:
      print(f" Weight: {result[0]:.2f} kg, Width: {result[1]*1000:.0f} mm, "
        f"Thickness: {result[2]*1000:.0f} mm, Length: {result[3]:.2f} m, "
        f"Bending Utilisation: {result[4]:.2f}%, Bending Status: {result[5]}, "
```

```
        f"Shear Utilisation: {result[6]:.2f}%, Shear Status: {result[7]}, "
        f"SLS Utilisation: {result[8]:.2f}%, SLS Status: {result[9]}, "
        f"Compression Utilisation: {result[10]:.2f}%, Compression status: {result[11]}, "
        f"Buckling Utilisation in plane: {result[12]:.2f}%, Buckling status in plane: {result[13]}, "
        f"Buckling Utilisation out of plane: {result[14]:.2f}%, Buckling status out of plane: {result[15]}, "
        f"Final Utilisation: {result[16]:.2f}%, Final utilisation status: {result[17]}, ")
    plot_results(results)
    plot_3d_surface_with_distinct_gradient_markers(results)
    save_results_to_csv(results)
if __name__ == "__main__":
    main()
```

Input script for load calculator

```
import math
# Functions from the first code
def calculate_kr(z0):
    z0_II = 0.05  # Fixed reference roughness length in meters
    return 0.19 * (z0 / z0_II)**0.07
def calculate_cr(kr, z, z0):
    return kr * math.log(z / z0)
def calculate_turbulence_intensity(k1, c0, z, z0):
    if z0 <= 0 or z <= z0:
        raise ValueError("z must be greater than z0 and z0 must be positive")
    return k1 / (c0 * math.log(z / z0))
def calculate_mean_wind_velocity(kr, c0, vb0, z, z0):
    cr = calculate_cr(kr, z, z0)
    return cr * c0 * vb0
def calculate_peak_wind_velocity_pressure(Iv, rho, vm):
    qp = ((1 + 7 * Iv) * 0.5 * rho * vm ** 2)/1000
    return qp
def calculate_wind_pressure(qp, b, d, h):
    e = min(b, 2 * h)
    if e > 5 * d:
        A_width = d
        B_width = 0
        C_width = 0
    elif e > d:
        A_width = e / 5
        B_width = (d - e) / 5
        C_width = 0
    else:
        A_width = e / 5
        B_width = e * (4 / 5)
```

```
        C_width = d - e
    h_d_ratio = h / d
    if h_d_ratio >= 5:
        cpe_values = {'A': -1.2, 'B': -0.8, 'C': -0.5, 'D': 0.8, 'E': -0.7}
    elif 1 <= h_d_ratio < 5:
        cpe_values = {'A': -1.2, 'B': -0.8, 'C': -0.5, 'D': 0.8, 'E': -0.5}
    elif 0.25 <= h_d_ratio < 1:
        cpe_values = {'A': -1.2, 'B': -0.8, 'C': -0.5, 'D': 0.7, 'E': -0.3}
    else:
        raise ValueError("h/d ratio out of range for defined cpe values")
    We_results = {}
    areas = ['A', 'B', 'C', 'D', 'E']
    for area in areas:
        We_results[area] = qp * cpe_values[area]
    return We_results, {'A_width': A_width, 'B_width': B_width, 'C_width': C_width}
def calculate_loads(We_direct, We_side, widths, h, d, n):
    max_pressures = {}
    areas = ['A', 'B', 'C', 'D', 'E']
    for area in areas:
        max_pressures[area] = max(We_direct[area], We_side[area])

    load_on_beam = (max(max_pressures.values()) * h) / 2
    load_on_column = max(
        max_pressures['A'] * widths['A_width'],
        max_pressures['B'] * widths['B_width'],
        max_pressures['C'] * widths['C_width'],
        max_pressures['D'] * d,
        max_pressures['E'] * d
    ) / (n / 2)
    return load_on_beam, load_on_column
def calculate_dead_load(rho, T_sl, W_sl, L_sl):
    volume = W_sl * L_sl * T_sl
    mass = volume * rho
    g = 9.81
    weight = mass * g

    dead_load_per_meter = (weight / L_sl) / 2 / 1000

    return dead_load_per_meter
def calculate_Live_load(W_sl, L_sl):
    Live_load = (1.5)* (W_sl * L_sl)  # Assume a live load of 1.5 kN/m²
    qk = (Live_load / L_sl) / 2 / 1000
    return qk
def calculate_snow_load(W_sl,L_sl):
    M_i = 0.8  # Snow load shape coefficient
    Ce = 1.0   # Exposure coefficient
    Ct = 1.0   # Thermal coefficient
    s_g = float(input("Enter the Characteristic value of snow load (s.g): "))
    snow_load = ((M_i * Ce * Ct * s_g)*(W_sl * L_sl))
```

```
    sk= ((snow_load)/ L_sl)/2/1000
    return sk

def Beam_load_combinations():
    # Constants
    γ_g = 1.35
    γ_q = 1.5
    Ψ_0_q = 0
    Ψ_0_w = 0.6
    altitude = float(input("Enter the altitude of the site: "))
    if altitude > 1000:
        height = 2
    else:
        height = 1
    if height == 1:
        Ψ_0_s = 0.7
    else:
        Ψ_0_s = 0.5
    # Inputs for dead load calculation
    rho = float(input("Enter the density of the slab material (kg/m³): "))
    T_sl = float(input("Enter the thickness of the slab (m): "))
    W_sl = float(input("Enter the width of the slab (m): "))
    L_sl = float(input("Enter the length of the slab (m): "))
    gk = calculate_dead_load(rho, T_sl, W_sl, L_sl)
    print(f"The calculated dead load on the beam (gk) is {gk:.2f} kN/m")
    qk = calculate_Live_load(W_sl, L_sl)

    sk= calculate_snow_load(W_sl,L_sl)
    # Get the wind load inputs
    h = float(input("Enter the height of the building h (m): "))
    z = h       #input("Enter the height at which the wind speed is considered (z) in (m)
    z0 = float(input("Enter the roughness length (z0) in meters: "))
    c0 = float(input("Enter the orography factor (c0): "))
    vb0 = float(input("Enter the basic wind speed (vb0) in m/s: "))
    b = W_sl    #input("Enter the width of the building b (m)
    d = L_sl    #input("Enter the length of the building d (m)
    n = int(input("Enter the number of columns n: "))
    # Calculating kr, Iv, Vm, and qp using the first code's functions
    kr = calculate_kr(z0)
    Iv = calculate_turbulence_intensity(1, c0, z, z0)
    vm = calculate_mean_wind_velocity(kr, c0, vb0, z, z0)
    qp = calculate_peak_wind_velocity_pressure(Iv, 1.25, vm)  # rho is 1.25 kg/m^3
    print(f"Calculated peak velocity pressure qp: {qp:.2f} Pa\n")
    # Calculate for direct wind
    We_direct, widths_direct = calculate_wind_pressure(qp, b, d, h)
    print_results(We_direct, "direct")
    # Calculate for side wind (just swapping b and d)
    We_side, widths_side = calculate_wind_pressure(qp, d, b, h)
    print_results(We_side, "side")
```

```
# Calculate wind loads
wk, load_on_column = calculate_loads(We_direct, We_side, widths_direct, h, d, n)
print(f"Wind load on the beam (wk): {wk:.2f} kN/m")
print(f"Load on the column: {load_on_column:.2f} kN")

ULS_category1 = [γ_g * gk]
ULS_category2 = [
    (γ_g * gk) + (γ_q * qk),
    (γ_g * gk) + (γ_q * qk) + (Ψ_0_s * γ_q * sk),
    (γ_g * gk) + (γ_q * qk) + (Ψ_0_w * γ_q * wk)
]
ULS_category3 = [
    (γ_g * gk) + (γ_q * qk) + (Ψ_0_s * γ_q * sk) + (Ψ_0_w * γ_q * wk),
    (γ_g * gk) + (Ψ_0_q * γ_q * qk) + (γ_q * sk) + (Ψ_0_w * γ_q * wk),
    (γ_g * gk) + (Ψ_0_q * γ_q * qk) + (Ψ_0_s * γ_q * sk) + (γ_q * wk),
    (γ_g * gk) + (γ_q * sk),
    (γ_g * gk) + (γ_q * wk),
    (γ_g * gk) + (γ_q * sk) + (Ψ_0_w * γ_q * wk),
    (γ_g * gk) + (γ_q * wk) + (Ψ_0_s * γ_q * sk),
    (γ_g * gk) + (Ψ_0_q * γ_q * qk) + (γ_q * sk),
    (γ_g * gk) + (Ψ_0_q * γ_q * qk) + (γ_q * wk)
]
max_category1 = max(ULS_category1)
max_category2 = max(ULS_category2)
max_category3 = max(ULS_category3)

SLS_combinations = [
    gk,
    gk + qk,
    gk + qk + Ψ_0_s * sk,
    gk + qk + Ψ_0_w * wk,
    gk + qk + Ψ_0_s * sk + Ψ_0_w * wk,
    gk + Ψ_0_q * qk + sk + Ψ_0_w * wk,
    gk + Ψ_0_q * qk + Ψ_0_s * sk + wk,
    gk + sk,
    gk + wk,
    gk + sk + Ψ_0_w * wk,
    gk + wk + Ψ_0_s * sk,
    gk + Ψ_0_q * qk + sk,
    gk + Ψ_0_q * qk + wk
]
max_SLS = max(SLS_combinations)

Lead_varbl = max(qk, sk, wk)

if Lead_varbl == qk:
    psi_lead = 0
elif Lead_varbl == sk:
    if height == 1:
```

```
            psi_lead = 0.2
        else:
            psi_lead = 0.5
    elif Lead_varbl == wk:
        psi_lead = 0.2
    values = [qk, sk, wk]
    values.remove(Lead_varbl)
    acmp_varbl = max(values)
    if acmp_varbl == qk:
        psi_acmp = 0
    elif acmp_varbl == sk:
        if height == 1:
            psi_acmp = 0
        else:
            psi_acmp = 0.2
    elif acmp_varbl == wk:
        psi_acmp = 0
    print(f"Maximum load for ULS Category 1 (Permanent): {max_category1:.2f} kN/m")
    print(f"Maximum load for ULS Category 2 (Medium-term): {max_category2:.2f} kN/m")
    print(f"Maximum load for ULS Category 3 (Instantaneous): {max_category3:.2f} kN/m")
    print(f"Maximum load for SLS: {max_SLS:.2f} kN/m")
    print(f"Leading varible action: {Lead_varbl:.2f} kN/m")
    print(f"accompanying variable action: {acmp_varbl:.2f} kN/m")
    print(f"psi_lead: {psi_lead:.2f}")
    print(f"psi_acmp: {psi_acmp:.2f}")
def print_results(We_results, wind_direction):
    print(f"Wind pressure results for {wind_direction} wind:")
    for area, pressure in We_results.items():
        print(f"We for area {area}: {pressure:.2f} Pa")
    print("\n")
# Call the function to run the combined code
Beam_load_combinations()
```

Input script for G-code Genrator

```
def generate_gcode(
    mortise_width,
    mortise_height,
    mortise_depth,
    tenon_width,
    tenon_height,
    tenon_length,
    peg_diameter,
    peg_depth,
    num_pegs,
    tool_diameter,
    feed_rate,
    spindle_speed,
    safe_z,
    step_down=2,  # Added step-down parameter
):
    """Generates G-code for a pegged mortise and tenon joint."""

    gcode = ""

    # Setup
    gcode += "G21\n"  # Set units to millimeters
    gcode += "G17\n"  # Set XY plane
```

```
gcode += "G90\n"  # Set to absolute coordinates

gcode += f"F{feed_rate}\n"

gcode += f"S{spindle_speed}\n"


# Mortise

gcode += mill_pocket(

    0, 0, -mortise_depth, mortise_width, mortise_height, tool_diameter, safe_z, step_down

)


# Tenon

gcode += mill_pocket(

    0,

    0,

    -tenon_length,

    tenon_width,

    tenon_height,

    tool_diameter,

    safe_z,

    step_down,

)


# Peg holes

peg_spacing = mortise_width / (num_pegs + 1)

for i in range(num_pegs):

    x_pos = peg_spacing * (i + 1)
```

```
        gcode += drill_hole(x_pos, mortise_height / 2, -peg_depth, peg_diameter, safe_z)

    # End of program
    gcode += "M30\n"

    return gcode

def mill_pocket(x_start, y_start, z_depth, width, height, tool_diameter, safe_z, step_down):
    """Generates G-code to mill a pocket."""

    gcode = ""
    current_z = 0
    while current_z > z_depth:
        current_z -= step_down
        gcode += f"G0 Z{safe_z}\n"
        gcode += f"G0 X{x_start + tool_diameter/2} Y{y_start + tool_diameter/2}\n"
        gcode += f"G1 Z{current_z}\n"
        gcode += f"G1 X{x_start + width - tool_diameter/2}\n"
        gcode += f"G1 Y{y_start + height - tool_diameter/2}\n"
        gcode += f"G1 X{x_start + tool_diameter/2}\n"
        gcode += f"G1 Y{y_start + tool_diameter/2}\n"
    gcode += f"G0 Z{safe_z}\n"
    return gcode

def drill_hole(x_pos, y_pos, z_depth, diameter, safe_z):
```

```
    """Generates G-code to drill a hole."""

    gcode = ""
    gcode += f"G0 Z{safe_z}\n"
    gcode += f"G0 X{x_pos} Y{y_pos}\n"
    gcode += f"G1 Z{z_depth}\n"  # Use a drilling cycle (e.g., G81) if supported
    gcode += f"G0 Z{safe_z}\n"
    return gcode

# Example usage
gcode_program = generate_gcode(
    mortise_width=20,
    mortise_height=40,
    mortise_depth=10,
    tenon_width=18,
    tenon_height=38,
    tenon_length=15,
    peg_diameter=6,
    peg_depth=20,
    num_pegs=2,
    tool_diameter=8,
    feed_rate=1000,
    spindle_speed=10000,
    safe_z=10,
) print(gcode_program)
```

Appendix F: Input script for Joint Optimiser

```
import math
import matplotlib.pyplot as plt
import numpy as np
# Calculate the capcity of peg and spacing requierments
def calculate_capacity_and_status_for_graph(
    w_clmn, b_clmn, w_t, tau_c, F_ed, F_em, F_es,
    required_load_kN, Ke, Re, k3, dtl_e, dtl_s, dtl_v, dtl_g,
    n, tm, ts ):
    D_values = []
    capacity_values = []
    statuses = []

    # Iterate over D values, converting floats to ints
    for D in range(int(0.5 * 100), int((b_clmn/4) * 100) + 1, int(0.01 * 100)):
        D = D / 100  # Convert back to float for calculations
        # 1. Calculate Capacity Components
        Pld = (n * D * tm * F_ed) / 2
        Plm = (n * D * tm * F_em) / 2
        Pls = n * D * ts * F_es
        PVd = (n * math.pi * (D ** 2) * tau_c) / 4
        # 2. Find Overall Capacity
        capacity = min(Pld, Plm, Pls, PVd)
        # 3. Check if the Joint is Strong Enough
        status = "Acceptable" if (
            capacity >= required_load and
            lim_v + lim_e < b_clmn and
            (2 * lim_g) + lim_s < w_t
        ) else "Not Acceptable"
        # 4. Calculate Equivalent Steel Diameter Bolt
        Z = capacity
        d_im = (4 * Ke * Z) / (tm * F_em)
        d_is = (2 * Ke * Z) / (ts * F_es)
        d_iiis = (1.6 * Ke * Z * (2 + Re)) / (k3 * ts * F_em)
        d_iv = (math.sqrt((1.6 * Ke * Z * math.sqrt(3 * (1 + Re))) / math.sqrt(2 * F_em * F_es))) / 2
        d_eq = max(d_im, d_is, d_iiis, d_iv)
        # 5. Calculate Limits for Placement of the Dowel
        lim_e = dtl_e * d_eq
        lim_s = dtl_s * d_eq
        lim_v = dtl_v * d_eq
        lim_g = dtl_g * d_eq
        # 6. Check if Dowel Placement is OK
        limit_check_v_e = lim_v + lim_e < b_clmn
        limit_check_g_s = (2 * lim_g) + lim_s < w_t
        # 7. Print the Results in the desired format
        D_mm = D * 25.4
```

```
        lim_e_mm = lim_e * 25.4
        lim_s_mm = lim_s * 25.4
        lim_v_mm = lim_v * 25.4
        lim_g_mm = lim_g * 25.4
        capacity_kN = capacity * 0.00444822

        print(f"{D_mm:.3f}, {lim_e_mm:.2f}, {lim_s_mm:.2f}, {lim_v_mm:.2f}, {lim_g_mm:.2f}, {capacity_kN:.2f}, {status} ")

        # Collect values for plotting
        D_values.append(D_mm)
        capacity_values.append(capacity_kN)
        statuses.append(status)
    return D_values, capacity_values, statuses
# Input parameters ( we are iterating over it D)
w_clmn = 3.93701 #100 mm
b_clmn = 4.4291339 #112.5 mm
w_t = 6 #152.4 mm
tau_c = 1518
F_ed = 2688
F_em = 5488
F_es = 2660
required_load = 1000
Ke = 0.625
Re = 2.063
k3 = 1.3
dtl_e = 2
dtl_s = 2.5
dtl_v = 1.5
dtl_g = 1.5
n = 2
tm = (w_clmn/3)
ts = tm
required_load_kN= required_load * 0.00444822
# Get the values for plotting
D_values, capacity_values, statuses = calculate_capacity_and_status_for_graph(
    w_clmn, b_clmn, w_t, tau_c, F_ed, F_em, F_es,
    required_load_kN, Ke, Re, k3, dtl_e, dtl_s, dtl_v, dtl_g,
    n, tm, ts,
)
```

Bibliography

- Agency, I. E. (2013). Modernising building energy codes to secure our global energy future, International Energy Agency.
- Allen, K. M. (2006). "Community-based disaster preparedness and climate adaptation: local capacity-building in the Philippines." Disasters 30(1): 81-101.
- Liina Transitional Shelter / Aalto University Wood Program" 11 Oct 2011. ArchDaily. <https://www.archdaily.com/174909/liina-transitional-shelter-aalto-university-wood-program> ISSN 0719-8884
- Arlet, J. L. (2021) Innovative Carpentry and Hybrid Joints in Contemporary Wooden Architecture. Arts 10, DOI: 10.3390/arts10030064
- ASTM (1995a). Practice for establishing clear wood strength values. West Conshohocken, PA, ASTM International.
- ASTM (2017). Practice for establishing clear wood strength values. West Conshohocken, PA, ASTM International.
- ASTM (2023). Standard Test Method for Evaluating Dowel-Bearing Strength of Wood and Wood-Based Products.
- Azzarello, N. (2013). "open source emergency habitat for haiti builds in five hours." from https://www.designboom.com/architecture/open-source-emergency-habitat-for-haiti-builds-in-five-hours-10-14-2013/.
- Banichuk, N. V., et al. (2010). Structural Optimization with Uncertainties, Springer.
- Barreca, F., et al. (2022). "Civil Engineering Journal A Highly Sustainable Timber-Cork Modular System for Lightweight Temporary Housing." Civil Engineering Journal 8: 2336-2352.

- Bendsoe, M. P. and O. Sigmund (2013). Topology Optimization: Theory, Methods, and Applications, Springer Berlin Heidelberg.
- Benson, T., and James Gruber. (1980). Building the timber frame house: the revival of a forgotten craft.
- Benson, T. (1997). The Timber-frame Home: Design, Construction, Finishing, Taunton Press.
- Binding, G. (1975). Kleine Kunstgeschichte des deutschen Fachwerkbaus, Wissenschaftliche Buchgesellschaft.
- Branco, J., et al. (2015). "Analysis and strengthening of carpentry joints". Construction and Building Materials 2015 Vol. 97
- Brown, A. (1995). The Genius of Japanese Carpentry: The Secrets of a Craft, Kodansha International.
- Burnett, D. T., et al. (2003). "Structural properties of pegged timber connections as affected by end distance." Forest Products Journal 53: 50-57.
- Casagrande, D., et al. (2021). "Structural performance of a hybrid timber wall system for emergency housing facilities." Journal of Building Engineering 33: 101566.
- Christensen, P. W. and A. Klarbring (2008). An Introduction to Structural Optimization, Springer Netherlands.
- Cook, R. D., et al. (2002). Concepts and applications of finite element analysis. New York, NY, John Wiley & Sons.
- Danish, M. S. S., et al. (2019). "A managed framework for energy-efficient building." Journal of Building Engineering 21: 120-128.
- Eckelman, C., et al. (2006). "Effect of shoulders on bending moment capacity of round mortise and tenon joints." 56.

- Falk, R. H., et al. (2019). Development of a ready-to-assemble tornado shelter from cross-laminated timber (CLT): impact and wind pressure testing, U.S. Department of Agriculture, Forest Service, Forest Products Laboratory.
- Fang, D. (2020). Timber joinery in modern construction: Mechanical behavior of wood-wood connections.
- Fang, D., et al. (2019). Modern timber design approaches for traditional Japanese architecture: analytical, experimental, and numerical approaches for the Nuki joint.
- Gustavsson, L., et al. (2006). "Carbon Dioxide Balance of Wood Substitution: Comparing Concrete- and Wood-Framed Buildings." Mitigation and Adaptation Strategies for Global Change 11(3): 667-691.
- Guan, Z., et al. (2008). "Experimental study and finite element modelling of Japanese “Nuki” joints — Part two: Racking resistance subjected to different wedge configurations." Engineering Structures - ENG STRUCT 30: 2041-2049.
- Holan, J. (1990). Norwegian Wood: A Tradition of Building, Rizzoli.
- Hudert, M. & Pfeiffer, S. (2019). Rethinking Wood: Future Dimensions of Timber Assembly. Berlin, Boston: Birkhäuser. https://doi.org/10.1515/9783035617061
- Haftka, R. T. and Z. Gürdal (2012). Elements of Structural Optimization, Springer Netherlands.
- Hewett C.A., English Historic Carpentry. London & Chichester: Phillimore & Co. Ltd., 1980, p.270.
- Hu, W. and B. Chen (2021). "A Methodology for Optimizing Tenon Geometry Dimensions of Mortise-and-Tenon Joint Wood Products." Forests 12.
- Iwata, T., et al. (2023). "Towards improving provision of wooden temporary housing: Analysis of repairs of temporary housing built by local contractors after the Great East Japan Earthquake." International Journal of Disaster Risk Reduction 86: 103537.

- Hu, W. and B. Chen (2021). "A Methodology for Optimizing Tenon Geometry Dimensions of Mortise-and-Tenon Joint Wood Products." Forests 12(4): 478.
- JELUŠIČ, P. (2018). "Determining optimal designs of timber beams with non-uniform cross-section." WIT Press.
- Kaijima, S., et al. (2015). Parametric Finite Element Contact Analysis for Topologically Interlocking Joinery.
- Kasal, A., et al. (2016). "Numerical Analyses of Various Sizes of Mortise and Tenon Furniture Joints." BioResources 11.
- Kessel, M. H. and Augustin, R., "Untersuchungen über das Tragverhalten von Verbindungen mit Eichenholznägeln," Bauen mit Holz, pp. 246-250, April, 1990.
- Kessel, M. H. a. A., R. (1996). "Load Bearing Capacity of Timber Connections with Wood Pegs." Journal of the Timber Framers Guild 39: 8-11.
- Kim, N.-H. (2015). Erratum to: Introduction to Nonlinear Finite Element Analysis. Introduction to Nonlinear Finite Element Analysis. N.-H. Kim. New York, NY, Springer US: E1-E1.
- In chapter 1 titled “Preliminary Concepts”, text and equations has been updated in pages 1, 5, 8, 9, 11, 13, 14, 15, 24, 41, 63, and 75.
- Kolb, J., et al. (2008). Systems in Timber Engineering: Loadbearing Structures and Component Layers, Birkhäuser.
- Kravanja, S. and T. Žula (2021). "Optimization of a single-storey timber building structure." International Journal of Computational Methods and Experimental Measurements 9: 126-140.
- Kłosowski, P., et al. (2018). "Historical carpentry corner log joints—Numerical analysis within stochastic framework." Engineering Structures 176: 64-73.

- Láng, E. M. and T. Fodor (2007). "Finite Element Analysis of Cross-halved Joints for Structural Composites." Wood and Fiber Science 34: 251-265.
- Larsen, H. J. (1973). The Yield Load of Bolted and Nailed Joints. Proceedings of the International Union of Forestry Research Organization. Division V Conference: 645-654.
- Latif, K., Adam, A., Yusof, Y. and Kadir, A.Z.A., 2021. A review of G code, STEP, STEP-NC, and open architecture control technologies based embedded CNC systems. The International Journal of Advanced Manufacturing Technology, 114, pp.2549-2566.
- Leichti, R. J., et al. (2000). "The continuum of connection rigidity in timber structures." Wood and fiber science: 11-19.
- Liu, K., et al. (2024). "Investigating the Influence of Tenon Dimensions on White Oak (Quercus alba) Mortise and Tenon Joint Strength." Forests 15(9): 1612.
- Nick Cater, Keith Ashton, and Brenda Puech, "How Kosovo Is Teaching Us the New Economics of Shelter," Humanitarian Affairs Review (June 15, 2000)
- McLain, T. (1993). Connector code development and application in the United States: Generic fasteners. Proc., 1992 Int. Workshop on Wood Connectors, Forest Products Society.
- McMullin, P. W. and J. S. Price (2017). Timber Design, Taylor & Francis.
- Moradei, J., et al. (2018). Structural Characterization of Traditional Moment-Resisting Timber Joinery.
- Oktaee, J., et al. (2014). "Bending moment capacity of simple and haunched mortise and tenon furniture joints under tension and compression loads." TURKISH JOURNAL OF AGRICULTURE AND FORESTRY 38: 291-297.
- Paul, W. M. and S. P. Jonathan (2017). Architect's Guidebooks to Structures. Stoodleigh, Devon, UK, Florence Production Ltd.

- Pech, S., et al. (2019). "Metamodel assisted optimization of glued laminated timber beams by using metaheuristic algorithms." Engineering Applications of Artificial Intelligence 79: 129-141.
- Querin, O. M., et al. (2017). Topology Design Methods for Structural Optimization, Elsevier Science.
- Richard J. Schmidt, R. B. M. (1997). TIMBER FRAME TENSION JOINERY, University of Wyoming.
- Roschlia, A., Borisha, M., Feldhausena, T., Barnesa, A., Wanga, P., & MacDonalda, E. (2023). The g-code file. Motion and Path Planning for Additive Manufacturing, 225.
- Sangree, R. H. and B. W. Schafer (2009). "Experimental and numerical analysis of a halved and tabled traditional timber scarf joint." Construction and Building Materials 23(2): 615-624.
- Schilderman, T. (2004). "Adapting traditional shelter for disaster mitigation and reconstruction: experiences with community-based approaches." Building Research & Information 32(5): 414-426.
- Schmidt, R. J. and R. Mackay (1997). TIMBER FRAME TENSION JOINERY.
- Schmidt, R. J. and C. E. J. Daniels (1999). DESIGN CONSIDERATIONS FOR MORTISE AND TENON.
- Schmidt, R. and J. Miller (2004). "CAPACITY OF PEGGED MORTISE AND TENON JOINERY."
- Shanks, J. D., et al. (2008). "Experimental study on mechanical performance of all-softwood pegged mortice and tenon connections." Biosystems Engineering 100(4): 562-570.
- Shanks, J. and P. Walker (2009). "Strength and Stiffness of All-Timber Pegged Connections." Journal of Materials in Civil Engineering - J MATER CIVIL ENG 21.

- Shaw, M. (2004). "Housing and public health." Annu Rev Public Health 25: 397-418.
- Shin, Seung-Jun, Suk-Hwan Suh, and Ian Stroud. "Reincarnation of G-code based part programs into STEP-NC for turning applications." Computer-Aided Design 39, no. 1 (2007): 1-16.
- Siem, J. (2017). "The single-step joint – a traditional carpentry joint with new possibilities." International Wood Products Journal 8(sup1): 45-49.
- Skog, K. E., et al. (2015). "Desirable properties of wood for sustainable development in the twenty-first century." Annals of Forest Science 72(6): 671-678.
- Smith, I. and G. Foliente (2002). "Load and Resistance Factor Design of Timber Joints: International Practice and Future Direction." Journal of Structural Engineering-asce - J STRUCT ENG-ASCE 128.
- Stanić, A., et al. (2016). "Economic-design optimization of cross laminated timber plates with ribs." Composite Structures 154: 527-537.
- Stern, Brenda G. "Minimizing embodied carbon in multi-material structural optimization of planar trusses." Thesis, Massachusetts Institute of Technology, 2018. http://hdl.handle.net/1721.1/119324.
- Thelandersson, S., Larsen, H. J. Timber Engineering. Chichester: John Wiley & Sons Ltd., 346 pages, 2003.
- Tran, V.-D., et al. (2014). "FE analysis and geometrical optimization of timber beech finger-joint under bending test." International Journal of Adhesion and Adhesives 52: 40-47.
- Tannert, Thomas, Daniel Schmidt, and Frank Lam. "CNC timber processing in research and teaching." In Proceedings of the 51st International Convention of Society of Wood Science and Technology, pp. 1-9. 2008.
- Topping, B. H. V. and D. J. Robinson (1984). "Optimization of timber framed structures." Computers & Structures 18(6): 1167-1177.

- Ulrich, R. B. (2007). Roman Woodworking, Yale University Press.
- United States Department of Agriculture, F. S. F. P. L. (2010). Wood handbook : wood as an engineering material, Centennial edition. Madison, WI : U.S. Dept. of Agriculture, Forest Service, Forest Products Laboratory, [2010] ©2010.
- University, R. r. (2010). Literature Review for Shelter After Disaster. World, Shelter Centre.
- Van de Kuilen, J.-W. and C. Sandhaas (2013). "Material model for wood." Heron 58: 173-194.
- Van Nimwegen, S. E. and P. Latteur (2023). "A state-of-the-art review of carpentry connections: From traditional designs to emerging trends in wood-wood structural joints." Journal of Building Engineering 78: 107089.
- VanRooyen, M. and J. Leaning "After the Tsunami — Facing the Public Health Challenges." New England Journal of Medicine 352(5): 435-438.
- Voulpiotis, K., et al. (2021). "A holistic framework for designing for structural robustness in tall timber buildings." Engineering Structures 227: 111432.
- Wielinga, E. (2023). Finite Element Analysis of Interlocking Timber Connections in Plywood Diaphragm Floors: Optimizing Form for Strength, Eindhoven University of Technology. Master.
- Wilczyński, A. P. and K. Warmbier (2003). Effect of joint dimensions on strength and stiffness of tenon joints.
- Wilson, M. (2011). "Emergency Shelter: An Architectural Perspective (2011)."
- Yang, B. (2005). 5 - Stress Analysis in Two-Dimensional Problems. Stress, Strain, and Structural Dynamics. B. Yang. Burlington, Academic Press: 135-156.
- Zwerger, K. and V. Olgiati (2015). Wood and Wood Joints: Building Traditions of Europe, Japan and China.

List of Figures